IN VITRO TOXICITY EVALUATION OF PIPERAZINE DESIGNER DRUGS

Marcelo Dutra Arbo

TESE APRESENTADA PARA ADMISSÃO A PROVAS DE DOUTORAMENTO À FACULDADE DE FARMÁCIA DA UNIVERSIDADE DO PORTO

The candidate performed the experimental work supported by a PhD grant (Proc. BEX 0593/10-9) of Capes Foundation (Coordenação para Aperfeiçoamento de Pessoal de Nível Superior), Brazil.

The Faculty of Pharmacy of the University of Porto, Portugal, the National Institute of Health Dr. Ricardo Jorge (INSA) – Porto and the Leibniz Research Centre for Working Environment and Human Factors (IFADO), Technical University of Dortmund – Dortmund (Germany) provided the facilities and logistical support for the experimental work.

Marcelo Dutra Arbo

IN VITRO TOXICITY EVALUATION OF PIPERAZINE DESIGNER DRUGS

Tese do 3º Ciclo de Estudos Conducente ao Grau de Doutor em Ciências Farmacêuticas – Especialidade: Toxicologia

Orientador: Professora Doutora Helena Maria Ferreira da Costa Ferreira Carmo

(Professora Auxiliar da Faculdade de Farmácia da Universidade do Porto)

Coorientador: Professora Doutora Maria de Lourdes Pinho de Almeida Souteiro Bastos

(Professora Catedrática da Faculdade de Farmácia da Universidade do Porto)

Porto

dezembro, 2014

“A ciência nunca resolve um problema sem criar pelos menos outros dez.“

(George Bernard Shaw)

ACKNOWLEDGMENTS / AGRADECIMENTOS

Foram quatro anos de doutoramento e muitos momentos, bons e não tão bons, muito trabalho, esforço, incontáveis experiências (científicas e de vida), novos amigos, novos lugares, novos hábitos, aos quais tive que me habituar ou me adaptar. Por tudo isso, antes de tudo, deixo um agradecimento as três instituições que me acolheram, o Laboratório de Toxicologia da Faculdade de Farmácia da Universidade do Porto, o Instituto Nacional de Saúde (INSA) Doutor Ricardo Jorge no Porto e o Leibniz Institute für Arbeitforschung an der TU Dortmund (IfADo, Alemanha).

Inicialmente, não posso deixar de agradecer a todos que apoiaram a minha ideia de fazer o doutorado longe de casa, incluindo a minha família, a minha tutora no Brasil, Profª Dr. Mirna Bainy Leal, e as professoras Dr. Solange Cristina Garcia e Dr. Renata Pereira Limberger pelos conselhos iniciais e ajuda no processo burocrático para a concessão da bolsa de doutorado.

A Professora Doutora Maria de Lourdes Bastos, minha co-orientadora, serei imensamente grato por ter me aceitado em seu grupo, desde aquele primeiro contato em 2008 até conseguir os meios para chegar a Portugal em 2010, não ter medido esforços para disponibilizar tudo que precisei para executar o trabalho e por todas as palavras de incentivo que me fizeram ter esperança em tempos difíceis. O seu trabalho, humildade e capacidade humana são inspiradores!

A minha orientadora, Professora Doutora Helena Carmo, quero agradecer a fundamental supervisão durante estes quatro anos e dizer que muito me orgulha ter partilhado comigo seus conhecimentos. Se hoje chego ao fim do doutoramento devo muito ao seu empenho, dedicação, incentivo e visão científica que me levaram mais longe do que eu pensava chegar.

Ao Professor Doutor Fernando Remião, agradeço as palavras amigas, o incentivo e ter me dado a oportunidade de participar de algumas aulas práticas que foram, sem dúvida, de grande valia. Quero deixar um reconhecimento pela preocupação constante que tem com os alunos e os problemas do laboratório em geral.

Ao Professor Doutor Félix Carvalho, seu otimismo é contagiante para todo o grupo, mesmo a passar poucos minutos em sua presença, acaba-se por aprender muito consigo.

À Doutora Paula Guedes, Doutora Sónia Fraga, Doutora Vera Costa e ao Doutor João Capela, obrigado pela ajuda, conselhos e estes anos de convivência quase diária. À Sra. Engenheira Maria Elisa Soares, muito obrigado pelo seu imenso carinho, amizade e por estar sempre preocupada com o bem-estar de todos no laboratório. À Cátia, um agradecimento especial por sempre aceitar mais um item na lista de compras e sempre nos socorrer quando precisamos de algum material com urgência. À Ana Margarida, não esqueço da amizade, dos ratos cedidos para tentarmos mais um isolamento de hepatócitos e da companhia nos tempos da antiga FFUP.

À Diana, não encontro palavras para descrever o quanto sou grato, passamos juntos por muitos infortúnios e isso só fez com que a minha admiração e amizade crescesse. Foste os braços

e pernas a mais que eu precisava ter e não tinha, muito deste trabalho devo a ti e por isso serei eternamente grato.

À Renata e ao Daniel, muito obrigado pela paciência, por toda a ajuda que me deram no laboratório e por estarem sempre disponíveis quando precisei. O vosso auxílio e amizade não serão esquecidos.

À Eliane e Luciana, e também ao Artur, vocês foram a minha família no Porto enquanto estiveram aqui e por isso sou grato. Ter começado essa aventura ao lado de caras conhecidas fez tudo ser mais fácil, sinto não ter vocês aqui presentes no final também.

Quero agradecer a todos os outros colaboradores do Laboratório de Toxicologia da FFUP pela ajuda, simpatia e companhia diária. Quero agradecer em especial às grandes colegas já Doutoras Ana e Teresa pelos nossos almoços, viagens, aventuras e por serem sempre um espalhanço de alegria no laboratório. Á Juliana (Juzinha), Rita e ao José Luís (Zé), muito obrigado pela companhia, especialmente nesse último ano, e a amizade, das quais vou sentir muita falta. Obrigado também a Vânia, Maria João, Márcia, Margarida, Mariline e Filipa.

Ao Doutor João Paulo Teixeira, sou muito grato pela colaboração que iniciamos para fazer os testes de genotoxicidade e a amizade. E pensar que tudo começou em um Eurotox... Também preciso agradecer à Susana a colaboração e todo o auxílio na preparação das lâminas e à Carla pelas ideias iniciais.

To Prof. Dr. Jan Hengstler, I am very thankful for all the contribution to this work and I feel honored to have worked at IfADo even for a few months. I also would like to thank everyone at IfADo that were so kind and pleasant in receiving me. Special thanks to my great friends and collegues Markus, Regina, Simone, Agata and Katharina for all the support and all the fun we had. Danke! Grazie! Dziękuję!

Aos meus amigos que ficaram no Brasil, da faculdade, do mestrado ou do Centro de Informação Toxicológica (CIT), especialmente à Gabriela, Rachel, Fernando, Viviane, Rafaela, Eduardo e Carolina, foram quatro anos de ausência, muitas vezes a minha vontade era ir e voltar, rapidinho, só para estar com vocês. O que me reconforta é saber que a distância não diminuiu em nada nossa amizade e a cada vez que conseguia ir ao Brasil, cada encontro era como se eu nunca estivesse saído.

Ao Airton, muito obrigado pela ajuda, pelas formatações, por estar sempre próximo e por todo apoio, especialmente nesse último ano, que passou tão rápido e muitas vezes eu achava que não conseguiria fazer tudo que faltava a tempo.

Por fim, obrigado a todos que de alguma forma colaboraram para esse doutoramento e que, porventura, eu possa ter esquecido. Com o fim desta tese, volto para casa mas não vou sozinho, levo um pouco de Portugal comigo, assim como acredito que deixei um pouco do Brasil em Portugal. Para os amigos que agora eu deixo cá, os laços de amizade são eternos, não será a distância que vai altera-los, espero encontrar-vos novamente muito em breve.

PUBLICATIONS

Articles in international peer-reviewed journals

1. Arbo MD, Silva R, Barbosa DJ, Dias da Silva D, Rossato LG, Bastos ML, Carmo H. Piperazine designer drugs induce toxicity in cardiomyoblast H9c2 cells through mitochondrial impairment. Toxicology Letters 229 (1): 178-189.

2. Arbo MD, Silva R, Barbosa DJ, Dias da Silva D, Silva SP, Teixeira JP, Bastos ML, Carmo H. In vitro neurotoxicity evaluation of piperazine designer drugs in differentiated human neuroblastoma SH-SY5Y cells. British Journal of Pharmacology. *Submitted for publication*

3. Arbo MD, Dias da Silva D, Valente MJ, Bastos ML, Carmo H. Hepatotoxicity of piperazine designer drugs: comparison of different in vitro models. Archives of Toxicology. *To be submitted for publication*

4. Arbo MD, Melega S, Stöber R, Schug M, Rempel E, Rahnenführer J, Bastos ML, Carmo H, Hengstler JG. Hepatotoxicity of piperazine designer drugs: a toxicogenomic approach. Archives of Toxicology. *To be submitted for publication*

ABSTRACT

In several countries, there is growing use of piperazine derivatives with recreational purposes. The most commonly piperaze derivatives used as drugs of abuse are 1-benzylpiperazine (BZP), 1-(3-trifluoromethylphenyl)piperazine (TFMPP), 1-(4-methoxyphenyl)piperazine (MeOPP) and 1-(3,4-methylenedioxybenzyl)piperazine (MDBP). Little is known about the toxic effects of these substances. The aim of this study was to conduct a toxicological evaluation of these drugs using *in vitro* models. The *in vitro* models used were: immortalized H9c2 rat cardiomyoblasts, human immortalized SH-SY5Y neuroblastoma cells, HepaRG and HepG2 human hepatoma cell lines and primary rat hepatocytes in monolayer and sandwich cultures. Cytotoxicity and toxicological parameters such as energy status, oxidative stress, mitochondrial function, and cell death pathways were evaluated. Microarray studies of gene expression were performed in primary hepatocytes in sandwich culture. The piperazine derivatives showed cytotoxicity in all evaluated models, and the TFMPP derivative was the most potent. The mitochondria seem to be an important target of toxicity. In H9c2 cells, the drugs increased intracellular Ca^{2+} levels, led to loss of mitochondrial membrane potential ($\Delta\psi m$) and ATP depletion, which was related to the opening of the mitochondrial permeability transition pore (MPTP). Similarly, mitochondrial depolarization and ATP depletion were observed in primary hepatocytes. On the other hand, in SH-SY5Y cells an increase in intracellular Ca^{2+} levels and a mitochondrial hyperpolarization were observed. In addition, a decrease in total glutathione levels was observed in all the models. With the exception of primary rat hepatocytes, oxidative stress did not appear to have a major influence on the cytotoxicity produced by piperazine derivatives. In all models, we observed an activation of apoptotic cell death pathways. Using the microarray technique in sandwich cultured primary rat hepatocytes, an up-regulation of genes linked to cholesterol biosynthesis was observed, which could be associated with a phospholipidosis toxicity mechanism. Overall, the results point to potential cardio-, neuro- and hepatotoxicity caused by piperazine-derived designer drugs, raising concern about their abuse.

Keywords: piperazine designer drugs, *in vitro* models, cytotoxicity, toxicogenomics.

RESUMO

Em diversos países do mundo, é crescente o uso de derivados da piperazina com fins recreacionais. Dentre os compostos piperazínicos mais comumente utilizados como drogas de abuso, estão a 1-benzilpiperazina (BZP), 1-(3-trifluormetilfenil)piperazina (TFMPP), 1-(4-metoxifenil)piperazina (MeOPP) e 1-(3,4-metilenodioxibenzil)piperazina (MDBP). Pouco se sabe ainda sobre os efeitos tóxicos destas substâncias. O objetivo deste trabalho foi realizar a avaliação toxicológica destes compostos por meio de modelos *in vitro*. Para tal, foram utilizados como modelos *in vitro* os cardiomioblastos de rato imortalizados H9c2, a linha imortalizada de neuroblastoma humano SH-SY5Y, as linhas imortalizadas de hepatoma humano HepG2 e HepaRG, bem como hepatócitos primários de rato cultivados em monocamada e em *sandwich*. Nestes sistemas, foram traçadas curvas de citoxicidade e avaliados parâmetros energéticos, de stress oxidativo, de função mitocondrial e vias de morte celular. Além disso, foram realizados estudos de expressão genética, através de *microarrays*, nos hepatócitos primários em *sandwich*. As drogas de abuso derivadas da piperazina demonstraram citotoxicidade em todos os modelos avaliados, e o derivado TFMPP mostrou ser o mais potente. A mitocôndria pareceu ser um importante alvo de toxicidade. Nas células H9c2 foi observado aumento dos níveis de Ca^{2+} intracelular, perda do potencial de membrana mitocondrial ($\Delta\psi m$) e depleção de ATP, o que estava relacionado a abertura do poro mitocondrial de permeabilidade transitória (MPTP). De modo semelhante, a despolarização mitocondrial e depleção de ATP também foram observados em hepatócitos primários. Por outro lado, em SH-SY5Y foi observado aumento dos níveis de Ca^{2+} intracelular e hiperpolarização da mitocôndria. Além disso, a diminuição dos níveis totais de glutationa foi observada em todos os modelos. Com exceção dos hepatócitos primários de rato, o stress oxidativo não pareceu ter grande influência na citotoxicidade produzida pelos derivados da piperazina. Em todos os modelos, foi verificada uma ativação de vias apoptóticas de morte celular. Utilizando a técnica de *microarrays* em hepatócitos primários de rato cultivados em *sandwich*, foi observada uma sobreexpressão de genes envolvidos na biossíntese do colesterol, o que poderá estar relacionado com um mecanismo de fosfolipidose. De um modo geral, os resultados apontam para uma potencial cardio, neuro e hepatotoxicidade causadas pelas *designer drugs* derivadas da piperazina, levantando séria preocupação acerca do seu abuso.

Palavras-chave: *designer drugs* derivadas da piperazina, modelos *in vitro*, citotoxicidade, estudos toxicogenómicos.

OUTLINE OF THE THESIS

The thesis is organized in 6 chapters.

Chapter I is an introduction to contextualize the state of art of the key topics within the thesis. The introduction summarizes current knowledge on dynamics, kinetics, and analytical methodologies for the identification of piperazine designer drugs, including BZP, MDBP, *m*CPP, TFMPP, and MeOPP.

Chapter II comprises the aims of the thesis and explains how these articulate with the subsequent experimental results presented.

Chapter III contains the main studies performed, including materials, methods, results and discussion which are presented in the form of published manuscripts or under submission in peer-reviewed journals. For each study, information concerning the journal and co-authors is provided.

Chapters IV to VI include a general discussion and main conclusions of the thesis, highlighting the most relevant achievements and also the prospects for future work.

TABLE OF CONTENTS

LIST OF FIGURES

LIST OF TABLES

LIST OF ABBREVIATIONS

5-HT	5-hydroxytryptamine / serotonin
Δψm	mitochondrial membrane potential
ACTH	adrenocorticotropic hormone
AIF	apoptosis inducing factor
API/MS	atmospheric pressure ionization mass spectrometry
BZP	*N*-benzylpiperazine
CAR	constitutive androstane receptor
CE	capillary electrophoresis
CD	chemiluminescence detector
COMT	catechol-*O*-methyltransferase
CPP	chlorophenylpiperazine
DA	dopamine
DAD	diode array detector
DAT	dopamine transporter
DIB-Cl	4-(4,5-diphenyl-1-H-imidazol-2-yl)benzoyl chloride
DOI	2,5-dimethoxy-4-iodoamphetamine
EMIT®	enzyme-multiple immunoassay technique
ER-α	α estrogen receptor
ESI-MS	electrospray ionization mass spectrometry
EU	European Union
FD	fluorescence detector
FPIA	fluorescence polarization immunoassay
GC	gas chromatography
GGT	γ-glutamyl transpeptidase
GPx	glutathione peroxidase
GR	glutathione reductase
GSH	glutathione
GSSG	oxidized glutathione
HPLC	high performance liquid chromatography
IL-1β	interleukine 1β
IT-MS	ion trap mass spectrometer
k’	capacity factor
LPS	lipopolysaccharide
MBDB	*N*-methyl-1-(3,4-methylenedioxyphenyl)-2-butanamine
*m*CPP	1-(3-chlorophenyl)piperazine
MDA	methylenedioxyamphetamine
MDBP	1-(3,4-methylenedioxybenzyl)piperazine
MDEA	3,4-methylenedioxyethylamphetamine

MDMA	3,4-methylenedioxymethamphetamine
MeOPP	1-(4-methoxyphenyl)piperazine
MPP^+	1-methyl-4-phenylpyridinium ion
MPTP	mitochondrial permeability transition pore
MS	mass spectrometer
NE	norepinephrine
NET	norepinephrine transporter
NFκB	nuclear factor-κ B
NPD	nitrogen phosphorus detector
*p*FPP	1-(4-fluorophenyl)piperazine
PXR	pregnane X receptor
RNS	reactive nitrogen species
ROS	reactive oxygen species
SERT	serotonin transporter
SPE	solid-phase extraction
t½	elimination half-life
TFAA	trifluoroaceticacid anhydride
TFMPP	1-(3-trifluoromethylphenyl)piperazine
T_{lag}	time from administration to first quantifiable concentration
TLC	thin-layer chromatography
TNF-α	tumor necrosis factor-α
TPA	12-*O*-tetradecanoylphorbol-13-acetate
UPLC	ultrahigh performance liquid chromatography
VMAT	vesicular monoamine transporter
WADA	World Anti-Doping Agency

CHAPTER I

INTRODUCTION

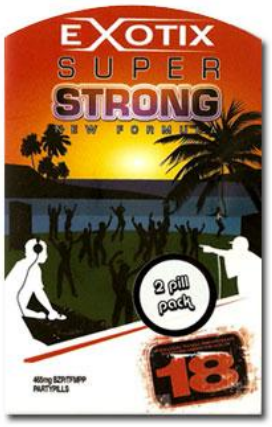

1.1. General aspects

The abuse of drugs is widespread all over the world. Synthetic drugs are among the most commonly abused and they are consumed mainly at parties and night clubs by young people. The so-called designer drugs are a heterogeneous group of psychoactive substances obtained through the modification of the chemical structure of some natural products or drugs (Mustata et al., 2009). The most common designer drugs are derived from phenylethylamine, as 3,4-methylenedioxymethamphetamine (MDMA). As soon as these drugs become forbidden, new derivatives appear in the market to evade the law. In this context, piperazine derived drugs appeared on the market, mainly head shops and the internet (Nelson et al., 2014), sold as ecstasy pills or under the names of “Rapture”, “Frenzy”, “Bliss”, “Charge”, “Herbal ecstasy”, “A2”, “Legal X” and “Legal E”. Generally, they are consumed as capsules, tablets or pills but also in powder or liquid forms (Gee et al., 2005). They can also appear as mixture of piperazines (as BZP/TFMPP) or in combination with other drugs of abuse, such as MDMA and cocaine (Staack et al., 2007).

The first documented abuse of a piperazine-derived drug occurred with *N*-benzylpiperazine (BZP), in the USA, in 1996 (Austin and Monasterio, 2004). In September 2004, the new ecstasy-like substance 1-(3-chlorophenyl)piperazine (*m*CPP) was detected in street drugs in Sweden and in the Netherlands by the Drug Information and Monitoring System (DIMS). *m*CPP has been found in 26 member states of European Union (EU) and in Norway (Bossong et al., 2005; Kovaleva et al., 2008). It was estimated that in 2006, approximately 823,000 tablets of *m*CPP were seized in the EU (Kovaleva et al., 2008). In the Netherlands, the number of *m*CPP tablets seized alone or in combination with MDMA increased significantly between 2004 and 2007 (Bossong et al., 2009). A survey in the UK, found that piperazines are among the most common active drugs in tablets purchased from internet supplier sites (Davies et al., 2010). In New Zealand, the piperazine designer drugs known as party pills became a recent phenomenon (Gee et al., 2005; Sheridan et al., 2007). Piperazine designer drugs have also been detected in Japan (Takahashi et al., 2009) and Brazil (Lanaro et al., 2010). Markets for these drugs have also developed in Bulgaria, Sweden (Helander et al., 2014), South Africa (Cohen and Butler, 2011), and Poland (Biliński et al., 2012). Nowadays, piperazine derived drugs including BZP and *m*CPP are under control in the EU, USA, New Zealand, Australia, and Japan (Gee and Fountain, 2007). In Brazil, besides BZP and *m*CPP, 1-(3-trifluoromethylphenyl)piperazine (TFMPP) is also under control. In competitive sports, the use of these substances is forbidden by the World Anti-Doping Agency (WADA).

Although in the corresponding drug scene the designer drugs have the reputation of being safe, several experimental, clinical, and epidemiological studies indicate risks to humans including a life-threatening serotonin syndrome, hepatotoxicity, neurotoxicity, psychopathology, and abuse potential (Maurer et al., 2004).

Chemically, the piperazinic compounds are derived from piperazine, a cyclic molecule containing two nitrogens in opposite positions and four carbons distributed between the two nitrogen atoms (figure 1). They were originally used as anti-helmintic agents in the 1950s, and presently remain in human and veterinary pharmacotherapy (Haroz and Greenberg, 2006). Piperazine designer drugs can be divided into two classes, the benzylpiperazines such as BZP and its methylenedioxy analogue 1-(3,4-methylenedioxybenzyl)piperazine (MDBP), and the phenylpiperazines such as *m*CPP, 1-(4-fluorophenyl)piperazine (*p*FPP), 1-(3-trifluoromethylphenyl)piperazine (TFMPP), and 1-(4-methoxyphenyl)piperazine (MeOPP) (figure 1).

BZP can be manufactured by reacting piperazine monohydrochloride with benzyl chloride. Other methods described include mixing of piperazine hexahydrate, piperazine dihydrochloride monohydrate and benzyl chloride, leading to the predominant product 1-BZP dihydrocloride, and the mixture of equal molar amounts of piperazine hexahydrate and benzyl chloride (Yeap et al., 2010).

BZP was originally synthesized by researchers from Burroughs, Wellcome & Co as a de-worming agent for cattle. However, there is no published data about the use of BZP as a treatment for intestinal parasites. In the 1970s, BZP was investigated as an anti-depressant agent. Clinical trials were performed but they were abandoned due to reinforcing effects similar to dexamphetamine. Despite this finding, in the 1980s, BZP-derived compounds were once more tested as anti-depressant agents, namely Trelibet (EGYT-475) and befuraline (DIV-145). There is evidence that they reached phase I and II clinical trials and were found to act as a pro-drug, being metabolized to active BZP in humans (Kerr and Davis, 2011, Monteiro et al., 2013).

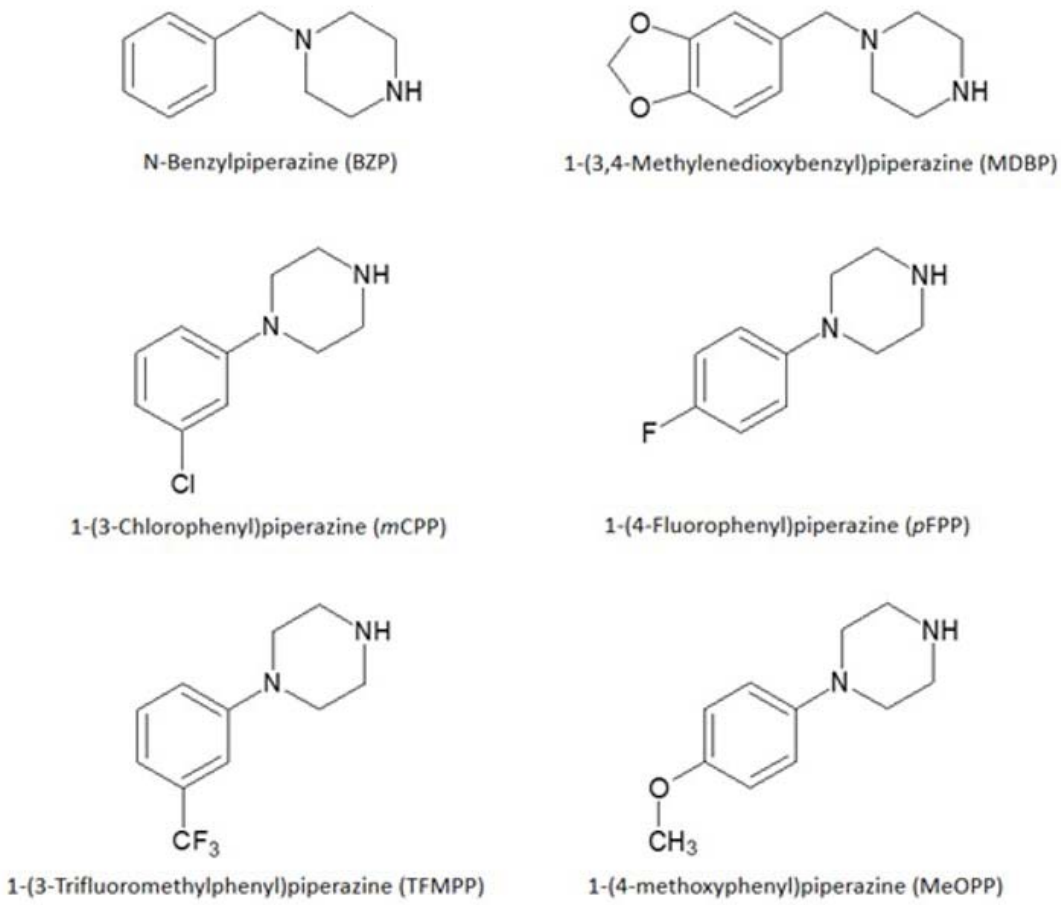

Figure 1. Chemical structure of some piperazine designer drugs.

1.2. Dynamics

Piperazine designer stimulants were designed to mimic the effects of traditional illicit stimulants such as cocaine or amphetamines. Because of this, comparison of their neurochemical and behavioural effects provides a logical starting point for evaluating relative abuse potential. Not surprisingly, as with the traditional illicit stimulants, designer stimulants primarily exert their behavioural and psychological effects by dynamically modulating monoamine transmission in brain (Watterson et al., 2013).

1.2.1. *In vitro* studies

Among the piperazinic compounds used as drugs of abuse, BZP is the most studied. It has been reported that the combination of BZP and TFMPP (2:1, in most documented cases) in pills mimics the effects of MDMA in humans (de Boer et al., 2001). Studies in synaptosomes demonstrated that BZP is a releaser of 1-methyl-4-phenylpyridinium ion ([^{3}H]MPP$^+$) (Baumann et al., 2005), whereas TFMPP and *m*CPP were releasers of serotonin ([^{3}H]5-HT), and inactive at releasing dopamine ([^{3}H]DA) (Baumann et al., 2014). These releasing properties are mediated by substrate activity at norepinephrine (NETs), dopamine (DATs) and serotonin (SERTs) transporters, although the piperazine derivatives were less potent than MDMA (Baumann et al., 2005). Indeed, TFMPP binds to all three transporters, however, it showed a higher releasing effect at SERT (Severinsen et al., 2012).

In synaptosomes, *m*CPP was found to induce the release of 5-HT through SERT and possess agonist properties at some 5-HT receptors, as 5-HT$_{2C}$, and antagonist properties at others, such as 5-HT$_{2B}$. An important difference between *m*CPP and MDMA was their effect on dopamine release in this *in vitro* model. *m*CPP exhibited only minimal effects, which could result in weak reinforcing effects as compared with other drugs such as MDMA. However, the abuse potential of *m*CPP was not assessed *in vivo* to confirm this findings. Furthermore, *m*CPP lacks neurotoxic potential. It is able to release 5-HT without causing a long-term depletion since it releases only the cytoplasmic 5-HT, while MDMA induces the release of both cytoplasmic and vesicular 5-HT (Baumann et al., 2001).

In rat brain synaptosomes, BZP strongly inhibited the re-uptake of DA and norepinephrine (NE), but had a small effect on 5-HT re-uptake, while *m*CPP and MeOPP strongly inhibited 5-HT re-uptake and also inhibited re-uptake of NE and DA. In the same synaptosomes preparations, BZP strongly stimulated DA and NE release, but hardly affected the release of 5-HT. On the other hand, *m*CPP strongly stimulated the release of 5-HT, DA and NE, while MeOPP had relatively high monoamine-releasing activity (Nagai et al., 2007).

*m*CPP significantly decreased the production of nitric oxide, tumor necrosis factor-α (TNF-α) and interleukin-1β (IL-1β) in rat microglia and astrocyte cultures. Also, *m*CPP attenuated the expression of inducible nitric oxide synthase and pro-inflammatory cytokines such as IL-1β and TNF-α at mRNA levels. In addition, *m*CPP inhibited nuclear factor-κ B (NFκB) activation and phosphorylation of p38 mitogen-activated protein kinase

in lipopolysaccharide (LPS)-stimulated microglia cells, indicating molecular mechanisms for anti-inflammatory effects for *m*CPP (Hwang et al., 2008).

BZP and TFMPP showed cell proliferative effects in human breast cancer MCF7-BUS cells, which were antagonized with tamoxifen co-incubation (Min et al., 2012). Both drugs presented binding affinities to the α estrogen receptor (ER-α) in a concentration-dependent trend. The treatment with 10 μM BZP or TFMPP increased the mRNA expressions of progesterone receptor and pS2 genes in MCF7-BUS cells.

1.2.2. *In vivo* studies

Surprisingly, in spite of the potential in vitro estrogenic effect of these piperazine derivatives, *in vivo* studies found limited evidence of hormonal activity. No significant differences were found in uterus weight in the uterotrophic assay with immature female rats. Also, treatments (1, 4, 10, 25 mg/kg BZP or TFMPP i.p. once a day for 3 days) had no effects on body weight, lung, liver, kidney, and adrenal to body weight ratios. (Min et al., 2012).

In mice, BZP exhibited a clear stimulant-like pattern of behavioural effects (Yarosh et al., 2007). BZP lacked hallucinogen-like actions in the test of drug-elicited head twitch response (1, 3, 10 and 30 mg/kg i.p.), induced a dose-dependent locomotor stimulant effect in the open-field (30 and 100 mg/kg i.p.), and fully substituted for the stimulant-like S(+)-enantiomer of MDMA (1, 3, 10 and 30 mg/kg i.p.). TFMPP and *m*CPP dose-dependently and fully substituted for S(+)-MDMA (1 and 3 mg/kg i.p.) but produced a decrease in locomotor activity (30 mg/kg TFMPP or 3 and 10 mg/kg *m*CPP). Interestingly, TFMPP was active in the head twitch assay (10 mg/kg i.p.), while BZP and *m*CPP (1, 3 and 10 mg/kg i.p.) showed no activity, but TFMPP failed to substitute for the hallucinogen-like R(-)-MDMA (1 and 3 mg/kg i.p.) (Yarosh et al., 2007). It is therefore believed that the BZP/TFMPP combination aggregates the stimulant effect of BZP, through a dopaminergic action, with the hallucinogenous effects of TFMPP that are mediated via serotonergic pathways (Rosenbaum et al., 2012).

When intravenously administered to rats, the behavioural effects of BZP (3 mg/kg iv at time 0 and 10 mg/kg iv 60 min later) were confirmed through the increase of DA and 5-HT in brain dialysates monitored through 120 min. However, the increase of DA release was more pronounced than the increase of 5-HT (Baumann et al., 2005). Similar to MDMA, BZP provoked hyperlocomotion and stereotypic behaviours. In the same study, TFMPP (3 mg/kg iv at time 0 and 10 mg/kg iv 60 min later) induced extracellular elevation

only in 5-HT levels, although it was 3-fold less potent than MDMA and caused no alterations in ambulation and stereotypy (Baumann et al., 2005). Based on these findings, the authors proposed that the TFMPP pharmacological mechanisms include: (i) full agonist activity at multiple 5-HT receptors, (ii) partial agonist or antagonist activity at 5-HT_{2A} receptors, and (iii) SERT-mediated 5-HT releasing activity. Also, the effects of the co-administration of BZP and TFMPP (1:1) were investigated in rats (3 mg/kg iv at time 0 and 10 mg/kg iv 60 min later). The drug mixture produced increased release of DA and 5-HT in nucleus accumbens, as well as increases in ambulation and stereotypy (Baumann et al., 2005). Comparing the effects of TFMPP and *m*CPP, both drugs increased extracellular 5-HT, however TFMPP was more potent. *m*CPP produced modest elevations in DA whereas TFMPP decreased DA levels at later time points (about 400 min) (Baumann et al., 2014).

BZP, administered at a single dose of 5 or 20 mg/kg intraperitoneally to rats, induced a dose-dependent increase in time spent in the compartment associated with the drug in the place-preference test experiment. Pharmacological blockade of dopamine D_1-like receptors attenuated BZP-produced conditioned place-preference, indicating that some acute effects of BZP can be due to the effects on central dopaminergic substrates (Meririne et al., 2006). Exposure of Sprague-Dawley rats to BZP (20 and 40 mg/kg i.p.) and methamphetamine (1 and 2 mg/kg i.p.) produced dose-dependent hyperactivity and stereotypy (Brennan et al., 2007). Repeated exposure to the same drugs for 5 days produced sensitized behavioural responses at 20 mg/kg BZP that were more apparent in the hyperactivity measures. Also, cross-sensitization between BZP and methamphetamine was evident hyperactivity and stereotypy when administering a low dose of methamphetamine (0.5 mg/kg i.p.) in BZP pre-treated rats (20 mg/kg i.p. for 5 days) after a 2 day-withdrawal period (Brennan et al., 2007).

Adolescent male and female rats treated intraperitoneally with 10mg/kg/day BZP from postnatal days 45 to 55 presented higher levels of anxiety-like behavior, compared to controls, 17 days after the last administration. The observed effects were possibly due to the interference of BZP with the maturation of anxiety-associated forebrain mechanisms (Aitchison and Hughes, 2006).

After *in vivo* microdialysis of rat nucleus accumbens locally infused with *m*CPP, significant elevations in dialysate 5-HT were observed at 1, 10 and 100 μM doses, and this effect was clearly dose-dependent. Furthermore, *m*CPP produced a significant rise in DA at 10 and 100 μM, but the magnitude of *m*CPP-evoked DA increase was always

smaller than the corresponding 5-HT increase. A significant 5-HT increase was also observed after intravenous injection of 1, 3 and 10 µmol/kg *m*CPP (Baumann et al., 2001).

An effective reinforcing activity of 0.03, 0.1 and 0.3 mg/kg/inj iv.) BZP in rhesus monkeys was reported (Fantegrossi et al., 2005). In the same study, TFMPP (0.01, 0.03, 0.1, 0.3 and 1 mg/kg/inj iv.) failed to maintain self-administration behaviour. When evaluated in monkeys trained to discriminate amphetamine from saline, BZP (ED_{50} 9.3 mg/kg iv.) had full amphetamine-like effects, suggesting that it has an abuse liability of the amphetamine type. When combinations of BZP and TFMPP were tested, they seemed to be less effective reinforcers than BZP alone (Fantegrossi et al., 2005). In the same study, high BZP intake by self administration produced several signs of intoxication, including stereotyped visual scanning around the room, involuntary head movements, jaw chattering, bizarre body postures, hyperactivity, and “fly catching” (fixating on an empty point in space and attempting to quickly grasp the area). In the same model, no signs of intoxication were observed for TFMPP (Fantegrossi et al., 2005).

Adverse effects reported in humans after the abuse of *m*CPP include anxiety, dizziness, hallucinations, nausea, warm and cold flushes, migraine and panic attacks. *m*CPP often induces severe hallucinations and nausea. Its subjective effects resemble those of MDMA, both positive as well as negative. The agonist properties of *m*CPP at 5-HT_2 receptors can explain its hallucinogenic features since other hallucinogenic substances such as lysergic acid diethylamide exert their effects through the activation of these receptors (Bossong et al., 2005, 2010). Indeed, *m*CPP is an agonist of 5-HT_{2C}, 5-HT_{1A}, 5-HT_{1B} and 5-HT_{1D} receptor subtypes, showing an entactogen profile different from other hallucinogens that act as 5-HT_{2A} agonists. Neuroendocrine properties, namely the release of hormones such as adrenocorticotropic hormone (ACTH), cortisol, and prolactin were noted. These effects are also mediated via 5-HT receptors (Feuchtl et al., 2004). The activation of 5-HT_3 receptors may be involved in the *m*CPP-induced nausea (Bossong et al., 2005, 2010).

The pharmacological effects described for piperazine designer drugs are summarized in table 1.

Table 1. Summary of pharmacological effects of piperazine designer drugs.

Drug	Effects	Reference
BZP	locomotor stimulant effect	
	substitution for S(+)-MDMA	Yarosh et al., 2007
	no hallucinogen-like actions in head twitch assay	
	increase in DA and 5-HT in brain dialysates	Baumann et al., 2005
	hyperlocomotion and stereotypic behaviours	
	reinforcing effects at place preference test in rats	Meririne et al., 2006
	cross-sensitization with methamphetamine	Brennan et al., 2007
	higher levels of anxiety-like behavior in adolescent rats	Aitchison and Hughes, 2006
	reinforcing effects in rhesus monkeys	Fantegrossi et al., 2005
TFMPP	decrease in locomotor activity	
	substitution for S(+)-MDMA	Yarosh et al., 2007
	hallucinogen-like actions in head twitch assay	
	increase in extracellular 5-HT	Baumann et al., 2005
	no self-administration behaviour in rhesus monkeys	Fantegrossi et al., 2005
*m*CPP	decrease in locomotor activity	
	substitution for S(+)-MDMA	Yarosh et al., 2007
	no hallucinogen-like actions in head twitch assay	
	increase in extracellular DA and 5-HT	Baumann et al., 2005

1.3. Kinetics

Piperazines are readily absorbed from the gastrointestinal tract. A portion of the absorbed drug is metabolized and excreted in urine. There is wide variation in the rates at which piperazines are excreted by different individuals, which adds to the variability of their toxicity (Austin and Monasterio, 2004; Elliott, 2011). The piperazine designer drugs are mainly metabolized in liver, being the phenylpiperazines more extensively metabolized than the benzylpiperazines, and excreted almost exclusively as metabolites (Maurer et al., 2004). The main metabolic reactions include hydroxylation, *N*-dealkylation and demethylenation.

Biodistribution data are scarce however, the fact that this drugs have effects on mood and behaviour suggests that they cross the blood-brain barrier. A study of tissue distribution in the rat found higher concentrations of BZP in the kidneys, with a concentration ratio between plasma and kidneys of approximately 1:20, while the TFMPP concentration ratio between the plasma and the lungs (the organ with the highest TFMPP concentration) had a ten-fold difference at approximately 1:200, 30 min after dose. This study also reported that the ratios of BZP and TFMPP between plasma and all other analysed tissues (brain,

liver, kidneys, lungs, heart) were 1:40 and 1:385 respectively, 30 min after dose (Antia et al., 2009d). Additional toxicokinetic data for *m*CPP in rodents suggest poor protein binding (about 30-40%), accumulation in the brain, and renal elimination (Caccia, 2007).

The metabolism of BZP was qualitatively studied in male Wistar rats and the proposed pathways are presented in figure 2. This piperazine derivative was not extensively metabolized and was mainly excreted unchanged. Three metabolic targets could be identified for BZP: (i) the aromatic ring, (ii) the benzyl carbon and (iii) the piperazine heterocycle. The aromatic ring was metabolically altered by single or double hydroxylation (2 and 3, figure 2) through CYP450 activity, followed by catechol-*O*-methyltransferase (COMT) catalyzed methylation to *N*-(4-hydroxy-3-methoxybenzyl)piperazine (4, figure 2). Formation of the corresponding glucuronides and/or sulfates was postulated. *N*-Dealkylation at the benzyl carbon led to the liberation of piperazine (5, in figure 2). The piperazine heterocycle was degraded by double *N*-dealkylation leading either to the formation of *N*-benzylethylenediamine (6, in figure 2) or benzylamine (7, in figure 2) (Staack et al., 2002; Staack and Maurer, 2005).

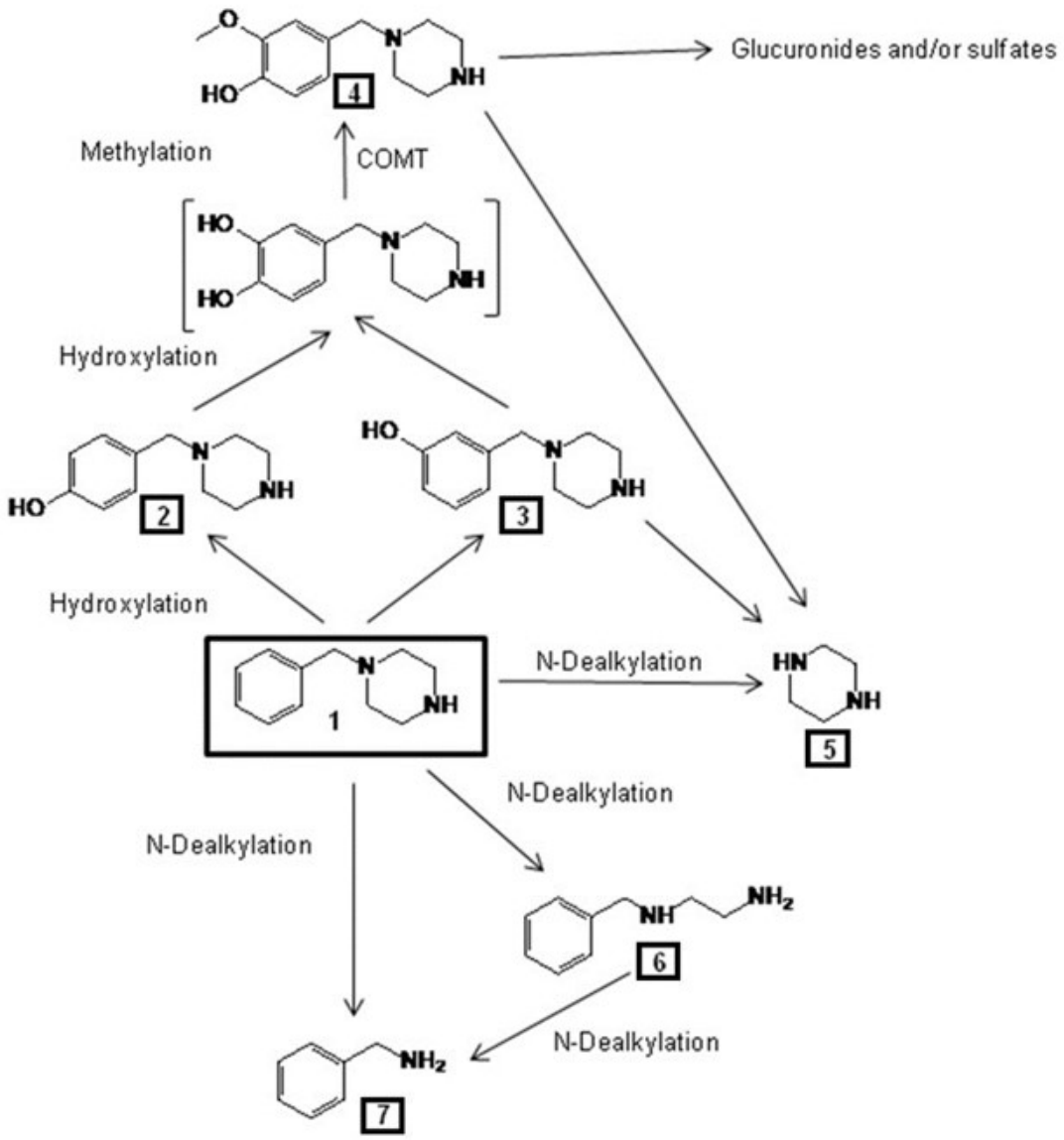

Figure 2. Proposed metabolism of 1-benzylpiperazine (BZP) in male Wistar rats. 1 = BZP; 2 = 4-hydroxybenzylpiperazine; 3 = 3-hydroxybenzylpiperazine; 4 = N-(4-hydroxy-3-methoxybenzyl)piperazine; 5 = piperazine; 6 = *N*-benzylethylenediamine; 7 = benzylamine. (Adapted from Staack & Maurer, 2005).

MDBP is the methylenedioxy derivative of BZP, and is also the main metabolite of the therapeutic drug fipexide (Vigilor®) that was withdrawn from the market worldwide due to adverse side effects, including liver toxicity (Sleno et al., 2007). The MDBP metabolism was qualitatively studied in male Wistar rats (figure 3) (Staack and Maurer, 2004). As described for BZP, MDBP was mainly excreted as unchanged parent compound. Metabolic alteration of the aromatic moiety, the benzyl carbon and the piperazine heterocycle was also described for MDBP. The main pathway is the demethylenation of

the 3,4-methylenedioxy moiety to the corresponding catechol and further methylation to *N*-(4-hydroxy-3-methoxybenzyl)piperazine (2, in figure 3) followed by partial glucuronidation or sulfation leading to the formation of metabolites common with BZP. Likewise, *N*-dealkylation at the benzyl carbon, leading to piperazine (3, in figure 3) was described. Degradation of the piperazine heterocycle by double *N*-dealkylation led to the corresponding benzylamine and *N*-benzylethylenediamine derivatives 3,4-methylenedioxybenzylamine (4, in figure 3) and *N*-(3,4-methylenedioxybenzyl)ethylenediamine (5, in figure 3) (Staack and Maurer, 2004; Staack and Maurer, 2005). Special concern regarding toxicity should be given to the catechol formation. Several drugs undergo bioactivation into *ortho*-quinone intermediates, via catechol metabolites, which have the ability to covalently bind to endogenous compounds such as the cysteinyl sulfhydryl group in gluthatione (GSH) to form GSH conjugates, as already described for MDMA metabolites (Carvalho et al., 2004; Jones et al., 2005).

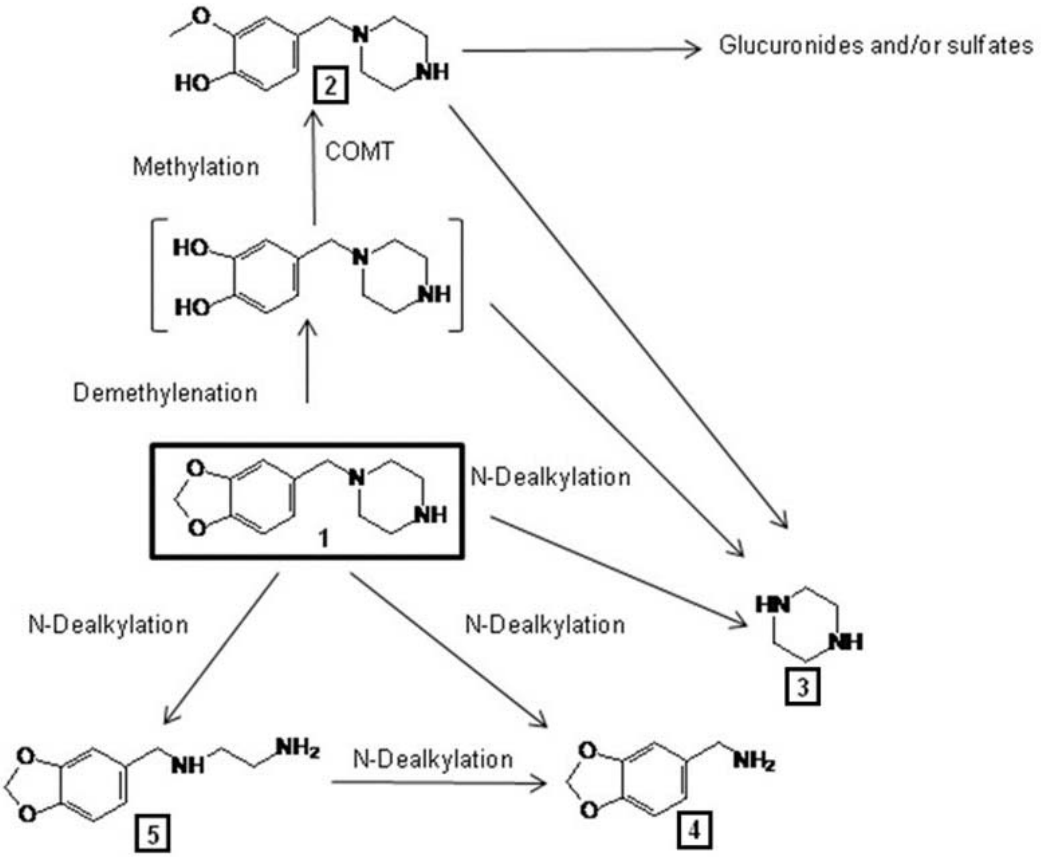

Figure 3. Proposed metabolism of 1-(3,4-methylenedioxy)benzylpiperazine (MDBP) in male Wistar rats. 1 = MDBP; 2 = *N*-(4-hydroxy-3-methoxybenzyl)piperazine; 3 = piperazine; 4 = 3,4-methylenedioxybenzylamine; 5 = *N*-(3,4-methylenedioxybenzyl)ethylenediamine. (Adapted from Staack & Maurer, 2004).

*m*CPP is an active metabolite of therapeutic drugs such as trazodone, nefazodone, etoperidone, and mepiprazol, used as antidepressants and minor tranquilizers. The *m*CPP metabolism, represented in figure 4, was qualitatively studied in male Wistar rats (Staack and Maurer, 2003). Extensive metabolism was reported. However, small amounts of unchanged *m*CPP could be detected in urine. *p*-Hydroxy-*m*CPP (2, in figure 4) was identified as the major metabolite. In addition to the aromatic hydroxylation, degradation of the piperazine heterocycle by double *N*-dealkylation of *m*CPP to *N*-(3-chlorophenyl)ethylenediamine (3, in figure 4) or to 3-chloroaniline (4, in figure 4) were described. Hydroxy-3-chloroaniline (5, in figure 4) was the only metabolite resulting from degradation of the piperazine moiety of hydroxy-*m*CPP. The aniline metabolites were partially *N*-acetylated (6 and 7, in figure 4). Glucuronidation and sulfation were postulated as phase II reactions (Staack and Maurer, 2003; Staack and Maurer, 2005).

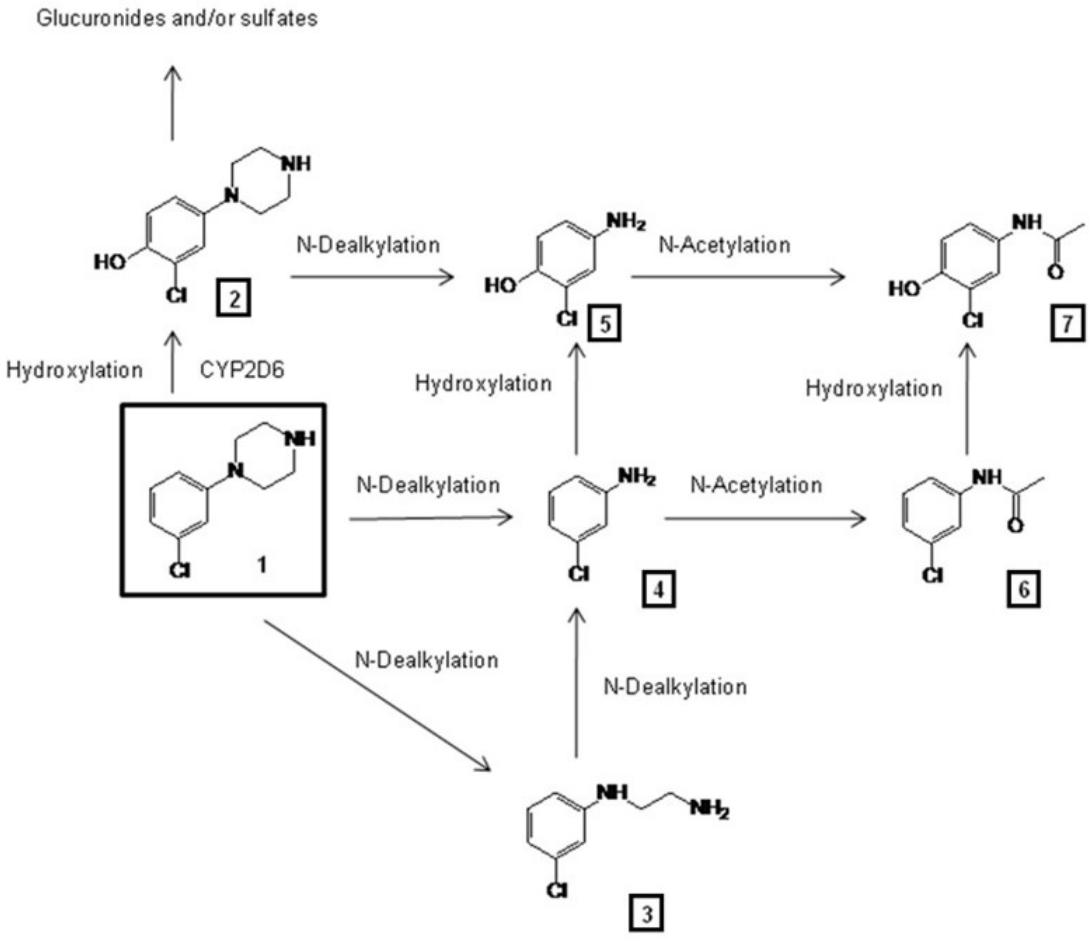

Figure 4. Proposed metabolism of 1-(3-chlorophenyl)piperazine (*m*CPP) in male Sprague-Dawley and Wistar rats. 1 = *m*CPP; 2 = *p*-hydroxy-*m*CPP; 3 = *N*-(3-chlorophenyl)ethylenediamine; 4 = 3-chloroaniline; 5 = 4-hydroxy-3-chloroaniline; 6 = *N*-acetyl-3-chloroaniline; 7= *N*-acetyl-4-hydroxy-3-chloroaniline.

TFMPP is structurally closely related to *m*CPP, with the chloro moiety exchanged by the bioisosteric trifluoromethyl group. The TFMPP metabolism was qualitatively studied in male Wistar rats and the scheme can be visualized in figure 5 (Staack et al., 2003). It was extensively metabolized and almost exclusively excreted as metabolites. The major metabolic reaction was the aromatic hydroxylation to hydroxy-TFMPP (2, in figure 5) followed by partial glucuronidation or sulfation. Degradation of the piperazine heterocycle by double *N*-dealkylation led to the formation of *N*-(3-trifluoromethylphenyl)ethylenediamine (3, in figure 5) or to 3-trifluoromethylaniline (5, in figure 5). The *N*-dealkylation of the hydroxylated TFMPP metabolite led to the formation of *N*-(hydroxy-3-trifluoromethylphenyl)ethylenediamine (4, in figure 5) or to hydroxy-3-trifluoromethylaniline (7, in figure 5). Partial *N*-acetylation was reported for the aniline derivatives (6 and 8, in figure 5) (Staack et al., 2003; Staack and Maurer, 2005).

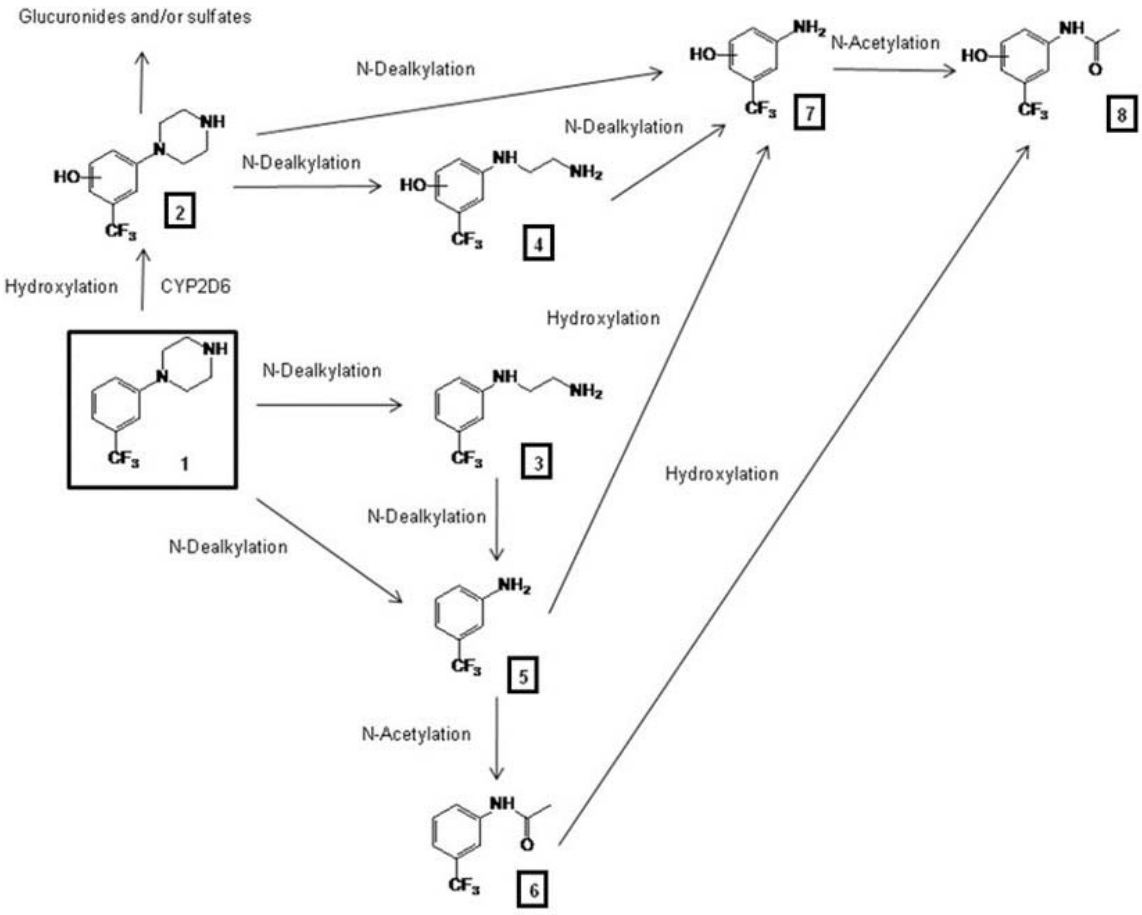

Figure 5. Proposed metabolism of 1-(3-trifluoromethylphenyl)piperazine (TFMPP) in male Wistar rats. 1 = TFMPP; 2 = hydroxy-TFMPP; 3 = N-(3-trifluoromethylphenyl)ethylenediamine; 4 = *N*-(hydroxy-3-trifluoromethylphenyl)ethylenediamine; 5 = 3-trifluoromethylaniline; 6 = *N*-acetyl-3-trifluoromethylaniline; 7 = hidroxy-3-trifluoromethylaniline; 8 = *N*-acetyl-hidroxy-3-trifluoromethylaniline. (Adapted from Staack et al., 2003).

In vivo studies using Wistar rats as extensive metabolizers and female Dark-Agouti rats as poor metabolizers identified CYP2D6 as being responsible for 80.9% of predicted total TFMPP hydroxylation clearance. For the same hydroxylation reaction, CYP1A2 and CYP3A4 were responsible for 11.5% and 7.6%, respectively (Staack et al., 2004a; Maurer et al., 2004).

The metabolism of MeOPP, shown in figure 6, was also qualitatively studied in male Wistar rats (Staack et al., 2004b). As with the other phenylpiperazines, MeOPP was extensively metabolized. *O*-Demethylation of the methoxy moiety was the major metabolic step. The formed hydroxyphenylpiperazine metabolite (2, in figure 6) was subsequently conjugated by partial glucuronidation or sulfation. 4-Methoxyaniline (3, in figure 6) and *N*-(4-methoxyphenyl)ethylenediamine (4, in figure 6) were formed by degradation of the piperazine moiety of MeOPP. 4-Hydroxyaniline (5, in figure 6) could be detected as the piperazine-degraded metabolite of hydroxyphenylpiperazine and it was found to be partially glucuronated or sulfated. Furthermore, it was *N*-acetylated to *N*-acetyl-4-hydroxyaniline (6, in figure 6), which corresponds to the analgesic drug acetaminophen (paracetamol) (Staack et al., 2004b; Staack and Maurer, 2005).

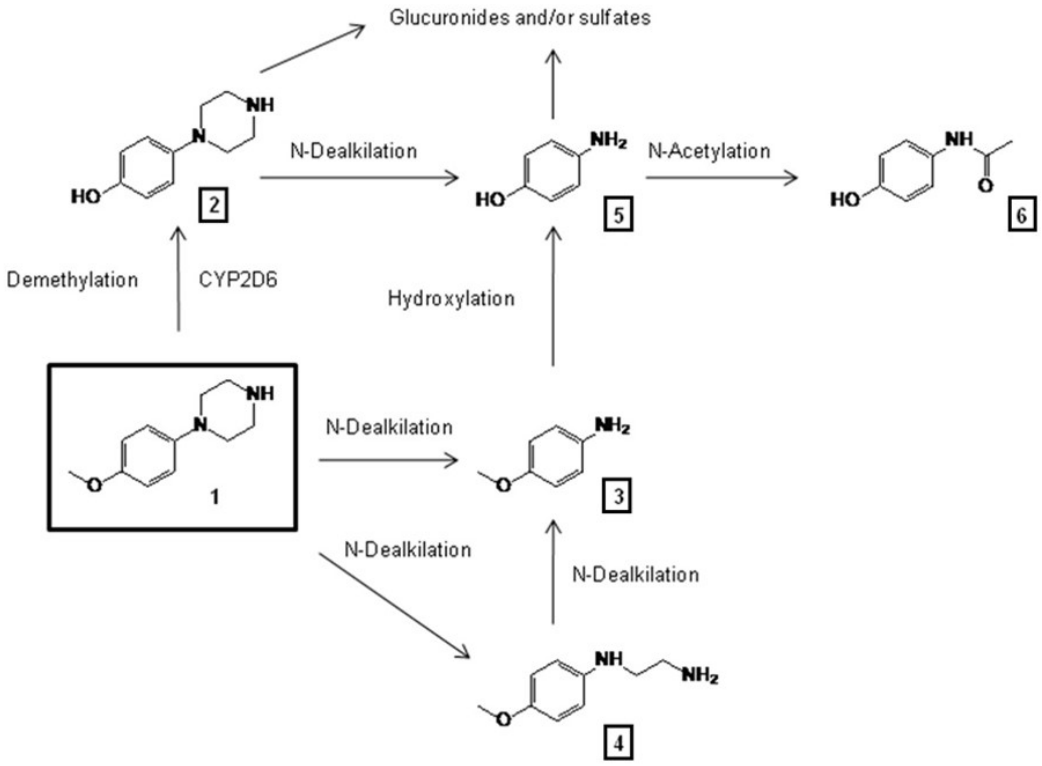

Figure 6. Proposed metabolism of 1-(4-methoxyphenyl)piperazine (MeOPP) in male Wistar rats. 1 = MeOPP; 2 = 4-hydroxyphenylpiperazine; 3 = 4-methoxyaniline; 4 = *N*-(4-methoxyphenyl)ethylenediamine; 5 = 4-hydroxyaniline; 6 = *N*-acetyl-4-hydroxyaniline.

Using baculovirus-infected insect cell microsomes containing human cDNA expressing CYP1A2, CYP2A6, CYP2B6, CYP2C8, CYP2C9, CYP2C19, CYP2D6, CYP2E1 and CYP3A4, Staack et al. (2004b) found that CYP2D6 is the main isoenzyme responsible for catalyzing the demethylation of MeOPP. These results were confirmed through the inhibition of CYP2D6 with quinidine. The metabolite formation rate was also significantly lower in liver microsomes of a single donor with poor CYP2D6 metabolizer genotype in comparison with pooled human liver microsomes (Stack et al., 2004b). Studies using human liver microsomes showed that the metabolism of BZP and TFMPP was significantly inhibited by the inhibitors of CYP2D6, CYP1A2 and CYP3A4. In the same study, it was observed that MDBP, TFMPP, MeOPP and mCPP inhibited CYP2C19. These data highlighted the potencial for interaction between piperazine-designer drugs and other drugs (Antia et al., 2009b).

The kinetics of BZP and TFMPP was studied in Wistar male rats after single or co-administration of a 2 mg/kg dose of each substance by the intraperitoneal route (Wada et al., 2011). The plasma concentrations of BZP administered alone were comparable to those after co-administration, whereas the TFMPP concentrations tended to be higher after co-administration than after individual administration. For single administration of BZP, it was found a 219 min elimination half-life ($t_{1/2}$), distribution volume of 5.1 L and a clearance of 0.017 L/min. For TFMPP single administration, there was a 147 min elimination half-life, distribution volume of 2.0 L and a clearance of 0.009 L/min. In co-administration, TFMPP clearance decreased to 0.005 L/min (Wada et al., 2011). This study corroborates previous *in vitro* findings of metabolic inhibition caused by co-incubation of BZP and TFMPP in human liver microsomes (Antia et al., 2009b).

The kinetics of BZP was studied in healthy male humans after a single oral dose of 200 mg BZP hydrochloride. The peak plasma concentration (C_{max}) was found to be 262 ng/mL, and it was reached 75 min (T_{max}) post-dose. Absorption half-life was calculated to be 6.2 min. The clearance was 58.3 L/h and the $t_{1/2}$ was 5.5 h. For the metabolites 3-hydroxy-BZP and 4-hydroxy-BZP, C_{max} was 13 ng/mL, reached at 75 min post-dose, and 7 ng/mL, at 60 min post-dose, respectively. It was calculated that the total amount of BZP excreted in urine over the 24 h was approximately 12.25% of the dose, being 6% excreted in the unconjugated form. The metabolites were only present at very low concentrations (0.11%). This low recovery of the drug suggests low bioavailability, other routes of excretion, such as biliary excretion, or strong tissue or protein binding (Antia et al., 2009a).

The TFMPP pharmacokinetics was studied in humans after a single oral dose of 60 mg. C_{max} was 24.1 ng/mL, reached 90 min post-dose. The absortion half-life was calculated to be 24.6 min. Apparent clearance was 384.24 L/h. A single metabolite, 4-hydroxy-TFMPP was detected in plasma, with a C_{max} of 20.2 ng/mL, a T_{max} of 90 min and a T_{lag} (time from administration to first quantifiable concentration) of 30 min. The authors demonstrated that there are two distinct disposition phases following C_{max}, indicating a redistribution of the drug into organs such as kidney, liver, and brain. Analyses of urine showed that TFMPP is excreted primarily in its conjugated form, probably as an *N*-glucuronide, accounting for around 70% of the excreted TFMPP. The metabolite 4-hydroxy-TFMPP was also excreted mainly as a conjugate (around 90%), probably as a *N*-glucuronide. The total amount of TFMPP excreted in urine was less than 1% of the dose administered, which, as well as for BZP, also suggests a low bioavailability, other routes of excretion (such as biliary excretion) or strong tissue or protein binding (Antia et al., 2010).

When BZP (100 mg) and TFMPP (30 mg) were co-administered to healthy volunteers, the formation of the metabolites 3-hydroxy-BZP and 4-hydroxy-TFMPP was inhibited. This is thought to be the result of CYP2D6 inhibition which catalyses the hydroxylation of both BZP and TFMPP (Antia et al., 2009c).

The pharmacokinetic profile of *m*CPP was evaluated in healthy volunteers (8 women and 6 men) who received an oral dosage of 0.5 mg/kg or an intravenous dose of 0.1 mg/kg. Oral *m*CPP presented an absorption half-life of 60 min, 54 ng/mL C_{max} in a 3.2 h T_{max}. The $t_{1/2}$ was 4.3 h with a bioavailability of 47.5%. After intravenous injection, C_{max} was 52 ng/mL reached at 18.6 min post-dose. The $t_{1/2}$ was 5.8 h and the clearance was 49.6 mL/h (Gijsman et al., 1998).

1.4. Clinical studies

Wilkins and collegues (2008) conducted a survey in New Zealand about patterns of uses and side effects of BZP/TFMPP party pills that included 2010 participants. The users were characterized as being mainly male (60%), from European origin (75%), and with mean age of 23 years. The majority of consumers (89%) used party pills in combination with other drugs such as alcohol (91%), tobacco (37%), and cannabis (21%). The most reported adverse physical symptoms were insomnia (54%), headaches (26%) and nausea (21%). Among the most reported psychological symptoms were short temper

(12%), confusion (11%), anxiety (10%), depression (10%), paranoia (9%) and auditory hallucinations (9%) (Wilkins et al., 2008).

In humans, common experienced symptoms after BZP intake include anxiety, vomiting, headache, palpitations, confusion, collapse, and seizures (Gee et al, 2005). Some symptoms persisted for up to 24 hours after ingestion. Vital signs showed expected sympathomimetic effects in patients with tachycardia and hypertension. Physiological effects of BZP were not felt for up to 2 hours after oral ingestion. To experience a faster onset of action, some users have injected BZP intravenously, although this is reported as being painful due to the alkalinity of the solution (raw BZP in solution has a pH≥12) (Gee et al., 2005). The cardiovascular effects are, to some extent, predictable. Drugs acting on serotonergic, dopaminergic, or noradrenergic systems are likely to induce vasoconstriction and/or tachycardia and arrhythmia (Dawson and Moffatt, 2012).

A study was performed with 27 adult women, divided in two groups, who received a single oral dose of 200 mg BZP (n=14) or placebo (n=13) and were submitted to physiological and mood measures. After 120 minutes of dosing, it was observed a significant increase in systolic and diastolic pressures and heart rate and a decrease in body temperature in BZP group. BZP was associated with a significant decrease in fatigue. The BZP group also reported feeling more vigorous and/or active by the end of the study (Lin et al., 2009). The physiological results were already expected, since in the periferic nervous system the actions of BZP are mediated by α2-adrenoceptors, which are related to reflex tachycardia and hypertension (Gee et al., 2005).

A survey was conducted at the Christchurch Hospital (Christchurch, New Zealand) with 184 patients presented at the Emergency Department with possible BZP poisoning (Gee et al., 2008). Ninety-six patients had plasma BZP levels measured on admission, ranging from 0 up to 6.29 μg/mL (mean 0.68 μg/mL). Logistic regression using plasma BZP levels versus incidence of seizures revealed a trend towards higher levels of BZP being associated with seizures. Furthermore, 53.4% of the patients admitted to take BZP pills together with alcohol. However, a positive correlation between seizures and co-ingestion of BZP and alcohol was not found (Gee et al., 2008).

The effects of BZP combined with TFMPP were investigated in adult men after an oral dose of 100 mg BZP and 30 mg TFMPP. BZP/TFMPP administration produced a significant increase in systolic and diastolic blood pressure and heart rate. Also, it was found an increase in vigour/activity, ‘dysphoria’ and ‘dexamphetamine-like effects’ through

subjective like scales completed by the participants before and 120 min after drug administration (Lin et al., 2011).

A study with 35 volunteers was performed to evaluate the effects of BZP/TFMPP association in party pills alone and in combination with alcohol (Thompson et al., 2010). The volunteers were divided into groups which received (i) double placebo, (ii) 300 mg BZP/74 mg TFMPP and alcohol placebo, (iii) placebo capsules and 57.6 g (6 units) of alcohol and (iv) 300 mg BZP/74 mg TFMPP and 57.6 g (6 units) of alcohol. Measures were taken between 3 and 6 h and 7 days after dosing. Blood levels of BZP and TFMPP peaked at 6.5 h with mean values of 585 and 41 ng/mL, respectively. Interestingly, BZP/TFMPP party pills alone significantly improved driving performance, by means of decreasing the standard deviation of the lateral position test. BZP/TFMPP also resulted in increased heart rate and blood pressure and in difficulty in getting to sleep. Nevertheless, BZP/TFMPP alone or with alcohol were accompanied by an increase in severe adverse events, such as agitation, anxiety, hallucinations, vomiting, insomnia and migraine, presented by 4 of 10 subjects in the BZP/TFMPP group and three of seven in the BZP/TFMPP combined with alcohol group. This led to the interruption of the study before getting a planned sample of 64 subjects (Thompson et al., 2010).

A randomized, double-blind, placebo-controlled study was conducted with 30 volunteer men to investigate the effects of TFMPP in human information processing. Before and 2 h after taking 60 mg TFMPP orally, the participants were tested using electroencephalogram acquisition. The treatment reduced the interhemispheric transfer time but did not affect reaction time, suggesting that TFMPP may affect neurotransmitter systems involved in speeding of interhemispheric communication, such as glutamatergic, serotonergic, gabaergic and dopaminergic pathway (Lee et al., 2011).

In a study with 14 healthy volunteers (8 women and 6 men) who received an oral dosage of 0.5 mg/kg or an intravenous dose of 0.1 mg/kg of *m*CPP, it was observed a significant increase in heart rate and body temperature as well as an increase in plasma prolactin and cortisol. The stimulating effect of *m*CPP was confirmed through an electroencephalographic reading (Gijsman et al., 1998). In another study conducted by Feuchtl et al. (2004) with 12 healthy men, after intravenous and oral *m*CPP administration it was observed a significant increase in clinical response (anxiety, shivering, dizziness, heightened sensitivity toward light and noise, and fear of losing control). Also, there was an increase in plasma ACTH, cortisol and prolactin levels compared to placebo (Feuchtl et al., 2004). In a trial with 15 patients with depressed mood, the treatment with a single oral

dose of 0.5 mg/kg *m*CPP also demonstrated a significant increase in plasma ACTH, cortisol and prolactin (Klaassen et al., 2002).

1.5. Case reports

The case-reports of documented piperazine-related intoxications are summarized in table 2.

There is a case report of a male young adult who attended a party and ingested four tablets of a substance called Rapture (containing BZP). Twelve hours after the ingestion, he developed an acute psychotic episode associated with intense persecutory delusional beliefs and auditory and visual hallucinations. The symptoms completely abated within 48 h, with only benzodiazepines treatment (Austin and Monasterio, 2004).

A case of nephrotoxicity was reported in a 17 year-old man who ingested five BZP-based herbal party pills and a small amount of alcohol. After a few hours he started to have bilateral loin pain, which gradually increased in the next day. After 36 h, he was admitted to a hospital because of the severity of the abdominal pain. He was found to have renal impairment with a serum creatinine level of 220 µmol/L, which increased to 320 µmol/L, 440 µmol/L and peaked at 778 µmol/L in the following days (reference value of serum creatinine in man: 80-115 µmol/L). He was dialysed once and three weeks after admission his serum creatinine had returned to 92 µmol/L. Although BZP intake confirmation was not done, the authors postulate that the acute renal failure observed may be related to a direct toxic effect of the party pills on the kidneys (Alansari and Hamilton, 2006).

Nephrotoxic symptoms were also reported by a 38 year-old man with a 4 day history of constant bilateral flank pain radiating to the midline and groin, nausea and vomiting. No fever or urinary symptoms were reported. The patient had taken two tablets of BZP one week prior to admission and had also smoked cannabis. He had been taking BZP for about a year, initially one to two times a week and more recently only every 2-3 weeks. Past medical history included long-standing depression, with regular intake of 20 mg fluoxetine for over 10 years. At the admission, the patient was afebrile and in pain, with blood pressure 140/80 mmHg. Abdominal examination demonstrated bilateral renal angle tenderness only. Urinalysis demonstrated microscopic haematuria, sterile pyuria and proteinuria. Biochemistry demonstrated acute kidney injury with a serum creatinine 200 µmol/L. Creatine kinase was 307 U/L (reference value of serum creatine kinase in

man is <200 U/L). A computed tomography urogram demonstrated two normal-sized kidneys with no evidence of renal calculi. After 48 h, renal function continued to decline. A renal biopsy was performed, pointing to interstitial nephritis. Electron microscopy showed swollen and convoluted epithelial cells pushing into urinary spaces. Management consisted of simple analgesia and i.v. rehydration. Renal function improved over the following 72 h (Berner-Meyer et al., 2012).

Another case of nephrotoxicity was reported for a 22 year-old man with 2 days of constant bilateral flank pain radiating to the groin. There was an associated fever but no urinary symptoms. The patient had been using cannabis oil regularly and had recently experimented it with BZP 3-4 days prior to admission. At presentation, he was febrile (38°C) and in pain. Blood pressure was 124/62 mmHg. Abdominal examination demonstrated bilateral renal angle tenderness only. Urinalysis revealed microscopic haematuria, sterile pyuria, proteinuria and no glycosuria. Biochemistry demonstrated acute kidney injury with a serum creatinine of 210 μmol/L. Renal function kept declining reaching a peak of 280 μmol/L. Renal biopsy demonstrated a mild mesangioproliferative glomerulonephritis. Due to the continuing renal flank pain and renal function deterioration, the patient was treated with corticosteroids with a rapid resolution of renal failure (Berner-Meyer et al., 2012).

In another case, 3 young male adults ingested 4 tablets of a drug thought to be Ecstasy and presented dissociative symptoms, agitation with bruxism, nausea and features of sympathomimetic toxicity, with dilated pupils and tachycardia. Toxicological screening of blood and urine of the patients revealed the presence of BZP and TFMPP. Although the dissociative symptoms are not typical of previous reports of BZP toxicity, it is likely that the cause of these symptoms was the combination of both, TFMPP and BZP drugs (Wood et al., 2008).

In New Zealand, it was reported a case of an adult female, with history of schizophrenia and substance abuse, who developed status epilepticus, hyperthermia, disseminated intravascular coagulation, rhabdomyolysis, and renal failure after BZP intake (Gee et al., 2010). In another case, the patient presented similar symptoms, however there was an association of BZP and MDMA. In spite of the serious adverse effects presented, after 30 and 25 days of hospitalization, respectively, the patients were discharged (Gee et al., 2010).

In a non-fatal case of overdose by *m*CPP, a female patient developed anxiety, agitation, drowsiness, flushing, visual disturbances and tachycardia. The *m*CPP

concentration was 320 ng/mL in plasma and 2300 ng/mL in urine. However, amphetamine, benzoilecgonine and alcohol were also detected in small quantities in plasma (Kovaleva et al., 2008).

A fatal case of a 23 year-old woman who ingested BZP and MDMA was described. She was admitted at the hospital with bradycardia, hypertension and reduced consciousness. The pacient died 57 h after admission with massive brain oedema (Balmelli et al., 2001). Another fatal case, in which BZP contributed to the death, was occured in Sweden. The victim was a man who had been taking ecstasy and A2 (containing BZP). For forensic analysis, a femoral blood sample was collected and screened for amphetamines with a positive result. Confirmatory analysis found 1.7 µg BZP/g blood, and also detected MDMA, methylenedioxyamphetamine (MDA) and tetrahydrocannabinol in the blood sample (Wikström et al., 2004).

A fatal case of a 20 year-old man with allergic asthma was reported. The medical history also included a posttraumatic pneumothorax. He was a regular user of ecstasy and cocaine, and in the late morning of the day of his death, he had taken half a scored “ecstasy” tablet. It was a white tablet, stamped with a “smiling sun” logo. In the afternoon his condition worsened. When he had a serious asthma attack, his mother gave him 2 tablets of 20 mg prednisone. As the corticosteroid did not have the desired effect and the attack had lasted over an hour, the patient was taken to the hospital. Upon the arrival at the emergency, he showed tachycardia (123 beats/min), his blood pressure was 160/90 mmHg, and the oxygen saturation was 90%. Auscultation revelead expiratory dyspnea with tachypnea, sibilant wheezing, and a symmetrical vesicular murmur. The patient condition worsered drastically, with agitation, diminished left vesicular murmur, and cardiorespiratory arrest, despite treatment with salbutamol aerosol. The patient was taken into intensive care, despite the intensive resuscitation attempts, with intubation and ventilation, external cardiac massage, the administration of vasopressive amines, external electric shocks and a total of 5 mg adrenaline, 120 mg methylprednisolone, 2 mg atropine, intravenous salbutamol, magnesium sulfate and sedation with midazolam and fentanyl, no cardiac activity reappeared and the patient was pronounced dead. Analysis of a tablet similar in appearance seized from the dealer by the police revealed the presence of 5.4 mg metoclopramide and 45.8 mg *m*CPP. After the autopsy, analysis of biological fluids (hepatic blood and urine) showed the presence of metabolites of cocaine (benzoylecgonine and ecgonine methyl ester), metoclopramide and therapeutic concentrations of the drugs used at the hospital. *m*CPP was found in urine (15 ng/mL), bile (5.1 ng/mL), liver (0.3 ng/g) and humor vitreous (4.7 ng/mL). Hair analysis showed

chronic MDMA use. As no trace of *m*CPP was detected in hair samples, a hypothesis of first use was put forward (Gaillard et al., 2013).

Table 2. Summary of case-reports of piperazine designer drugs.

Piperazine	Street name	Age	Sex	Amount ingested	Symptoms	Toxicological screening	Reference
BZP	A2	23	F		bradicardia, hypertension, reduced consciousness and death by brain oedema	BZP and MDMA	Balmelli et al., 2001
BZP	Rapture	20	M	4 tablets	acute psychotic episode and auditory and visual hallucinations	BZP	Austin and Monasterio, 2004
BZP	A2		M			BZP (1.7 µg/g blood), MDMA, MDA, tetrahydrocannabinol	Wikström et al., 2004
	"Party-pills"	17	M	5 tablets	bilateral loin pain "renal impairment"		Alansari and Hamilton, 2006
mCPP		29	F	3 tablets	agitation, visual hallucinations, tachycardia	mCPP (320ng/mL in plasma and 2300ng/mL in urine), alcohol (0.7 g/L), amphetamine (40ng/mL), benzoylecgonine (47ng/mL)	Kovaleva et al., 2008
BZP/TFMPP	Ecstasy	18	M	4 tablets	nausea, dissociative symptoms, agitation, bruxism, tachicardia	BZP (260-270ng/mL in serum), TFMPP (30-60ng/mL in serum)	Wood et al., 2008
	Ecstasy	18	M				
	Ecstasy	19	M				

BZP		19	F		generalized tonic clonic activity, tachycardia, hyperthermia, tachypnea	BZP (0.2mg/L in plasma), metabolites of benztropine, caffeine and nicotine	Gee et al., 2010
BZP	"Party-pills"	22	M	3-4 tablets	hyperthermia, tachycardia, muscle rigidity, hypotension, coma	BZP (2.23mg/L in plasma), MDMA (1.05mg/L)	Gee et al., 2010
BZP		38	M	2 tablets	constant bilateral flank pain, nausea and vomiting		Berney-Meyer et al., 2012
BZP		22	M		constant bilateral flank pain, fever		Berney-Meyer et al., 2012
*m*CPP	Ecstasy	20	M	½ tablet	tachycardia, hypertension, dyspnea with tachypnea, sibilant wheezing and simetrical vesicular murmur	mCPP (15 ng/mL in urine; 5.1 ng/mL in bile; 4.7 ng/mL in humor vitreous, 0.3 ng/g of liver), metoclopramide and metabolites of cocaine in biological fluids and MDMA in hair	Gaillard et al., 2013

1.6. Analysis

There are several techniques used to detect and/or quantify piperazine designer drugs, from colorimetric tests to chromatographic analysis in different matrices.

1.6.1. Colorimetric tests

Colorimetric reactions are used for screening or preliminary identification of seized materials and residues extracted from biological samples. Colorimetric reagents that react with nitrogen are usually used for detection tests (Namera et al., 2011). An isomer of chlorophenylpiperazine (CPP) was identified in seized tablets using different strategies. Tablets were submitted to three common preliminary colorimetric tests, used to identify alkaloids (Marquis test), cocaine and derivatives (Scott test) and methamphetamines (Simons test). There is no specific colour test for piperazines derivatives. CPP presented no colour in the Marquis test, blue colour in the Scott test, and orange colour (untill 30s) and dark brown colour (after 2 min) in the Simons test (Lanaro et al., 2010).

1.6.2. Immunoassays

When piperazine designer drugs are analyzed by the current available test for the detection of amphetamines, false positive results may occur. In order to evaluate a broad range of clinical and forensic toxicological techniques, BZP was analyzed in two different amphetamine-like immunoassays. BZP presented cross reactivity at 300 and 12,000 ng/mL in enzyme-multiple immunoassay technique (EMIT®) d.a.u.® Amphetamines system but was not detected by fluorescence polarization immunoassay (FPIA) using AxSYM® Amphetamine/Methamphetamine assay (de Boer et al., 2001). Indeed, false positive results for amphetamine compounds analyzed through EMIT® probably occur due to the formation of primary amines (Domingos et al., 2008), which are products of BZP biotransformation. Besides BZP and the product of its biotransformation *N*-benzylethylenediamine, also TFMPP presents crossreactivity with amphetamines. Presently, there are no commercially available immunoassay tests for detection of piperazine derivatives (Peters et al., 2010).

1.6.3. Chromatography

Chromatographic methods are commonly used to identify and quantify designer drugs. The chromatographic methods described for the analysis of piperazine designer drugs are summarized in table 3.

Table 3. Summary of instrumental chromatographic analysis of piperazine designer drugs.

Method	Chromatographic Conditions	Matrix	Pre-treatment	Derivatization	Piperazine-derivatives	Reference
HPLC/UV	Ultrasphere ODS C18 (150 mm x 4.6 mm x 5 µm), gradient of acetonitrile and 40 mM acetate buffer (pH 4.5) at 1.5 mL/min flow rate	capsules or tablets			BZP and TFMPP	Young et al., 2013
HPLC/DAD	LiChrospher 60 RP Select B column (250 mm x 5 mm x 50 µm) at 30°C, isocratic mode, mobile phase of acetonitrile and phosphate buffer 0.02 M (pH 2; 36:64, w/w) at 0.9 mL/min flow rate	plasma	liquid-liquid extraction with 1-chlorbutan		*m*CPP	Staack et al., 2007
HPLC/DAD	L-column ODS (4.6 x 150 mm; 5 µm), gradient of SDS 10 mM in acetonitrile/water/phosphoric acid (300:700:1) and SDS 10 mM in actonitrile/water/phosphoric acid (700:300:1), at 1.0 mL/min flow rate	capsules and tablets			BZP, *m*CPP, MeOPP and MDBP	Takahashi et al., 2009
HPLC/DAD	Zorbax Eclipse column (4.6 x 150 mm; 5 µm) at 30°C, gradient of phosphoric acid 10mM (pH 3.0) and acetonitrile at 1.0 mL/min flow rate	tablets			*m*CPP, *o*CPP, *p*CPP	Lanaro et al., 2010

HPLC/FD	Daisopak-SP-ODS-BP column (250 x 4.6 mm, 5 µm), gradient of acetate buffer 0.1 M (pH 3.5) and acetonitrile at 1.0 mL/min flow rate, column at 35°C, λ_{ex} 340 nm and λ_{em} 445nm	rat plasma	SPE	DIB-Cl at room temperature for 30 min	BZP, TFMPP and hydroxylated metabolites	Wada et al., 2011
HPLC/CD	Chromolith SpeedROD RP-18 column, 2 mL/min flow rate	tablets		$[Ru(bipy)_3]^{3+}$	BZP, TFMPP, MeOPP, *m*CPP and others	Waite et al., 2013
HPLC/ESI-MS	SCX column (2.0 mm x 150 mm), mobile phase of ammonium acetate buffer 40 mM (pH 4)/acetonitrile (25:75, v/v) at 0.15 mL/min	urine	enzimatic hydrolysis, liquid-liquid extraction at pH 9 with chloroform/2-propanol (3:1, v/v), SPE	TFA:ethylacetate (1:1, v/v), 60°C, 1h	BZP, TFMPP and hydroxylated metabolites	Tsutsumi et al., 2005
HPLC/ESI-MS	Synergi™ Polar-RP C18 column (150 x 2.0 mm; 4 mm) at 35°C, gradient elution of 0.1% formic acid/acetonitrile at 0.4 mL/min flow rate	urine			BZP and TFMPP	Vorce et al., 2008
HPLC/ESI-MS	C18 Agilent Zorbax column (150 mm x 4,6 mm, 5 µm), gradient of ammonium formate buffer 0.01 M (pH 4.5) and acetonitrile at 20°C	plasma and urine	deproteinization of plasma with $ZnSO_4$ and enzymatic hydrolysis of urine		BZP, TFMPP and hydroxylated metabolites	Antia et al., 2010

HPLC/MS/MS	Synergi Polar RP column (150 mm x 2 mm x 4 µm) at 40°C, gradient elution of ammonium formate 1 mM/formic acid 0.1% and methanol/formic acid 0.1% at 0.25 mL/min flow rate	plasma	SPE		BZP, TFMPP, *m*CPP, MeOPP and MDBP	Wohlfarth et al., 2010
HPLC/MS/MS	Hypersil Gold C18 column (100 mm x 2.1 mm x 3 µM) at 35°C, gradient elution mode of 95% formate buffer and 5% acetonitrile at 0.25 mL/min flow rate	Tablets, biological fluids and hair	Liquis-liquid extraction in Toxi-Tube A® (Varian)		*o*CPP, *m*CPP, *p*CPP	Gaillard et al., 2013
HPLC/MS/MS	Gemini C18 column (10 cm x 2 mm x 3 µm), gradient mode with acetonitrile and 30 mM acetate buffer pH 4.5 at a 0.4 mL/min flow-rate and 1:4 split	urine	SPE		TFMPP, MeOPP, MDBP, *p*FPP, *p*CPP	Montesano et al., 2013
UPLC/IT-MS	Kintex PFP column (50 mm x 2.1 mm x 1.8 µm), gradient mode with 2 mM ammonium formate/formic acid 2% and acetonitrile/formic acid 0.1% at 0.5 mL/min flow rate	urine, plasma and whole blood	SPE		BZP and TFMPP	Johnson and Botch-Jones, 2013
GC/NPD	HP-5MS column (14 m x 0.25 mm x 0.25 µm), injection temperature of 250°C, helium at 1.0 mL/min	capsules	liquid-liquid extraction with *tert*-butyl methyl ether		BZP, TFMPP, MeOPP	de Boer et al., 2001
GC/MS	HP-5MS column (19 m x 0.25 mm x 0.25 µm), injector at 270°C and transferline at 300°C, helium at a flow rate of 1.0 mL/min	capsules	liquid-liquid extraction with *tert*-butyl methyl ether	TFAA and ethyl acetate (1:1, v/v) , 30 min at 65°C	BZP, TFMPP, MeOPP	de Boer et al., 2001
GC/MS	HP-5MS column (30 m x 0.25 mm x 0.25 µm), injection temperature 280°C, helium at 0.6 mL/min, splitless mode	plasma	SPE	HFBA under microwave irradiation (440 V, 5 min)	BZP, TFMPP, *m*CPP, MeOPP and MDBP	Peters et al., 2003

GC/MS	HP-5MS column (30 m x 0.25 mm x 0.25 µm), helium at 0.9 mL/min, splitless mode	blood and urine	liquid-liquid extraction with ethylacetate (blood) and isooctane (urine)	TFAA, 60°C, 15 min	BZP	Wikström et al., 2004
GC/MS	DB-5MS column (30 m x 0.25 mm; 0.25 µm), injection temperature of 270°C in splitless mode, transferline at 250°C, helium at 1.0 mL/min, source temperature of 200°C	urine	enzimatic hydrolysis, liquid-liquid extraction at pH 9 with chloroform/2-propanol (3:1, v/v), SPE	TFA:ethylacetate (1:1, v/v), 60°C, 1h	BZP, TFMPP and hydroxylated metabolites	Tsutsumi et al., 2005
GC/MS	VF-5MS column (30 m x 0.25 mm x 0.25 µm), injector at 280°C in splitless mode, helium flow rate at 1.0 mL/min, transferline at 280°C and ion source at 230°C	urine	acidic hydrolysis and liquid-liquid extraction at pH 8-9 with dichloromethane/isopropanol/ ethyl acetate (1:1:3, v/v/v)	acetic anhydride/pyridine (3:2, v/v) for 5 min under microwase irradiation at 440 W	*m*CPP	Staack et al., 2007
GC/MS	DB-5MS column (20 m x 0.18 mm), helium at 1.0 mL/min, initial oven temperature at 70°C, transferline at 280°C and source at 230°C, split mode (10:1)	urine	SPE		BZP and TFMPP	Vorce et al., 2008
GC/MS	DB-5MS column ODS (30 m x 0.25 mm x 0.25 µm), helium flow rate of 1.1 mL/min, injector temperature 250°C, splitless mode, transferline 290°C	capsules and tablets			BZP, *m*CPP, MeOPP and MDBP	Takahashi et al., 2009

GC/MS	HP-5MS column (30 m x 0.25 mm x 0.25 µm) injector at 220°C, detector at 280°C, oven 90°C for 2 min, increased by 15°C/min to 300°C helium flow rate of 0.8 mL/min	hair	wash with dichloromethane, deionised water and methanol, SPE	MSTFA with 5% TMS at 80°C for 30 min	TFMPP, *m*CPP and MeOPP	Barroso et al., 2010

Abbreviations: HPLC (high performance liquid chromatography), UPLC (ultra-high performance liquid chromatography), GC (gas chromatography), UV (ultraviolet detector), DAD (diode array detector), FD (fluorescence detector), CD (chemioluminescence detector), ESI-MS (electrospray ionization mass spectrometry), MS/MS (tandem mass spectrometry), IT-MS (ion trap mass spectrometer), NPD (nitrogen-phosphorus detector), DIB-Cl (4-(4,5-diphenyl-1-*H*-imidazol-2-yl)benzoyl chloride), $[Ru(bipy)_3]^{3+}$ (tris(2,2'-bipyridine)ruthenium(III)), $ZnSO_4$ (zinc sulfate).

1.6.3.1. Planar chromatography

Due to its simplicity and low cost, thin-layer chromatography (TLC) is widely used for detection of drugs of abuse. For an isomer of CPP, TLC was performed in three different solvent systems using iodoplatinate and Dragendorff´s reagents. CPP presented Rf values of 0.32 in methanol:ammonia (100:1.5; v/v), 0.58 in cyclohexane:toluene:diethylamine (75:15:10; v/v) and 0.21 in chloroform:acetone (4:1; v/v) (Lanaro et al., 2010).

1.6.3.2. Column chromatography

Lanaro and co-works tried to use a HPLC with diode array detector (DAD) method to identify the CPP isomers in tablets. The CPP presented a retention time of 7.4 min between 215 and 236 nm. The UV/Vis spectra presented a significative absortion at 208 and 248 nm, however the corresponding isomer of CPP (*ortho*-, *meta*-, or *para*-) could not be identified (Lanaro et al., 2010).

HPLC/UV analysis was performed in capsules through the REMEDi™ HS Drug Profiling System. Although BZP was not part of the standard library and therefore not identified, the system indicated some candidate drugs for the peak observed, namely the cyclic derivative of dinorpropoxyphene, 4-hydroxyphencyclidine, alphaprodine and phencyclidine itself. When analyzed by gas chromatography (GC) with a nitrogen phosphorous detector (NPD), BZP, TFMPP and MeOPP showed prominent peaks with good response factors as expected from molecules with two nitrogens. The GC mass spectrometry (MS) analyses of BZP, TFMPP and MeOPP was performed before and after acetylation and trifluoroacetylation. The analysis of non-derivatized piperazines was difficult due to the asymmetric peak shapes and tailing. Acetylation seemed to stabilize the piperazine ring, resulting in more stable ions and more characteristic mass spectra. The *N*-trifluoroacetyl derivatives showed to be even more stable than the *N*-acetyl derivatives however, the derivatization of MeOPP resulted in two different bis-*N*-trifluoroacetyl derivatives instead of one mono-*N*-trifluoroacetyl derivative (de Boer et al., 2001).

A GC/MS method was validated for screening of amphetamine and piperazine derivatives (including BZP, TFMPP, *m*CPP, MeOPP and MDBP) in human blood plasma (Peters et al., 2003). Tsutsumi et al. (2005) developed a GC/MS and a HPLC with electrospray ionization and mass spectrometry (ESI-MS) methods for determination of BZP, TFMPP and their main hydroxylated metabolites in urine. The authors concluded that both methods were sensitive, however, the derivatization process for GC/MS

presented a low reproducibility for the hydroxylated metabolites while the HPLC/ESI-MS allowed accurate quantitation (Tsutsumi et al., 2005).

A GC/MS method for forensic purposes was described by Wikström et al. (2004). The method applied liquid-liquid extraction in urine and blood samples, and a derivatization step with trifluoroacetic acid anhydride (TFAA). It was used a SIM analysis with m/z 181, corresponding to the trifluoroacetylpiperazine, as quantifier ion. The method was applied in 56 individual cases from southern Sweden, including prison cases, autopsies, drug abusers, traffic drivers and treatment care. This confirmatory analysis also differentiate BZP from 10 amphetamine analogues, including amphetamine, metamphetamine, phenmetrazine, ephredrine, norephedrine, 3,4-methylenedioxyamphetamine (MDA), MDMA, 3,4-methylenedioxyethylamphetamine (MDEA), *N*-methyl-1-(3,4-methylenedioxyphenyl)-2-butanamine (MBDB) and phentermine (Wikström et al., 2004).

Urine of seven U.S. service members was submitted to immunoassay and GC/MS screening, after solid phase extraction (SPE) and without previous derivatization (Vorce et al., 2008). BZP and TFMPP were identified. For quantitation by HLPC-ESI/MS, the ions m/z 91, 177 (MH+), and 178 were selected for the SIM monitoring for BZP and m/z 188, 231 (MH+), and 232 for TFMPP. *m*CPP was used as internal standard with monitoring m/z 154 and 197 (MH+) ions. The MH+ ion was used for quantitation (Vorce et al., 2008). BZP and TFMPP were also detected in postmortem blood through HPLC/UV in three fatalities (road traffic deaths and a fatal fall). However, in these cases BZP and TFMPP were not the direct cause of death. In all cases, other drugs and/or ethanol were found. BZP was found at concentrations of 0.71, <0.50, and 1.39 mg/L and TFMPP was found at concentrations of 0.05 and 0.15 mg/L (Elliott and Smith, 2008). Antia et al. (2010) validated a method by HPLC/MS for quantification of BZP, TFMPP and the metabolites 3-hydrozy-BZP, 4-hydroxy-BZP and 4-hydroxy-TFMPP in plasma and urine samples. Using human hair as biological matrice, TFMPP, *m*CPP and MeOPP were analyzed by GC/MS as trimethylsilyl derivatives (Barroso et al., 2010).

A HPLC with atmospheric pressure ionization mass spectrometry (API/MS) method was proposed for the determination of hallucinogenic designer drugs in urine of users, which included *m*CPP (Pichini et al., 2008). In another method, the isomers *o*CPP, *m*CPP and *p*CPP were differentiated by retention time and the *m*CPP could be identified and quantified by a HPLC MS/MS method in tablets, biological fluids and hair (Gaillard et al., 2013). A HPLC/MS method for screening of MDA and piperazine-derived designer

drugs in urine was validated. The method appeared to be suitable for identification of designer drugs and could also provide semi-quantitative data (Montesano et al., 2013).

A psychoactive drugs data library was developed in order to quickly confirm the presence of a potentially hazardous designer drug. Data in this library is based on capacity factor (k') ratio of each drug with the internal standard, the UV spectrum and the MS data, after HPLC/DAD and GC/MS analysis. The piperazinic compounds include BZP, *m*CPP, MeOPP and MDBP. Surprisingly, TFMPP was used as internal standard (Takahashi et al., 2009). An extensive HPLC/MS/MS screening method was also proposed for identification of several amphetamines, tryptamines and piperazines in serum (Wohlfarth et al., 2010). BZP and TFMPP were identified in plasma of rats after derivatization with 4-(4,5-diphenyl-1-H-imidazol-2-yl)benzoyl chloride (DIB-Cl), a fluorescence labeling reagent, by HPLC-fluorescence detection (FD) (Wada et al., 2011). Chemiluminescence detection (CD) was also applied in the determination of piperazines in party pills, after a chromatographic separation. The method explored the chemiluminescent reaction of benzyl and phenylpiperazines with tris(2,2'-bipyridine)ruthenium(III) (Waite et al., 2013).

The stability of BZP and TFMPP in biological matrices for up to 14 days were evaluated (whole blood, plasma and urine) through ultrahigh performance liquid chromatography (UPLC) coupled to triple quadrupole ion trap mass spectrometer (IT-MS). Three conditions were tested, which includes storage at -20°C (freezer), 4°C (refrigerator) and 22°C (room temperature). Samples proved to be relatively stable except for whole blood and plasma samples at room temperature (Johnson and Botch-Jones, 2013).

1.6.4. Capillary electrophoresis (CE)

A method based on a chiral capillary electrophoresis (CE) separation was optimized for analysis of amphetamine and piperazine designer drugs in tablets (Bishop et al., 2005). CE was also successfully applied on the analysis of 17 confiscated pills in Brazil. The method allowed the separation of the three CPP isomers (*o*CPP, *m*CPP and *p*CPP) and identified *m*CPP as the main ingredient in such pills (Široká et al., 2013).

1.7. Intoxication and treatment

At low doses, the effects of BZP (50 – 100 mg) and TFMPP (5 – 25 mg) tend to be mild, producing feelings of euphoria and wakefulness. Ingestion of high doses of piperazine derivatives results in symptoms similar to sympathomimetic toxicity. Most common symptoms include insomnia, headaches, nausea, anxiety, depression, paranoia and auditory hallucinations. At high doses, patients may experience palpitations, tachycardia, hypertension and hyperthermia. Neurological effects at high doses can include tremors, myoclonus and seizures (Schep et al., 2011). Renal manifestations are generally considered a consequence of sympathomimetic toxicity. However, severe toxicity may cause prolonged seizures and hyperthermia that can lead to rhabdomyolysis and acute tubular necrosis (Luciano & Perazella, 2014).

Patients with seizure disorders, psychiatric illness or coronary disease should avoid BZP as should those taking prescribed sympathomimetics or anticholinergics. Coingestion with MDMA or amphetamine should also be cautioned against, as this combination could lead to fatal toxicity (Gee et al., 2005).

When patients present to healthcare facilities with BZP toxicity, an electrocardiogram and an estimation of plasma sodium should be done. Those with moderate to severe toxicity may require treatment with benzodiazepines, intravenous fluids, and antiemetics (Gee et al, 2005). The efficacy of gastric lavage and activated charcoal following piperazine designer drugs ingestion has not been assessed formally but is unlikely to be of clinical importance in patients presenting more than 1 h after ingestion (Schep et al., 2011). These patients should be observed for 6-8 h post-BZP ingestion in case of delayed seizures. Seizures should be treated with benzodiazepines and airway management. Barbiturates may be required in status epilepticus (Gee et al., 2005). Antipsychotics have not usually been recommended as first line agents for the control of agitation as they may interfere with thermoregulation, precipitate extrapyramidal side-effects including dystonic reactions, or induce cardiac dysrhythmias or hypotension (Schep et al., 2011).

If control of blood pressure is required, intravenous isosorbide dinitrate, nitroglycerine, α-adrenergic blocking agents or sodium nitroprusside should be administered until blood pressure elevation is controlled. Clonidine has also been used successfully to control blood pressure in a patient with BZP poisoning (Gee et al., 2010; Schep et al., 2011).

1.8. References

Aitchinson LK, Hughes RN. Treatment of adolescent rats with 1-benzylpiperazine: a preliminary study of subsequent behavioral effects. Neurotoxicol Teratol 2006, 28: 453-458.

Alansari M, Hamilton D. Nephrotoxicity of BZP-based herbal party pills: a New Zealand case report. N Z Med J 2006, 119: U1959.

Antia U, Lee HS, Kydd RR, Tingle MD, Russell BR. Pharmacokinetics of 'party pill' drug N-benzylpiperazine (BZP) in healthy human participants. Forensic Sci Int 2009a, 186, 63-67.

Antia U, Tingle MD, Russell BR. Metabolic interactions with piperazine-based 'party pill' drugs. J Pharm Pharmacol 2009b, 61: 877-882.

Antia U, Tingle MD, Russel BR. In vivo interactions between BZP and TFMPP (party pill drugs). N Z Med J 2009c, 122: 29-38.

Antia U, Tingle MD, Russel BR. 'Party pill' drugs - BZP and TFMPP. N Z Med J 2009d, 122: 55-68.

Antia U, Tingle MD, Russel BR. Validation of an LC-MS method for the detection and quantification of BZP and TFMPP and their hydroxylated metabolites in human plasma and its application to the pharmacokinetic study of TFMPP in humans. J Forensic Sci 2010, 55: 1311-1318.

Austin H, Monasterio E. Acute psychosis following ingestion of 'Rapture'. Australas Psychiatry 2004, 12: 406-408.

Balmelli C, Kupferschmidt H, Rentsch K, Schneemann M. Fatal brain edema after ingestion of ecstasy and benzylpiperazine. Dtsch Med Wochenschr 2001, 126: 809-811.

Barroso M, Costa S, Dias M, Vieira DN, Queiroz JA, López-Rivadulla M. Analysis of phenylpiperazine-like stimulants in human hair as trimethylsilyl derivatives by gas chromatography-mass spectrometry. J Chromatogr A 2010, 1217: 6274-6280.

Baumann MH, Ayestas MA, Dersch CM, Rothman RB. 1-(m-Chlorophenyl)piperazine (mCPP) dissociates in vivo serotonin release from long-term serotonin depletion in rat brain. Neuropsychopharmacol 2001, 24: 492-501.

Baumann MH, Bulling S, Benaderet TS, Saha K, Ayestas MA, Partilla JS, et al. Evidence for a role of transporter-mediated currents in the depletion of brain serotonin induced by serotonin transporter substrates. Neuropsychopharmacol 2014, 39: 1355-1365.

Baumann MH, Clark RD, Budzynski AG, Partilla JS, Blough BE, Rothman RB. N-Substituted piperazines abused by humans mimic the molecular mechanism of 3,4-methylenedioxymethamphetamine (MDMA, or 'Ectasy'). Neuropsychopharmacol 2005, 30: 550-560.

Berney-Meyer L, Putt T, Schollum J, Walker R. Nephrotoxicity of recreational party drugs. Nephrol 2012, 17: 99-103.

Biliński P, Hołownia P, Kapka-Skrzypczak L, Wojtyła A. Designer drugs (DD) abuse in Poland; a review of the psychoactive and toxic properties of substances found from seizures of illegal drug products and the legal consequences thereof. Part II -

Piperazines/piperidines, phenylethylamines, tryptamines and miscellaneous 'others'. Ann Agric Environ Med 2012, 19: 871-882.

Bishop SC, McCord BR, Gratz SR, Loeliger JR, Witkowski MR. Simultaneous separation of different types of amphetamine and piperazine designer drugs by capillary electrophoresis with a chiral selector. J Forensic Sci 2005, 50: 326-335.

Bossong MG, Brunt TM, Van Dijk JP, Rigter SM, Hoek J, Goldschmidt HMJ, et al. mCPP: an undesired addition to the ecstasy market. J Psychopharmacol 2009, 29: 1395-1401.

Bossong MG, Van Dijk JP, Niesink RJM. Methylone and mCPP, two new drugs of abuse? Addict Biol 2005, 10: 321-323.

Brennan K, Johnstone A, Fitzmaurice P, Lea R, Schenk S. Chronic benzylpiperazine (BZP) exposure produces behavioral sensitization and cross-sensitization to methamphetamine (MA). Drug Alcohol Depend 2007, 88: 204-213.

Carvalho M, Milhazes N, Remião F, Borges F, Fernandes E, Amado F, et al. Hepatotoxicity of 3,4-methylenedioxyamphetamine and α-methyldopamine in isolated rat hepatocytes: formation of glutathione conjugates. Arch Toxicol 2004, 78, 16-24.

Caccia S. N-Dealkylation of arylpiperazine derivatives: disposition and metabolism of the 1-aryl-piperazines formed. Curr Drug Metab 2007, 8: 612-622.

Cohen BMZ, Butler R. BZP-party pills: a review of research on benzylpiperazine as recreational drug. Int. J Drug Policy 2011, 22: 95-101.

Davies S, Wood DM, Smith G, Button J, Ramsey J, Archer R, et al. Purchasing ‘legal highs’ on the internet – is there consistency in what you get? Q J Med 2010, 103: 489-493.

Dawson P, Moffatt JD. Cardiovascular toxicity of novel psychoactive drugs: lessons from the past. Prog Neuropsychopharmacol Biol Psychiatry 2012, 39: 244-252.

de Boer D, Bosman IJ, Hidvégi E, Manzoni C, Benkö AA, Reys LJAL, et al. Piperazine-like compounds: a new group of designer drugs-of-abuse on the European market. Forensic Sci Int 2001, 121: 47-56.

Domingos VB, Sebben VC, Paliosa P, Limberger RP. Determinação da clorpromazina e de seus produtos de biotransformação na presença de compostos anfetamínicos. Latin Am J Pharm 2008, 27: 165-171.

Elliott S. Current awareness of piperazines: pharmacology and toxicology. Drug Test Analysis 2011, 3: 430-438.

Elliott S, Smith C. Investigation of the first deaths in the United Kingdom involving the detection and quantitation of the piperazines BZP and 3-TFMPP. J Anal Toxicol 2008, 32: 172-177.

Fantegrossi WE, Winger G, Woods JH, Woolverton WL, Coop A. Reinforcing and discriminative stimulus effects of 1-benzylpiperazine and trifluoromethylphenylpiperazine in rhesus monkeys. Drug Alcohol Depend 2005, 77: 161-168.

Feuchtl A, Bagli M, Stephan R, Frahnert C, Kölsch H, Kühn KU, et al. Pharmacokinetics of m-chlorophenylpiperazine after intravenous and oral administration in healthy male volunteers: implication for the pharmacodynamic profile. Pharmacopsychiatry 2004, 37: 180-188.

Gaillard YP, Cuquel AC, Boucher A, Romeuf L, Bevalot F, Prevosto JM, et al. A fatality following ingestion of the designer drug meta-chlorophenylpiperazine (mCPP) in an asthmatic - HPLC MS/MS detection in biofluids and hair. J Forensic Sci 2013, 58: 263-269.

Gee P, Fountain J. Party on? BZP party pills in New Zealand. N Z Med J 2007, 120: U2422.

Gee P, Gilbert M, Richardson S, Moore G, Paterson S, Graham P. Toxicity from the recreational use of 1-benzylpiperazine. Clin Toxicol, 2008, 46: 802-807.

Gee P, Jerram T, Bowie D. Multiorgan failure from 1-benzylpiperazine ingestion – legal high or lethal high? Clin Toxicol, 2010, 48: 230-233.

Gee P, Richardson S, Woltersdorf W, Moore G. Toxic effects of BZP-based herbal party pills in humans: a prospective study in Christchurch, New Zealand. N Z Med J 2005, 118: 1784-1794.

Gijsman HJ, Van Gerven JMA, Tieleman MC, Schoemaker RC, Pieters MSM, Ferrari MD, et al. Pharmacokinetic and pharmacodynamic profile of oral and intravenous meta-chlorophenylpiperazine in healthy volunteers. J Clin Psycopharmacol 1998, 18: 289-295.

Haroz R, Greenberg M. New drugs of abuse in North America. Clin Lab Med 2006, 26: 147-164.

Helander A, Bäckber M, Hultén P, Al-Saffar Y, Beck O. Detection of new psychoactive substance use among emergency room patients: results from the Swedish STRIDA project. Forensic Sci Int 2014, 243: 23-29.

Hwang J, Zheng LT, Ock J, Lee MG, Suk K. Anti-inflammatory effects of *m*-chlorophenylpiperazine in brain glia cells. Int Immunopharmacol 2008, 8: 1686-1694.

Johnson RD, Botch-Jones SR. The stability of four designer drugs: MDPV, mephedrone, BZP and TFMPP in three biological matrices under various storage conditions. J Anal Toxicol 2013, 37: 51-55.

Jones DC, Duvauchelle C, Ikegami A, Olsen CM, Lau SS, de la Torre R, et al. Serotonergic neurotoxic metabolites of ecstasy identified in rat brain. J Pharmacol Exp Ther 2005, 313: 422-431.

Kerr JR, Davis LS. Benzylpiperazine in New Zealand: brief history and current implications. NZJR 2011, 41: 155-164.

Klaassen T, Riedel WJ, van Praag HM, Menheere PPCA, Griez E. Neuroendocrine response to meta-chlorophenylpiperazine and ipsapirone in relation to anxiety and aggression. Psychiatry Res 2002, 113: 29-40.

Kovaleva J, Devuyst E, De Paepe P, Verstraete A. Acute chlorophenylpiperazine overdose: a case report and review of the literature. Ther Drug Monit 2008, 30: 394-398.

Lanaro R, Costa JL, Zanolli-Filho LA, Cazenave SOS. Identificação química da clorofenilpiperazina (CPP)em comprimidos apreendidos. Quim Nova 2010, 33: 725-729.

Lee HS, Kydd RR, Lim VK, Kirk IJ, Russel BR. Effects of trifluoromethylphenylpiperazine (TFMPP) on interhemispheric communication. Psychopharmacol 2011, 213: 707-714.

Lin JC, Bangs N, Lee HS, Kydd RR, Russell BR. Determining the subjective and physiological effects of BZP on human females. Psychopharmacol 2009, 207: 439-446.

Lin JC, Jam RK, Lee HS, Jensen MA, Kydd RR, Russell BR. Determining the subjective and physiological effects of BZP combined with TFMPP in human males. Psycopharmacol 2011, 214: 761-768.

Luciano RL, Perazella MA. Nephrotoxic effects of designer drugs: synthetic is not better! Nat Rev Neprol 2014, 10: 314-324.

Maurer HH, Kraemer T, Springer D, Staack RF. Chemistry, pharmacology, toxicology and hepatic metabolism of designer drugs of the amphetamine (ecstasy), piperazine, and pyrrolidinophenone types. Ther Drug Monit 2004, 26: 127-131.

Meririne E, Kajos M, Kankaanpää A, Seppälä T. Rewarding properties of 1-benzylpiperazine, a new drug of abuse, in rats. Basic Clin Pharmacol Toxicol 2006, 98: 346-250.

Min CR, Kim MJ, Park YJ, Kim RH, Lee SY, Chung KH, et al. Estrogenic effects and their action mechanism of the major active components of party pill drugs. Toxicol Lett 2012, 214: 339-347.

Monteiro MS, Bastos ML, Pinho PG, Carvalho M. Update on 1-benzylpiperazine (BZP) party pills. Arch Toxicol 2013, 87: 929-947.

Montesano M, Sergi M, Moro M, Napoletano S, Romolo FS,Del Carlo M, et al. Screening of methylenedioxyamphetamine- and piperazine-derived designer drugs in urine by LC-MS/MS using neutral loss and precursor ion scan. J Mass Spectrom 2013, 48: 49-59.

Mustata C, Torrens M, Pardo R, Pérez C, Psychonaut Web Mapping Group, Farré M. Spice drugs: los cannabinoides como nuevas drogas de diseño. Addiciones 2009, 21: 181-186.

Nagai F, Nonaka R, Kamimura KSH. The effects of non-medically used psychoactive drugs on monoamine neurotransmission in rat brain. Eur J Pharmacol 2007, 559: 132-137.

Namera A, Nakamoto A, Saito T, Nagao M. Colorimetric detection and chromatographic analyses of designer drugs in biological materials: a comprehensive review. Forensic Toxicol 2011, 29: 1-24.

Nelson ME, Bryant SM, Aks SE. Emerging drugs of abuse. Emerg Med Clin N Am 2014, 32: 1-28.

Peters FT, Martinez-Ramirez JA. Analytical toxicology of emerging drugs of abuse. Ther Drug Monit 2010, 32: 532-539.

Peters FT, Schaefer S, Staack RF, Kraemer T, Maurer HH. Screening for and validated quantification of amphetamines and of amphetamine- and piperazine-derived designer drugs in human blood plasma by gas-chromatography/mass spectrometry. J Mass Spectrom 2003, 38: 659-676.

Pichini S, Pujadas M, Marchei E, Pellegrini M, Fiz J, Pacifici R, Zuccaro P, et al. Liquid chromatography-atmospheric pressure ionization electrospray mass spectrometry determination of “hallucinogenic designer drugs” in urine of consumers. J Pharm Biomed Anal 2008, 47: 335-342.

Rosenbaum CD, Carreiro SP, Babu KM. Here tofay, gone tomorrow... and back again? A review of herbal marijuana alternatives (K2, spice), synthetic cathinones (bath salts), kratom, *Salvia divinorum*, methoxetamine, and piperazines. J Med Toxicol 2012, 8: 15-32.

Schep LJ, Slaughter RJ, Vale A, Beasley MG, Gee P. The clinical toxicology of the designer “party pills” benzylpiperazine and trifluoromethylphenylpiperazine. Clin Toxicol 2011, 49: 131-141.

Severinsen K, Kraft JF, KoldsØ H, Vinberg KA, Rothman RB, Partilla JS, et al. Binding of the amphetamine-like 1-phenyl-piperazine to monoamine transporters. ACS Chem Neurosci 2012, 3: 693-705.

Sheridan J, Butler R, Wilkins C, Russel B. Legal piperazine- containing party pills – a new trend in substance misuse. Drug Alcohol Rev 2007, 26: 335-343.

Široká J, Polesel DN, Costa JL, Lanaro R, Tavares MFM, Polášek M. Separation and determination of chlorophenylpiperazine isomers in confiscated pills by capillary electrophoresis. J Pharm Biomed Anal 2013, 84: 140-147.

Sleno L, Staack RF, Varesio E, Hopfgartner G. Investigating the in vitro metabolism of fipexide: characterization of reactive metabolites using liquid chromatography/mass spectrometry. Rapid Commun Mass Spectrom 2007, 21: 2301-2311.

Staack RF, Fritschi G, Maurer HH. Studies on the metabolism and toxicological detection of the new designer drug *N*-benzylpiperazine in urine using gas chromatography-mass spectrometry. J Chromatogr B 2002, 773: 35-46.

Staack RF, Fritschi G, Maurer HH. New designer drug 1-(3-trifluoromethylphenyl)piperazine (TFMPP): gas chromatography/mass spectrometry and liquid chromatography/mass spectrometry studies on its phase I and II metabolism and on its toxicological detection in rat urine. J Mass Spectrom 2003, 38: 971-981.

Staack RF, Maurer HH. Piperazine-derived designer drug 1-(3-chlorophenyl)piperazine (mCPP): GC-MS studies on its metabolism and its toxicological detection in rat urine including analytical differentiation from its precursor drugs trazodone and nefazodone. J Anal Toxicol 2003, 27: 560-568.

Staack RF, Maurer HH. New designer drug 1-(3,4-methylenedioxybenzyl)piperazine (MDBP): studies on its metabolism and toxicological detection in rat urine using gas chromatography/mass spectrometry. J Mass Stectrom 2004, 39: 255-261.

Staack RF, Maurer HH. Metabolism of designer drugs of abuse. Curr Drug Metab 2005, 6: 259-274.

Staack RF, Paul LD, Schmid D, Roider G, Rolf B. Proof of 1-(3-chlorophenyl)piperazine (mCPP) intake – Use as adulterant of cocaine resulting in drug-drug interations? J Chromatog B 2007, 855: 127-133.

Staack RF, Paul LD, Springer D, Kraemer T, Maurer HH. Cytochrome P450 dependent metabolism of the new designer drug 1-(3-trifluoromethylphenyl)piperazine (TFMPP) in vivo studies in Wistar and Dark Agouti rats as well as in vitro studies in human liver microssomes. Biochem Pharmacol 2004a, 67: 235-244.

Staack RF, Theobald DS, Paul LD, Springer D, Kraemer T, Maurer HH. In vivo metabolism of the new designer drug 1-(4-methoxyphenyl)piperazine (MeOPP) in rat and identification of the human cytochrome P450 enzymes responsible for the major metabolic step. Xenobiotica 2004b, 34: 179-192.

Takahashi M, Nagashima M, Suzuki J, Seto T, Yasuda I, Yoshida T. Creation and application of psychoactive designer drugs data library using liquid chromatography with photodiode array spectrophotometry detector and gas chromatography-mass spectrometry. Talanta 2009, 77: 1245-1272.

Thompson I, Williams G, Caldwell B, Aldington S, Dickson S, Lucas N, et al. Randomised double-blind, placebo-controlled trial of the effects of the ‘party pills’ BZP/TFMPP alone and in combination with alcohol. Psychopharm 2010, 24: 1299-1308.

Tsutsumi H, Katagi M, Miki A, Shima N, Kamata T, Nishikawa M, et al. Development of simultaneous gas chromatography-mass spectrometric and liquid chromatography-electrospray ionization mass spectrometric determination method for the new designer drugs, N-benzylpiperazine (BZP), 1-(3-trifluoromethylphenyl)piperazine (TFMPP) and their main metabolites in urine. J Chromatog B 2005, 819: 315-322.

Vorce SP, Holler JM, Levine B, Past MR. Detection of 1-benzylpiperazine and 1-(3-trifluoromethylphenyl)-piperazine in urine analysis specimens using GC-MS and LC-ESI-MS. J Anal Toxicol 2008, 32: 444-450.

Wada M, Yamahara K, Ikeda R, Kikura-Hanajiri R, Kuroda N, Nakashima K. Simultaneous determination of N-benzylpiperazine and 1-(3-trifluoromethylphenyl)piperazine in rat plasma by HPLC-fluorescence detection and its application to monitoring of these drugs. Biomed Chromatogr 2012, 26: 21-25.

Waite RJ, Barbante GJ, Barnett NW, Zammit EM, Francis PS. Chemiluminescence detection of piperazine designer drugs and related compounds using tris(2,2'-bipyridine)ruthenium(III). Talanta 2013, 116: 1067-1072.

Watterson LR, Watterson E, Olive MF. Abuse liability of novel 'legal high' designer stimulants: evidence from animal models. Behav Pharmacol 2013, 24: 341-355.

Wikström M, Holmgren P, Ahlner J. A2 (*N*-benzylpiperazine) a new drug of abuse in Sweden. J Anal Toxicol 2004, 28: 67-70.

Wilkins C, Sweetsur P, Girling M. Patterns of benzylpiperazine/trifluoromethylphenylpiperazine party pill use and adverse effects in a population sample in New Zealand. Drug Alcohol Rev 2008, 27: 633-639.

Wood DM, Button J, Lidder S, Ramsey J, Holt DW, Dargan PI. Dissociative and sympathomimetic toxicity associated with recreational use of 1-(3-trifluoromethylphenyl)piperazine (TFMPP) and 1-benzylpiperazine (BZP). J Med Toxicol 2008, 4: 254-257.

Wohlfarth A, Weinmann W, Dresen S. LC-MS/MS screening method for designer amphetamines, tryptamines, and piperazines in serum. Anal Bioanal Chem 2010, 396: 2403-2414.

Yarosh HL, Katz EB, Coop A, Fantegrossi WE. MDMA-like behavioral effects of N-substituted piperazines in the mouse. Pharmacol Biochem Behav 2007, 88: 18-27.

Yeap CW, Bian CK, Abdullah AFL. A review on benzylpiperazine and triflouromethylphenylpiperazine: origins, effects, prevalence and legal status. Health Environ J 2010, 2: 38-50.

Young SA, Thrimawithana TR, Antia U, Fredatovich JD, Na Y, Neale PT, et al. Pharmaceutical quality of "party pills" raises additional safety concerns im the use of illicit recreational drugs.N Z Med J 2013, 126: 61-70.

CHAPTER II

OBJECTIVES

The use of designer drugs has substantially increased since the 1990s. They have been produced clandestinely with the intent of eliciting feelings of euphoria similar to those experienced with the use of controlled substances and the internet has been primarily used in the production, sale, and purchase of these compounds. Among these new substances, piperazine designer drugs emerged in the market in the early 2000s. In the drug scene, piperazines have the reputation of being safe. Although several reports indicate a potential risk to humans, there are presently no studies regarding their toxicity at the cellular level that could help understanding the detrimental effects of these drugs. The overall aim of the present thesis was to study the toxicity of the piperazine designer drugs BZP, TFMPP, MeOPP and MDBP using different *in vitro* models.

The strategy pursued to achieve the main objective proposed comprised the following steps:

a) To evaluate the potential cardiotoxicity of BZP, TFMPP, MeOPP and MDBP in the rat cardiomyoblast H9c2 cell line.

b) To evaluate the potential neurotoxicity of BZP, TFMPP, MeOPP and MDBP in human neuroblastoma SH-SY5Y differentiated cells.

c) To evaluate the potential hepatotoxicity of BZP, TFMPP, MeOPP and MDBP in the human hepatoma cell lines, HepG2 and HepaRG, and in primary rat hepatocytes.

d) To predict hepatotoxic mechanisms with a toxicogenomic approach using sandwich cultured rat hepatocytes.

CHAPTER III

ORIGINAL RESEARCH

Study I

Piperazine designer drugs induce toxicity in cardiomyoblast h9c2 cells through mitochondrial impairment

(Published in Toxicology Letters)

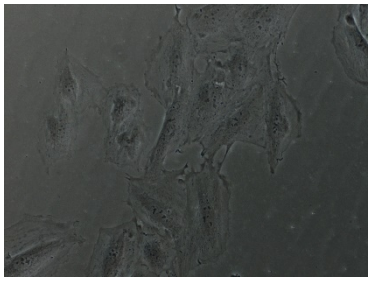

Toxicology Letters 229 (2014) 178–189

Contents lists available at ScienceDirect

Toxicology Letters

journal homepage: www.elsevier.com/locate/toxlet

Piperazine designer drugs induce toxicity in cardiomyoblast h9c2 cells through mitochondrial impairment

Marcelo Dutra Arbo [a,*], Renata Silva [a], Daniel José Barbosa [a], Diana Dias da Silva [a], Luciana Grazziotin Rossato [a,b], Maria de Lourdes Bastos [a], Helena Carmo [a]

[a] REQUIMTE, Laboratório de Toxicologia, Departamento de Ciências Biológicas, Faculdade de Farmácia, Universidade do Porto, Rua Jorge Viterbo Ferreira 228, Porto 4050-313, Portugal

[b] Instituto de Ciências Biológicas, Curso de Farmácia, Universidade de Passo Fundo (UPF) Campus I, Km 292, BR 285, Passo Fundo, Rio Grande do Sul 99052-900, Brazil

HIGHLIGHTS

- Piperazine derivatives presented cytotoxicity, being TFMPP the most cytotoxic.
- Piperazine designer drugs significantly increased Ca^{2+} intracellular levels.
- All drugs caused decreased intracellular ATP and mitochondrial membrane potential.
- Mitochondrial permeability transition pore seems to play a role in cytoxicity.
- There were found early apoptotic cells and cells undergoing secondary necrosis.

ARTICLE INFO

Article history:
Received 14 April 2014
Received in revised form 18 June 2014
Accepted 20 June 2014
Available online 23 June 2014

Keywords:
Piperazine designer drugs
Mitochondrial impairment
Ca^{2+} overload
Mitochondrial membrane potential
Apoptosis
Mitochondrial permeability transition pore

ABSTRACT

Abuse of synthetic drugs is widespread among young people worldwide. In this context, piperazine derived drugs recently appeared in the recreational drug market. Clinical studies and case-reports describe sympathomimetic effects including hypertension, tachycardia, and increased heart rate. Our aim was to investigate the cytotoxicity of *N*-benzylpiperazine (BZP), 1-(3-trifluoromethylphenyl) piperazine (TFMPP), 1-(4-methoxyphenyl) piperazine (MeOPP), and 1-(3,4-methylenedioxybenzyl) piperazine (MDBP) in the H9c2 rat cardiac cell line. Complete cytotoxicity curves were obtained at a 0–20 mM concentration range after 24 h incubations with each drug. The EC_{50} values (μM) were 343.9, 59.6, 570.1, and 702.5 for BZP, TFMPP, MeOPP, and MDBP, respectively. There was no change in oxidative stress markers. However, a decrease in total GSH content was noted for MDBP, probably due to metabolic conjugation reactions. All drugs caused significant decreases in intracellular ATP, accompanied by increased intracellular calcium levels and a decrease in mitochondrial membrane potential that seems to involve the mitochondrial permeability transition pore. The cell death mode revealed early apoptotic cells and high number of cells undergoing secondary necrosis. Among the tested drugs, TFMPP seems to be the most potent cytotoxic compound. Overall, piperazine designer drugs are potentially cardiotoxic and support concerns on risks associated with the intake of these drugs.

1. Introduction

Piperazine designer drugs emerged in the drug market for recreational purposes in the early 2000s. They can be divided into two classes, the benzylpiperazines such as *N*-benzylpiperazine (BZP) and its methylenedioxy-analogue 1-(3,4-methylenedioxybenzyl) piperazine (MDBP), and the phenylpiperazines such as 1-(3-chlorophenyl) piperazine (*m* CPP), 1-(4-fluorophenyl) piperazine (*p* FPP), 1-(3-trifluoromethylphenyl) piperazine (TFMPP), and 1-(4-methoxyphenyl) piperazine (MeOPP) (Fig. 1). Generally, they are consumed as capsules, tablets or pills but also in powder or liquid forms (Gee et al., 2005) under

* Corresponding author. Tel.: +351 220428597.
E-mail addresses: m.arbo@terra.com.br, marcelo.arbo@gmail.com (M.D. Arbo).

http://dx.doi.org/10.1016/j.toxlet.2014.06.031
0378-4274/

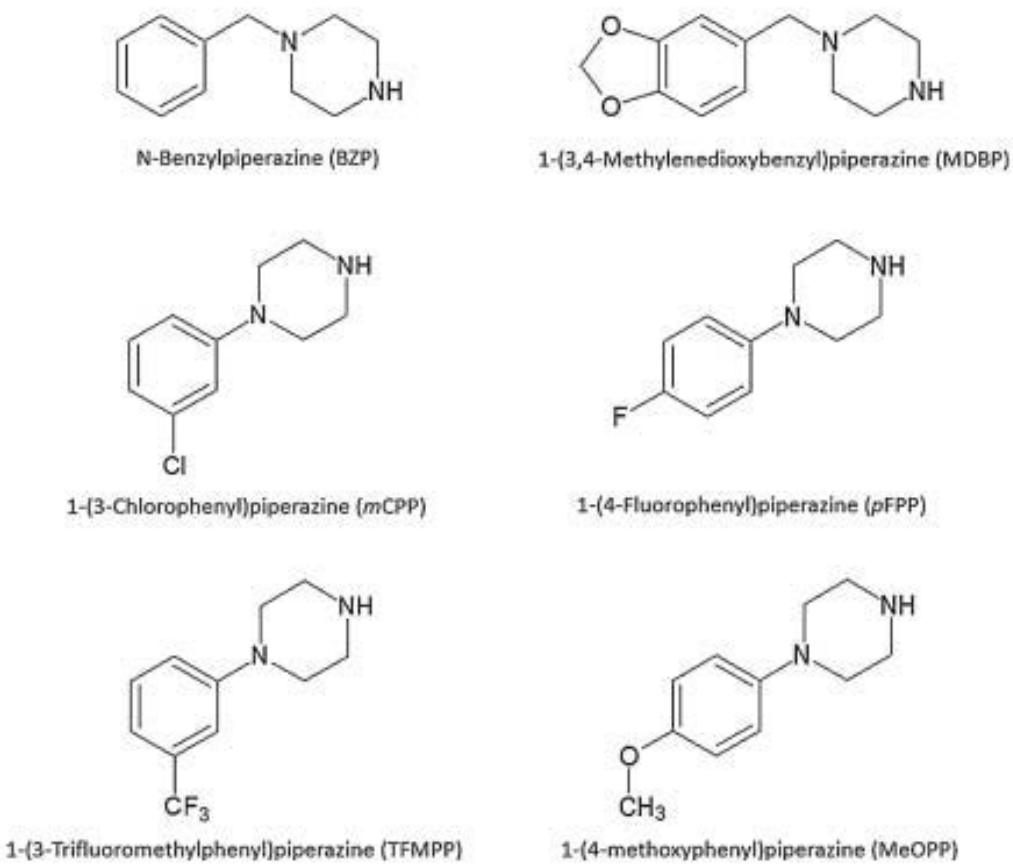

Fig. 1. Chemical structure of some piperazine designer drugs.

several names, such as "Rapture," "Frenzy," "Bliss," "Charge," "Herbal ecstasy," "A2," "Legal X," "Legal E," or simply party pills. They can also appear as adulterants of MDMA and cocaine (Staack et al., 2007).

In humans, piperazines are readily absorbed from the gastrointestinal tract (Antia et al., 2009; Schep et al., 2011). The information available on blood concentrations and pharmacokinetic distribution data is extremely limited. Blood concentrations measured at clinical studies with human volunteers reached approximately 1 μM after 200 mg of orally administrated BZP (Antia et al., 2009) and 0.1 μM after 60 mg of TFMPP (Antia et al., 2010). However, higher (up to 25 times) and largely discrepant blood concentrations were reported after intoxication with BZP and TFMPP (Gee et al., 2008; Kovaleva et al., 2008; Wood et al., 2008; Antia et al., 2009, 2010; Gee et al., 2010). Moreover, it is known that piperazine designer drugs readily cross the blood–brain barrier and interestingly, animal studies have shown that the TFMPP C_{max} brain-to-blood concentration ratio was in excess of one order of magnitude (Schep et al., 2011) indicating that these drugs achieve high tissue concentrations. The piperazine designer drugs are mainly metabolized in the liver, being the phenylpiperazines more extensively metabolized than the benzylpiperazines, and excreted almost exclusively as metabolites (Maurer et al., 2004). The main metabolic pathways that were already described for the piperazine designer drugs in animals and in humans are the aromatic hydroxylation of BZP (Staack and Maurer, 2005), TFMPP (Staack et al., 2003), and MeOPP (Staack et al., 2004), and the demethylenation of MDBP (Staack and Maurer, 2004). The rates of urinary excretion of the drugs and metabolites seem to vary widely among individuals (Austin and Monasterio, 2004).

Phenylpiperazine designer drugs, such as TFMPP, are non-selective 5-HT agonists, and also act as substrates for serotonin transporters (SERTs). On the other hand, benzylpiperazine derivatives, namely BZP, act on central dopaminergic substrates such as D_1-like receptors and dopamine transporters (DATs). It has been reported that the combined use of BZP and TFMPP in pills (mixed at a 2:1 ratio, in most cases) mimics the effects of 3,4-methylenedioxymethamphetamine (MDMA, ecstasy) in humans. It is, therefore, believed that this combination aggregates the stimulant effect of BZP, through its dopaminergic action, with the hallucinogenic effects of TFMPP, via serotonergic activation (for review see Arbo et al., 2012).

Accordingly, cardiovascular effects dependent on both dopaminergic and serotonergic stimulation were noted after the intake of piperazine designer drugs, and a predominance of adrenergic effects in the peripheral system, characteristic of a sympathomimetic toxindrome, was observed (Schep et al., 2011). Most common effects include *d*-amphetamine-like effects (Lin et al., 2011), tachycardia, hypertension, anxiety, vomiting, headache, migraine, palpitations, confusion, collapse, and seizure (Gijsman et al., 1998; Gee et al., 2005; Feuchtl et al., 2004; Thompson et al., 2010). In a randomized, double-blind, placebo-controlled study, a single administration of 200 mg BZP to women induced an increase in systolic and diastolic blood pressure and heart rate comparing to placebo (Lin et al., 2009). The same cardiovascular effects were found in other studies using a single administration of a BZP/

TFMPP combination (Thompson et al., 2010; Lin et al., 2011). Wood et al. (2008) reported a case of three male young adults presenting dissociative symptoms, agitation with bruxism, nausea, and features of sympathomimetic toxicity, with dilated pupils and tachycardia after the intake of four tablets of a drug thought to be ecstasy but contaning BZP and TFMPP. In New Zealand, two cases involving an adult woman and a young man were reported, in which the patients developed status epilepticus, hyperthermia, tachycardia, and tachypnea after BZP intake (Gee et al., 2010). In a non-fatal case of mCPP overdose, a female patient developed anxiety, agitation, drowsiness, flushing, visual disturbances, and tachycardia (Kovaleva et al., 2008).

The cardiovascular effects of recreational drugs are, to some extent, predictable because the receptors and transporters on which they act are located both in the central nervous system and in the periphery. Drugs acting on serotonergic, dopaminergic, or noradrenergic systems are, therefore, likely to induce vasoconstriction and/or tachycardia and arrhythmia. Extreme activation of the sympathetic control of the cardiovascular system can lead to profound vasoconstriction and ischemia. The resultant hypertension is a risk factor for strokes and myocardial infarcts, which are more common in chronic sympathomimetic drug abusers. The cardiac effect of sympathetic stimulation produces both ischemia (coronary vasoconstriction) and an increased oxygen demand (as a consequence of increased myocardial contractility). Sympathomimetic drugs also induce arrhythmias, which probably contribute to fatalities (Dawson and Moffatt, 2012).

Besides the activation of central and peripheral neurotransmission, these drugs may act directly at the cardiomyocyte level to produce cytotoxicity. This has been noted for example with the cardiotoxicity mechanisms of amphetamines, such as MDMA, that seem to involve mitochondrial impairment and metabolic bioactivation of the drugs and intracellular Ca^{2+} homeostasis, which can, in turn, abnormally alter myocardial excitability and contractility (Tiangco et al., 2005; Carvalho et al., 2012).

Notwithstanding, in the corresponding drug scene, piperazines have the reputation of being safe, and there are presently no studies regarding their toxicity at the cellular level that could help understanding the aforementioned detrimental effects of these drugs. The aim of this work was to study the in vitro cardiotoxicity of the piperazine designer drugs BZP, TFMPP, MeOPP, and MDBP using the H9c2 cardiac cell line. The H9c2 is a cell line derived from rat heart (Kimes and Brandt, 1976), that is considered a valuable model to assess in vitro cardiotoxicity, especially because these cells biochemical and electrophysiological properties are comparable to those of adult cardiomyocytes and adequately mimic the metabolic capacity of the rat heart (Zordoky and El-Kadi, 2007).

2. Material and methods

2.1. Chemicals

N-Benzylpiperazine (BZP, 99.3% purity) was purchased from Chemos GmbH (Regenstauf, Germany), 1-(3-trifluoromethylphenyl) piperazine (TFMPP, 98% purity) was acquired from Alfa Aesar (Karlsruhe, Germany), 1-(4-methoxyphenyl) piperazine (MeOPP, 96% purity) was purchased from Acros Organics (New Jersey, USA), and 1-(3,4-methylenedioxybenzyl) piperazine (MDBP, 97% purity) was purchased from Aldrich Chemistry (Steinheim, Germany). Fetal bovine serum (FBS), trypsin (0.25%)–EDTA (1 mM), and antibiotic (10,000 U/mL penicillin, 10,000 μg/mL streptomycin), Hanks balanced salt solution (HBSS), and phosphate buffer (PBS) were obtained from Gibco Laboratories (Lenexa, KS, USA). Dulbecco's modified eagle's medium (DMEM) with 4500 mg/L glucose, dichlorodihydrofluorescein diacetate (DCFH-DA), tetramethylrhodamine ethyl ester perchlorate (TMRE), reduced glutathione (GSH), oxidized glutathione (GSSG), glutathione reductase (GR, EC 1.6.4.2), 2-vinylpyridine, reduced β-nicotinamide adenine dinucleotide (β-NADH), 3-(4,5-dimethylthiazol-2-yl)-2,5-diphenyltetrazolium bromide (MTT), 5,5-dithio-bis(2-nitrobenzoic) acid (DTNB), *N*-acetyl-Asp-Glu-Val-Asp-*p*-nitroaniline (Ac-DEVD-pNA), 4-(2-hydroxyethyl) piperazine-1-ethanesulfonic acid (HEPES), 3-[(3-cholamidopropyl) dimethylammonio]-1-propanesulfonate hydrate (CHAPS), dithiothreitol (DTT), ethylenediaminetetraacetic acid (EDTA), luciferin, luciferase, campthotecin, and cyclosporine A were obtained from Sigma–Aldrich (St. Louis, USA). Fluo-3 AM was obtained from Molecular Probes (Eugene, OR). Dimethylsulfoxide (DMSO), perchloric acid ($HClO_4$), sodium phosphate dibasic (Na_2HPO_4), sodium phosphate monobasic (NaH_2PO_4), potassium bicarbonate ($KHCO_3$), hydrogen peroxide (H_2O_2), sodium chloride (NaCl), and glycerol were obtained from Merck (Darmstadt, Germany). Flow cytometry reagents (BD Facs-Flow™ and Facs-Clean™) were purchased from BD (Becton, Dickinson and Company, San Jose, CA, USA).

2.2. H9c2 cell culture

The H9c2 cell line was a generous gift from Dr. Vilma Sardão, Center for Neurosciences and Cellular Biology, University of Coimbra, Portugal. The cells were cultured in DMEM supplemented with 10% FBS, 100 U/mL of penicillin, and 100 μg/mL of streptomycin in 75 cm^2 tissue culture flasks at 37 °C in a humidified 5% CO_2–95% air atmosphere. The cells were fed every 2–3 days, and sub-cultured once 70–80% confluence was reached.

2.3. Cytotoxicity assay

For the evaluation of cytotoxicity, the MTT reduction assay was performed as previously described (Rossato et al., 2013). This assay measures dehydrogenase activity, an indicator of metabolically active mitochondria, and therefore, of cell viability. Cells were seeded at a density of 35,000 cells/mL in 48-well plates (final volume of 250 μL; ~8000 cells/cm^2). Stock solutions of BZP were made up in PBS. Stock solutions of TFMPP, MeOPP, and MDBP were made in DMSO. In these cases, 0.1% DMSO in culture medium was used as negative control. All stock solutions were stored at −20 °C and freshly diluted on the day of the experiment. Concentration–response curves were obtained incubating the cells with 0–20 mM of BZP, TFMPP, MeOPP, or MDBP for 24 h at 37 °C. Triton X-100 1% was used as positive control. After the incubation period, the medium was removed and replaced with fresh medium containing 0.5 mg/L MTT. The cells were incubated at 37 °C for 4 h. After incubation, the cell culture medium was removed, and the formed formazan crystals dissolved in DMSO. The absorbance was measured at 550 nm in a multi-well plate reader (BioTek Instruments, Vermont, USA). To reduce inter-experimental variability, data were normalized and scaled between 0% (negative controls) and 100% effect (positive controls). Results were graphically presented as percentage of cell death vs concentration (μM). All drugs were tested in three independent experiments with each concentration tested in six replicates within each experiment.

2.4. Neutral red (NR) uptake assay

To confirm the results obtained with the MTT reduction assay, we performed the NR uptake assay. This assay is based on the ability of viable cells to incorporate and bind the weak cationic dye NR, which penetrates into the cells by non-ionic diffusion, accumulating in lysossomes by interaction with anionic sites in the lysosomal matrix (Labonne et al., 2009). At the end of 24 h incubations of H9c2 cells with 0–20 mM of BZP, TFMPP, MeOPP, or

MDBP, the medium was replaced by new medium containing 50 μg/mL NR. The cells were incubated at 37 °C in a humidified, 5% CO_2–95% air atmosphere for 3 h allowing the lysosomes of viable cells to take up the dye. Thereafter, the cells were carefully washed with 200 μL of HBSS to eliminate extracellular dye and lysed with a 50% ethanol–1% glacial acid acetic solution. Triton X-100 1% was used as positive control. The absorbance was measured at 540 nm in a multi-well plate reader (BioTek Instruments, Vermont, USA). The percent cell death relative to that of the control cells was used as the cytotoxicity measure.

2.5. Intracellular ROS and RNS production

The intracellular reactive oxygen (ROS) and nitrogen (RNS) species production was monitored by means of the DCFH-DA assay as previously described (Dias da Silva et al., 2013b). The sensitive DCFH-DA lipophilic probe readily penetrates the cells producing 2′,7′-dichlorodihydrofluorescein (DCFH) after hydrolysis, which further reacts with intracellular ROS and RNS, including the hydroxyl radical and hydrogen peroxide, generating green fluorescent 2′,7′-dichlorofluorescein (DCF), which is polar and trapped within the cells (Rao et al., 1992; Smith and Weidemann, 1993). For this determination, cells were seeded at a density of 35,000 cells/mL in 48-well plates (final volume of 250 μL, ~8000 cells/cm^2) and allowed to grow for 48 h. On the day of the experiment, the cells were pre-incubated with 10 μM DCFH-DA for 30 min, at 37 °C, in the dark. As DCFH-DA is a non-water-soluble powder, it was initially prepared as a 4 mM stock solution in DMSO and made up to the final concentration in fresh culture medium (ensuring that the final concentration of DMSO did not exceed 0.05%) immediately before each experiment. The cells were then rinsed with HBSS and incubated with the piperazine designer drugs (1000 and 2000 μM BZP, MeOPP, or MDBP or 50 and 500 μM for TFMPP) at 37 °C. H_2O_2 (150 μM) was used as a positive control. Fluorescence was recorded on a fluorescence microplate reader (BioTek Instruments, Vermont, USA) set to 485 nm excitation and 530 nm emission at times 0, 1, 2, 3, 4, 5, 6, 7, 8, and 24 h after incubation. The data obtained were normalized to negative controls on a plate-by-plate basis and calculated as fold increase over control conditions from three independent experiments with each concentration tested in three replicates within each experiment.

2.6. Measurement of intracellular total glutathione (tGSH), GSH, and GSSG levels

Cells were seeded at a density of 35,000 cells/mL in 55 cm^2 Petri dishes (final volume of 12.5 mL, ~8000 cell/cm^2) and grown for 48 h. The medium was then replaced and cells were incubated at 37 °C with the piperazine designer drugs (1000 and 2000 μM BZP, MeOPP, or MDBP or 50 and 500 μM for TFMPP). After a 24 h incubation period, the medium was removed, and the cells were kept on ice while being scraped in PBS, pH 7.4. After centrifugation (210 × *g*, 5 min, 4 °C), the supernatant was removed. The pellet of cells was lysed with 5% $HClO_4$ and centrifuged (16,000 × *g*, 10 min, 4 °C). The obtained supernatant was frozen at −20 °C until further determination of tGSH and GSSG levels, evaluated by the DTNB–GSSG reductase recycling assay, as previously described (Rossato et al., 2013). Briefly, the acidic supernatant was neutralized with an equal volume of 0.76 M $KHCO_3$ and centrifuged (16,000 × *g*, 2 min, 4 °C). Total glutathione was determined by transfering, in triplicate, 100 μL of the neutralized supernatants, standards or blank (5% $HClO_4$, w/v) to a 96-well plate, followed by the addition of 65 μL of freshly prepared reagent containing 0.24 mM NADPH and 0.7 mM DTNB in phosphate buffer (71.5 mM Na_2HPO_4, 71.5 mM NaH_2PO_4, and 0.63 mM EDTA; pH 7.5). The plates were then incubated for 15 min, at 30 °C, in a microplate reader (BioTek Instruments, Vermont, USA), prior to the addition of 40 μL per well of a freshly prepared 10 U/mL glutathione reductase solution in phosphate buffer. The stoichiometric formation of 5-thio-2-nitrobenzoic acid (TNB) was followed every 10 s for 3 min at 415 nm at 30 °C, and compared with a standard curve performed for all readings. For the determination of GSSG, 10 μL of 2-vinylpyridine was added to 200 μL aliquots of the acidic supernatants and mixed continuously for 1 h at 0 °C for derivatization of the sulfhydryl groups (SH). GSSG was then measured as described for tGSH. The GSH content was calculated by subtracting the GSSG from the tGSH values [GSH = tGSH − (2 × GSSG)]. The final results were expressed as percentage of control conditions from five independent experiments with each concentration tested in three replicates within each experiment.

2.7. Influence of piperazine designer drugs on glutathione reductase (GR) activity

The activity of GR was evaluated by following the oxidation of NADPH consumed during the reduction of GSSG at 340 nm, at a constant temperature of 30 °C (Remião et al., 2000). The enzyme activity was determined by transferring 170 μL of a reaction mixture containing 1 mM GSSG, 71.5 mM Na_2HPO_4, 71.5 mM NaH_2PO_4, and 0.63 mM EDTA; pH 7.5, to which 50 μL of a freshly prepared 0.5 U/mL glutathione reductase solution in phosphate buffer and 100, 500, 1000, and 2000 μM BZP, MeOPP, or MDBP or 5, 50, 100, and 500 μM TFMPP were added. After 2 min pre-incubation, the reaction was initiated by the addition of 30 μL 1 mM NAPH in phosphate buffer. The kinectics of the reaction was monitored for 5 min at 20 s intervals. A blank assay containing all components of the reaction mixture except the enzyme was performed to evaluate the non-enzymatic oxidation of NADPH, which was subtracted from the assay values. As a positive control, DHBA (3,4-dihydroxybenzylamine) was used. The final results were expressed as percentage of control conditions from three independent experiments with each concentration tested in three replicates within each experiment.

2.8. Measurement of intracellular ATP levels

Cells were seeded, treated and incubated following the same protocol used for the measurement of glutathione levels. After centrifugation (210 × *g*, 5 min, 4 °C), the supernatant was removed. The pellet of cells was lysed with 5% $HClO_4$, centrifuged (16,000 × *g*, 10 min, 4 °C), and the supernatant obtained was frozen at −20 °C until further determination of the ATP intracellular content. The ATP levels were quantified by a bioluminescence assay, as described by Rossato et al. (2013). Briefly, the acidic supernatant was neutralized with an equal volume of 0.76 M $KHCO_3$ and centrifuged (16,000 × *g*, 1 min, 4 °C). The ATP contents were then measured in duplicate in 96-well white plates, by adding 100 μL of the neutralized supernatants, standards or blank (5% $HClO_4$, w/v) and 100 μL of the luciferin/luciferase solution [0.15 mM luciferin, 300,000 light units of luciferase from *Photinus pyralis* (American firefly), 50 mM glycine, 10 mM $MgSO_4$, 1 mM Tris, 0.55 mM EDTA, 1% BSA (pH 7.6)]. The emitted light intensity was determined using a luminescence microplate reader (BioTek Instruments, Vermont, USA) and compared with a standard curve performed within each experiment. The final results were expressed as percentage of control conditions from five independent experiments with each concentration tested in two replicates within each experiment.

2.9. Flow cytometry analysis of intracellular Ca^{2+} levels

Intracellular Ca^{2+} levels were evaluated with the sensitive fluorochrome Fluo3-AM. After uptake by live cells, Fluo3-AM is enzymatically hydrolyzed by intracellular esterases to Fluo3,

which binds Ca^{2+} and exhibits an increase in fluorescence intensity. A protocol previously described (Rossato et al., 2013) was used with minor modifications. Cells were seeded at a density of 35,000 cells/mL in six-well plates (final volume of 2.5 mL, ~9,000 cells/cm^2). After 48 h, the medium was replaced by fresh medium containing 500 and 1000 μM BZP or MDBP, or 250 and 500 μM MeOPP, or 10, 50, and 100 μM TFMPP. Twenty-four hours after exposure, the cells were harvested by trypsinization (0.05% trypsin/EDTA), centrifuged (300 × *g*, 5 min, 4 °C), and then loaded with 10 μM Fluo3-AM in 50 μL of heated serum-free DMEM without phenol red, for 30 min, at 37 °C, in a water bath with shaking. After this incubation period, the cells were centrifuged (300 × *g*, 5 min, 4 °C) washed by resuspending in 500 μL of heated HBSS (with Ca^{2+} and Mg^{2+}), centrifuged again (300 × *g*, 5 min, 4 °C), and kept on ice until flow cytometry analysis.

Sample analysis was performed in a FACSCalibur™ flow cytometer (BD, CA, USA), equipped with a 488 nm argon ion laser, using CellQuest software (BD Biosciences). The green fluorescence of Fluo3 was measured by a 530 ± 15 nm band-pass filter (FL1). After resuspending the cell pellet in HBSS (+/+) with 0.5 μg/mL propidium iodide (PI) (after permeating death cells, PI interlaces with the nucleic acid helix with consequent increase in fluorescence intensity emission at 615 nm), data from at least 15,000 viable cells (based on their forward and side light scatter) were collected from each test condition. In order to detect a possible contribution from cells auto-fluorescence to the analyzed fluorescence signals, portions of cell suspension (with or without exposure to the drugs), which were not incubated with Fluo3-AM, were analyzed in the 530 ± 15 nm band-pass filter (FL1). Results are presented as Fluo3 fluorescence intensity (percentage of control) from at least six independent experiments with each concentration tested in two replicates within each experiment.

2.10. Assesment of mitochondrial membrane potential ($\Delta\psi m$)

Assessment of mitochondrial integrity was performed by measuring TMRE inclusion as described by Dias da Silva et al. (2013c). TMRE is a cell permeable fluorescent dye that specifically stains live mitochondria, and accumulates in proportion to the mitochondrial membrane potential ($\Delta\psi m$) (Scaduto and Grotyohann, 1999). Cells were seeded at a density of 35,000 cells/mL in 48-well plates (final volume of 250 μL; ~8000 cells/cm^2). After 48 h, the medium was gently aspirated, and the cells were incubated with the piperazine designer drugs (500, 1000, and 2000 μM for BZP, MeOPP, or MDBP or 10, 50, 100, 500, and 1000 μM for TFMPP). At the end of the 24 h incubation period, the medium was replaced by fresh medium containing 2 μM TMRE, and incubated at 37 °C, for 30 min, in the dark. As TMRE is a non water-soluble powder, a 2 mM stock solution was initially prepared in DMSO and stored in the dark. Afterwards, the medium was gently aspirated and replaced by 0.2% BSA in HBSS. Fluorescence was measured on a fluorescence microplate reader (BioTek Instruments, Vermont, USA) set to 544 nm excitation and 590 nm emission. The data obtained were normalized on a plate-by-plate basis to the values of the respective controls and calculated as the percentage of control conditions from at least six independent experiments with each concentration tested in three replicates within each experiment. Although rhodamines can undergo self-quenching at high concentrations (up to 150 nM), the use of low concentrations may cause a loss of sensibility in detecting small $\Delta\psi m$ depolarizations. The 2 μM TMRE tested concentration has been successful in detecting $\Delta\psi m$ alterations in previous works (Dias da Silva et al., 2013c).

2.11. Inhibition of the mitochondrial permeability transition pore (MPTP)

The mitochondrial permeability transition pore is sensitive to cyclosporin A (CsA) that blocks the opening of this pore. To evaluate the role of MPTP in the cytotoxicity mediated by piperazine designer drugs, H9c2 cells were seeded at a density of 35,000 cells/mL in 48-well plates (final volume of 250 μL; ~8000 cells/cm^2). After 48 h cells were pre-treated for 30 min, and co-incubated with 1 μM CsA to inhibit the MPTP. After the pre-incubation, cells were incubated with 500, 1000, 1500, and 2000 μM BZP, MeOPP, or MDBP or 50, 100, 250, and 500 μM TFMPP. After 24 h, cell mortality was determined through the MTT reduction assay. The final results were expressed as percentage of control conditions from four independent experiments with each concentration tested in three replicates within each experiment.

2.12. Cell death mode: apoptosis vs necrosis

Cell death analysis was performed by staining H9c2 cells with Annexin V-FITC and propidium iodide (PI) (FITC Annexin V Apoptosis Detection Kit BD Biosciences, USA). Annexin V binds to exposed phosphatidylserine on the plasma membrane of the early apoptotic cells, while late apoptotic and/or necrotic cells are stained by PI. To perform the assay, H9c2 cells were seeded at a density of 12,000 cells/mL in 48-well plates (final volume of 250 μL; ~3,000 cells/cm^2). After 48 h, the cells were incubated with 360 μM BZP, 70 μM TFMPP, 380 μM MeOPP, and 500 μM MDBP. After the 24 h incubation period, the medium was removed, and 100 μL binding buffer was added, followed by 2 μL PI and 3 μL annexin V-FITC. Plates were incubated in the dark at room temperature. After 15 min, the cells were observed under a fluorescence microscope (Nikon, Tokyo, Japan). Five pictures per well were taken, and the percentages of early apoptotic cells were estimated by counting the annexin V-positive but PI-negative cells, whereas the percentages of late apoptotic cells were estimated by counting the number of cells which were both annexin V-positive and PI-positive. Necrotic cells were the PI-positive but annexin V-negative ones. Campthotecin 12 μM was used as a positive control for apoptosis. The results are expressed as percentage cell population from 4 independent experiments.

2.13. Caspase-3 activity assay

Cells were seeded at a density of 35,000 cells/mL in six-well plates (final volume of 2.5 mL, ~9000 cells/cm^2) and allowed to grow. After 48 h, the medium was replaced, and cells were incubated with piperazine designer drugs at 37 °C (1000 and 2000 μM for BZP, MeOPP, or MDBP or 50 and 500 μM for TFMPP). After a 24 h incubation period, the cells were detached and collected to a tube (two wells per tube), centrifuged (210 × *g*, 5 min, 4 °C), and the supernatant was discarded. One hundred and fifty microliters of lysis buffer (50 mM HEPES, 0.1 mM EDTA, 0.1% CHAPS, supplemented with 1 mM DTT, pH 7.4) were added to the pellets, votex-mixed and incubated on ice for 5 min before centrifugation (16,000 × *g*, 10 min, 4 °C). In a 96-well plate, 50 μL of the supernatant, which contains the cytoplasmic fraction, was mixed with 200 μL of assay buffer (100 mM NaCl, 50 mM HEPES, 1 mM EDTA, 0.1% CHAPS, 10% glycerol, supplemented with 10 mM DTT, pH 7.4). The reaction was started by adding 5 μL of caspase-3 peptide substrate Ac-DEVD-pNA (final concentration 80 μM) and subsequent incubation at 37 °C for 24 h. Caspase-3 releases the *p*-nitroaniline moiety of the substrate, which presents high absorbance at 405 nm. All steps were performed on ice, and the caspase-3 activity was determined at 405 nm in a multi-well plate reader (BioTech Instruments, Vermont, US) as previously

described (Barbosa et al., 2014). Caspase-3 substrate Ac-DEVD-pNA (stock solution at 4 mM) and DTT were prepared in DMSO. The absorbance of blanks, used as non-enzymatic control, was subtracted from each value of absorbance. Final results of caspase-3 activity were expressed as optical density at 405 nm/mg of protein. The protein content in the cytoplasmic fraction was quantified using the Bio-Rad DC protein assay kit as described by the manufacturer, and bovine albumin solutions were used as standards. Campthotecin (12 μM) was used as positive control.

2.14. Statistical analysis

Concentration–response curves were obtained from six replicates of each tested concentration from three independent experiments. They were fitted by the least squares method. The comparisons between curves (bottom, top and log EC_{50}) were made using the extra sum-of-squares F test. Results of all other biochemical measures are presented as mean ± standard error of the mean (SEM) from at least three independent experiments. Normality of the data distribution was assessed by the Kolmogorov–Smirnov normality test. Significance was accepted at $p < 0.05$. Statistical comparisons between groups were performed with one-way ANOVA (when data followed normal distribution) or with the Kruskal–Wallis test (one-way ANOVA on ranks in case data distribution was not normal). A two-way ANOVA analysis was conducted when the cells were submitted to a drug challenge after pre-incubation with the MTPT opening inhibitor CsA. Details of the statistical analysis are provided in the text and legend of the figures.

3. Results

3.1. Piperazine designer drugs elicit concentration-dependent cytotoxicity in H9c2 cells

A comprehensive concentration–response analysis was carried out by incubating the H9c2 cells with 0–20 mM of each piperazine designer drug for 24 h. Fig. 2 presents the obtained concentration–response curves showing that in the MTT (A) and NR (B) assays, all tested drugs produced concentration-dependent cytotoxic effects. A summary of the calculated EC_{50} values (representing the half-maximum-effect concentrations from the fitted curves) is presented in Table 1. Significant differences were observed for the EC_{50} values of the curves. Based on these data, it was evident that, under our experimental conditions, TFMPP (EC_{50} 59.6 μM) was the most cytotoxic of the tested piperazine designer drugs to H9c2 cells, followed by BZP (EC_{50} 343.9 μM), MeOPP (EC_{50} 570.1 μM), and MDBP (EC_{50} 702.5 μM). To confirm these results, we also performed the NR uptake assay. The EC_{50} values were higher than those obtained with the MTT assay, but the cytotoxicity profile of the piperazine designer drugs was the same (Table 1, Fig. 2B).

3.2. Oxidative stress does not contribute to the cytotoxic effects elicited by the piperazine designer drugs

Oxidative stress plays an important role in drug-induced cardiotoxicity for many different compounds including drugs of abuse (e.g., cocaine and amphetamines), and pharmaceuticals (e.g., doxorubicin and cyclophosphamide) (Costa et al., 2013). The effect of piperazine designer drugs in the generation of reactive species was, therefore, evaluated by the DCFH-DA assay at different time-points, but no significant changes in reactive species generation were found for any of the tested piperazine drugs even when tested at highly cytotoxic concentrations (data not shown).

Changes in the intracellular amounts of GSH and GSSG are also strong indicators of redox disturbances and were investigated with the DTNB–GSSG reductase recycling assay. In accordance with the data from the DCFH-DA assay, the intracellular GSH levels were not depleted by the piperazine test drugs, even at highly cytotoxic concentrations, with the exception of MDBP. As can be seen in Fig. 3, total GSH levels were significantly decreased ($p < 0.05$, ANOVA/Bonferroni) after 24 h incubations with 1000 and 2000 μM MDBP as compared to control (representing a 23% and 37% decrease, respectively). GSSG was also detected in H9c2 cells: however, no changes in the intracellular levels of the dissulfide were observed for any of the tested drugs (data not shown). Thus, the observed depletions in total GSH levels are probably due to a decrease in reduced GSH intracellular levels as a consequence of

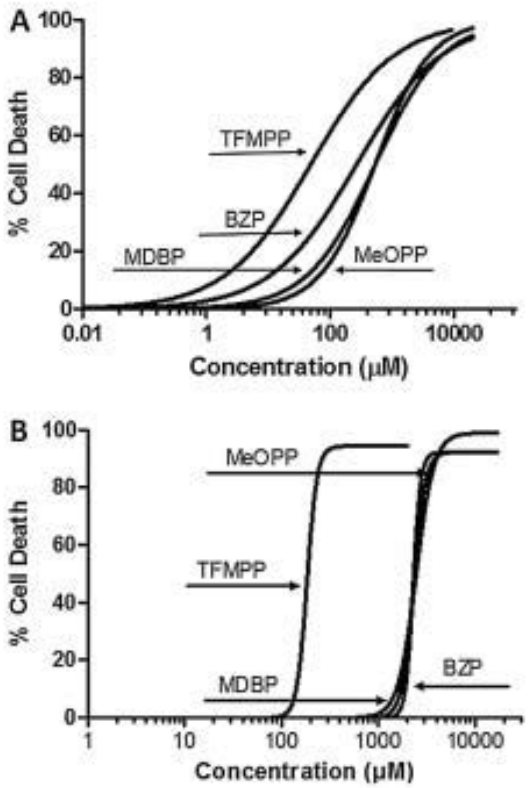

Fig. 2. Concentration–response (cell death) curves of the tested piperazine designer drugs after 24 h incubation in H9c2 cells at 37 °C. Cell viability was evaluated by the MTT reduction (A) and the neutral red uptake (B) assays. Data are presented as percentage of cell death relative to the respective negative controls. Three independent experiments were performed (six replicates tested for each concentration within each experiment). Curves were fitted using least squares as the fitting method.

Table 1
EC_{50} values of the piperazine designer drugs.

Designer drug	EC_{50} MTT (μM)	EC_{50} NR (μM)
BZP	343.9	2332[b]
TFMPP	59.6[a]	186.4[a,c,d]
MeOPP	570.1[a,b]	2366[b]
MDBP	702.5[a,b]	2469[b]

The cytotoxicity curves were fitted using least squares as the fitting method. Comparisons were made using the extra sum-of-squares F test ($p < 0.05$).
[a] Compares to BZP.
[b] Compares to TFMPP.
[c] Compares to MeOPP.
[d] Compares to MDBP.

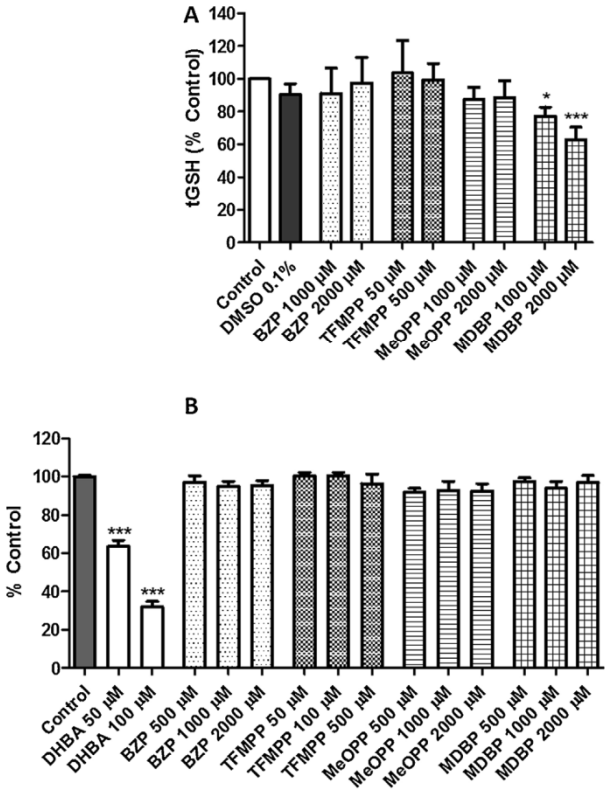

Fig. 3. (A) Intracellular contents of total glutathione (tGSH) in H9c2 cells after 24 h incubations with the tested piperazine designer drugs at 37 °C. (B) Effect of piperazine designer drugs in the activity of GSH reductase (GR). Results are expressed as percentage control ± SEM ($n = 5$ independent experiments run in triplicates). Statistical comparisons were made using one-way ANOVA/Bonferroni post-hoc test ($^{*}p < 0.05$; $^{***}p < 0.001$ vs control).

the metabolic bioactivation of MDBP into reactive metabolites that can conjugate GSH but an interference with the enzymes involved in GSH homeostasis, namely with glutathione reductase (GR), cannot be discarded. To test this hypothesis, the influence of the piperazine designer drugs on the activity of the GR enzyme was measured, and no differences were found at the concentration range tested (Fig. 3B).

3.3. Piperazine designer drugs disturb the cellular energetic status and Ca^{2+} homeostasis

ATP, the key intermediate for energy exchange, is engaged in a variety of cellular activities, including cellular energetics, metabolic regulation, and signalling. Since all cells require ATP to remain alive and carry out their specific functions and, because ATP is transiently depressed by many forms of cellular stress, its levels reflect the functional integrity of viable cells. Fig. 4 shows that the ATP levels measured in H9c2 cells after 24 h incubations with the tested piperazine designer drugs at 37 °C were significantly depleted at highly cytotoxic concentrations. Significant ($p < 0.05$, ANOVA/Bonferroni) 23 and 45% decreases in ATP levels in relation to negative controls were observed at 1000 and 2000 µM BZP. For 500 µM TFMPP, a 45% decrease was noted, while this decrease was of 28% for 2000 µM MeOPP, and 27% and 35%, respectively, for 1000 and 2000 µM MDBP.

Intracellular Ca^{2+} homeostasis is also critical for maintaining the normal function of the cell, in that variations in the

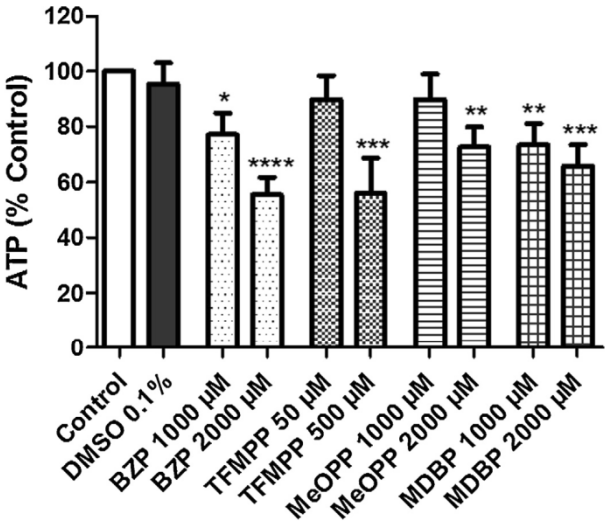

Fig. 4. Intracellular contents of ATP in H9c2 cells after 24 h incubations with the tested piperazine designer drugs at 37 °C. Results are expressed as percentage control ± SEM ($n = 5$ independent experiments run in duplicates). Statistical comparisons were made using one-way ANOVA/Bonferroni post-hoc test ($^{*}p < 0.05$; $^{**}p < 0.01$; $^{***}p < 0.001$; $^{****}p < 0.0001$ vs control).

concentration of Ca^{2+} in cells can determine cell survival or death (Oliveira and Gonçalves, 2009). Incubation with piperazine designer drugs significantly increased ($p < 0.05$, Kruskal–Wallis) the intracelular Ca^{2+} levels in a concentration-dependent manner. As shown in Fig. 5, a 37% increase occured at 1000 µM BZP in relation to negative controls. At 50 and 100 µM TFMPP, mean fluorescence markedly increased up to 89% and 123% over control values, respectively. At 500 µM MeOPP and 1000 µM MDBP increases of 130% and 118% relative to control, respectively, could also be observed.

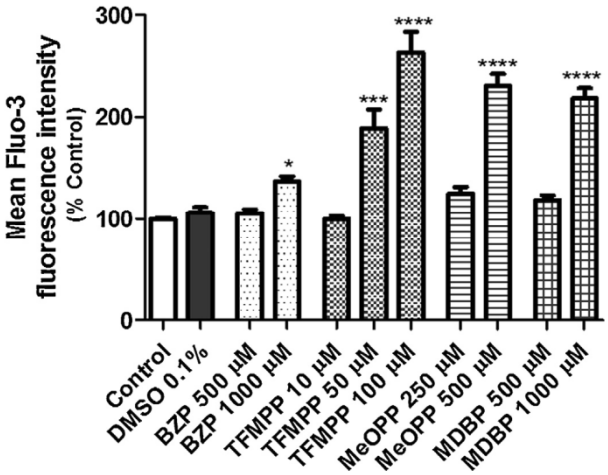

Fig. 5. Intracellular levels of Ca^{2+} in H9c2 cells after 24 h incubations with the tested piperazine designer drugs at 37 °C. Results are expressed as percentage control ± SEM ($n = 6$ independent experiments run in duplicates). Statistical comparisons were made using the non-parametric Kruskal–Wallis test ($^{*}p < 0.05$; $^{***}p < 0.001$; $^{****}p < 0.0001$ vs control).

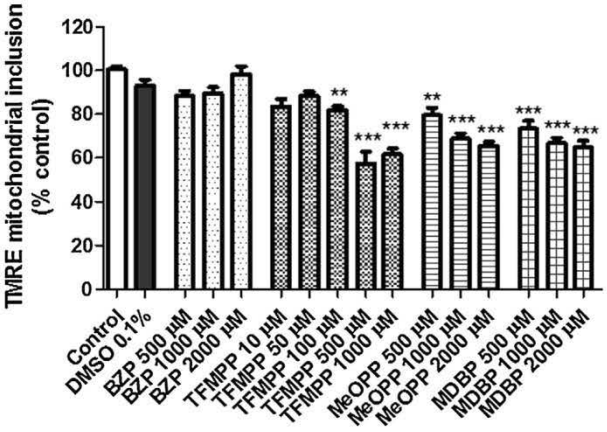

Fig. 6. Mitochondrial membrane potential ($\Delta\psi m$) measured as TMRE incorporation in mitochondria of H9c2 cells after 24 h incubations with the tested piperazine designer drugs at 37 °C. Results are expressed as percentage control ± SEM ($n = 6$ independent experiments run in triplicates). Statistical comparisons were made using one-way ANOVA/Bonferroni post-hoc test (**$p < 0.01$; ***$p < 0.001$ vs control).

3.4. Mitochondrial function is severely affected by the piperazine designer drugs

To investigate whether the piperazine drugs could disturb the mitochondrial function, the mitochondrial membrane potential ($\Delta\psi m$) was evaluated. A significant loss of $\Delta\psi m$ impairs oxidative phosphorylation, depleting cells of energy, and inducing cell death. In Fig. 6, a significant loss in $\Delta\psi m$ ($p < 0.01$, ANOVA/Bonferroni) can be observed after 24 h incubations of H9c2 cells with 100, 500, and 1000 μM TFMPP (with decreases of 18, 43 and 39%, respectively) in relation to control values. At 500, 1000, and 2000 μM MeOPP, this loss comprises 21, 33, and 35% of control $\Delta\psi m$, while 27, 33, and 36% decreases in $\Delta\psi m$ relative to control occurred at 500, 1000, and 2000 μM MDBP, respectively. BZP did not produce any measurable modifications in $\Delta\psi m$ even at highly cytotoxic concentrations.

Increase of intracellular Ca^{2+} levels, loss of $\Delta\psi m$, and ATP depletion are indicative signals of MPTP opening. Fig. 7 shows the involvement of MPTP in the cytotoxic effects of the tested piperazine designer drugs. When the H9c2 cells were incubated with the tested drugs in the presence of 1 μM cyclosporine A (CsA) (including a pre-incubation period of 30 min), it was possible to observe a partial reversion of the piperazine designer drugs cytotoxic effects. In fact, the cytotoxic effects produced by 1500 and 2000 μM BZP after pre-incubation with 1 μM CsA were significantly lower ($p < 0.05$, ANOVA/Bonferroni) than those observed in the absence of CsA. In these set of experiments, the BZP control incubations without CsA revealed lower toxicity levels than those expected from the cytotoxicity curves, but this is likely explained by the steepness of the MTT cytotoxicity assay curve at these concentration ranges. The cells incubated with 50, 100, 250, and 500 μM TFMPP presented a significant ($p < 0.001$, ANOVA/Bonferroni) cytotoxic effect in the MTT assay. The incubation with CsA 1 μM was capable to slightly but significantly increase cell survival at the tested 50 and 100 μM TFMPP concentrations. However, the protective effects of CsA were not observed for the higher and more cytotoxic TFMPP concentrations. Incubation with MeOPP also resulted in a significant ($p < 0.001$, ANOVA/Bonferroni) cell death. CsA was able to significantly ($p < 0.05$, ANOVA/Bonferroni) increase cell survival only at 2000 μM MeOPP. The

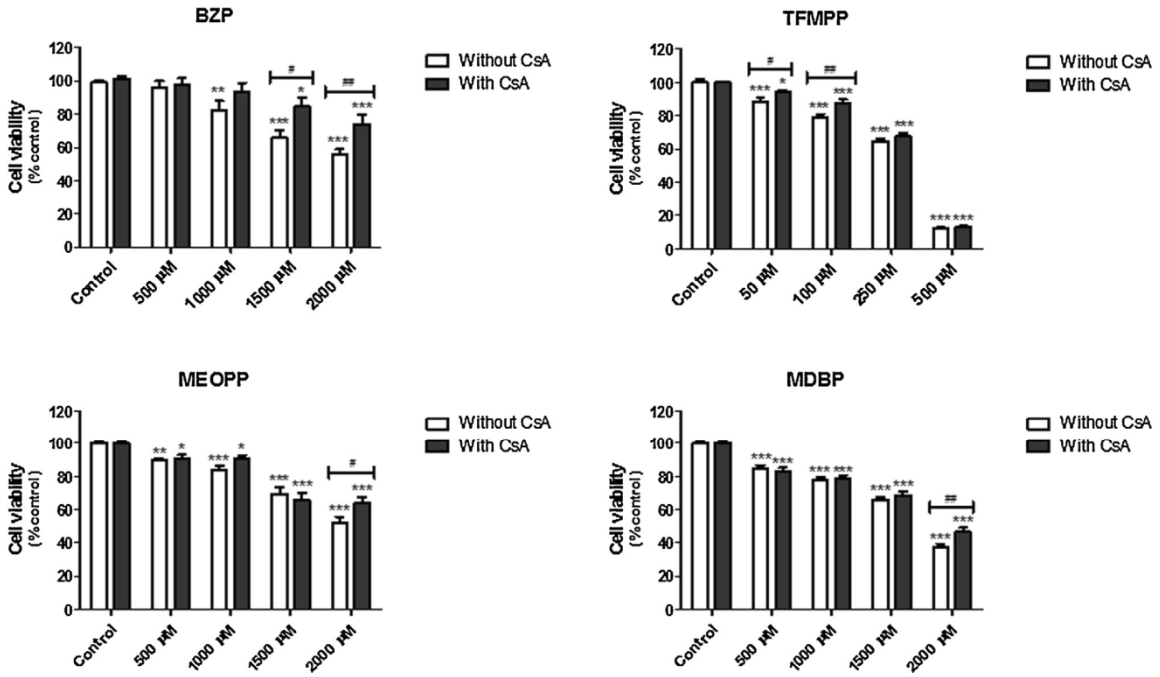

Fig. 7. Involvement of the mitochondrial permeability transition pore (MPTP) in the piperazine designer drugs-induced cell death. Viability was evaluated by the MTT reduction assay in H9c2 cells after 24 h incubations with the tested piperazine designer drugs with and without 30 min pre-incubation followed by co-incubation with 1 μM cyclosporine A (CsA) at 37 °C. Results are expressed as percentage control ± SEM ($n = 4$ independent experiments run in triplicates). Statistical comparisons were made using two-way ANOVA/Bonferroni post-hoc test, for comparisons vs the respective control condition (*$p < 0.05$; **$p < 0.01$; ***$p < 0.001$ vs control) and for comparison between the same concentration with or without 1 μM CsA (#$p < 0.05$; ##$p < 0.01$ vs incubation without 1 μM CsA).

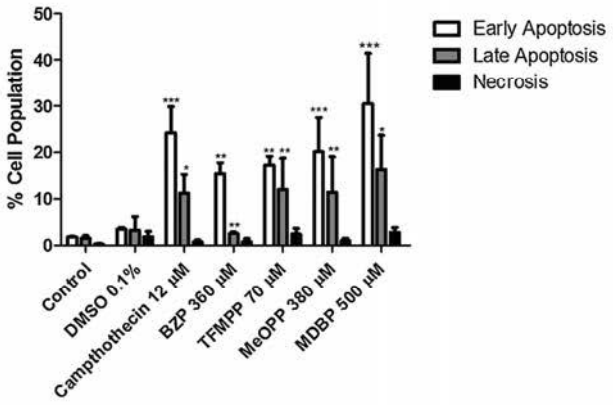

Fig. 8. Annexin V/PI staining of H9c2 cells after 24 h incubations with the tested piperazine designer drugs at 37 °C. The H9c2 cell population was divided into early apoptotic (annexin V+/PI−), late apoptotic (annexin V+/PI+), and necrotic (annexin V−/PI+) cells. Results are expressed as percentage cell population ± SEM ($n = 4$ independent experiments). Statistical comparisons were made using one-way ANOVA/Bonferroni post-hoc test (*$p < 0.05$; **$p < 0.01$; ***$p < 0.001$ vs control).

incubation with 1 μM CsA was also able to increase cell viability after MDBP incubations but only at the highest 2000 μM tested concentration of the drug. In spite of the observed increases in survival, cell viability after CsA incubations was still significantly lower than control ($p < 0.05$, ANOVA/Bonferroni).

In order to evaluate the mode of death, the cells were stained with annexin V-FITC and PI after 24 h incubations with the piperazine designer drugs at concentrations that approximately corresponded to their EC_{50} levels, as determined by the MTT assay. Fig. 8 depicts the relative number (percentage of cell population) of early apoptotic, late apoptotic (undergoing secondary necrosis) and necrotic H9c2 cells. At the tested concentrations, after incubation with all piperazine test drugs a high number of cells presenting early apoptosis features, i.e., stained only with annexin V-FITC could be observed relative to the control cell population (Fig. S1, Supplemented material). A high number of cells that were double-stained with both annexin V-FITC and PI were also found after the drug incubations. These cells are likely undergoing secondary necrosis and present features of both types of cell death. The number of necrotic cells did not significantly differ from control cells for any of the piperazine designer drugs.

Supplementry material related to this article found, in the online version, at http://dx.doi.org/10.1016/j.toxlet.2014.06.031.

Notwithstanding, when the activation of caspase-3, that is involved in the apoptotic cascade, was investigated, no significant changes in this downstream effector caspase activity were observed after 24 h incubations (data not shown).

4. Discussion

A recent survey in the UK found that piperazines are among the most common active recreational drugs in tablets purchased from internet supplier sites (Davies et al., 2010). These so-called party pills gained popularity in the 2000s as a legal and arguably safer alternative to MDMA. However, the available information on the toxic effects of piperazine designer drugs is currently very limited.

For the first time, we demonstrate that piperazine designer drugs produce cytotoxicity to H9c2 cells, a commercially available myogenic cell line derived from embryonic rat heart ventricle that has been considered suitable for the study of drug-induced cardiotoxicity (Watkins et al., 2011), specially due to their metabolic competence that parallels the metabolic capacity of the heart (Zordoky and El-Kadi, 2007). Among the four tested piperazine designer drugs, TFMPP was the most potent drug to elicit cytotoxic effects. This is in accordance with the cardiovascular effects experienced by users (Wood et al., 2008; Kovaleva et al., 2008; Gee et al., 2010). In this work, we used two viability tests, the MTT reduction and the NR uptake assays, to determine the cytotoxicity of the piperazine designer drugs. In spite of the differences in the obtained EC_{50} values, the cytotoxicity profile of the drugs was the same for the two tests. Discrepancies among different viability tests are quite commonly noted in the literature (Putnam et al., 2002; Weyermann et al., 2005; Pohjala et al., 2007; Kim et al., 2009; Zwolak, 2013). The main difference between these two assays is that MTT measures the activity of succinate dehydrogenase, which is present in the mitochondrial inner membrane (Putnam et al., 2002), while NR is based on the storage of NR dye in the lysosomes and probably in the golgi apparatus (Zwolak, 2013). Any damage to lysosomes/golgi apparatus decreases the cellular accumulation of the dye. On the other hand, mitochondrial succinate dehydrogenase is sensitive to local changes in ion concentrations and ion flux. It is not uncommon for some chemicals to increase metabolic activity in a cell, which would result in increased mitochondrial succinate dehydrogenase activity (Putnam et al., 2002). Also, MTT does not seem to be appropriate for the evaluation of cytotoxicity in cells with an unchanged reduction fluctuation by a high level of basal cellular reduction capacity and/or oxidant defense (Kim et al., 2009). In the present case, oxidative stress does not seem to contribute to the toxic effect of piperazine designer drugs in H9c2 cells, and the piperazine derivatives alter ionic concentration through the disruption of Ca^{2+} homeostasis. Therefore, MTT is probably not the best test for evaluation the cytotoxicity of the piperazine designer drugs. Accordingly, the NR cytotoxicty data agree much better with the oxidative stress and energetic imbalance endpoints additionally measured, while the MTT seems to overestimate the cytotoxic potential of the piperazine designer drugs.

Oxidative stress is a well-described mechanism underlying the toxicity of many xenobiotics, which plays an essential role in the cytotoxic effects of several amphetamine derivatives that induce the formation of highly reactive species (Dias da Silva et al., 2013b). Interestingly, piperazine designer drugs failed to induce reactive species formation, as measured through the DCFH-DA assay. GSH has an important protective role which involves its oxidant neutralizing and lipid peroxidase and/or tocopheryl radical-regenerating activities. Changes in the intracellular amounts of GSH and GSSG are, therefore, strong indicators of redox disturbances. In agreement with the DCFH-DA assay data, the intracellular GSH level remained significantly unchanged upon incubation with the piperazine designer drugs with the exception of MBDP. Our data indicate a decrease in intracelular tGSH content after incubation with MDBP for 24 h. However, these decreases were not accompanied by significant alterations in GSSG levels or inhibition of the GR enzymatic activity. A possible explanation for this result is that the GSSG formed through the free radicals neutralizing reactions of GSH could be extruded for the extracellular medium, contributing to the decrease in the tGSH levels. This GSSG efflux is a cellular response that protects the cells from oxidative stress (Rossato et al., 2011). However, since no formation of reactive species could be observed, it is not likely that the observed depletion in tGSH levels is due to increased GSSG formation. Depletion may be caused by inhibition of GSH biosynthesis (Gao et al., 2010), which occurs in the cytosol, and involves two enzymes: γ-glutamylcysteine ligase and GSH synthase, the first catalyzing the rate-limiting step of this biosynthetic pathway (Marí et al., 2013). A key role in GSH homeostasis is also played by γ-glutamyl transpeptidase (GGT), which breaks down extracellular GSH and provides cysteine, the rate-limiting substrate, for intracellular de novo synthesis of GSH

(Zhang et al., 2005). Another pathway involves the reduction of GSSG by GR producing two molecules of GSH. GR is known to be sensitive to chemical modification of its active thiol groups. Thus, the activity of GR can be modulated by the redox conditions of the reactive environment. Under extreme oxidising conditions, aggregates of GR may be formed, which decrease GR activity (Remião et al., 2000). However, according to our results, the piperazine designer drugs do not seem to have any influence on the GR activity.

In fact, it has been previously described that the cardiotoxicity of MDMA involves the formation of catechol metabolites that are oxidized into quinone intermediates following the demethylenation of MDMA (Hiramatsu et al., 1990) and methylenedioxyamphetamine (MDA) (Carvalho et al., 2004) leading to the production of the corresponding glutathione-*S*-yl-*N*-methyl-α-methyldopamine and glutathione-*S*-yl-α-methyldopamine conjugates. There is a striking similarity with the main metabolic pathways that were already described for MDBP in animals and in humans, namely the demethylenation of MDBP (Staack and Maurer, 2004), which can lead to the formation of similar GSH adducts, since a catechol intermediate is also formed. Although such conjugate formation is yet to be demonstrated, this possible metabolic bioactivation affords an alternative and reasonable explanation for the GSH decreases that were observed with only MDBP.

Cardiac myocytes are endowed with high content of mitochondria, equivalent to approximately 30% of the cellular volume, and maintain an elevated rate of ATP synthesis to satisfy the energy demand of the heart (Lax et al., 2009). Depletion of ATP is a typical feature of hypoxic and toxic injury and could be due to an alteration in mitochondrial function. Indeed, mitochondria seems to play an essential role in piperazine designer drugs-induced cardiotoxicity. Mitochondria is generally considered the 'powerhouse' of the cell in generating ATP, but they also play an important role in other aspects of normal cell functioning. Apart from ATP synthesis, mitochondrial Ca^{2+} uptake represents a major function of mitochondria; thus, regulating Ca^{2+}-dependent signalling pathways (Griffiths, 2000). Ca^{2+} uptake is driven by the electrochemical potential gradient generated by the combination of the $\Delta\psi m$ and the low concentration of Ca^{2+} in the matrix (Duchen, 1999). It is well established that mitochondria accumulate Ca^{2+} ions during cytosolic Ca^{2+} elevations in a variety of cell types including cardiomyocytes (Kumar et al., 2012). The downward electrochemical gradient across the inner membrane directs Ca^{2+} into the mitochondria through an uniporter. If mitochondrial buffering capacity is overwhelmed by elevated Ca^{2+}, mitochondrial matrix Ca^{2+} increases to levels high enough to trigger the opening of the mitochondrial permeability transition pore (MPTP). This involves the formation of pores in the inner membranes of pores with $\leq$1.5 kDa, allowing the influx of water and solutes into the matrix. Although MPTP can 'flicker' and be reversible, sustained transitions lead to the collapse of $\Delta\psi m$, cessation of ATP production, and cell death (Dong et al., 2006). Disruptions in Ca^{2+} homeostasis may abnormally alter myocardial excitability and contractility and induce arrhythmia or ventricular fibrillation. Increased intracellular Ca^{2+} may also affect signalling pathways, leading to diverse responses including fibrosis and hypertrophy (Tiangco et al., 2005).

Our data show that piperazine designer drugs alter the Ca^{2+} homeostasis, leading to an increase in cytosolic free Ca^{2+} levels, observed with 1000 μM BZP and MDBP, 500 μM MeOPP, and 50 μM TFMPP. At higher concentrations, the mitochondria buffering capacity was overwhelmed and led to the loss of $\Delta\psi m$ and mitochondrial depolarization and the depletion of ATP. In response to mitochondrial depolarization, the ATP synthase reverts to an ATPase activity, consuming ATP and pumping protons outwards, in a futile, energy consuming cycle (Duchen, 1999). According to the chemiosmotic theory of mitochondrial oxidative phosphorylation, $\Delta\psi m$ is the driving force behind oxidative phosphorylation. Thus, maintenance of $\Delta\psi m$ is extremely important for normal cell function (Mathur et al., 2000). Generation of $\Delta\psi m$ depends on a proton gradient across the inner mitochondrial membrane. It is known that translocation of protons from the matrix to the intermembrane space to establish $\Delta\psi m$ is coupled to the mitochondrial electron transport chain (Yuan and Acosta, 1996). Inhibition of chain activity undoubtedly diminishes $\Delta\psi m$, and this could be another pathway through which piperazine designer drugs decrease cellular energy and impair mitochondrial function. Using the same H9c2 cellular model, other studies conducted with MDMA, a drug which mimics the piperazine designer drugs effects, similarly demonstrated the involvement of increased intracellular Ca^{2+} concentrations and loss of $\Delta\psi m$ in the cytotoxic effects of the drug (Tiangco et al., 2005).

Since these results suggest the involvement of MPTP in these cytotoxic events, we pre-incubated cells with CsA and then further incubated the piperazines designer drugs in the presence of CsA. Cyclosporin A binds to cyclophilin D, part of the MPTP, causing inhibition of the MPTP opening and preventing cell death (Crompton, 1999). The incubations with CsA only partially, but significantly, prevented cell death induced by the tested piperazine drugs. It is plausible that the inhibition of MPTP open did not block Ca^{2+} influx and, therefore, did not prevent the alteration in the electron gradient across the inner membrane. Also, Ca^{2+} may possibly enter the matrix through alternative pathways other than the Ca^{2+} uniporter. Recently, growing bodies of evidence of other mechanisms related to the mitochondrial Ca^{2+} influx have been reported. These mechanisms involve the mitochondrial ryanodine receptor, a rapid mode of Ca^{2+} uptake, mitochondrial uncoupling proteins, and leucine zipper EF hand-containing transmembrane protein 1 (LETM1) Ca^{2+}/H^{+} antiporter. Ca^{2+} influx through these alternative Ca^{2+} uptake channels could also trigger MPTP opening (Yarana et al., 2012).

MPTP opening generally represents a catastrophe for the cell and will lead inexorably to cell death, either through ATP consumption, acute energy failure and necrosis or through the initiation of apoptosis (Duchen, 1999). Whereas the loss of ion homeostasis resulting from ATP depletion can lead to necrosis, MPTP opening also causes a leakage of cytochrome c from mitochondria, and thus, triggers a cascade of events that eventually lead to apoptosis (Chiu et al., 2008). Apoptotic cells are characterized by a set of distinct morphological changes, which can be classified as early and late apoptotic changes. The early marker of apoptosis is the exposition of phosphatidilserine on the cell surface (it is normally concentrated in the luminal layer of the cytoplasmic membrane), while, at the later stage, the entire phosphatidylserine is flipped on the outer membrane (Kumar et al., 2012). When the rate of apoptosis is substantially increased, the cells undergo secondary necrosis (or late apoptosis) with breakdown of membrane potential, cell swelling and cell contents release. These cells present features of both the apoptotic and necrotic cells and in many cases can only be accurately distinguished with detailed morphological analysis. When the mode of cell death was investigated, we found an unexpected high number of cells that were at an early apoptotic stage and a low number of necrotic cells. However, an elevated number of cells that were double-stained and most likely undergoing secondary necrosis was also noted for all the piperazine drugs; thus, agreeing with the previous data that clearly indicated a preferential necrotic cell death pathway characterized by the loss of $\Delta\psi m$, ATP depletion and MPTP opening. Accordingly, under our experimental conditions, we did not observe any activation of downstream effector caspase-3,

which also suggests that necrotic cell death would predominate. However, alternative mechanisms for apoptosis induction that are independent of caspases activation have been described. In fact, activation of calpains due to increased intracellular Ca^{2+} concentrations has been linked to cardiomyocyte death. A mechanism for ceramide-induced cardiomyocyte death with apoptosis induction, which can turn into necrosis, following ATP depletion, increased Ca^{2+} influx, mitochondrial network fragmentation and loss of the mitochondrial Ca^{2+} buffer capacity dependent on calpains activation and independent of caspases or reactive species production has been described (Parra et al., 2013). Nevertheless, the involvement of apoptotic and necrotic pathways should be further investigated for a better comprehension of the cell death mechanisms involved in the cytotoxicity of the piperazine designer drugs.

In conclusion, we describe, for the first time, the cardiotoxic effects of piperazine designer drugs in an in vitro model. Among the tested designer drugs, TFMPP was the most potent in inducing cytotoxicity. In H9c2 cells, piperazine designer drugs induced cell death by causing disturbances in Ca^{2+} homeostasis, ATP depletion, loss of $\Delta\psi m$ and MPTP opening. It should be noted that these drugs are frequently consumed in associations, such as TFMPP with BZP or BZP/TFMPP with MDMA, often in the same tablet. As previously observed with amphetamine designer drugs, marked toxicity can occur when the drugs are combined at individually non-cytotoxic concentrations (Dias da Silva et al., 2013a, 2013b, 2013c). Since combinations of piperazine designer drugs have already been implicated in human intoxications, further studies are needed not only to clarify the mechanisms involved in the observed cytotoxic effects of the isolated drugs but also to address the effects of such drug combinations.

Conflict of interest

The authors declare that there are no conflicts of interest.

Transparency document

The Transparency document associated with this article can be found in the online version.

Acknowledgements

Marcelo Dutra Arbo is the recipient of Coordenação de Aperfeiçoamento de Pessoal de Nível Superior (CAPES Foundation – Brazil) fellowship (Proc. BEX 0593/10-9). Renata Silva, Daniel José Barbosa and Luciana Grazziotin Rossato, were supported by fellowships (SFRH/BD/29559/2006, SFRH/BD/64939/2009 and SFRH/BD/63473/2009, respectively) from Fundação para a Ciência e Tecnologia (FCT), Portugal. This work was sponsored by the Portuguese Research Council Fundação para a Ciência e para a Tecnologia (FCT) [Grant No. PEst-C/EQB/LA0006/2011] and co-funded by the European Community Financial Support Program "Programa Operacional Factores de Competitividade do Quadro de Referência Estratégico Nacional (QREN POFC)".

References

Antia, U., Lee, H.S., Kydd, R.R., Tingle, M.D., Russell, B.R., 2009. Pharmacokinetics of 'party pill' drug *N*-benzylpiperazine (BZP) in healthy human participants. Forensic Sci. Int. 186, 63–67.

Antia, U., Tingle, M.D., Russel, B.R., 2010. Validation of an LC-MS method for the detection and quantification of BZP and TFMPP and their hydroxylated metabolites in human plasma and its application to the pharmacokinetic study of TFMPP in humans. J. Forensic Sci. 55, 1311–1318.

Arbo, M.D., Bastos, M.L., Carmo, H., 2012. Piperazine compounds as drugs of abuse. Drug Alcohol Depend. 122, 174–185.

Austin, H., Monasterio, E., 2004. Acute psychosis following ingestion of 'Rapture'. Australas. Psychiatry 12, 406–408.

Barbosa, D.J., Capela, J.P., Silva, R., Ferreira, L.M., Branco, P.S., Fernandes, E., Bastos, M. L., Carvalho, F., 2014. "Ecstasy"-induced toxicity in SH-SY5Y differentiated cells: role of hyperthermia and metabolites. Arch. Toxicol. 88, 515–531.

Carvalho, M., Carmo, H., Costa, V.M., Capela, J.P., Pontes, H., Remião, F., Carvalho, F., Bastos, M.L., 2012. Toxicity of amphetamines: an update. Arch. Toxicol. 86, 1167–1231.

Carvalho, M., Remião, F., Milhazes, N., Borges, F., Fernandes, E., Monteiro do, M.C., Gonçalves, M.J., Seabra, V., Amado, F., Carvalho, F., Bastos, M.L., 2004. Metabolism is required for the expression of ecstasy-induced cardiotoxicity in vitro. Chem. Res. Toxicol. 17, 623–632.

Chiu, P.Y., Luk, K.F., Leung, H.Y., Ng, K.M., Ko, K.M., 2008. Schisandrin B stereoisomers protect against hypoxia/reoxygenation-induced apoptosis and inhibit associated changes in Ca^{2+}-induced mitochondrial permeability transition and mitochondrial membrane potential in H9c2 cardiomyocytes. Life Sci. 82, 1092–1101.

Costa, V.M., Carvalho, F., Duarte, J.A., Bastos, M.L., Remião, F., 2013. The heart as a target for xenobiotic toxicity: the cardiac susceptibility to oxidative stress. Chem. Res. Toxicol. 26, 1285–1311.

Crompton, M., 1999. The mitochondrial permeability transition pore and its role in cell death. Biochem. J. 341, 233–249.

Davies, S., Wood, D.M., Smith, G., Button, J., Ramsey, J., Archer, R., Holt, D.W., Dargan, P.I., 2010. Purchasing 'legal highs' on the internet – is there consistency in what you get? QJM 103, 489–493.

Dawson, P., Moffatt, J.D., 2012. Cardiovascular toxicity of novel psychoactive drugs: lessons from the past. Prog. Neuro-Psychopharmacol. Biol. Psychiatry 39, 244–252.

Dias da Silva, D., Carmo, H., Silva, E., 2013a. The risky cocktail: what combination effects can we expect between ecstasy and other amphetamines? Arch. Toxicol. 87, 111–122.

Dias da Silva, D., Silva, E., Carmo, H., 2013c. Combination effects of amphetamines under hyperthermia – the role played by oxidative stress. J. Appl. Toxicol. doi: http://dx.doi.org/10.1002/jat.2889.

Dias da Silva, D., Carmo, H., Lynch, A., Silva, E., 2013b. An insight into hepatocellular death induced by amphetamines, individually and in combination: the involvement of necrosis and apoptosis. Arch. Toxicol. 87, 2165–2185.

Dong, Z., Saikumar, P., Weinberg, J.M., Venkatachalam, M.A., 2006. Calcium in cell injury and death. Annu. Rev. Pathol. Mech. Dis. 1, 405–434.

Duchen, M.R., 1999. Contributions of mitochondria to animal physiology: from homeostatic sensor to calcium signalling and cell death. J. Physiol. 516, 1–17.

Feuchtl, A., Bagli, M., Stephan, R., Frahnert, C., Kölsch, H., Kühn, K.U., Rao, M.L., 2004. Pharmacokinetics of m-chlorophenylpiperazine after intravenous and oral administration in healthy male volunteers: implication for the pharmacodynamic profile. Pharmacopsychiatry 37, 180–188.

Gao, W., Mizukawa, Y., Nakatsu, N., Minowa, Y., Yamada, H., Ohno, Y., Urushidani, T., 2010. Mechanism-based biomarker gene sets for glutathione depletion-related hepatotoxicity in rats. Toxicol. Appl. Pharmacol. 247, 211–221.

Gee, P., Gilbert, M., Richardson, S., Moore, G., Paterson, S., Graham, P., 2008. Toxicity from the recreational use of 1-benzylpiperazine. Clin. Toxicol. 46, 802–807.

Gee, P., Jerram, T., Bowie, D., 2010. Multiorgan failure from 1-benzylpiperazine ingestion – legal high or lethal high? Clin. Toxicol. 48, 230–233.

Gee, P., Richardson, S., Woltersdorf, W., Moore, G., 2005. Toxic effects of BZP-based herbal party pills in humans: a prospective study in Christchurch, New Zealand. NZ Med. J. 118, 1784–1794.

Gijsman, H.J., Van Gerven, J.M.A., Tieleman, M.C., Schoemaker, R.C., Pieters, M.S.M., Ferrari, M.D., Cohen, A.F., Van Kempen, G.M.J., 1998. Pharmacokinetic and pharmacodynamic profile of oral and intravenous meta-chlorophenylpiperazine in healthy volunteers. J. Clin. Psycopharmacol. 18, 289–295.

Griffiths, E.J., 2000. Mitochondria – potential role in cell life and death. Cardiovasc. Res. 46, 24–27.

Hiramatsu, M., Kumagai, Y., Unger, S.E., Cho, A.K., 1990. Metabolism of methylenedioxymethamphetamine: formation of dihydroxymethamphetamine and a quinone identified as its glutathione adduct. J. Pharmacol. Exp. Ther. 254, 521–527.

Kim, H., Toon, S.C., Lee, T.Y., Jeong, D., 2009. Discriminative cytotoxicity assessment based on various cellular damages. Toxicol. Lett. 184, 13–17.

Kimes, B.W., Brandt, B.L., 1976. Properties of a clonal muscle cell line from rat heart. Exp. Cell Res. 98, 367–381.

Kovaleva, J., Devuyst, E., De Paepe, P., Verstraete, A., 2008. Acute chlorophenylpiperazine overdose: a case report and review of the literature. Ther. Drug Monit. 30, 394–398.

Kumar, S., Kain, V., Sitasawad, S.L., 2012. High glucose-induced Ca^{2+} overload and oxidative stress contribute to apoptosis of cardiac cells through mitochondrial dependent and independent pathways. Biochim. Biophys. Acta 1820, 907–920.

Labonne, B.E.F., Gutiérrez, M., Gómez-Quiroz, L.E., Fainstein, M.K., Bucio, L., Souza, V., Flores, O., Ortíz, V., Hernández, E., Kershenobich, D., Gutiérrez-Ruiz, M.C., 2009. Acetaldehyde-induced mitochondrial dysfunction sensitizes hepatocytes to oxidative damage. Cell Biol. Toxicol. 25, 599–609.

Lax, A., Soler, F., Fernández-Belda, F., 2009. Mitochondrial damage as death inducer in heart-derived H9c2 cells: more than one way for an early demise. J. Bioenerg. Biomembr. 41, 369–377.

Lin, J.C., Bangs, N., Lee, H.S., Kydd, R.R., Russell, B.R., 2009. Determining the subjective and physiological effects of BZP on human females. Psychopharmacology (Berl.) 207, 439–446.

Lin, J.C., Jam, R.K., Lee, H.S., Jensen, M.A., Kydd, R.R., Russell, B.R., 2011. Determining the subjective and physiological effects of BZP combined with TFMPP in human males. Psycopharmacology 214, 761–768.

Marí, M., Morales, A., Colell, A., García-Ruiz, C., Kaplowitz, N., Fernández-Checa, J.C., 2013. Mitochondrial glutathione: features, regulation and role in disease. Biochim. Biophys. Acta 1830, 3317–3328.

Maurer, H.H., Kraemer, T., Springer, D., Staack, R.F., 2004. Chemistry, pharmacology, toxicology and hepatic metabolism of designer drugs of the amphetamine (ecstasy), piperazine, and pyrrolidinophenone types. Ther. Drug Monit. 26, 127–131.

Mathur, A., Hong, Y., Kemp, B.K., Barrientos, A.A., Erusalimsky, J.D., 2000. Evaluation of fluorescent dyes for the detection of mitochondrial membrane potential changes in cultured cardiomyocytes. Cardiovasc. Res. 46, 126–138.

Oliveira, J.M.A., Gonçalves, J., 2009. In situ mitochondrial Ca^{2+} buffering diferences of intact neurons and astrocytes from cortex and striatum. J. Biol. Chem. 284, 5010–5020.

Parra, V., Moraga, F., Kuzmicic, J., López-Crisosto, C., Troncoso, R., Torrealba, N., Criollo, A., Díaz-Elizondo, J., Rothermel, B.A., Quest, A.F.G., Lavandero, S., 2013. Calcium and mitochondrial metabolism in ceramide-induced cardiomyocyte death. Biochim. Biophys. Acta 1832, 1334–1344.

Pohjala, L., Tammela, P., Samanta, S.W., Yli-Kauhaluoma, J., Vuorela, P., 2007. Assessing the data quality in predictive toxicology using a panel of cell lines and cytotoxicity assays. Anal. Biochem. 362, 221–228.

Putnam, K.P., Bombick, D.W., Doolittle, D.J., 2002. Evaluation of eight in vitro assays for assessing the cytotoxicity of cigarette smoke condensate. Toxicol. in Vitro 16, 599–607.

Rao, K.M., Padmanabhan, J., Kilby, D.L., Cohen, H.J., Currie, M.S., Weinberg, J.B., 1992. Flow cytometric analysis of nitric oxide production in human neutrophils using dichlorofluorescein diacetate in the presence of a calmodulin inhibitor. J. Leukocyte Biol. 51, 496–500.

Remião, F., Carmo, H., Carvalho, F.D., Bastos, M.L., 2000. Inhibition of glutathione reductase by isoproterenol oxidation products. J. Enzym. Inhib. 15, 47–61.

Rossato, L.G., Costa, V.M., de Pinho, P.G., Carvalho, F., de Lourdes Bastos, M., Remião, F., 2011. Structural isomerization of synephrine influences its uptake and ensuing glutathione depletion in rat-isolated cardiomyocytes. Arch. Toxicol. 85, 929–939.

Rossato, L.G., Costa, V.M., Vilas-Boas, V., Bastos, M.L., Rolo, A., Palmeira, C., Remião, F., 2013. Therapeutic concentrations of mitoxantrone elicit energetic imbalance in H9c2 cells as an earlier event. Cardiovasc. Toxicol. 13, 413–425.

Scaduto Jr, R.C., Grotyohann, L.W., 1999. Measurement of mitochondrial membrane potential using fluorescent rhodamine derivatives. Biophys. J. 76, 469–477.

Schep, L.J., Slaughter, R.J., Vale, A., Beasley, M., Gee, G.P., 2011. The clinical toxicology of the designer "party pills" benzylpiperazine and trifluoromethylphenylpiperazine. Clin. Toxicol. 49, 131–141.

Smith, J.A., Weidemann, M.J., 1993. Further characterization of theneutrophil oxidative burst by flow cytometry. J. Immunol. Methods 162, 261–268.

Staack, R.F., Fritschi, G., Maurer, H.H., 2003. New designer drug 1-(3-trifluoromethylphenyl)piperazine (TFMPP): gas chromatography/mass spectrometry and liquid chromatography/mass spectrometry studies on its phase I and II metabolism and on its toxicological detection in rat urine. J. Mass Spectrom. 38, 971–981.

Staack, R.F., Maurer, H.H., 2004. New designer drug 1-(3,4-methylenedioxybenzyl) piperazine (MDBP): studies on its metabolism and toxicological detection in rat urine using gas chromatography/mass spectrometry. J. Mass Spectrom. 39, 255–261.

Staack, R.F., Maurer, H.H., 2005. Metabolism of designer drugs of abuse. Curr. Drug Metab. 6, 259–274.

Staack, R.F., Paul, L.D., Schmid, D., Roider, G., Rolf, B., 2007. Proof of 1-(3-chlorophenyl)piperazine (mCPP) intake – use as adulterant of cocaine resulting in drug–drug interations? J. Chromatogr. B 855, 127–133.

Staack, R.F., Theobald, D.S., Paul, L.D., Springer, D., Kraemer, T., Maurer, H.H., 2004. In vivo metabolism of the new designer drug 1-(4-methoxyphenyl)piperazine (MeOPP) in rat and identification of the human cytochrome P450 enzymes responsible for the major metabolic step. Xenobiotica 34, 179–192.

Thompson, I., Williams, G., Caldwell, B., Aldington, S., Dickson, S., Lucas, N., McDowall, J., Weatherall, M., Robinson, G., Beasley, R., 2010. Randomised double-blind, placebo-controlled trial of the effects of the 'party pills' BZP/TFMPP alone and in combination with alcohol. Psychopharmacology (Berl.) 24, 1208–1299.

Tiangco, D.A., Lattanzio Jr, F.A., Osgood, C.J., Beebe, S.J., Kerry, J.A., Hargrave, B.Y., 2005. 3,4-Methylenedioxymethamphetamine activates nuclear factor-κB, increases intracellular calcium, and modulates gene transcription in rat heart cells. Cardiovasc. Toxicol. 5, 301–310.

Watkins, S.J., Borthwick, G.M., Arthur, H.M., 2011. The H9C2 cell line and primary neonatal cardiomyocyte cells show similar hypertrophic responses in vitro. In Vitro Cell. Dev. Biol. Anim. 47, 125–131.

Weyermann, J., Lochmann, D., Zimmer, A., 2005. A practical note on the use of cytotoxicity assays. Int. J. Pharm. 288, 369–376.

Wood, D.M., Button, J., Lidder, S., Ramsey, J., Holt, D.W., Dargan, P.I., 2008. Dissociative and sympathomimetic toxicity associated with recreational use of 1-(3-trifluoromethylphenyl)piperazine (TFMPP) and 1-benzylpiperazine (BZP). J. Med. Toxicol. 4, 254–257.

Yarana, C., Sripetchwandee, J., Sanit, J., Chattipakorn, S., Chattipakorn, N., 2012. Calcium-induced cardiac mitochondrial dysfunction is predominantly mediated by cyclosporine A-dependent mitochondrial permeability transition pore. Arch. Med. Res. 43, 333–338.

Yuan, C., Acosta Jr, D., 1996. Cocaine-induced mitochondrial dysfunction in primary culture of rat cardiomyocytes. Toxicology 112, 1–10.

Zhang, H., Forman, H.J., Choi, J., 2005. Gamma-glutamyl transpeptidase in glutathione biosynthesis. Methods Enzymol. 401, 468–483.

Zordoky, B.N.M., El-Kadi, A.O.S., 2007. H9c2 cell line is a valuable in vitro model to study the drug metabolizing enzymes in the heart. J. Pharmacol. Toxicol. Methods 56, 317–322.

Zwolak, I., 2013. Comparison of five different *in vitro* assays for assessment of sodium metavanadate cytotoxicity in Chinese hamster ovary cells (CHO-KI line). Toxicol. Ind. Health 1–14 doi:http://dx.doi.org/10.1177/0748233713483199.

Study II

In vitro neurotoxicity evaluation of piperazine designer drugs in differentiated human neuroblastoma SH-SY5Y cells

(Submitted for publication in British Journal of Pharmacology)

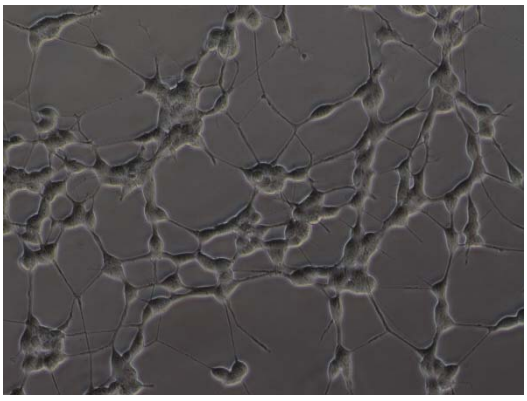

In vitro neurotoxicity evaluation of piperazine designer drugs in differentiated human neuroblastoma SH-SY5Y cells

M D Arbo[1a], R Silva[1], D J Barbosa[1,2], D Dias da Silva[1], S P Silva[3], J P Teixeira[3], M L Bastos[1], H Carmo[1]

[1]REQUI*M*TE, Laboratório de Toxicologia, Departamento de Ciências Biológicas, Faculdade de Farmácia, Universidade do Porto, Rua Jorge Viterbo Ferreira, 228, 4050-313, Porto, Portugal.

[2] Cell Division Mechanisms Group, Institute for Molecular and Cell Biology – IBMC, Rua do Campo Alegre, 823, 4150-180, Porto, Portugal.

[3] Instituto Nacional de Saúde Dr. Ricardo Jorge (INSA), Rua Alexandre Herculano, 321, 4000-055, Porto, Portugal.

Running title: *In vitro* neurotoxicity of piperazine designer drugs

- MD Arbo, R Silva, DJ Barbosa, D Dias da Silva and S Silva performed the research
- MD Arbo, ML Bastos and H Carmo designed the research
- JP Teixeira, ML Bastos and H Carmo supervised the research
- MD Arbo, R Silva, DJ Barbosa, D Dias da Silva, ML Bastos and H Carmo analysed the data
- MD Arbo wrote the paper
- JP Teixeira, ML Bastos and H Carmo revised the work critically

[a] Corresponding author:
M. D. Arbo (m.arbo@terra.com.br)
REQUI*M*TE, Laboratório de Toxicologia, Departamento de Ciências Biológicas, Faculdade de Farmácia, Universidade do Porto.
Rua Jorge Viterbo Ferreira, 228, Porto, 4050-313, Portugal.
Tel: +(351) 220428597

Abstract

Background and purpose

Abuse of synthetic drugs is widespread worldwide. Studies indicate that piperazine designer drugs act as dopaminergic and serotonergic substrates in the brain. This work aimed to investigate the cytotoxicity of N-benzylpiperazine (BZP), 1-(3-trifluoromethylphenyl)piperazine (TFMPP), 1-(4-methoxyphenyl)piperazine (MeOPP) and 1-(3,4-methylenedioxybenzyl)piperazine (MDBP) in the differentiated human neuroblastoma SH-SY5Y cell line.

Experimental approach

Cytotoxicity was evaluated after 24 h incubations through the MTT reduction and neutral red uptake assays. Oxidative stress (ROS/RNS production and GSH content) and energetic (ATP content) parameters, as well as intracellular Ca^{2+}, mitochondrial membrane potential, DNA damage (commet and LMW assays) and cell death mode were also evaluated.

Key results

Complete cytotoxicity curves were obtained after 24 h incubations with each drug. A significant decrease in intracellular total GSH content was noted for all the tested drugs. All drugs caused a significant increase of intracellular free Ca^{2+} levels, accompanied by mitochondrial hyperpolarization. However, ATP levels remained unchanged. The investigation of cell death mode revealed a predominance of early apoptotic cells. The commet and the LMW assays revealed that, under our experimental conditions, piperazine designer drugs elicited cytotoxicity but not genotoxicity in differentiated SH-SY5Y cells.

Conclusions and implications

Among the tested drugs, TFMPP seemed to be the most cytotoxic. Overall, piperazine designer drugs are potentially neurotoxic compounds, supporting concerns on risks associated with the abuse of these drugs.

Keywords: piperazine designer drugs, cytotoxicity, Ca^{2+} overload, mitochondrial hyperpolarization, apoptosis.

Abbreviations

5-HT, serotonin; % TDNA, percentage of DNA in the comet tail; ATP, adenosine triphosphate; BZP, N-benzylpiperazine; BSA, bovine serum albumin; DAT, dopamine transporter; DCFH-DA, dichlorodihydrofluorescein diacetate; DCFH, dichlorodihydrofluorescein; DMEM, Dulbecco's modified Eagle's medium; DTNB, 5,5'-dithio-bis(2-nitrobenzoic) acid; EDTA, ethylenediaminetetracetic acid; FBS, fetal bovine serum; GSH, reduced glutathione; GSSG, oxidized glutathione; LMW, low molecular weight; *m*CPP, 1-(3-chlorophenyl)piperazine; MDBP, 1-(3,4-methylenedioxybenzyl)piperazine; MDMA, 3,4-methylenedioxymethamphetamine; MeOPP, 1-(4-methoxyphenyl)piperazine; MTT, 3-(4,5-dimethylthiazol-2-yl)-2,5-diphenyltetrazolium bromide; β-NADPH, reduced β-nicotinamide adenine dinucleotide; NEAA, non-essential aminoacids; *p*FPP, 1-(4-fluorophenyl)piperazine; PI, propidium iodide; ROS, reactive oxygen species; RNS, reactive nitrogen species; SERT, serotonin transporter; TFMPP, 1-(3-trifluoromethylphenyl)piperazine; TMRE, tetramethylrhodamine ethyl ester perchlorate; TNB, 5-thio-2-nitrobenzoic acid; TPA, 12-*O*-tetradecanoylphorbol-13-acetate

Introduction

Designer drugs, synthethic drugs, new psychoactive substances or, more recently, legal highs, are terms used to designate a class of substances synthesized from chemical precursors to produce compounds with similar effects but structurally different from controlled substances. The abuse of designer drugs has increased substantially since the 1990s. They have been produced clandestinely and the internet has been used for the production, sale and purchase of these compounds. It is estimated that more than 70% of users of legal highs manifest adverse effects, with approximately 5% of these individuals requiring hospitalization (Bilinski et al., 2012; Albertson, 2013). Among these new substances, piperazine designer drugs emerged in the market in the early 2000s. They can be divided into two classes, the benzylpiperazines, such as *N*-benzylpiperazine (BZP) and its methylenedioxy- analogue 1-(3,4-methylenedioxybenzyl)piperazine (MDBP), and the phenylpiperazines, such as 1-(3-chlorophenyl)piperazine (*m*CPP), 1-(4-fluorophenyl)piperazine (*p*FPP), 1-(3-trifluoromethylphenyl)piperazine (TFMPP), and 1-(4-

methoxyphenyl)piperazine (MeOPP) (figure 1). Generally, they are consumed as capsules, tablets or pills but also in powder or liquid forms (Gee et al., 2005) under several names, such as “Rapture,” “Frenzy,” “Bliss,” “Charge,” “Herbal ecstasy,” “A2,” “Legal X”, “Legal E” or simply party pills. Very often these are mixtures of different piperazines combined with adulterants including caffeine, vitamins or even drugs, such as 3,4-methylenedioxymethamphetmine (MDMA, “Ecstasy”) and cocaine (Staack et al., 2007).

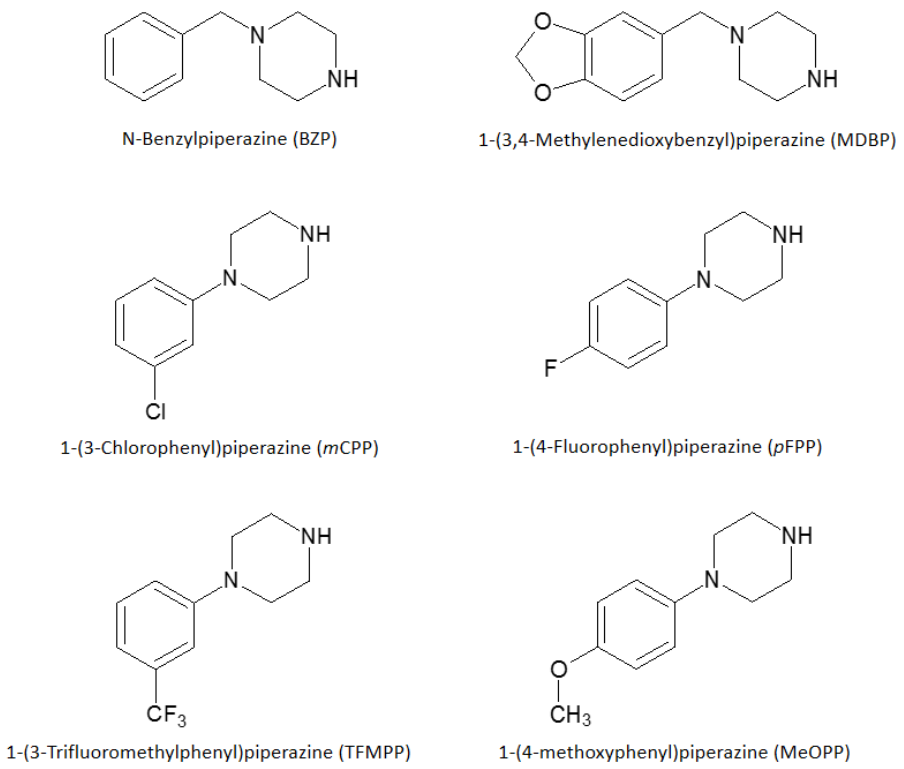

Figure 1. Chemical structure of some piperazine designer drugs.

The most commonly abused piperazines are BZP and TFMPP. TFMPP acts both presynaptically, as a substrate releaser at the serotonin transporter (SERT), and as a non-selective 5-HT receptor agonist. On the other hand, BZP acts on central dopaminergic substrates such as D_1-like receptors and dopamine transporters (DATs). It has been reported that the combined use of BZP and TFMPP in pills (mixed at a 2:1 ratio, in most cases) mimics the effects of MDMA in humans. It is therefore believed that this combination aggregates the stimulant effect of BZP, through its dopaminergic action, with the hallucinogenic effects of TFMPP, via serotonergic activation. Less information is available on MeOPP and MDBP derivatives, however they have relatively high

monoamine reuptake and releasing activities, as revealed in rat brain synaptossomes (for review see Arbo et al., 2012).

The nervous system is particularly sensitive to toxic insults due to a number of intrinsic characteristics, such as dependence upon aerobic metabolism, the presence of axonal transport, or the processes of neurotransmission. Piperazine designer drugs cross the blood-brain barrier and animal studies reported that tissue concentrations were up to 40 times higher than blood for BZP and 385 times higher for TFMPP (Antia et al., 2009), indicating that they achieve high tissue concentrations. High plasma levels of BZP were associated with seizures in party pills abusers (Gee et al., 2008). In case-reports, neurobehavioral symptoms already described include psychotic episode (Austin and Monasterio, 2004), dissociative symptoms (Wood et al., 2008), status epilepticus (Gee et al., 2010), anxiety, agitation and drowsiness (Kovaleva et al., 2008). There is one case of death after BZP intake in who a 23 year-old woman died after a massive brain oedema, but the patient ingested MDMA concomitantly (Balmelli et al., 2001), and therefore an inequivocal direct relationship between BZP intake and death could not be established.

Notwithstanding, in the drug scene, piperazines have the reputation of being safe, and there are presently no studies regarding their neurotoxicity that could help understanding the aforementioned detrimental effects of these drugs. Thus, the aim of this work was to study the *in vitro* neurotoxicity of the piperazine designer drugs BZP, TFMPP, MeOPP, and MDBP using the differentiated human neuroblastoma SH-SY5Y cell line.

Methods

Chemicals

N-Benzylpiperazine (BZP, 99.3% purity) was purchased from Chemos GmbH (Regenstauf, Germany), 1-(3-trifluoromethylphenyl)piperazine (TFMPP, 98% purity) was acquired from Alfa Aesar (Karlsruhe, Germany), 1-(4-methoxyphenyl)piperazine (MeOPP, 96% purity) was purchased from Acros Organics (New Jersey, USA), and 1-(3,4-methylenedioxybenzyl)piperazine (MDBP, 97% purity) was purchased from Aldrich Chemistry (Steinheim, Germany). Heat inactivated fetal bovine serum (FBS), trypsin (0.25%)-ethylenediamine tetraacetic acid (EDTA) (1 mM), antibiotic (10,000 U/mL

penicillin, 10,000 µg/mL streptomycin), Hanks balanced salt solution (HBSS), and phosphate buffer (PBS) and non-essential aminoacids (NEAA) were obtained from Gibco Laboratories (Lenexa, KS, USA). Fluo-3 AM and SyberGold were obtained from Molecular Probes (Eugene, OR). Agarose was obtained from Bioron (Ludwigshafen, Germany). Flow cytometry reagents (BD Facs-Flow™ and Facs-Clean™) were purchased from BD Biosciences (Becton, Dickinson, and Company, San Jose, CA, USA). All other chemicals and reagents were obtained from Sigma-Aldrich (St. Louis, USA)

Cell culture and differentiation

SH-SY5Y cells (ATCC, Manassas, VA, USA) were routinely cultured in 25 cm^2 flasks (Corning Costar, Corning, NY, USA) using DMEM with GlutMAX™ and 4.5 g/L glucose, supplemented with 10% heat inactivated FBS, 1% NEAA, 100 U/mL of penicillin, and 100 µg/mL of streptomycin. Cells were maintained at 37 °C in a humidified 5% CO_2-95% air atmosphere. Cultures were subcultivated weekly by trypsinization (0.25% trypsin/EDTA). The SH-SY5Y cells used in all experiments were taken between the 21st and 31st passages. To increase the dopaminergic neuronal phenotype, SH-SY5Y cells were differentiated as described previously (Barbosa et al., 2014a,b). Briefly, cells were seeded at an initial density of 25,000 cells/cm^2, in complete medium containing 10 µM retinoic acid, and cultured for 3 days. After seeding, the final volume of medium in 48- and 6-well culture plates (Corning Costar, Corning, NY, USA) was 250 µL and 2 mL, respectively. After 3 days *in vitro*, 50 or 400 µL of medium containing 480 nM 12-*O*-tetradecanoylphorbol-13-acetate (TPA) were added to each well of the 48- or 6-well culture plates (80 nM final TPA concentration), respectively, and cells were cultured for another 3 days. Stock solutions of retinoic acid (10 mM) and TPA (80 µM) were prepared in DMSO. Final concentration of DMSO in each well was 0.2% (v/v).

Cytotoxicity assays

The cytotoxicity was evaluated through the MTT reduction and NR uptake assays. Cells were seeded at a density of 100,000 cells/mL in 48-well plates (final volume of 250 µL; ~25,000 cells/cm^2). Stock solutions of BZP were made up in PBS. Stock solutions of TFMPP, MeOPP and MDBP were made in DMSO. In these cases, 0.1% DMSO in culture medium was used as negative control. All stock solutions were stored at -20 °C and

freshly diluted on the day of the experiment. Concentration-response curves were obtained incubating the cells with 0 – 20 mM of BZP, TFMPP, MeOPP, or MDBP for 24 h at 37°C. Triton X-100 1% was used as positive control.

MTT reduction assay

The MTT reduction assay was performed as previously described (Barbosa et al., 2014b). This assay measures cellular dehydrogenases activity, an indicator of metabolically active mitochondria, and therefore of cell viability. After the 24h incubation period, the cells were incubated at 37°C with fresh medium containing 0.5 mg/mL MTT. After 3 h incubation, the cell culture medium was removed, and the formed formazan crystals dissolved in DMSO. The absorbance was measured at 550 nm in a multi-well plate reader (BioTek Instruments, Vermont, USA). Results were presented as percentage of cell death versus concentration. All drugs were tested in 3 independent experiments with each concentration tested in 6 replicates within each experiment.

Neutral red (NR) uptake assay

The NR uptake assay was performed as described by Arbo et al. (2014). At the end of 24 h incubations of differentiated SH-SY5Y cells, the medium was replaced by fresh medium containing 50 µg/mL NR. The cells were incubated at 37°C for 3 h. Thereafter, the cells were lysed with a 50% ethanol:1% glacial acid acetic solution. The absorbance was measured at 540 nm in a multi-well plate reader. The percent cell death relative to the control cells was used as the cytotoxicity measure. All drugs were tested in 3 independent experiments with each concentration tested in 6 replicates within each experiment.

Measurement of intracellular reactive oxygen (ROS) and nitrogen (RNS) species

The intracellular ROS and RNS production was monitored by means of the DCFH-DA assay as previously described (Barbosa et al., 2014b). Cells were seeded as described for cytotoxicity and differentiated for 6 days. The cells were incubated with the piperazine designer drugs (500 or 1000 µM BZP, 5, 50 or 100 µM TFMPP, and 250 or 500

μM MeOPP or MDBP) at 37 °C for 24 h. H_2O_2 (150 μM) was used as a positive control. Fluorescence was recorded on a fluorescence microplate reader set to 485 nm excitation and 530 nm emission at times 0, 1, 2, 3, 4, 5, 6, 7, 8, and 24 h after incubation. The data obtained were calculated as fold increase over control conditions from 3 independent experiments with each concentration tested in 3 replicates within each experiment.

Measurement of intracellular glutathione levels

Cells were seeded at a density of 119,000 cells/mL in 6-well plates (final volume of 2 mL, ~25,000 cell/cm^2) and differentiated for 6 days. Cells were incubated at 37°C with the piperazine designer drugs (500 or 1000 μM BZP, 5, 50 or 100 μM TFMPP, and 250 or 500 μM MeOPP or MDBP). After a 24 h incubation period, the medium was removed and the cells were scraped with PBS in ice (pH=7.4). After centrifugation (210 g, 5 min, 4 °C), the supernatant was removed and the cell pellet was lysed with 5% $HClO_4$ and centrifuged (16,000 g, 10 min, 4 °C). The tGSH levels were evaluated by the DTNB/GSSG reductase assay, as previously described (Barbosa et al., 2014b). The stoichiometric formation of 5-thio-2-nitrobenzoic acid (TNB) was followed every 10 s for 3 min at 415 nm and at 30 °C, and then compared with a standard curve. For the determination of GSSG, 10 μL of 2-vinylpyridine were added to 200 μL aliquots of the acidic supernatants and mixed continuously for 1 h, in ice, for derivatization of the sulfhydryl groups (SH). GSSG was then measured by the same DTNB-GSH reductase recycling assay. The GSH content was calculated according to the formula: [GSH = tGSH – (2 x GSSG)]. The final results were expressed as % of control from 5 independent experiments with each concentration tested in 3 replicates within each experiment.

Measurement of intracellular ATP levels

Cells were seeded, treated, and incubated following the same protocol used for the measurement of GSH levels. After centrifugation (210 g, 5 min, 4 °C), the supernatant was removed. The pellet was lysed with 5% $HClO_4$, centrifuged (16,000 g, 10 min, 4 °C), and the supernatant obtained was frozen at -20°C until further determination of the ATP intracellular content. The ATP levels were quantified by a bioluminescence assay, as described by Rossato et al. (2013). The emitted light intensity was determined using a luminescence microplate reader and compared with a standard curve. The final results

were expressed as % of control from 5 independent experiments with each concentration tested in 2 replicates within each experiment.

Flow cytometry analysis of intracellular Ca^{2+} levels

Intracellular Ca^{2+} levels were evaluated with the sensitive fluorochrome Fluo3-AM. A protocol previously described (Barbosa et al., 2014b) was used with minor modifications. Cells were seeded at a density of 119,000 cells/mL in 6-well plates (final volume of 2 mL, ~25,000 cells/cm^2). After 6 days of differentiation, the medium was replaced by fresh medium containing 100 or 350 μM BZP, 0.5, 1 or 5 μM TFMPP, and 25 or 50 μM MeOPP or MDBP. Twenty-four hours after exposure, the cells were harvested by trypsinization (0.25% trypsin/EDTA), centrifuged (300 g, 5 min, 4 °C), and then loaded with 10 μM Fluo3-AM in 50 μL serum-free DMEM without phenol red, for 30 min, at 37 °C, in a water bath with shaking. After this incubation period, the cells were centrifuged (300 g, 5 min, 4 °C) washed with HBSS (with Ca^{2+} and Mg^{2+}), centrifuged again and kept on ice until flow cytometry analysis.

Sample analysis was performed in a FACSCalibur™ flow cytometer (BD, CA, USA), equipped with a 488 nm argon ion laser, using CellQuest software (BD Biosciences). The green fluorescence of Fluo3 was measured by a 530 ± 15 nm band-pass filter (FL1). After resuspending the cell pellet in HBSS (with Ca^{2+} and Mg^{2+}) with 0.5 μg/mL propidium iodide (PI) (after permeating dead cells, PI interlaces with the nucleic acid helix with consequent increase in fluorescence intensity emission at 615 nm), data from at least 15,000 viable cells (based on their forward and side light scatter) were collected from each test condition. In order to detect a possible contribution from cells auto-fluorescence to the analyzed fluorescence signals, portions of cell suspension (with or without exposure to the drugs), which were not incubated with Fluo3-AM, were analyzed in the 530 ± 15 nm band-pass filter (FL1). Results are presented as Fluo3 fluorescence intensity (% of control) from at least 6 independent experiments with each concentration tested in 2 replicates within each experiment.

Assessment of mitochondrial membrane potential (Δψm)

Assessment of mitochondrial integrity was performed by measuring TMRE inclusion as described by Dias da Silva et al. (2013). Cells were seeded as described for cytotoxicity. After 6 days of differentiation, the medium was gently aspirated and the cells were incubated with the piperazine designer drugs (500 or 1000 µM for BZP, 5, 50 or 100 µM for TFMPP, and 250, 500, 1000 or 2000 µM MeOPP or MDBP). Fluorescence was measured on a fluorescence microplate reader set to 544 nm excitation and 590 nm emission. The data obtained were calculated as the percentage of control conditions from at least 6 independent experiments with each concentration tested in 2 replicates within each experiment.

Cell death mode: apoptosis vs necrosis

Cell death analysis was performed by staining differentiated SH-SY5Y cells with Annexin V-FITC and PI (FITC Annexin V Apoptosis Detection Kit, BD Biosciences, USA) as described by Arbo et al. (2014). To perform the assay, SH-SY5Y cells were seeded at a density of 100,000 cells/mL in 48-well plates (final volume of 250 µL, ~25,000 cells/cm^2). After 6 days of differentiation, the cells were incubated with 17.5 µM BZP, 0.92 µM TFMPP, 3.7 µM MeOPP and 2.3 µM MDBP. After the 24 h incubation period, the medium was removed and 100 µL binding buffer was added, followed by 2 µL PI and 3 µL annexin V-FITC. Plates were incubated in the dark at room temperature. After 15 min, the cells were observed under a fluorescence microscope (Nikon, Tokyo, Japan). Five pictures per well were taken and the percentages of early apoptotic cells were estimated by counting the annexin V-positive but PI-negative cells, whereas the percentages of late apoptotic cells were estimated by counting the number of cells which were both annexin V-positive and PI-positive. Necrotic cells were the PI-positive but annexin V-negative ones. Campthotecin 12 µM was used as a positive control for apoptosis. The results are expressed as % cell population from 4 independent experiments.

Comet Assay

Cells were seeded as described for cytotoxicity. After 6 days of differentiation, the medium was aspirated and the cells were incubated with the piperazine designer drugs (500 or 1000 µM for BZP, 5, 50 or 100 µM for TFMPP, and 250 or 500 µM MeOPP or

MDBP). At the end of the 24 h incubation period, cells were harvested by trypsinization (0.05% trypsin/EDTA), centrifuged (300 g, 5 min, 4 °C), and then ressuspended in HBSS (without Ca^{2+} and Mg^{2+}). The alkaline comet assay was performed as described by Singh et al (1988) with minor modifications (Costa el al., 2008). A medium-throughput version of the comet assay, 12-Gel Comet Assay Unit ™ (Severn Biotech Ltd) was used. Briefly, two aliquots of 5 µl of each cell suspension were dispersed in 0.6% (w/v) low-melting point agarose in PBS and dropped onto a frosted slide pre-coated with 1% layer of normal melting point agarose. Slides were immersed into cold (4ºC) lysis solution (2.5 M NaCl, 100 mM Na_2EDTA, 10 mM Tris-base, 0.25 M NaOH, pH 10; 1% Triton X100) for at least 1 h at 4 ºC in the dark. Slides were then incubated with electrophoresis solution (1 mM Na_2EDTA, 300 mM NaOH) for 20 min at 4 ºC before electrophoresis, carried out for 20 min at 30 V (1.1 V/cm). After that, the slides were neutralised by washing them in PBS for 10 min and rinsed in distilled water for a further 10 min. DNA was fixed by immersing the slides in 70% ethanol for 15 min and in absolute ethanol for a further 15 min before letting them dry overnight. Dryed slides were stained with SYBR®Gold and 100 cells (50 cells per gel) were scored using the semi-automated image analysis system Comet Assay IV (Perceptive Instruments, UK). Microscopic analyses were performed on a Nikon Eclipse E400 Epi-fluorescence microscope. The percentage of DNA in the comet tail (% TDNA) was the DNA damage parameter evaluated to describe comet formation (Doktorovova et al., 2014). Concurrently with the comet assay, an extra and identical replicate comet slide was prepared, lysed and immediately fixed and stained without electrophoresis for evaluation of the cytotoxicity through the Low Molecular Weight (LMW) DNA diffusion assay (Vasquez, 2010). Gels were prepared from at least 4 independent experiments with each concentration tested in 2 replicates in each experiment.

Statistical analysis

For the cytotoxicity evaluation, concentration-response curves were fitted by the least squares method. The comparisons between curves (bottom, top and $logEC_{50}$) were made using the extra sum-of-squares F test. Results of all other biochemical measures are presented as mean ± standard error of the mean (SEM) from at least 3 independent experiments. Normality of the data distribution was assessed by the Kolmogorov–Smirnov test. Statistical comparisons between groups were performed with one-way ANOVA (when data followed normal distribution) or the Kruskal–Wallis test. Significance was

accepted at $p<0.05$. Details of the statistical analysis are provided in the text and legend of the figures.

Results

Piperazine designer drugs elicited concentration-dependent cytotoxicity in differentiated SH-SY5Y cells

Figure 2 presents the obtained concentration-response curves for MTT (A) and NR (B) assays. All tested drugs produced concentration-dependent cytotoxic effects. A summary of the calculated EC_{50} values (representing the half-maximum-effect concentrations from the fitted curves) is presented in Table 1. Significant differences were observed for the EC_{50} values of the curves. It was evident that TFMPP was the most cytotoxic of the tested piperazine designer drugs. For the NR uptake assay, the EC_{50} values were higher than those obtained for the MTT assay. However, the cytotoxicity profile observed was quite similar to those observed for the MTT reduction assay (Table 1, figure 2B).

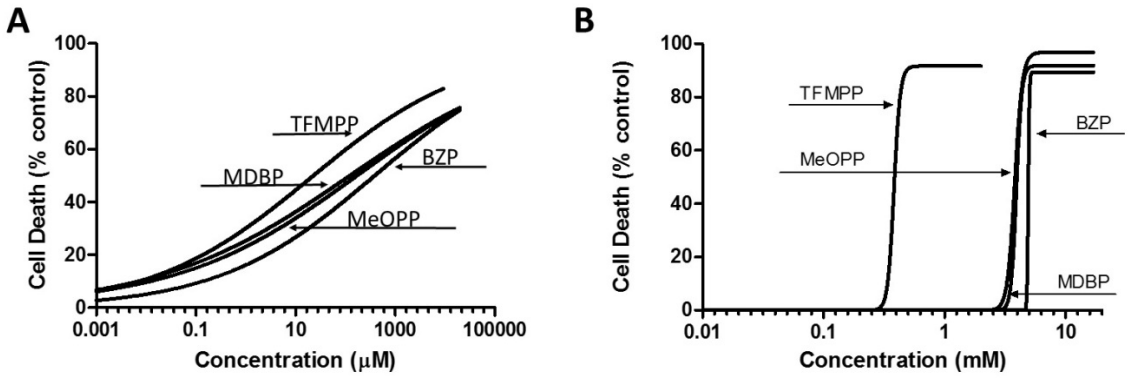

Figure 2. Concentration-response (cell death) curves of the tested piperazine designer drugs after 24 h incubation in differentiated SH-SY5Y cells at 37°C. Cell viability was evaluated by the MTT reduction (A) and the neutral red uptake (B) assays. Data are presented as percentage of cell death relative to the respective negative controls. Three independent experiments were performed (six replicates tested for each concentration within each experiment). Curves were fitted using least squares as the fitting method.

Table 1. EC_{50} values of the piperazine designer drugs

Designer Drug	EC_{50} MTT (μM)	EC_{50} NR (μM)
BZP	$721.4^{\#\$\&}$	$4920^{\#\$\&}$
TFMPP	$41.0^{*\$\&}$	$386^{*\$\&}$
MeOPP	$274.7^{\#}$	$3819^{*\#}$
MDBP	$144.3^{*\#}$	$3954^{*\#}$

* compares to BZP, # compares to TFMPP; $ compares to MeOPP; & compares to MDBP. The cytotoxicity curves were fitted using least squares as the fitting method. Comparisons were made using the extra sum-of-squares F test ($p<0.05$).

Piperazine designer drugs elicited tGSH depletion in differentiated SH-SY5Y cells

Under our experimental conditions no significant changes in reactive species generation were found for any of the tested piperazine drugs (data not shown).

Changes in the intracellular amounts of GSH and GSSG are strong indicators of redox disturbances. Intracellular levels of oxidized glutathione (GSSG) were found to be below the quantification limit of the method (0.25 μM). Therefore, only intracellular total GSH results are presented. Piperazine designer drugs elicited a significant ($p<0.01$, ANOVA/Bonferroni) concentration-dependent depletion of the intracellular total GSH levels (figure 3).

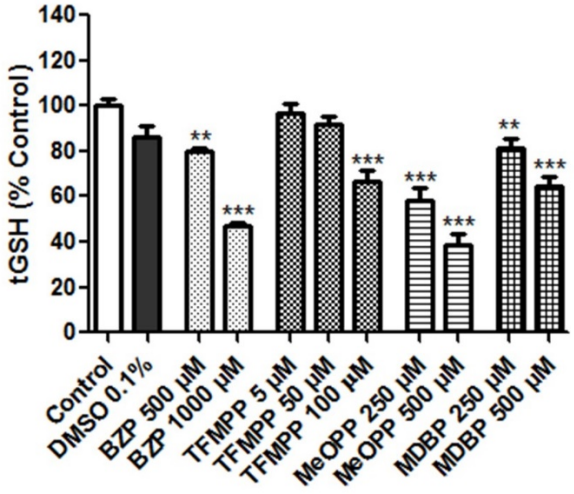

Figure 3. Intracellular contents of total glutathione (tGSH) in differentiated SH-SY5Y cells after 24 h incubations with the tested piperazine designer drugs at 37 °C. Results are expressed as % control±SEM (n=5 independent experiments run in triplicates). Statistical comparisons were made using one-way ANOVA/Bonferroni post-hoc test (** $p<0.01$; *** $p<0.001$ vs control).

Piperazine designer drugs disturbed Ca^{2+} homeostasis

Intracellular Ca^{2+} homeostasis is critical for maintaining the normal cell function and variations in intracellular Ca^{2+} levels can determine cell survival or death (Oliveira and Gonçalves, 2009). As depicted in figure 4, incubation of differentiated SH-SY5Y cells with piperazine designer drugs significantly increased the intracelular Ca^{+2} levels in a concentration-dependent manner ($p<0.05$, Kruskal-Wallis/Dunn's).

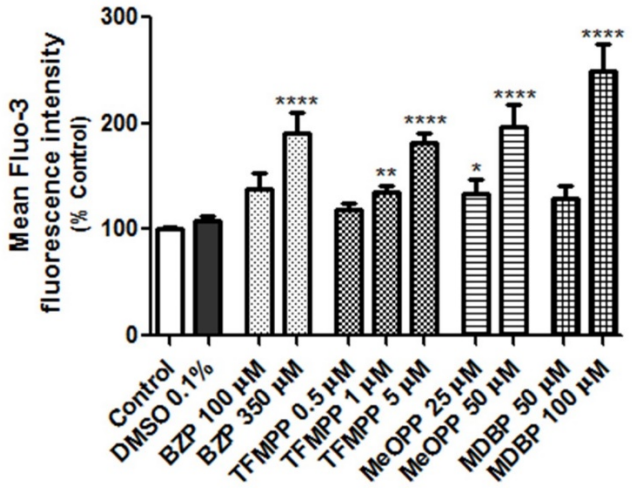

Figure 4. Intracellular levels of Ca^{2+} in differentiated SH-SY5Y cells after 24 h incubations with the tested piperazine designer drugs at 37 °C. Results are expressed as % control±SEM (n=6 independent experiments run in duplicate). Statistical comparisons were made using the non-parametric Kruskal-Wallis/Dunn's post hoc test (* $p<0.05$; ** $p<0.01$; **** $p<0.0001$ vs control).

Piperazine designer drugs hyperpolarized mitochondria

As shown in figure 5, a significant increase in Δψm ($p<0.05$, ANOVA/Bonferroni) can be observed after 24 h incubations of differentiated SH-SY5Y cells.

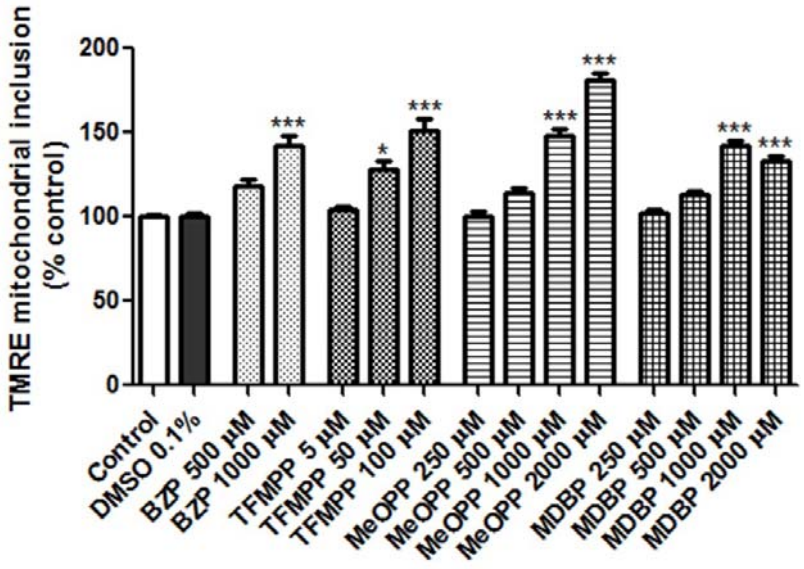

Figure 5. Mitochondrial membrane potential (Δψm) measured as TMRE incorporation in mitochondria of differetiated SH-SY5Y cells after 24 h incubations with the tested piperazine designer drugs at 37 °C. Results are expressed as % control±SEM (n=6 independent experiments run in duplicate). Statistical comparisons were made using one-way ANOVA/Bonferroni post-hoc test (* $p<0.05$; *** $p<0.001$ vs control).

Energetic status was evaluated through the measurement of intracellular ATP levels, which remained unaltered under our experimental conditions at the concentrations tested.

Piperazine designer drugs induced apoptosis in differentiated SH-SY5Y cells

The mode of cell death was investigated with the piperazine designer drugs at non cytotoxic concentrations. Figure 6 depicts the relative number (% of cell population) of viable, early apoptotic, late apoptotic and necrotic differentiated SH-SY5Y cells. At the tested concentrations, a high number of cells presenting early apoptosis features, i.e., stained only with annexin V-FITC could be observed relative to the control cell population. For TFMPP and MeOPP, also a significant number of cells that were double-stained with both annexin V-FITC and PI were found after the drug incubations. These cells are likely undergoing secondary necrosis and present features of both types of cell death. The number of necrotic cells did not significantly differ from control cells for any of the piperazine designer drugs.

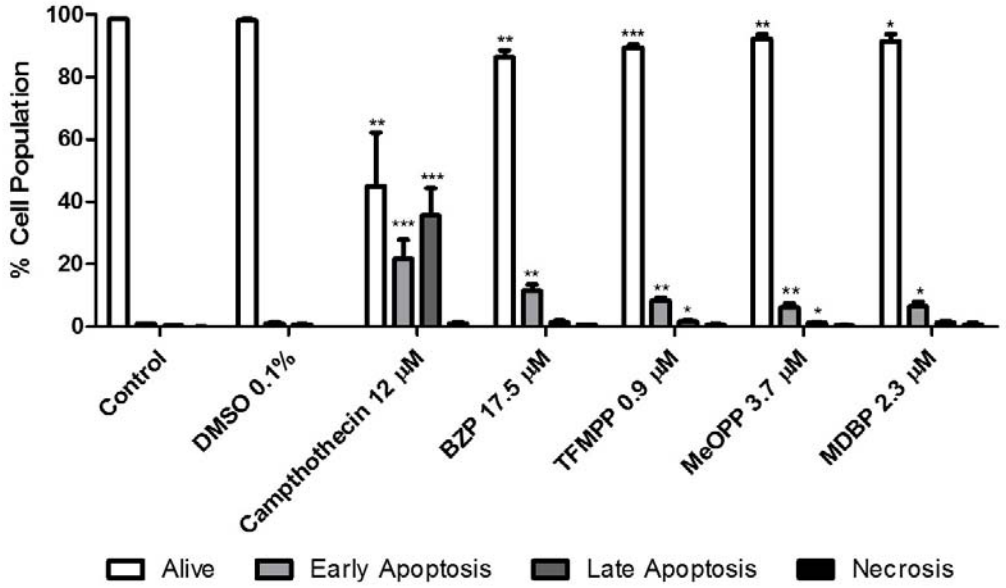

Figure 6. Annexin V/PI staining of differentiated SH-SY5Y cells after 24 h incubations with the tested piperazine designer drugs at 37 °C. The differentiated SH-SY5Y cell population was divided into alive, early apoptotic (annexin V+/PI-), late apoptotic (annexin V+/PI+), and necrotic (annexin V-/PI+) cells. Results are expressed as % cell population±SEM (n=3 independent experiments). Statistical comparisons were made using one-way ANOVA/Bonferroni post-hoc test (* $p<0.05$; ** $p<0.01$; *** $p<0.001$ vs control).

Piperazine designer drugs elicited cytototoxicity but not genotoxicity in differentiated SH-SY5Y cells

Genotoxicity is the capacity of a compound or material to damage DNA. DNA damage is generally considered as the underlying cause of hereditary changes. However, cell death also leads to DNA fragmentation. Depending on the degree and stage of apoptosis/necrosis of the cells at the time that the comet slides are prepared, cytotoxicity-related DNA fragmentation can contribute to increased DNA migration levels in the total cell population that can be misinterpreted as a genotoxic effect (i.e. 'false positive') or it can contribute to decreasing DNA migration levels (i.e. 'false negative') due to the loss of detectable DNA following lysis and electrophoresis (Vasquez, 2010). Therefore, it must be ascertained whether detected positive responses in the comet assay are due to genotoxicity rather than cytotoxicity.

As shown in figure 7A, piperazine designer drugs did not induce DNA breaks in the alkaline comet assay under our experimental conditions. However there was a significant increase ($p<0.01$, ANOVA/Bonferroni) in DNA migration in LMW DNA diffusion test as depicted in figure 7B. The DNA degradation caused by endonuclease activity during

apoptosis or necrosis indicates that piperazine designer drugs caused cytotoxicity, but not genotoxicity, to the tested cells.

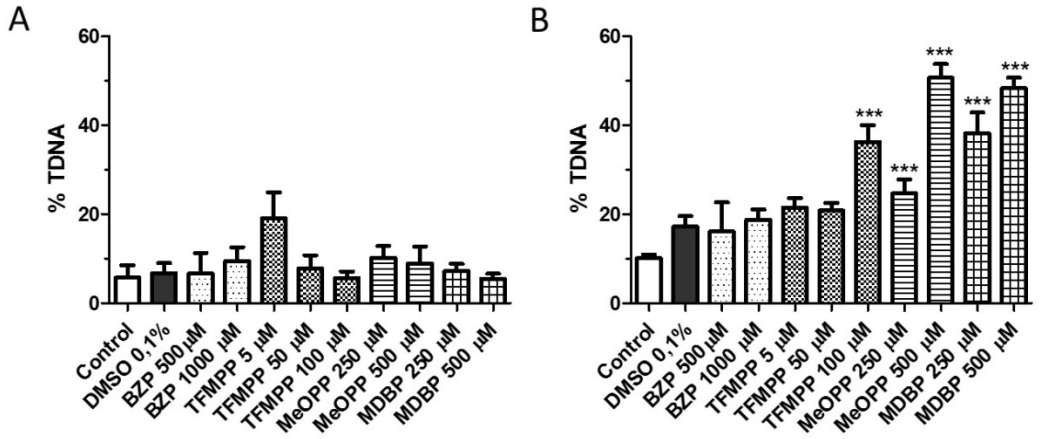

Figure 7. DNA damaged in alkaline comet assay (A) and low molecular weight (LMW) DNA diffusion assay (B) in differentiated SH-SY5Y cells after 24 h incubations with the tested piperazine designer drugs. Values are expressed as means±SEM from 4 independent experiments (n=4). Statistical comparisons were made using one-way ANOVA/Bonferroni post-hoc test (** $p<0.01$; *** $p<0.001$ vs control).

Discussion & Conclusions

For the first time, we demonstrate that piperazine designer drugs produce cytotoxicity to differentiated SH-SY5Y cells. These cells are a fairly homogeneous neuroblast-like cell line. They exhibit neuronal marker enzyme activity (tyrosine and dopamine-β-hydroxylases), specific uptake of norepinephrine (NA), and express neurofilament proteins. They also express opioid, muscarinic, and nerve growth factor receptors. Retinoic acid/TPA-differentiated SH-SY5Y cells develop a dopaminergic phenotype and have higher levels of tyrosine hydroxylase, DAT (Barbosa et al., 2014b), and dopaminergic D_2 and D_3 receptors but lower levels of VMAT than undifferentiated cells (Xie et al., 2010).

Among the four tested piperazine designer drugs, TFMPP was the most potent cytotoxic compound. The MTT reduction and the NR uptake assays were used to determine the cytotoxicity profile of the piperazine designer drugs. In spite of the differences in the obtained EC_{50} values, the cytotoxicity profile of the drugs was similar for the two tests. Discrepancies among different viability tests are quite commonly noted in the literature (Putnam et al., 2002; Weyermann et al., 2005; Pohjala et al., 2007; Kim et

al., 2009; Zwolak, 2013) and were also observed in our previous study on the *in vitro* cardiotoxicity of piperazine designer drugs (Arbo et al., 2014). The difference between these two assays is that MTT measures the activity of succinate dehydrogenase, an enzyme present in the mitochondrial inner membrane (Putnam et al., 2002), while NR is based on the storage of NR dye in the lysosomes and Golgi apparatus (Zwolak, 2013). Any damage to lysosomes/Golgi apparatus decreases the cellular accumulation of the dye. On the other hand, mitochondrial succinate dehydrogenase is sensitive to local changes in ion concentrations and flux. It is not uncommon for some chemicals to induce an increase in cellular metabolic activity, which would result in increased mitochondrial succinate dehydrogenase activity (Putnam et al., 2002). Thus, as piperazine derivatives alter ionic concentration through the disruption of Ca^{2+} homeostasis, MTT is probably not the best test to evaluate the cytotoxicity of these drugs, but could be a good marker of the mitochondrial disfunction.

Oxidative stress is a well-described mechanism underlying the toxicity of many xenobiotics, which plays an essential role in the cytotoxic effects of several amphetamine derivatives that induce the formation of highly reactive species (Barbosa et al., 2014b; Dias da Silva et al., 2014). Interestingly, piperazine designer drugs did not induce significant changes in reactive species formation. In spite of this, our data indicate a decrease in intracelular tGSH content after 24 h incubation with all piperazine designer drugs. GSH has an important protective role in the cell. Changes in the intracellular amounts of GSH and GSSG are therefore strong indicators of redox disturbances. A previous *in vitro* study showed that these drugs do not interfere with the activity of GSH reductase (GR), the enzyme responsible for the reduction of GSSG into GSH (Arbo et al., 2014). As a protection of the cells against oxidative stress, the GSSG formed through the free radicals neutralizing reactions of GSH could be extruded to the extracellular medium, contributing to the decrease in the tGSH levels. Also, depletion may be caused by inhibition of GSH biosynthesis (Gao et al., 2010), which occurs in the cytosol and involves two enzymes: γ-glutamylcysteine ligase and GSH synthase, the first catalyzing the rate-limiting step of this biosynthetic pathway (Marí et al., 2013). A key role in GSH homeostasis is also played by γ-glutamyl transpeptidase (GGT), which breaks down extracellular GSH and provides cysteine, the rate-limiting substrate for intracellular *de novo* synthesis of GSH (Zhang et al., 2005). Further studies to clarify the mechanisms involved are therefore necessary to better understand the changes in the redox status of the cells caused by these piperazine designer drugs.

Apart from ATP synthesis, mitochondrial Ca^{2+} uptake represents a major function of mitochondria, thus regulating Ca^{2+}-dependent signalling pathways (Griffths, 2000). Perturbations of sequestration of Ca^{2+} within the mitochondrial matrix have been reported to play an integral role in glutamatergic excitotoxic injury (Vergun et al., 1999; Vergun et al., 2001). Alterations in cytosolic Ca^{2+} levels can be induced by several factors. The best known is that mitochondria and other intracellular Ca^{2+} stores, such as the endoplasmic reticulum, become overfilled with Ca^{2+}, leading to exaggerated increases in cytosolic Ca^{2+} levels. Modulation of Ca^{2+} re-uptake due to changes in Ca^{2+}-ATPase expression or Ca^{2+}-ATPase inhibition are also responsible for increasing cytosolic Ca^{2+} levels. Although the effects of excess cytosolic Ca^{2+} can initially be subtle and have negligible effects, with increasing age (or chronic low level toxicological exposure), the Ca^{2+} homeostatic machinery becomes less effective, ultimately leading to Ca^{2+}-induced neuronal cell death (Al-Mousa and Michelangeli, 2012). Piperazine designer drugs altered the Ca^{2+} homeostasis, increasing free Ca^{2+} levels. In the same cellular model, MDMA and its metabolites increased the intracellular free Ca^{2+} levels but when an intracellular Ca^{2+} quelator was used, it was shown that Ca^{2+} did not influence the cell death induced by the compounds (Barbosa et al., 2014b). Methadone caused necrotic-like death in SH-SY5Y cells after Ca^{2+} homeostasis perturbation and mitochondrial dysfunction (Perez-Alvarez et al., 2010). In our previous study, using H9c2 cardiomyoblasts, piperazine designer drugs increased intracellular Ca^{2+} levels, and led to mitochondrial permeability transition pore opening and cell death (Arbo et al., 2014).

The $\Delta\psi m$ is the central parameter controlling the accumulation of Ca^{2+} and ATP synthesis. Piperazine designer drugs induced an increase in $\Delta\psi m$, which can be seen as mitochondrial hyperpolarization. A hyperpolarization of $\Delta\psi m$ has been previously described in hippocampal neurons exposed to staurosporine (Poppe et al., 2001) and 30 min oxygen glucose deprivation (Iijima et al., 2003), and also in primary rodent cortical neurons exposed to HIV-1 regulatory protein transactivator of transcription protein (Perry et al., 2005). A positive correlation was established between $\Delta\psi m$ and neuronal survival, with neurons displaying a more pronounced $\Delta\psi m$ hyperpolarization surviving longer (Ward et al., 2007). Hyperpolarization silences DA-containing neurons by inhibiting their spontaneous activity, which ultimately controls DA release in the somatodendritic and terminal areas. Transient reduction in neuronal activity could be neuroprotective, as it lowers ATP consumption necessary to maintain ion gradients, but it may also reduce the expression of activity-dependent genes, such as neurotrophins. Notably, the hyperpolarized state is also accompanied by intracellular accumulation of Ca^{2+} and Na^{+}

ions that might initiate a cascade of unfavourable events that establish a permanent damage to neurons (Guatteo et al., 2005). According to our findings, the increase in intracellular Ca^{2+} levels may lead to mitochondrial hyperpolarization and this, in turn, to the conservation of ATP levels.

Apoptotic cells are characterized by a set of distinct morphological changes, which can be classified as early and late apoptotic changes. The early marker of apoptosis is the release of phosphatidilserine on the cell surface (it is normally concentrated in the luminal layer of the cytoplasmic membrane), while, at the later stage, the entire phosphatidylserine is flipped on the outer membrane (Kumar et al., 2012). When the rate of apoptosis is substantially increased, the cells undergo secondary necrosis (or late apoptosis) with breakdown of membrane potential, cell swelling and cell contents release. When the cell death mode was investigated, we found a high number of cells that were at an early apoptotic stage and a low number of necrotic cells. This indicates that piperazine designer drugs probably activate preferentially apoptotic cell death cascade instead of necrotic process.

Apoptotic cell cascade comprise several pathways, the most common involves downstream caspase activation. Another important pathway involves calpains, that are Ca^{2+}-dependent proteases involved in apoptotic and necrotic processes which could, in turn, be activated by piperazine designer drugs due to the increased intracellular Ca^{2+} levels (Jiang et al., 2010). Previous studies in SH-SY5Y cells showed that increased intracellular Ca^{2+} levels induced the degradation of the apoptotic protease-activating factor-1 (APAF-1), reducing the ability of cytochrome c to activate caspase-3-like proteases and inducing apoptotic pathways dependent on calpains (Reimertz et al., 2001). This pathway was also observed after incubation of SH-SY5Y cells with prion protein fragment PrP-(106-126) (O'Donovan et al., 2001).

In conclusion, we describe, for the first time, the potential of piperazine designer drugs to induce neurotoxicity in an *in vitro* model. Among the tested designer drugs, TFMPP was the most potent in inducing cytotoxicity. In differentiated SH-SY5Y cells, piperazine designer drugs induced cell death by causing disturbances in Ca^{2+} homeostasis, leading to apoptosis. Considering that these drugs have already been implicated in human intoxications, further studies are needed not only to clarify the mechanisms involved in the observed cytotoxic effects of the isolated drugs but also to address the effects of combinations of them.

Acknowledgements

Marcelo Dutra Arbo is the recipient of Coordenação de Aperfeiçoamento de Pessoal de Nível Superior (CAPES Foundation – Brazil) fellowship (Proc. BEX 0593/10-9). Renata Silva and Daniel José Barbosa were supported by fellowships (SFRH/BD/29559/2006 and SFRH/BD/64939/2009, respectively) from Fundação para a Ciência e Tecnologia (FCT), Portugal. This work was sponsored by the Portuguese Research Council Fundação para a Ciência e para a Tecnologia (FCT) [Grant No. PEst-C/EQB/LA0006/2011] and co-funded by the European Community financial support program "Programa Operacional Factores de Competitividade do Quadro de Referência Estratégico Nacional (QREN POFC)".

Conflict of interest statement

The authors declare that there is no conflict of interest.

References

Albertson TE (2013). Recreational drugs of abuse. Clin Rev Allergy Immunol 46: 1-2.

Al-Mousa F, Michelangeli F (2012). Some commonly used brominated flame retardants cause Ca^{2+}-ATPase inhibition, beta-amyloid peptide release and apoptosis in SH-SY5Y neuronal cells. PLoS One 7: e33059.

Antia U, Tingle MD, Russel BR (2009) 'Party pill' drugs - BZP and TFMPP. N Z Med J 122: 55-68.

Arbo MD, Bastos ML, Carmo H (2012). Piperazine compounds as drugs of abuse. Drug Alcohol Depend 122: 174-185.

Arbo MD, Silva R, Barbosa DJ, Dias da Silva D, Rossato LG, Bastos ML *et al.* (2014). Piperazine designer drugs induce toxicity in cardiomyoblast h9c2 cells through mitochondrial impairment. Toxicol Lett 229: 178-189.

Austin H, Monasterio E (2004). Acute psychosis following ingestion of 'Rapture'. Australas Psychiatry 12: 406–408.

Balmelli C, Kupferschmidt H, Rentsch K, Schneemann M (2001). Fatal brain edema after ingestion of ecstasy and benzylpiperazine. Dtsch Med Wochenschr 126: 809–811.

Barbosa DJ, Capela JP, Silva R, Ferreira LM, Branco PS, Fernandes E *et al.* (2014a). "Ecstasy"-induced toxicity in SH-SY5Y differentiated cells: role of hyperthermia and metabolites. Arch Toxicol 88: 515-531.

Barbosa DJ, Capela JP, Silva R, Villas-Boas V, Ferreira LM, Branco OS *et al.* (2014b). The mixture of "ecstasy" and its metabolites is toxic to human SH-SY5Y differentiated cells at in vivo relevant concentrations. Arch Toxicol 88: 455-473.

Bilinski P, Kapka-Skrzypczak L, Jablonski P (2012). Determining the scale of designer drugs (DD) abuse and risk to public health in Poland through an epidemiological study in adolescents. Ann Agric Environ Med 19: 357-364.

Costa S, Coelho P, Costa C, Silva S, Mayan O, Santos LS *et al.* (2008). Genotoxic damage in pathology anatomy laboratory workers exposed to formaldehyde. Toxicology, 252: 40-48.

Dias da Silva D, Carmo H, Lynch A, Silva E. (2013). An insight into hepatocellular death induced by amphetamines, individually and in combination: the involvement of necrosis and apoptosis. Arch Toxicol 87: 2165-2185.

Dias da Silva D, Silva E, Carmo H (2014). Combination effects of amphetamines under hyperthermia – the role played by oxidative stress. J Appl Toxicol 34: 637-650.

Doktorovova S, Silva AM, Gaivão I, Souto EB, Teixeira JP, Martins-Lopes P (2014). Comet assay reveals no genotoxicity risk of cationic solid lipid nanoparticles. J Appl Toxicol 34: 395-403.

Gao W, Mizukawa Y, Nakatsu N, Minowa Y, Yamada H, Ohno Y *et al.* (2010). Mechanism-based biomarker gene sets for glutathione depletion-related hepatotoxicity in rats. Toxicol Appl Pharmacol 247: 211-221.

Gee P, Gilbert M, Richardson S, Moore G, Paterson S, Graham P (2008). Toxicity from the recreational use of 1-benzylpiperazine. Clin Toxicol 46: 802-807.

Gee P, Jerram T, Bowie D (2010). Multiorgan failure from 1-benzylpiperazine ingestion – legal high or lethal high? Clin Toxicol 48: 230-233.

Gee P, Richardson S, Woltersdorf W, Moore G (2005). Toxic effects of BZP-based herbal party pills in humans: a prospective study in Christchurch, New Zealand. NZ Med J 118: 1784–1794.

Griffiths EJ (2000). Mitochondria – potential role in cell life and death. Cardiovasc Res 46: 24-27.

Guatteo E, Marinelli S, Geracitano R, Tozzi A, Federici M, Bernardi G *et al.* (2005). Dopamine-containing neurons are silenced by energy deprivation: a defensive response or beginning of cell death? Neurotoxicology 26: 857-868.

Iijima T, Mishima T, Akagawa K, Iwao Y (2003). Mitochondrial hyperpolarization after transient oxygen-glucose deprivation and subsequent apoptosis in cultured rat hippocampal neurons. Brain Res 993: 140-145.

Jiang SX, Zheng R-Y, Zeng J-Q, Li X-L, Han, Z, Hou ST (2010). Reversible inhibition of intracellular calcium influx through NMDA receptors by imidazoline I_2 receptor antagonists. Eur J Pharmacol 629: 12-19.

Kim H, Toon SC, Lee TY, Jeong D (2009). Discriminative cytotoxicity assessment based on various cellular damages. Toxicol Lett 184: 13-17.

Kovaleva J, Devuyst E, De Paepe P, Verstraete A (2008). Acute chlorophenylpiperazine overdose: a case report and review of the literature. Ther Drug Monit 30: 394-398.

Kumar S, Kain V, Sitasawad SL (2012). High glucose-induced Ca^{2+} overload and oxidative stress contribute to apoptosis of cardiac cells through mitochondrial dependent and independent pathways. Biochim Biophys Acta 1820: 907-920.

Marí M. Morales A, Colell A, García-Ruiz C, Kaplowitz N, Fernández-Checa JC (2013). Mitochondrial glutathione: features, regulation and role in disease. Biochim Biophys Acta 1830: 3317-3328.

O'Donovan CN, Tobin D, Cotter TG (2001). Prion protein fragment PrP-(106-126) induce apoptosis via mitochondrial disruption in human neuronal SH-SY5Y cells. J Biol Chem 23: 43516-43523.

Oliveira JMA, Gonçalves J (2009). In situ mitochondrial Ca^{2+} buffering diferences of intact neurons and astrocytes from cortex and striatum. J Biol Chem 284: 5010-5020.

Perez-Alvarez S, Cuenca-Lopez MD, Melero-Fernández de Mera RM, Puerta E, Karachitos A, Bednarczyk P *et al.* (2010). Methadone induces necrotic-like cell death in SH-SY5Y cells by an impairment of mitochondrial ATP synthesis. Biophys Biochem Acta 1802: 1036-1047.

Perry SW, Norman JP, Litzburg A, Zhang D, Dewhurst S, Gelbard HA (2005). HIV-1 transactivator of transcription protein induces mitochondrial hyperpolarization and synaptic stress leading to apoptosis. J Immunol 174: 4333-4344.

Pohjala L, Tammela P, Samanta SW, Yli-Kauhaluoma J, Vuorela P (2007). Assessing the data quality in predictive toxicology using a panel of cell lines and cytotoxicity assays. Anal Biochem 362: 221-228.

Poppe M, Reimertz C, Dussmann H, Krohn AJ, Luetjens CM, Bockelmann D *et al.* (2001). Dissipation of potassium and proton gradients inhibits mitochondrial hyperpolarization and cytochrome c release during neural apoptosis. J Neurosci 21: 4551-4563.

Putnam KP, Bombick DW, Doolittle DJ (2002). Evaluation of eight in vitro assays for assessing the cytotoxicity of cigarette smoke condensate. Toxicol In Vitro 16: 599-607.

Reimertz C, Kögel D, Lankiewicz S, Poppe M, Prehn JHM (2001). Ca^{2+}-induced inhibition of apoptosis in human SH-SY5Y neuroblastoma cells: degradation of apoptotic protease activating factor-1 (APAF-1). J Neurochem 78: 1256-1266.

Rossato LG, Costa VM, Vilas-Boas V, Bastos ML, Rolo A, Palmeira C *et al.* (2013). Therapeutic concentrations of mitoxantrone elicit energetic imbalance in H9c2 cells as an earlier event. Cardiovasc Toxicol 13: 413-425.

Singh N, McCoy M, Tice R, Schneider E (1988). A simple technique for quantitation of low levels of DNA damage in individual cells. Exp Cell Res 175: 184-191.

Staack RF, Paul LD, Schmid D, Roider G, Rolf B (2007). Proof of 1-(3-chlorophenyl)piperazine (mCPP) intake – use as adulterant of cocaine resulting in drug-drug interations? J Chromatogr B 855: 127–133.

Vasquez MZ (2010). Combining the *in vivo* comet and micronucleus assays: a practical approach to genotoxicity testing and data interpretation. Mutagenesis 25: 187-199.

Vergun O, Keelan J, Khodorov BI, Duchen MR (1999). Glutamate-induced mitochondrial depolarisation and perturbation of calcium homeostasis in cultured rat hippocampal meurones. J Physiol 519: 451-466.

Vergun O, Sobolevsky AI, Yelshansky MV, Keelan J, Khodorov BI, Duchen MR (2001). Exploration of the role of reactive oxygen species in glutamate neurotoxicity in rat hippocampal neurones in culture. J Physiol 531: 147-163.

Ward MW, Huber HJ, Weisová P, Düssmann H, Nicholls DG, Prehn JHM (2007). Mitochondrial and plasma membrane potential of cultured cerebellar neurons during glutamate-induced necrosis, apoptosis, and tolerance. J Neurosci 27: 8238-8249.

Weyermann J, Lochmann D, Zimmer A (2005). A practical note on the use of cytotoxicity assays. Int J Pharm 288: 369-376.

Wood DM, Button J, Lidder S, Ramsey J, Holt DW, Dargan PI (2008). Dissociative and sympathomimetic toxicity associated with recreational use of 1-(3-trifluoromethylphenyl)piperazine (TFMPP) and 1-benzylpiperazine (BZP). J. Med. Toxicol. 4: 254-257.

Xie H, Hu L, Li G (2010). SH-SY5Y human neuroblastoma cell line: in vitro cell model of dopaminergic neurons in Parkinson´s disease. Chin Med J 123: 1086-1092.

Zhang H, Forman HJ, Choi J (2005). Gamma-glutamyl transpeptidase in glutathione biosynthesis. Methods Enzymol 401: 468-483.

Zwolak I (2013). Comparison of five different in vitro assays for assessment of sodium metavanadate cytotoxicity in Chinese hamster ovary cells (CHO-KI line). Toxicol Ind Health 1-14. Doi 10.1177/0748233713483199

Study III

Hepatotoxicity of piperazine designer drugs: comparison of different *in vitro* models

(To be submitted to Archives of Toxicology)

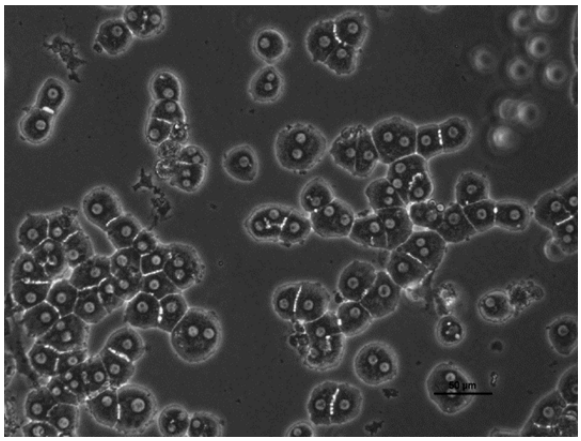

Hepatotoxicity of piperazine designer drugs: comparison of different *in vitro* models

Marcelo Dutra Arbo[*#], Diana Dias-da-Silva[*#], Maria João Valente, Maria de Lourdes Bastos, Helena Carmo

REQUI*M*TE, Laboratório de Toxicologia, Departamento de Ciências Biológicas, Faculdade de Farmácia, Universidade do Porto, Rua Jorge Viterbo Ferreira, 228, Porto, 4050-313, Portugal.

[#]Both authors contributed equally to this work

*Corresponding authors:

D. Dias da Silva (diana.dds@gmail.com)

M. D. Arbo (m.arbo@terra.com.br)

REQUIMTE, Laboratório de Toxicologia, Departamento de Ciências Biológicas, Faculdade de Farmácia, Universidade do Porto.

Rua Jorge Viterbo Ferreira, 228, Porto, 4050-313, Portugal.

Tel: +351 220428597

Abstract

Piperazine derived drugs emerged on the drug market in the last decade and have been often found as one of the main psychoactive substances present in tablets and pills sold on the internet. The aim of this study was to investigate *in vitro* the potential hepatotoxicity of the designer drugs N-benzylpiperazine (BZP), 1-(3-trifluoromethylphenyl)piperazine (TFMPP), 1-(4-methoxyphenyl)piperazine (MeOPP) and 1-(3,4-methylenedioxybenzyl)piperazine (MDBP) in two human hepatic cell lines (HepaRG and HepG2) and in primary rat hepatocytes. Cell death was evaluated by the MTT assay, after 24h-incubations. Among the tested drugs, TFMPP was the most potent. HepaRG cells and primary hepatocytes revealed to be the most and the least resistant cellular models, respectively. To ascertain whether the CYP450 metabolism could explain their higher susceptibility, primary hepatocytes were co-incubated with the piperazines and the CYP450 inhibitors metyrapone and quinidine. Our results support that the CYP450-mediated metabolism contributes to the detoxification of these drugs. Additionally, we further evaluated in primary cells the intracellular contents of reactive species, ATP, reduced (GSH) and oxidized (GSSG) glutathione, changes in mitochondrial membrane potential ($\Delta\psi m$) and caspase-3 activation. Overall, an increase in reactive species formation, followed by intracellular GSH and ATP depletion, loss of $\Delta\psi m$ and caspase-3 activation could be observed for all piperazines, in a concentration-dependent manner. In conclusion, piperazine designer drugs produce hepatic detrimental effects that can vary in magnitude among the different analogues. The observed cytotoxic effects highlight the risk associated with the abuse of these drugs.

Keywords: piperazine designer drugs, hepatotoxicity, HepaRG cells, HepG2 cells, primary rat hepatocytes.

Introduction

Piperazine derived drugs emerged on the drug market in last decade and have been often found as one of the main psychoactive substances present in tablets and pills sold on the internet (Davies et al. 2010). Initially, these drugs were commercialized as a legal alternative to 3,4-methylenedioxymethamphetamine (MDMA or ecstasy) but nowadays they are prohibited in most countries (Bulcão et al. 2012; Arbo et al. 2012).

Pharmacologically, piperazine designer drugs present a clear stimulant-like pattern of behavioural effects associated with increases in monoamines release (Baumann et al. 2005; Meririne et al. 2006; Yarosh et al. 2007). Users have experienced amphetamine-like sympathomimetic effects including, tachycardia, hypertension, anxiety, vomiting, headache, migraine, palpitations, confusion, collapse, and seizures (Gijsman et al. 1998; Feutchtl et al. 2004; Gee et al. 2005; Thompson et al. 2010; Lin et al. 2011). Acute psychotic episodes and hallucinations (Austin and Monasterio, 2004), severe nephrotoxicity (Alansari and Hamilton, 2006), hyperthermia, disseminated intravascular coagulation, rhabdomyolysis and renal failure (Gee et al., 2010), sympathomimetic toxicity (Wood et al., 2008; Kovaleva et al., 2008), and even a lethal intoxication case with death after massive brain oedema (Balmelli et al., 2001) have also occurred. Recent preliminary evidence suggest that BZP is highly toxic to heart and kidney cell lines, which may explain the symptoms of renal and cardiovascular toxicity in users (Arbo et al., 2012; Monteiro et al., 2013, Arbo et al., 2014). Hepatic liver failure has also been reported after BZP intake (Cole, 2011; Monteiro et al., 2013).

Pharmacokinetic data is limited, however, there is evidence indicating that piperazine designer drugs are mainly metabolized in the liver, where they can also accumulate (Antia et al. 2009), being the phenylpiperazines, such as 1-(3-trifluoromethylphenyl)piperazine (TFMPP), and 1-(4-methoxyphenyl)piperazine (MeOPP) more extensively metabolized than the benzylpiperazines, such as N-benzylpiperazine (BZP) and its methylenedioxy-analogue 1-(3,4-methylenedioxybenzyl)piperazine (MDBP) (Maurer et al. 2004). They are excreted almost exclusively as metabolites in urine in humans and animal models (Maurer et al. 2004) but there is wide variation in the excretion rate by different individuals, which can add to the variability of their toxic effects (Austin and Monasterio 2004).

Hepatocytes are of particular interest as they have a central function in the metabolic fate and, consequently, in the process of detoxification and toxification of xenobiotics. Also, the liver is known to be one of the main targets for the toxicity of amphetamine like-drugs in humans (Carvalho et al. 2010). Therefore, the study of the hepatic deleterious effects triggered by piperazine designer drugs is of particular interest. The aim of the current work was to evaluate and compare the potential hepatotoxicity of BZP, TFMPP, MeOPP, and MDBP in different *in vitro* models, including human hepatoma HepG2 and HepaRG cell lines, and rat primary hepatocytes.

Material and Methods

Chemicals

N-Benzylpiperazine (BZP, 99.3% purity) was purchased from Chemos GmbH (Regenstauf, Germany), 1-(3-trifluoromethylphenyl)piperazine (TFMPP, 98% purity) from Alfa Aesar (Karlsruhe, Germany), 1-(4-methoxyphenyl)piperazine (MeOPP, 96% purity) from Acros Organics (New Jersey, USA), and 1-(3,4-methylenedioxybenzyl)piperazine (MDBP, 97% purity) from Aldrich Chemistry (Steinheim, Germany). Dulbecco's modified eagle's medium (DMEM) with high glucose, heat-inactivated fetal bovine serum (FBS), 0.25% trypsin/1 mM EDTA, antibiotic solution (10,000 U/mL penicillin, 10,000 µg/mL streptomycin), Hanks balanced salt solution (HBSS), and phosphate buffer (PBS) were purchased from Invitrogen Corporations (Paisley, UK). Unless stated otherwise, all other chemicals and reagents were obtained from Sigma-Aldrich (St. Louis, USA).

Stock solutions of BZP were made up in PBS. Stock solutions of TFMPP, MeOPP and MDBP were made in dimethyl sulfoxide (DMSO). In these cases, DMSO did not exceed 1% in culture media and it was used as solvent control. In all experiments, a comparison between solvent and negative (cells treated with cell culture medium) control was performed and no statistically significant differences between negative and solvent controls were observed ($p>0.05$). All stock solutions were stored at -20 °C and freshly diluted on the day of the experiment.

Immortalized Cell Culture

HepG2 cells were kindly provided by Prof. Ricardo Dinis-Oliveira (Department of Sciences, Advanced Institute of Health Sciences—North, CESPU, CRL, Gandra, Portugal). Cells were routinely cultured in 75 cm^2 flasks using DMEM with high glucose medium, supplemented with 10% FBS and 1% antibiotic solution. Cells were maintained in a humidified 5% CO_2 – 95% air atmosphere at 37°C, and the medium was changed every 2-3 days. Cultures were passaged by trypsinization (0.25% trypsin/1 mM EDTA) when cells reached 70-80% confluence, and were subcultured over a maximum of 10 passages. For the MTT assay, cells were seeded at a density of 80,000 cells/well onto 96-well plates (BD Biosciences, Oxford, UK) in a volume of 100 µL of complete culture medium, to obtain confluent monolayers within 24 hours. The following day the cells were incubated with the test drugs in cell culture medium without FBS. To enable reliable, complete concentration–response curves for each drug, HepG2 cells were exposed in triplicates to a wide range of concentrations (from 39 µM to 35 mM for BZP; 4.6 µM to 3 mM for TFMPP; 51.4 µM to 16.36 mM for MeOPP; and 68.5 µM to 30 mM for MDBP), in four independent experiments.

HepaRG cells were purchased from Life Technologies (Invitrogen, France) and cultured in 75 cm^2 flasks using Williams' Medium E with L-glutamine, supplemented with 10% FBS and 1% antibiotic solution, 50 µM hydrocortisone 21-hemisuccinate sodium salt and 5 µg/mL insulin. Cells were maintained in a humidified 5% CO_2 – 95% air atmosphere at 37°C, and the medium was changed every 2-3 days. Cultures were passaged by trypsinization (0.25% trypsin/1 mM EDTA) when cells reached 70-80% confluence, and were subcultured over a maximum of 10 passages. For the MTT assay, cells were seeded at a density of 144,000 cells/well onto 96-well plates (BD Biosciences, Oxford, UK) in a volume of 100 µL of complete culture medium and allowed to grow. When cells reached confluence, differentiation was induced by replacing the complete culture medium with differentiation medium (Williams' Medium E with L-glutamine with no FBS, supplemented with 1% antibiotic solution, 50 µM hydrocortisone 21-hemisuccinate sodium salt, 5 µg/mL insulin, and 2% DMSO). The differentiation medium was replaced every 48h, during 15 days. The following day, HepaRG cells were incubated with the test drugs in culture medium without FBS to a wide range of concentrations (from 14 µM to 40 mM for BZP; 1 µM to 3 mM for TFMPP; 3 µM to 20 mM for MeOPP; and 3 µM to 20 mM for MDBP), in triplicates, in eight independent experiments.

Animals

Male Wistar rats with a body weight of 200–250 g were purchased from Charles-River Laboratories (Barcelona, Spain). The animals had access to food (standard rat chow) and tap water *ad libitum* and were kept under controlled temperature (20±2°C), humidity (40 – 60%) and lighting (12 h light/dark cycle conditions). The animals were acclimatized in polyethylene cages, for 1 week prior to use. Surgical procedures for the isolation of hepatocytes were performed under anesthesia with isoflurane (IsoFlo®, Abbot Laboratories, Berkshire, UK), and were carried out always between 10:00 and 11:00 a.m. This study was approved by the local committee for the welfare of experimental animals and was performed in accordance with national legislation.

Isolation and culture of primary rat hepatocytes

Hepatocytes isolation was performed by collagenase perfusion as previously described (Moldéus et al. 1978) with some modifications. Briefly, after perfusion with a chelating agent (600 µM EGTA) to allow the cleavage of the hepatic desmosomes, hepatic collagen was hydrolyzed by *ex situ* perfusion with a 100 U/mL collagenase type 1, from *Clostridium histolyticum* solution supplemented with 5.3 µM $CaCl_2$. The hepatocytes were dissociated in Krebs–Henseleit buffer and the obtained suspension was purified by low-speed centrifugations and incubated for 30 min, at 4 °C, with 1% antibiotic. The initial viability of the isolated hepatocytes suspensions was always above 85%, as estimated by the trypan blue exclusion test. A suspension of $5x10^5$ viable cells/mL in complete culture medium (William's E medium supplemented with 10 % FBS, 2 ng/mL insulin, 5 nM dexamethasone, 1% antibiotic solution, 10 µg/mL gentamicin, and 0.25 µg/mL amphotericin B) was seeded onto 96-well plates (BD Biosciences, Oxford, UK). Cells were incubated at 36.5 °C with 5% CO_2, overnight for cell adhesion. The following day, the cells were incubated in cell culture medium without FBS with a wide range of concentrations (from 45 µM to 40 mM for BZP; 0.4 µM to 2.5 mM for TFMPP; 2.22 µM to 20 mM for MeOPP; and 2.22 µM to 20 mM for MDBP) of the test drugs for the cytotoxicity experiments. Each concentration was tested in triplicate in nine independent experiments. Since primary rat hepatocytes proved to be the most sensitive model to the cytotoxicity induced by the piperazine designer drugs, all the subsequent assays to clarify the hepatotoxic mechanisms were performed in this cellular model by testing three different concentrations for each test substance that corresponded to 3 different cytotoxicity levels, the EC_{20}, EC_{40} and EC_{60} of each drug according to the MTT concentration-response

curves. The concentrations tested were: 1.06, 1.66, and 2.78 mM for BZP; 88, 113, and 152 µM for TFMPP; 1.44, 1.82, and 2.37 mM for MeOPP; and 2.40, 3.18, and 4.38 mM for MDBP.

Cytotoxicity Assays

For the evaluation of cytotoxicity, the MTT reduction assay was performed. The MTT assay measures succinate dehydrogenase activity, an indicator of metabolically active mitochondria, and therefore of cell viability. A protocol previously described by Dias da Silva et al. (2013a) was used with some modifications. Briefly, after 24 h incubations with piperazine designer drugs, the medium was removed and fresh medium containing 0.5 mg/L MTT in HBSS was added. The cells were incubated at 37°C, for 30 min. Then, the cell culture medium was removed and the formed formazan crystals dissolved in 100 µL of DMSO. The absorbance was measured at 550 nm in a multi-well plate reader (BioTek Instruments, Vermont, USA) after 15 min shaking. Since MTT is photosensitive all steps of the procedure were executed under light protection. Results were graphically presented as percentage of cell death related to control *versus* concentration (mM). 1% DMSO was used as solvent control and 1% Triton X-100 as positive control.

Influence of CYP metabolism on piperazine designer drugs cytotoxicity

To clarify the influence of CYP450 metabolism on the cytotoxicity elicited by the tested piperazines, primary rat hepatocytes were seeded at $5x10^5$ viable cells/mL density onto 96 well-plates. After 24 h, the cells were co-incubated with each tested piperazine designer drug and 500 µM metyrapone (non selective inhibitor of the cytochrome P450) or 100 µM quinidine hydrochloride monohydrate (CYP2D6 inhibitor) (Turpeinen et al. 2004). The CYP2D6 was specifically inhibited because it is the main CYP450 isoenzyme responsible for the piperazine designer drug metabolism *in vivo* (Staack and Maurer, 2005). After 24 h, cell mortality was determined through the MTT assay. The final results were expressed as % of control conditions from 3 independent experiments with each concentration tested in 3 replicates within each experiment.

Measurement of intracellular reactive oxygen (ROS) and nitrogen (RNS) species

The intracellular ROS and RNS production was monitored by means of the DCFH-DA assay as previously described (Dias da Silva et al. 2014a). On the day of the experiment, primary rat hepatocytes seeded onto 96-well plates at a density of $5x10^4$ viable cells/well and incubated with 10 µM DCFH-DA for 30 min, at 37 °C, in the dark. As DCFH-DA is a non-water-soluble powder, it was initially prepared as a 4 mM stock solution in DMSO and made up to the final concentration in fresh culture medium (ensuring that the final concentration of DMSO did not exceed 0.05%) immediately before each experiment. The cells were then rinsed with HBSS and incubated with the EC_{20}, EC_{40} and EC_{60} of each piperazine designer drug (based on the MTT concentration-response curves), at 37 °C during 24h. Fluorescence was recorded on a fluorescence microplate reader (BioTek Instruments, Vermont, USA) set to 485 nm excitation and 530 nm emission. The data are presented as the percentage of control conditions from four independent experiments with each concentration tested in six replicates within each experiment.

Measurement of intracellular reduced glutathione (GSH), and oxidized glutathione (GSSG)

Primary rat hepatocytes were seeded onto 6-well plates at $1x10^6$ viable cells/well density. After 24 h incubations with the EC_{20}, EC_{40} and EC_{60} of each drug at 37 °C, the cells were rinsed with HBSS and scrapped/precipitated with 5% perchloric acid ($HClO_4$, w/v). After centrifugation (16,000 g, 10 min, 4°C), the supernatants were collected and kept at -80°C until further determination of GSH and GSSG. The pellet obtained was resuspended in 0.3 M NaOH and used for protein quantification, determined by the Lowry assay (Lowry et al. 1951).

The intracellular levels of GSH and GSSG were evaluated by the DTNB-GSSG reductase-recycling assay, as previously described (Dias da Silva et al. 2014a). Data from four independent experiments were normalized to the protein content and the final results were expressed as nmol per mg of protein.

Measurement of intracellular ATP

Samples were prepared as described for the GSH and GSSG measurement. The ATP levels were quantified by a bioluminescence assay, as described by Pontes et al. (2008). Briefly, the thawed acidic supernatant was neutralized with an equal volume of 0.76 M $KHCO_3$ and centrifuged for 1 min at 16,000 g, at 4 °C). The ATP contents were then measured in duplicate in 96-well white plates, by adding 75 µL of the neutralized supernatants, standards or blank (5% $HClO_4$, w/v) and 75 µL of the luciferin/luciferase solution [0.15 mM luciferin, 300,000 light units of luciferase from *Photinus pyralis* (American firefly), 50 mM glycine, 10mM $MgSO_4$, 1 mM Tris, 0.55 mM EDTA, 1% BSA (pH 7.6)]. The emitted light intensity was determined using a luminescence microplate reader (BioTek Instruments, Vermont, USA) and compared with a standard curve performed within each experiment. Data were normalized to the protein content, determined by the Lowry assay (Lowry et al. 1951), and results from four independent experiments were expressed as nmol per mg of protein.

Assessment of mitochondrial membrane potential (Δψm)

Assessment of mitochondrial integrity was performed by measuring TMRE inclusion as described by Dias da Silva et al. (2014a). Primary rat hepatocytes, seeded at a $5x10^4$ viable cells/well density onto 96-well plates, were incubated with each piperazine designer drug at EC_{20}, EC_{40} and EC_{60} for 24 h. At the end of the incubation period, the medium was replaced by fresh medium containing 2 µM TMRE, and incubated at 37 °C, for 30 min, in the dark. As TMRE is a non water-soluble powder, a 2 mM stock solution was initially prepared in DMSO and stored at -20 ^oC, protected from light. Afterwards, the medium was gently aspirated and replaced by 0.2% BSA in HBSS. Fluorescence was measured on a fluorescence microplate reader (BioTek Instruments, Vermont, USA) set to 544 nm excitation and 590 nm emission. The data obtained were calculated as the percentage of control conditions from four independent experiments with each concentration tested in six replicates within each experiment.

Caspase-3 activity assay

Primary rat hepatocytes were seeded at a density of $1x10^6$ viable cells/well onto 6-well plates. After 24 h incubation, at 37°C, with each piperazine designer drug at EC_{20},

EC_{40} and EC_{60}, the cells were detached and collected to a tube (2 wells per tube), centrifuged (210 g, 5 min, 4 °C), and the supernatant was discarded. One hundred and fifty microliters of lysis buffer (50 mM HEPES, 0.1 mM EDTA, 0.1 % CHAPS, supplemented with 1 mM DTT, pH 7.4) were added to the pellets, vortex-mixed and incubated on ice for 5 min before centrifugation (16,000 g, 10 min, 4 °C). In a 96-well plate, 50 µL of the supernatant, which contains the cytoplasmic fraction, was mixed with 200 µL of assay buffer (100 mM NaCl, 50 mM HEPES, 1 mM EDTA, 0.1% CHAPS, 10% glycerol, supplemented with 10 mM DTT, pH 7.4). The reaction was started by adding 5 µL of caspase-3 peptide substrate Ac-DEVD-pNA (final concentration 80 µM), with subsequent incubation at 37 °C for 24h. Caspase-3 releases the *p*-nitroaniline moiety of the substrate, which presents high absorbance at 405 nm. All steps were performed on ice and the caspase-3 activity was determined at 405 nm in a multi-well plate reader (BioTech Instruments, Vermont, US) as previously described (Arbo et al. 2014). Caspase-3 substrate Ac-DEVD-*p*NA (stock solution at 4 mM) and DTT were prepared in DMSO. The absorbance of blanks, used as non-enzymatic control, was subtracted from each value of absorbance and the data normalized with the amount of protein of each sample. The protein content in the cytoplasmic fraction was quantified using the Bio-Rad DC protein assay kit as described by the manufacturer, and bovine albumin solutions were used as standards. Results from four independent experiments were expressed as fold increase of controls. Campthotecin (12 µM) was used as positive control.

Statistical Analysis

The normalized MTT data were fitted to the dosimetric logit model (Dias da Silva et al. 2014a), that was chosen based on a statistical goodness-of-fit principle (Scholze et al. 2001). Comparisons between concentration-response curves were performed using the extra sum-of-squares *F* test. Results of ROS/RNS GSH, GSSG, Δψm, ATP, and caspase-3 assays are presented as mean ± standard error of the mean (SEM) from 4 independent experiments. Normality of the data distribution was assessed by the Kolmogorov–Smirnov normality test. Statistical comparisons between groups were performed by one-way analysis of variance (ANOVA) followed by Dunn's multiple comparison test. Solvent and negative control values obtained in the MTT assay were compared by the Student's unpaired t-test. In all cases, significance was accepted at p values <0.05. All statistical calculations were performed using GraphPad Prism software, version 5.01 (GraphPad Software, San Diego, CA, USA).

Results

Piperazine designer drugs elicited hepatotoxicity in vitro

Figure 1 presents the concentration-response curves of each piperazine designer drug in the three *in vitro* models evaluated in this work, human derived HepG2 and HepaRG cells and primary rat hepatocytes. Exposure to piperazine drugs resulted in concentration-dependent cytotoxicity. A summary of the calculated EC_{50} values (representing the half-maximum-effect concentrations from the curves) is presented in Table 1. Significant differences were observed for the EC_{50} values of the curves ($p<0.05$, *F* test). Based on these data, it was evident that, under our experimental conditions, TFMPP was the most cytotoxic piperazine designer drug in the three *in vitro* models evaluated. HepaRG cells proved to be the most resistant model to the toxicity elicited by all piperazine drugs, except for MDBP, when cells were exposed to concentrations higher than the EC50. In the case of BZP, there was no significant difference between HepG2 and HepaRG cytotoxicity curves. Primary rat hepatocytes showed to be the most sensitive cells to study the hepatotoxicity of the piperazine designer drugs, and therefore all further toxicological evaluations were carried out in this model.

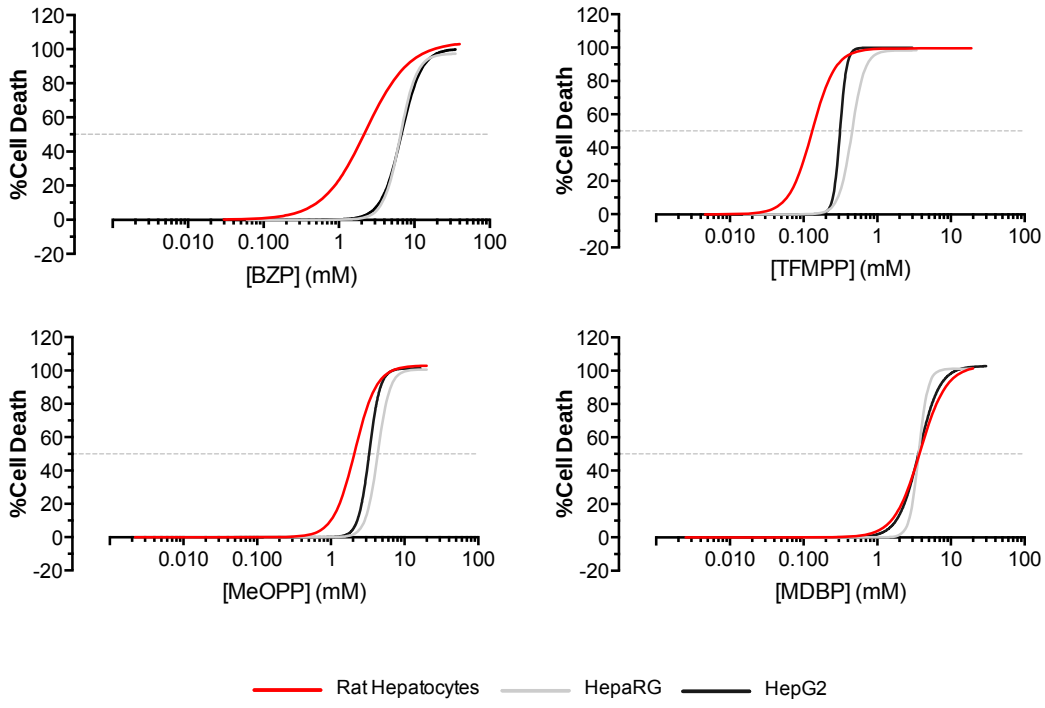

Figure 1. Concentration-response (cell death) curves of piperazine designer drugs in HepG2 and HepaRG cells and primary rat hepatocytes after 24h incubations at 37°C. Viability was evaluated through the MTT reduction assay. Data are presented as percentage of cell death relative to the respective negative controls. At least four independent experiments were performed (six replicates tested for each concentration within each experiment). Curves were fitted using the dosimetric logit model.

Table 1. EC50 values of the piperazine designer drugs in the MTT assay, after 24h-incubations at 37 °C.

Designer Drug	EC_{50} (mM)		
	HepG2	HepaRG	Rat Hepatocytes
BZP	6.75^{bcd}	6.58^{bcd}	2.15^{bd}
TFMPP	0.31^{acd}	0.46^{acd}	0.13^{acd}
MeOPP	3.31^{ab}	4.33^{abd}	2.08^{bd}
MDBP	3.62^{ab}	3.65^{abc}	3.74^{abc}

The cytotoxicity curves were fitted using the dosimetric logit model, p values <0.05 were considered statistically significant. [a] Compares to BZP. [b] Compares with TFMPP. [c] Compares with MeOPP. [d] Compares with MDBP.

Metabolism does not contribute to the cytotoxicity of piperazine designer drugs in rat primary hepatocytes

The metabolism of piperazine designer drugs is dependent of CYP450 activity. Figure 2 presents the concentration-response curves obtained after the co-incubation with each piperazine designer drug and 500 µM metyrapone (non selective inhibitor of CYP450) or 100 µM quinidine (inhibitor of CYP2D6) in primary rat hepatocytes. There was no significant difference between negative and solvent controls and the CYP450 inhibitors alone at the concentrations tested. The attained EC50 values are displayed in Table 2. With the exception of MDBP incubations with metyrapone, where no differences were observed, all other curves representing the co-incubation of the piperazine designer drugs with the CYP inhibitors showed a deviation to the left in relation to the curves obtained with the drugs alone. This indicates that the CYP450-mediated metabolism has a detoxifying effect, and it is most likely that the parent compounds are more toxic than their metabolites.

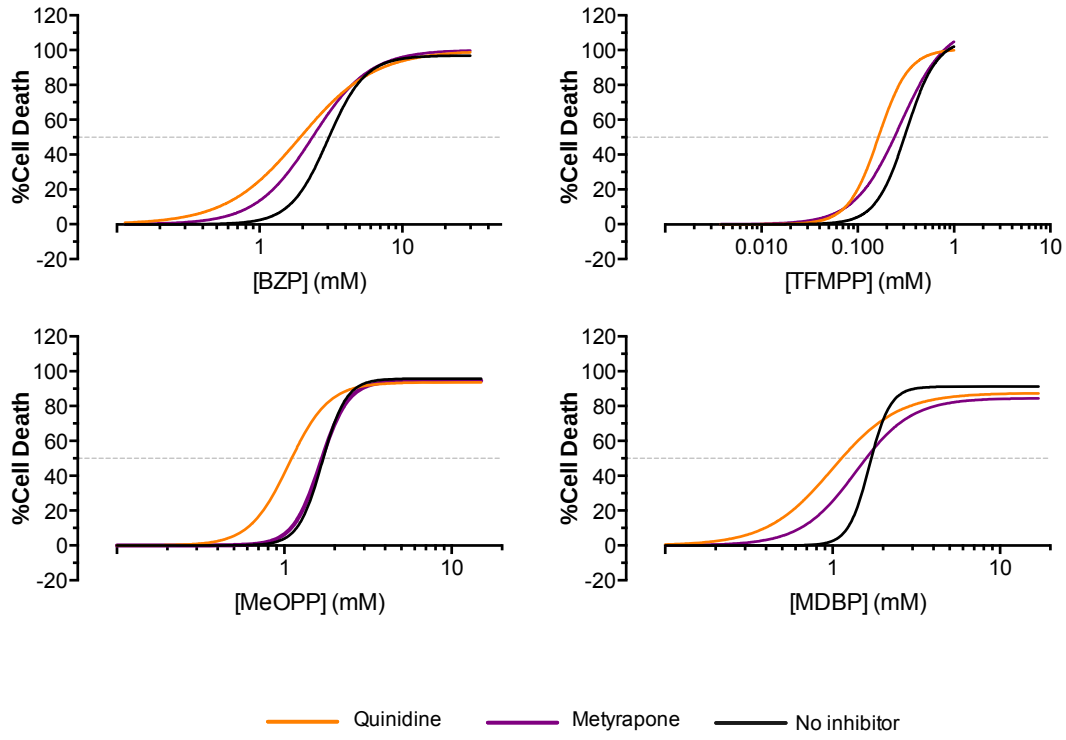

Figure 2. Concentration-response (cell death) curves of primary rat hepatocytes after 24h of co-incubation of each piperazine designer drug with 500 µM metyrapone or 100 µM quinidine at 37°C. Viability was evaluated through the MTT reduction assay. Data are presented as percentage of cell death relative to the respective negative controls. Three independent experiments were performed (six replicates tested for each concentration within each experiment). Curves were fitted using the dosimetric logit model.

Table 2. EC50 values of the piperazine designer drugs co-incubated with CYP450 inhibitors metyrapone (500 µM) and quinidine (100 µM) in the MTT assay, after 24h at 37 °C.

Designer Drug	**EC_{50} (mM)**		
		Metyrapone	Quinidine
	No inhibitor	(500 µM)	(100 µM)
BZP	3.06	2.35*	1.93*
TFMPP	0.30	0.24*	0.16*
MeOPP	1.71	1.68	1.10*
MDBP	1.70	1.58	1.13*

The cytotoxicity curves were fitted using the dosimetric logit model, *statistically significant comparing to the piperazine drugs alone ($p<0.05$).

Piperazine designer drugs induce oxidative stress in rat primary hepatocytes

Oxidative stress plays an important role in drug-induced hepatotoxicity for many different compounds including drugs of abuse (e.g. cocaine and amphetamines), and pharmaceuticals (e.g. azathioprine and paracetamol) (Pandit et al. 2012). As depicted in figure 3, piperazine designer drugs induced the production of reactive species after 24h incubations in primary rat hepatocytes, as evaluated by the DCFH-DA assay. This effect was significant ($p<0.05$, ANOVA/Dunn's) and concentration-dependent to all drugs tested. Interestingly, among the same cytotoxicity level, MeOPP significantly ($p<0.0001$, ANOVA/Dunn's) induced more reactive species formation than the other drugs. At equipotent cytotoxic concentrations, no significant differences were observed among BZP, TFMPP and MDBP.

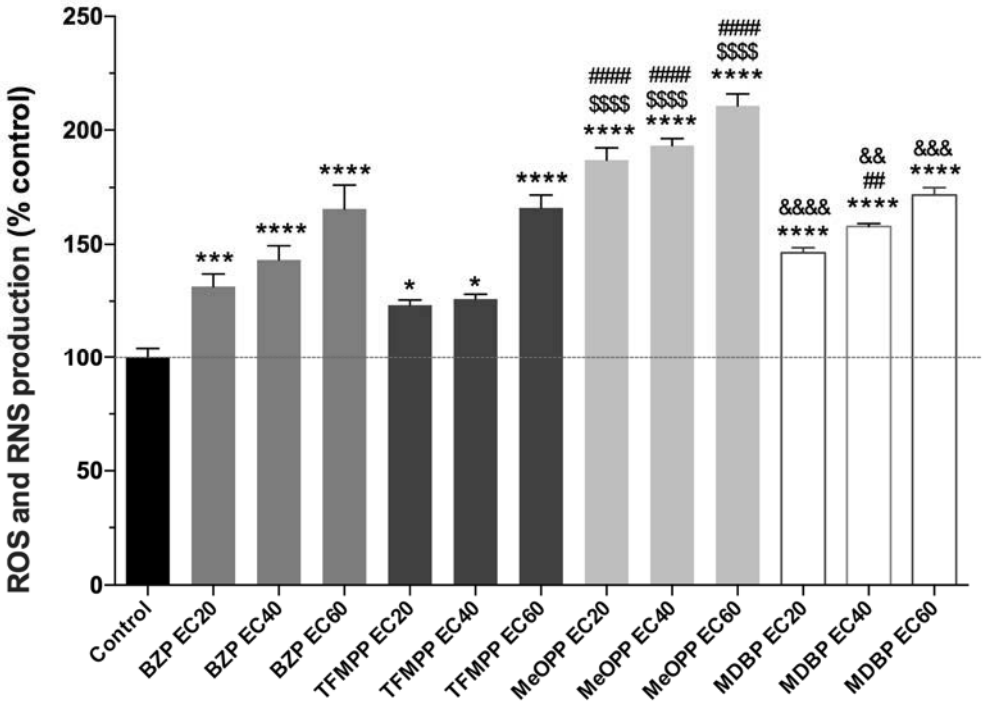

Figure 3. Reactive species (ROS/RNS) production, measured through the DCFH-DA assay, in rat primary hepatocytes after 24h-incubations with each piperazine designer drug at 37°C. Results are expressed as percentage control ± SEM (n = 4 independent experiments run in triplicates). Statistical comparisons were made using one-way ANOVA/Dunn's post-hoc test (*p<0.05; **p<0.01; ***p<0.001; ****p<0.0001 vs control). Comparing the same cytotoxicity levels $ vs BZP, # vs TFMPP, & vs MeOPP.

Changes in the intracellular amounts of GSH and GSSG are also strong indicators of redox disturbances and were investigated with the DTNB–GSSG reductase recycling assay. In figure 4, a significant ($p<0.001$, ANOVA/Dunn's) GSH depletion was noted at all concentrations of BZP and MDBP. A concentration-dependent effect was observed for

MeOPP, where a significant ($p<0.001$, ANOVA/Dunn's) depletion was observed at EC_{40} and EC_{60} compared to control. For BZP it was also possible to observe a significant ($p<0.01$, ANOVA/Dunn's) increase in GSSG levels at the tested EC_{20} and EC_{40}. Interestingly, these results agree with the generation of reactive species, since the highest GSH depletion was observed at EC60 MeOPP, which also induced the highest formation of reactive species. Comparing all piperazine designer drugs at equipotent cytotoxic concentrations, MDBP and BZP had a greater effect in GSH depletion. BZP significantly increased ($p<0.01$, ANOVA/Dunn's) the GSSG intracellular levels to a greater extent than that observed for any of the other drugs. TFMPP did not induce any alteration in GSH homeostasis.

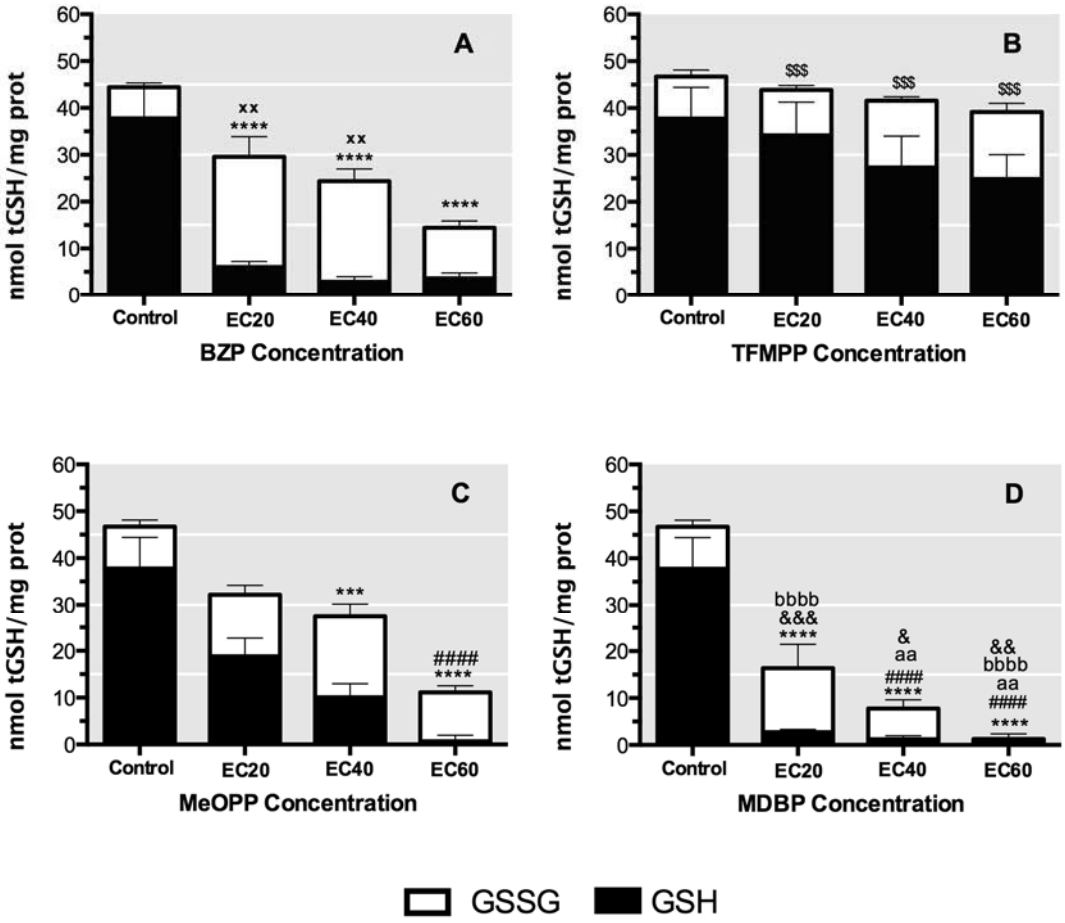

Figure 4. Intracellular contents of GSH and GSSG in rat primary hepatocytes after 24h of incubation with BZP (A), TFMPP (B), MeOPP (C) and MDBP (D). Results are expressed as mean ± SEM (n=4 independent experiments). Statistical comparisons were made using one-way ANOVA/Dunn's post-hoc test (*p<0.05; **p<0.01; ***p<0.001; ****p<0.0001 vs control GSH; xx p<0.01 vs control GSSG). Comparing the same cytotoxicity levels $ vs BZP GSH, # vs TFMPP GSH, & vs MeOPP GSH; a vs BZP GSSG, b vs TFMPP GSSG, c vs MeOPP GSSG.

Piperazine designer drugs induce mitochondrial impairment and disturb energetic status in rat primary hepatocytes

To investigate whether the piperazine drugs could disturb the mitochondrial function, the mitochondrial membrane potential (Δψm) was evaluated. A significant loss of Δψm impairs oxidative phosphorylation, depleting cells of energy, and inducing cell death. In figure 5, a significant ($p < 0.01$, ANOVA/Dunn's) loss in Δψm can be observed after 24 h incubations of primary rat hepatocytes with all drugs at all concentrations, except for EC_{20} TFMPP, in relation to control. Comparing all drugs at the same toxicity levels, the highest mitochondrial depolarization was observed with MDBP, at EC20 and EC40. This loss of Δψm was significantly higher ($p<0.01$, ANOVA/Dunn's) than for all the other drugs at equipotent concentrations. MeOPP and BZP presented similar effects at the same cytotoxicity level. On the other hand, TFMPP presented the lowest effect on Δψm.

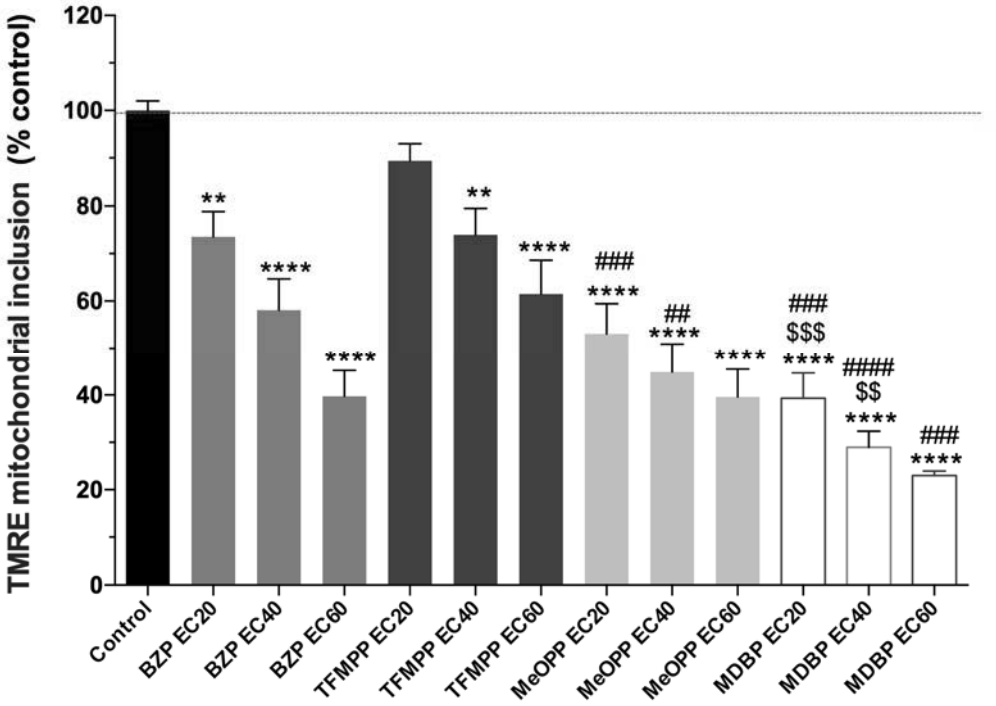

Figure 5. Mitochondrial membrane potential (Δψm) measured as TMRE incorporation in mitochondria of rat primary hepatocytes after 24 h incubations with the tested piperazine designer drugs at 37 °C. Results are expressed as percentage control ± SEM (n = 4 independent experiments run in triplicates). Statistical comparisons were made using one-way ANOVA/Dunn's post-hoc test (**p<0.01; ****p<0.0001 vs control). Comparing the same cytotoxicity levels $ vs BZP, # vs TFMPP.

ATP is the key intermediate for energy exchange, it is related with cellular energetics, metabolic regulation, and signaling. All cells require ATP to remain alive and carry out their specific functions and, because ATP is transiently depressed by many

forms of cellular stress, its levels reflect the functional integrity of viable cells. Figure 6 shows that the intracellular ATP levels measured in primary rat hepatocytes exposed to the tested piperazine designer drugs for 24 h at 37 °C were significantly depleted for all concentrations, with the exception of EC20 BZP, and EC20 and EC40 TFMPP. Interestingly, the drug presenting the highest ATP depletion ($p<0.05$ ANOVA/Dunn's) was MDBP, which also presented the highest Δψm loss. As observed for the Δψm loss induced by MeOPP and BZP, a similar effect in the same cytotoxicity level for these two drugs was observed for ATP depletion. Among all drugs, TFMPP exerted the lowest effect on ATP levels.

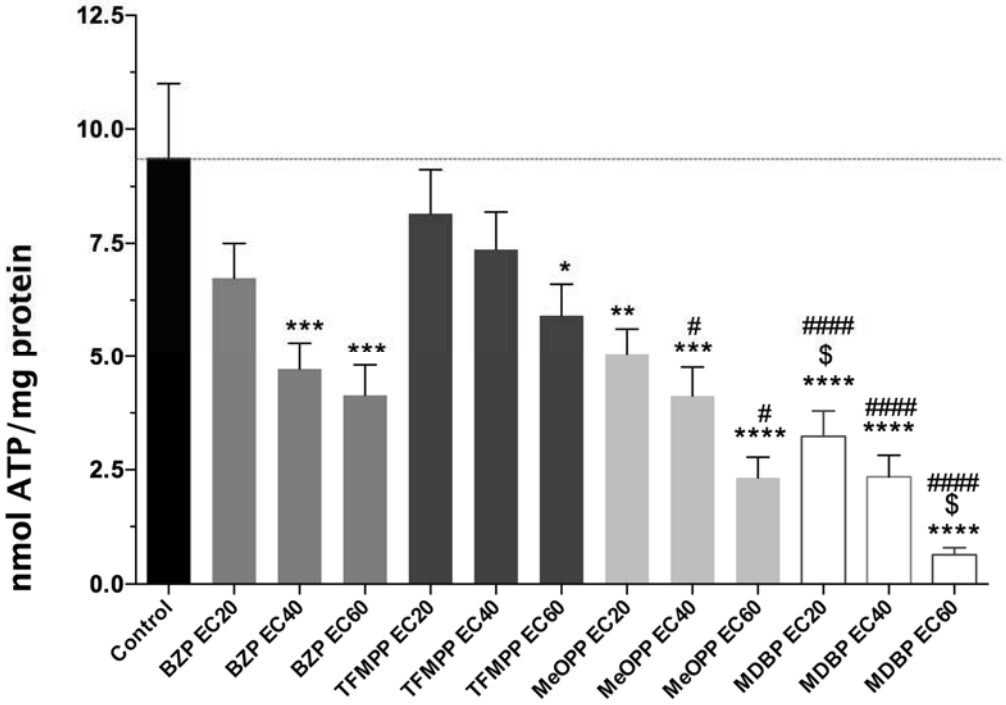

Figure 6. Intracellular ATP levels in primary rat hepatocytes after 24h of incubation with piperazine designer drugs at 37 °C. Results are expressed as mean ± SEM (n=4 independent experiments). Statistical comparisons were made using one-way ANOVA/Dunn's (*p<0.05; **p<0.01; ***p<0.001; ****p<0.0001 vs control). Comparing the same cytotoxicity levels $ vs BZP, # vs TFMPP.

Piperazine designer drugs induce caspase activation in primary rat hepatocytes

Caspase activation is one the main events leading to apoptosis. As can be seen in figure 7, a significant ($p<0.01$, ANOVA/Dunn's) increase in caspase-3 activity occurred at almost all concentrations of the tested piperazine designer drugs after 24 h incubations in primary rat hepatocytes. Among all tested drugs, the highest caspase-3 activation was observed with MDBP ($p<0.01$, ANOVA/Dunn's). A concentration-response effect was noted for MeOPP and BZP. At equipotent concentrations, TFMPP presented the lowest caspase-3 activation.

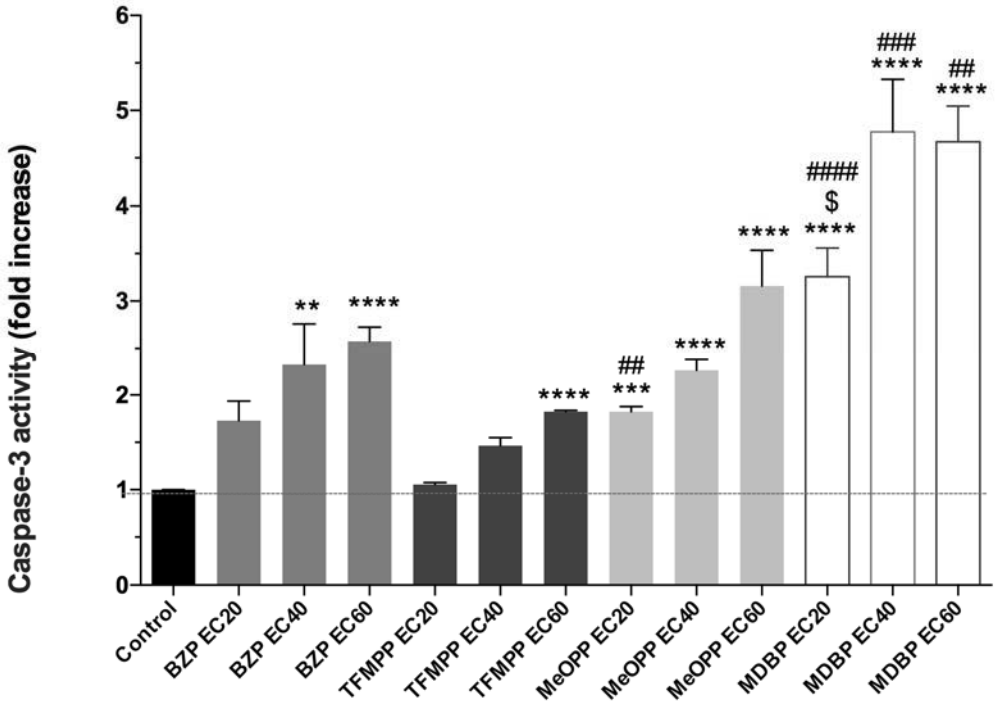

Figure 7. Caspase-3 activity fold increase in primary rat hepatocytes after 24h incubations with piperazine designer drugs at 37 °C. Results are expressed as mean ± SEM (n=4 independent experiments). Statistical comparisons were made using one-way ANOVA/Dunn's (*p<0.05; **p<0.01; ***p<0.001; ****p<0.0001 vs control). Comparing the same cytotoxicity levels $ vs BZP, # vs TFMPP.

Discussion

Synthetic drugs are highly abused and consumed mainly at parties and night clubs, especially by young people. The effects experienced by users after piperazine designer drugs intake resemble those of the amphetamines (Lin et al. 2011). The liver is acknowledged to be one of the main targets of toxicity for amphetamine-like compounds (Carvalho et al. 2010) and cathinone derivatives (Araujo et al. 2014). The available information on the toxic effects of piperazine designer drugs of abuse is currently very limited, but recent studies indicate that these drugs present cardiotoxic effects *in vitro* (Arbo et al. 2014).

For the first time, we demonstrate that piperazine designer drugs produced hepatotoxicity to three different *in vitro* models (HepG2 and HepaRG cells, and primary rat hepatocytes) being TFMPP the most potent designer drug in all of them. We select the human-derived hepatoblastoma cell line HepG2 not only because these cells have been extensively used as a test system for the prediction of toxicity, carcinogenicity and cell mutagenicity in humans (Donato et al. 2008; Liu and Zeng 2009) but also because they have been previously used for the characterization of the cytotoxic effects of other

designer drugs of abuse, including amphetamines (Dias da Silva et al. 2013abc, 2014a). However, there is a major limitation of this cellular model concerning drug metabolism since, in these hepatic cells, drug-metabolizing enzymes, namely CYP isoforms, are expressed at very low levels when compared with primary hepatocytes or with the *in vivo* situation (Guo et al. 2011; Lin et al. 2012). To overcome this limitation, the cytotoxicity studies were also conducted in HepaRG cells. This is another human cell line derived from a hepatocellular carcinoma which exhibits extensive differentiation after 2 weeks in culture. After acquiring a differentiated hepatocyte-like morphology, they retain a unique set of drug-metabolizing enzymes at levels comparable to those observed with primary human hepatocytes in culture. Comparing to HepG2 cells, HepaRG present a higher level of CYP1A1, CYP2B6, CYP2C9, CYP2E1 and CYP3A4 mRNA but lower CYP2D6 mRNA (Aninat et al. 2006, Rodrigues et al. 2013). The main metabolic pathways described for the piperazine designer drugs in animals and in humans comprise reactions catalyzed by CYP2D6 which include the hydroxylation of BZP (Staack and Maurer 2005), TFMPP (Staack et al. 2003), and MeOPP (Staack et al. 2004) and the demethylenation of MDBP (Staack and Maurer 2004). Since CYP2D6 is present at low levels in both immortalized cellular models, we also included rat primary hepatocytes in this study. Primary hepatocytes have some drawbacks such as, unpredictable viability, limited growth activity and lifespan, early phenotypic alterations after seeding, besides huge variations in functional activities, especially CYP levels. Nevertheless, primary hepatocytes are the most suitable model for investigating the induction of CYPs by chemical inducers and the metabolic profiles of new drugs (Aninat et al. 2006).

In all models, TFMPP was the most cytotoxic drug, which agrees with previous findings in cardiomyoblast H9c2 cells (Arbo et al. 2014). The main differences among the *in vitro* models used in this work concerns their metabolic capacity. Since the susceptibility of the primary hepatocytes to the cytotoxicity of the piperazine drugs was remarkably higher than those of the HepG2 and HepaRG cells, except for MDBP, it could be anticipated that their higher metabolic competence could explain these differences. Surprisingly, when we co-incubated the piperazine designer drugs with the CYP inhibitor metyrapone and the CYP2D6 inhibitor quinidine, an increase in the potency of the drug was observed. The deviation of the curves to the left, which is even more evident when cells were co-incubated with quinidine, suggests that metabolism plays a detoxifying role for the piperazine designer drugs.

The discrepancies in EC_{50} values of immortalized cells and primary hepatocytes are quite expected. The immortalization process adds new characteristics to the cells,

namely the continuous growth and an almost unlimited life-span, which can induce different physiological responses compared to the primary cells. Therefore, an advantage of the use of primary cells is that the cell phenotype comprises a much more reliable situation (Astashkina et al., 2012). Since the immortalized cells are from human origin and the primary hepatocytes from rats, it is also necessary to consider possible interspecies differences that could explain different rates of metabolism and toxicological susceptibilities.

Oxidative stress is a well-described mechanism underlying the toxicity of many xenobiotics, which plays an essential role in the cytotoxic effects of several amphetamine derivatives that induce the formation of highly reactive species (Dias da Silva et al. 2014b). Piperazine designer drugs induce the formation of these reactive species in primary rat hepatocytes, a situation also observed with amphetamine derivatives in primary rat hepatocytes (Pontes et al. 2008) and HepG2 cells (Dias da Silva et al. 2014a). Interestingly, MeOPP presented a pro-oxidant effect higher than the other drugs, and this could be due to the MeOPP metabolism. Two possible metabolic reactions, which include an *N*-dealkylation, followed by an *N*-acetylation, lead to the formation of *N*-acetyl-4-hydroxyaniline that corresponds to the analgesic drug acetaminophen (paracetamol) (Staack et al., 2004; Staack and Maurer, 2005), that can be further metabolized into *N*-acetyl-*p*-benzoquinone imine, a highly oxidative and GSH depleting chemical. On the other hand, this finding is not corroborated by our previous works with these piperazine designer drugs in rat cardiomyoblasts H9c2, where there was not observed any significant increase of reactive species (Arbo et al. 2014). However, comparing the two *in vitro* models, rat hepatocytes have a much more efficient metabolic capacity than the rat derived cardiomyoblast cells, which could lead to an exacerbated production of free radicals.

GSH has an important protective role which involves its oxidant neutralizing and its lipid peroxidase and/or tocopheryl radical-regenerating activities. GSH depletion may render the cells more vulnerable to the deleterious effects of free radicals, increasing their susceptibility towards oxidative injury. Events reflecting GSH depletion have been considered as potential biomarkers of drug-induced hepatotoxicity (Yuan and Kaplowitz 2009). Piperazine designer drugs elicited intracellular GSH depletion, which is related to the increased intracellular production of reactive species. The expected increases in intracellular GSSG levels were not observed for all drugs, possibly due to GSSG efflux. The formed GSSG is extruded for the extracellular medium as a protective response of the cells against oxidative stress. With the exception of BZP, the decreases in intracellular

GSH contents were not accompanied by an increase in GSSG levels. This is not surprising, and has been previously reported for amphetamine derivatives in hepatocytes (Hiramatsu et al. 1990; Carvalho et al. 1996; Carvalho et al. 2004; Dias da Silva et al. 2014a).

Regarding GSH homeostasis, an important role, contributing to GSH depletion, can be played by the metabolism of hepatocytes, leading to conjugation reactions with GSH (Carvalho et al. 2001), which was also verified with cardiomyoblasts (Arbo et al. 2014). In fact, it has been shown that the aromatic hydroxylation of amphetamine into *p*-hydroxyamphetamine leads to the formation of the glutathione-S-yl-*p*-hydroxyamphetamine conjugate through a reaction that is catalyzed by CYP2D6 and likely involves the formation of an arene epoxide intermediate (Carvalho et al. 1996). An alternative mechanism involving the formation of catechol metabolites that are oxidized into quinone intermediates following demethylenation of MDMA (Hiramatsu et al. 1990) and methylenedioxyamphetamine (MDA) (Carvalho et al. 2004) has also been shown to produce the corresponding glutathione-S-yl-N-methyl-α-methyldopamine and glutathione-S-yl-α-methyldopamine conjugates. There is a striking similarity between these metabolic pathways and those that were already described for the piperazine designer drugs in animals and in humans (Staack and Maurer 2005). Interestingly, MDBP, which produces a catechol intermediate as a metabolite, induced a significant GSH depletion at all tested concentrations. In addition, depletion may also be caused by inhibition of GSH biosynthesis (Gao et al. 2010). For example, γ-glutamyl transpeptidase (GGT) plays a key role in GSH homeostasis by breaking down extracellular GSH and providing cysteine, the rate-limiting substrate, for intracellular *de novo* synthesis of GSH (Zhang et al. 2005).

There are growing reports that mitochondria is a primary or secondary drug target and that its impairment is one of the major contributors to drug-induced liver injury (Scatena et al. 2007). Our data point to a depolarization of mitochondria, and ATP depletion after 24 h incubations of primary rat hepatocytes with piperazine designer drugs. The Δψm is crucial for maintaining the physiological function of the mitochondrial respiratory chain, a process responsible for ATP generation. A significant loss of Δψm impairs oxidative phosphorylation, depleting cells of energy and inducing cell death. Translocation of protons from the matrix to the intermembrane space to establish Δψm is coupled to the mitochondrial electron transport chain (Yuan and Acosta 1996). Inhibition of complex I and/or II of the electron transport chain leads to an increase of reactive oxygen species and a decrease in ATP production with subsequent accumulation of dysfunctional proteins, which impairs mitochondrial function (Usta et al. 2009). Depletion

of ATP is a typical feature of hypoxic and toxic injury, and leads to inhibition of two hepatic anabolic processes, namely gluconeogenesis and plasma protein synthesis, which have in common a substantial requirement for ATP (Ponsoda et al. 1995). Interestingly, the impairment of mitochondrial function, leading to ATP depletion, was also observed in our previous studies using H9c2 rat cardiomyoblasts (Arbo et al. 2014), which can indicate that this as one of the main mechanism of toxicity of piperazine designers drugs. Among all the tested drugs, the highest mitochondrial depolarization, and consequently, ATP depletion, was observed with MDBP.

Mitochondria also play a major role in apoptosis, by mediating and propagating death signals originated from the inside (intrinsic apoptotic pathway) or outside (extrinsic apoptotic pathway) of the cell, and loss of Δψm is an early apoptotic event. The observed activation of downstream caspase-3 is an indicative of the preference for apoptosis, as the main cell death mode and agrees well to what has already been described for amphetamines tested under normothermic conditions (Capela et al. 2013; Dias da Silva et al. 2013c). As with the effects observed in Δψm and ATP depletion, MDBP presented the highest downstream caspase-3 activation. Interestingly, after 24h incubations of rat cardiomyoblasts with these piperazine designer drugs, signs of apoptosis were also found, but no activation of caspase-3 was observed (Arbo et al. 2014).

In conclusion, we have demonstrated for the first time the *in vitro* hepatotoxic effects of piperazine designer drugs in three *in vitro* models, the HepG2, HepaRG cells, and primary rat hepatocytes. The rat primary hepatocytes were the most sensitive model in detecting deleterious effects and TFMPP was the most potent drug. In rat hepatocytes, piperazine designer drugs induced oxidative stress, loss of Δψm, ATP depletion and caspase-3 activation. Comparing all drugs at equipotent cytotoxic concentrations, differences in mechanisms of toxicity were evident, especially for TFMPP, indicating that additional toxicity endpoints should be evaluated for a better comprehension of the mechanisms involved in the cytotoxicity of the piperazine designer drugs. It should be noted that these drugs are frequently consumed in associations [the most common is BZP:TFMPP (2:1)] in the same tablet, or as adulterants of ecstasy tablets. As previously observed with amphetamine designer drugs, marked toxicity can occur when the drugs are combined at individually non-cytotoxic concentrations (Dias da Silva et al 2013ab, 2014ab). Since different combinations of piperazine designer drugs have already been implicated in human intoxications, further studies are needed not only to clarify the mechanisms involved in the observed cytotoxic effects but also to address the effects of drug combinations.

Acknowledgements

M.D. Arbo is the recipient of *Coordenação de Aperfeiçoamento de Pessoal de Nível Superior* (CAPES Foundation – Brazil) fellowship (Proc. BEX 0593/10-9). This work was sponsored by the Portuguese Research Council *Fundação para a Ciência e para a Tecnologia* (FCT) [Grant No. PEst-C/EQB/LA0006/2011] and co-funded by the European Community financial support program "*Programa Operacional Factores de Competitividade do Quadro de Referência Estratégico Nacional (QREN POFC)*".

Conflict of interest statement

The authors declare that there are no conflicts of interest.

References

Alansari M, Hamilton D (2006) Nephrotoxicity of BZP-based herbal party pills: a New Zealand case report. N Z Med J 119: U1959.

Aninat C, Piton A, Glaise D, Le Charpentier T, Langouët S, Morel F, Guguen-Guillouzo C, Guillouzo A (2006) Expression of cytochromes P450, conjugating enzymes and nuclear receptors in human hepatoma HepaRG cells. Drug Met Disp 34: 75-83.

Antia U, Tingle MD, Russel BR (2009) 'Party pill' drugs - BZP and TFMPP. N Z Med J 122: 55-68.

Araújo AM, Valente MJ, Carvalho M, Dias da Silva D, Gaspar H, Carvalho F, Bastos ML, Pinho PG (2014) Raising awareness of new psychoactive substances: chemical analysis and in vitro toxicity screening of 'legal high' packages containing synthetic cathinones. Arch Toxicol. doi: 10.1007/s00204-014-1278-7

Arbo MD, Bastos ML, Carmo H (2012) Piperazine compounds as drugs of abuse. Drug Alcohol Depend 122: 174-185.

Arbo MD, Silva R, Barbosa DJ, Dias da Silva D, Rossato LG, Bastos ML, Carmo H (2014) Piperazine designer drugs induce toxicity in rat cardiomyoblast h9c2 cells through mitochondrial impairment. Toxicol Lett 229: 178-189.

Astashkina A, Mann B, Grainger DW (2012) A critical evaluation of in vitro cell culture models for high-throughput drug screening and toxicity. Pharmacol Ther 134: 82-106.

Austin H, Monasterio E (2004) Acute psychosis following ingestion of 'Rapture'. Australas Psychiatry 12: 406–408.

Balmelli C, Kupferschmidt H, Rentsch K, Schneemann M (2001) Fatal brain edema after ingestion of ecstasy and benzylpiperazine. DMW 126: 809-11.

Baumann MH, Clark RD, Budzynski AG, Partilla JS, Blough BE, Rothman RB (2005) N-Substituted piperazines abused by humans mimic the molecular mechanism of 3,4-methylenedioxymethamphetamine (MDMA, or 'Ecstasy'). Neuropsychopharmacol 30: 550-560.

Bulcão R, Garcia SG, Limberger RP, Baierle M, Arbo MD, Chasin AAM, Thiesen FV, Tavares R (2012) *Designer drugs*: aspectos analíticos e biológicos. Química Nova 35: 149-158.

Carvalho F, Remião F, Amado F, Domingues P, Ferrer Correia AJ, Bastos ML (1996) *d*-Amphetamine interactions with glutathione in freshly isolated rat hepatocytes. Chem Res Toxicol 9: 1031-1036.

Carvalho M, Pontes H, Remião F, Bastos ML, Carvalho F (2010) Mechanisms underlying the hepatotoxic effects of ecstasy. Curr Pharm Biotechnol 11: 476-495.

Carvalho M, Carvalho F, Bastos ML (2001) Is hyperthermia the triggering factor for hepatotoxicity induced by 3,4-methylenedioxymethamphetamine (ecstasy)? An in vitro study using freshly isolated mouse hepatocytes. Arch Toxicol 74: 789-793.

Carvalho M, Milhazes N, Remião F, Borges F, Fernandes E, Amado F, Monks TJ, Carvalho F, Bastos ML (2004) Hepatotoxicity of 3,4-methylenedioxyamphetamine and α-methyldopamine in isolated rat hepatocytes: formation of glutathione conjugates. Arch Toxicol 78: 16-24.

Capela JP, da Costa Araújo S, Costa VM, Ruscher K, Fernandes E, Bastos ML, Dirnagl U, Meisel A, Carvalho F (2013) The neurotoxicity of hallucinogenic amphetamines in primary cultures of hippocampal neurons. Neurotoxicology 34: 254-263.

Cole M (2011) Poison in party pills is too much to swallow. Nature 474: 253.

Davies S, Wood DM, Smith G, Button J, Ramsey J, Archer R, Holt DW, Dargan PI (2010) Purchasing 'legal highs' on the internet – is there consistency in what you get? QJM 103: 489–493.

Dias da Silva D, Carmo H, Silva E (2013a) The risky cocktail: what combination effects can we expect between *ecstasy* and other amphetamines? Arch Toxicol 87: 111-122.

Dias da Silva D, Silva E, Carmo H (2013b) Cytotoxic effects of amphetamine mixtures in primary hepatocytes are severely aggravated under hyperthermic conditions. Toxicol in Vitro 27: 1670-1678.

Dias da Silva D, Carmo H, Lynch A, Silva E (2013c) An insight into the hepatocellular death induced by amphetamines, individually and in combination: the involvement of necrosis and apoptosis. Arch Toxicol 87: 2165-2185.

Dias da Silva D, Silva E, Carmo H (2014a) Combination effects of amphetamines under hyperthermia – the role played by oxidative stress. J Appl Toxicol 34: 637-650.

Dias da Silva D, Silva E, Carmo H (2014b) Mixtures of 3,4-methylenedioxymethamphetamine (ecstasy) and its major human metabolites act additively to induce significant toxicity to liver cells when combined at low, non-cytotoxic concentrations. J Appl Toxicol 34: 618-627.

Donato MT, Lahoz A, Castell JV, Gómez-Lechón MJ (2008) Cell lines: a tool for in vitro drug metabolism studies. Curr Drug Metab 9: 1-11.

Feuchtl A, Bagli M, Stephan R, Frahnert C, Kölsch H, Kühn KU, Rao ML (2004) Pharmacokinetics of m-chlorophenylpiperazine after intravenous and oral administration in healthy male volunteers: implication for the pharmacodynamic profile. Pharmacopsychiatry 37: 180-188.

Gao W, Mizukawa Y, Nakatsu N, Minowa Y, Yamada H, Ohno Y, Urushidani T (2010) Mechanism-based biomarker gene sets for glutathione depletion-related hepatotoxicity in rats. Toxicol Appl Pharmacol 247: 211-221.

Gee P, Jerram T, Bowie D (2010) Multiorgan failure from 1-benzylpiperazine ingestion – legal high or lethal high? Clin Toxicol 48: 230-3.

Gee P, Richardson S, Woltersdorf W, Moore G (2005) Toxic effects of BZP-based herbal party pills in humans: a prospective study in Christchurch, New Zealand. N Z Med J 118: 1784–1794.

Gijsman HJ, Van Gerven JMA, Tieleman MC, Schoemaker, RC, Pieters MSM, Ferrari MD, Cohen AF, Van Kempen GMJ (1998) Pharmacokinetic and pharmacodynamic profile of oral and intravenous meta-chlorophenylpiperazine in healthy volunteers. J Clin Psycopharmacol 18: 289-295.

Guo L, Dial S, Shi L, Branham W, Liu J, Fang JL, Green B, Deng H, Kaput J, Ning B (2011) Similarities and differences in the expression of drug-metabolizing enzymes between human hepatic cell lines and primary human hepatocytes. Drug Metab Dispos 39: 528-538.

Hiramatsu M, Kumagai Y, Unger SE, Cho AK (1990) Metabolism of methylenedioxymethamphetamine: formation of dihydroxymethamphetamine and a quinone identified as its glutathione adduct. J Pharmacol Exp Ther 254: 521-527.

Kovaleva J, Devuyst E, De Paepe P, Verstraete A (2008) Acute chlorophenylpiperazine overdose: a case report and review of the literature. Ther Drug Monitor 30: 394-8.

Lin JC, Jam RK, Lee HS, Jensen MA, Kydd RR, Russell BR (2011) Determining the subjective and physiological effects of BZP combined with TFMPP in human males. Psycopharmacology 214: 761-768.

Lin J, Schyschka L, Mühl-Benninghaus R, Neumann J, Hao L, Nussler N, Dooley S, Liu L, Stöckle U, Nussler AK, Ehnert S (2012) Comparative analysis of phase I and II enzyme activities in 5 hepatic cell lines identifies Huh-7 and HCC-T cells with the highest potential to study drug metabolism. Arch Toxicol 86: 87-95.

Liu ZH, Zeng S (2009) Cytotoxicity of ginkgolic acid in HepG2 cells and primary rat hepatocytes. Toxicol Lett 187: 131-136.

Lowry OH, Rosebrough NJ, Farr AL, Randall RJ (1951) Protein measurement with the folin-phenol reagent. J Biol Chem 193: 265-275.

Maurer HH, Kraemer T, Springer D, Staack RF (2004) Chemistry, pharmacology, toxicology and hepatic metabolism of designer drugs of the amphetamine (ecstasy), piperazine, and pyrrolidinophenone types. Ther Drug Monitor 26: 127–131.

Meririne E, Kajos M, Kankaanpää A, Seppälä T (2006) Rewarding properties of 1-benzylpiperazine, a new drug of abuse, in rats. Basic Clin. Pharmacol. Toxicol. 98: 346-350.

Moldéus P, Högberg J, Orrenius S (1978) Isolation and use of liver cells. Methods Enzymol 52: 60-71.

Monteiro MS, Bastos ML, Guedes de Pinho P, Carvalho M (2013) Update on 1-benzylpiperazine (BZP) party pills. Arch Toxicol 87: 929-47.

Pandit A, Sachdeva S, Bafna P (2012) Drug-induced hepatotoxicity: a review. J Appl Pharm Sci 02: 233-243.

Ponsoda X, Bort R, Jover R, Gómez-Lechón MJ, Castell JV (1995) Molecular mechanism of diclofenac hepatotoxicity: association of cell injury with oxidative metabolism and decrease in ATP levels. Toxicol in Vitro 9: 439-444.

Pontes H, Santos-Marques MJ, Fernandes E, Duarte JA, Remião F, Carvalho F, Bastos ML (2008) Effect of chronic ethanol exposure on the hepatotoxicity of ecstasy in mice: an *ex vivo* study. Toxicol in vitro 22: 910-920.

Rodrigues RM, Bouhifd M, Bories G, Sacco MG, Gribaldo L, Fabbri M, Coecke S, Whelan MP (2013) Assessment of an automated *in vitro* basal cytotoxicity test system based on metabolically-competent cells. Toxicol in Vitro 27: 760-767.

Scatena R, Bottoni P, Botta G, Martorana GE, Giardina B (2007) The role of mitochondria in pharmacotoxicology: a reevaluation of an old, newly topic. Am J Physiol Cell Physiol 293: C12-C21.

Staack RF, Fritschi G, Maurer HH (2003) New designer drug 1-(3-trifluoromethylphenyl)piperazine (TFMPP): gas chromatography/mass spectrometry and liquid chromatography/mass spectrometry studies on its phase I and II metabolism and on its toxicological detection in rat urine. J Mass Spectrom 38: 971–981.

Staack RF, Maurer HH (2004) New designer drug 1-(3,4-methylenedioxybenzyl)piperazine (MDBP): studies on its metabolism and toxicological detection in rat urine using gas chromatography/mass spectrometry. J Mass Spectrom 39: 255–261.

Staack RF, Maurer HH (2005) Metabolism of designer drugs of abuse. Cur Drug Metab 6: 259–274.

Staack RF, Theobald DS, Paul LD, Springer D, Kraemer T, Maurer HH (2004) In vivo metabolism of the new designer drug 1-(4-methoxyphenyl)piperazine (MeOPP) in rat and identification of the human cytochrome P450 enzymes responsible for the major metabolic step. Xenobiotica 34: 179–192.

Thompson I, Williams G, Caldwell B, Aldington S, Dickson S, Lucas N, McDowall J, Weatherall M, Robinson G, Beasley R (2010) Randomised double-blind, placebo-controlled trial of the effects of the 'party pills' BZP/TFMPP alone and in combination with alcohol. Psychopharmacology 24: 1299-1308.

Turpeinen M, Nieminen R, Juntunen T, Taavitsainen P, Raunio H, Pelkonen O (2004) Selective inhibition of Cyp2B6-catalyzed bupropion hydroxylation in human liver microssomes in vitro. Drug Metab Dispos 2004; 32: 626-631.

Usta J, Kreydiyyeh S, Knio K, Barnabe P, Bou-Moughlabay Y, Dagher S (2009) Linalool decreases HepG2 viability by inhibiting mitochondrial complexes I and II, increasing reactive oxygen species and decreasing ATP and GSH levels. Chem Biol Interact 180: 39-46.

Wood DM, Button J, Lidder S, Ramsey J, Holt DW, Dargan PI (2008) Dissociative and sympathomimetic toxicity associated with recreational use of 1-(3-trifluoromethylphenyl)piperazine (TFMPP) and 1-benzylpiperazine (BZP). J Med Toxicol 4: 254-7.

Yarosh HL, Katz EB, Coop A, Fantegrossi WE (2007) MDMA-like behavioral effects of N-substituted piperazines in the mouse. Pharmacol Biochem Behav 88:18-27.

Yuan, C., Acosta Jr, D (1996) Cocaine-induced mitochondrial dysfunction in primary culture of rat cardiomyocytes. Toxicology 112: 1–10.

Yuan L, Kaplowitz N (2009) Glutathione in liver diseases and hepatotoxicity. Mol Aspects Med 30: 29-41.

Zhang H, Forman HJ, Choi J (2005) Gamma-glutamyl transpeptidase in glutathione biosynthesis. Methods Enzymol 401: 468-483.

Study IV

Hepatotoxicity of piperazine designer drugs: a toxicogenomic approach

(To be submitted for publication)

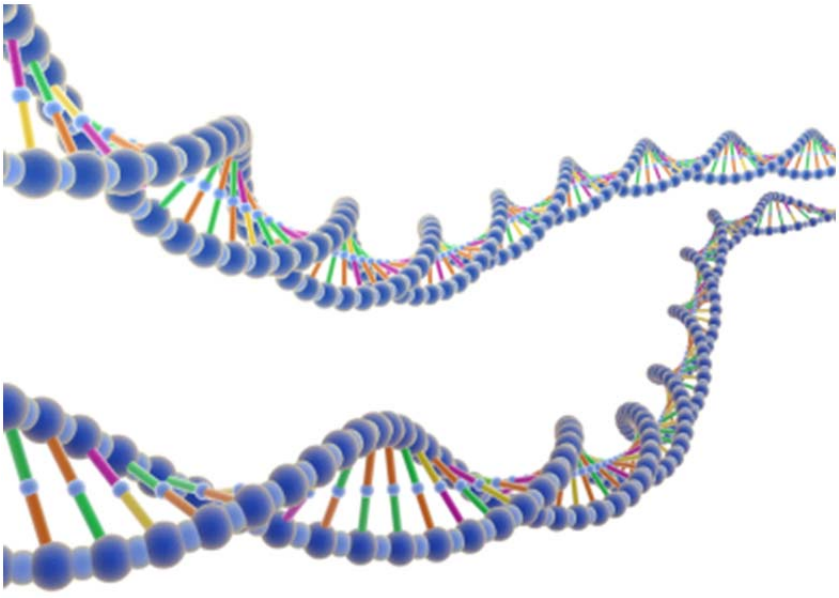

Hepatotoxicity of piperazine designer drugs: a toxicogenomic approach

Marcelo Dutra Arbo[1]*, Simone Melega[2], Regina Stöber[2], Markus Schug[2], Eugen Rempel[3], Jörg Rahnenführer[3], Maria de Lourdes Bastos[1], Helena Carmo[1], Jan Hengstler[2]

[1]REQUI*M*TE, Laboratório de Toxicologia, Departamento de Ciências Biológicas, Faculdade de Farmácia, Universidade do Porto, 4050-313 Porto, Portugal.

[2]Leibniz Research Centre for Working Environment and Human Factors (IFADO), Technical University of Dortmund, 44139 Dortmund, Germany.

[3]Department of Statistics, Technical University of Dortmund, 44221 Dortmund, Germany.

*Corresponding author:

M. D. Arbo (m.arbo@terra.com.br)

REQUI*M*TE, Laboratório de Toxicologia, Departamento de Ciências Biológicas, Faculdade de Farmácia, Universidade do Porto.

Rua Jorge Viterbo Ferreira, 228, Porto, 4050-313, Portugal.

Tel: +351 220428597

Abstract

The piperazine derivatives most frequently consumed for recreational purposes are 1-benzylpiperazine (BZP), 1-(3,4-methylenedioxybenzyl)piperazine (MDBP), 1-(3-trifluoromethylphenyl)piperazine (TFMPP), and 1-(4-methoxyphenyl)piperazine (MeOPP). Generally, they are consumed as capsules, tablets or pills but also in powder or liquid forms. In the corresponding drug scene piperazine designer drugs have the reputation of being safe, but preliminary data show that these compounds exhibit cytototoxicity in different in vitro models. The aim of this work was to evaluate the hepatotoxicity of BZP, TFMPP, MeOPP, and MDBP, using primary cultured rat hepatocytes, using a toxicogenomic approach. MDBP presented the highest number of altered probe sets. Among the four piperazine designer drugs, 65 probe sets and 4 transcription factors were found to be overlapped. From the total number of probe sets, genes with a fold change higher than 2.0 were selected as up-regulated, while genes with a fold change less than 0.3 were selected as down-regulated. The majority of up-regulated genes are related to cholesterol biosynthesis, which is, in turn, one of the events related to liver phospholipidosis.

Keywords: piperazine designer drugs, hepatotoxicity, primary rat hepatocytes, microarrays.

Introduction

Piperazines were originally developed as antihelminthic drugs for the management of intestinal roundworm and tapeworm infestations. In the 1970s, 1-benzylpiperazine (BZP) was investigated as an anti-depressant agent. Clinical trials were performed but they were abandoned due to reinforcing effects similar to dexamphetamine (Musselman and Hampton, 2014). The first documented BZP abuse occurred in the USA in 1996 (Austin and Monasterio, 2004). Since then, piperazine derived drugs appeared on the market, mainly in the internet, sold as “party pills” or under different street names, such as “Rapture”, “Frenzy”, “Bliss”, “Charge”, “Herbal ecstasy”, “A2”, “Legal X”, “Legal E.”, “Nemesis”, “Head Rush”, “XXX”, “Strong as Hell” and “Exotic Super Strong”. The most common derivatives are the benzylpiperazines, such as BZP and its methylenedioxy-analogue 1-(3,4-methylenedioxybenzyl)piperazine (MDBP), and the phenylpiperazines,

such as 1-(3-chlorophenyl)piperazine (mCPP), 1-(3-trifluoromethylphenyl)piperazine (TFMPP), and 1-(4-methoxyphenyl)piperazine (MeOPP) (Arbo et al., 2012). Generally, they can be consumed as capsules, tablets or pills but also in powder or liquid forms (Gee et al., 2005).

Studies using synaptossomes have shown that, although less potent than amphetamine designer drugs, the piperazines have substrate activity at the dopamine and serotonin transporters (Baumann et al., 2005). Several in vivo studies have confirmed a clear stimulant-like pattern of behavioural effects associated with increases in dopamine and serotonin release (Baumann et al., 2005; Meririne et al., 2006; Yarosh et al., 2007). At low doses, the effects tend to be mild, producing feelings of euphoria and wakefulness. Most common symptoms include insomnia, headaches, nausea, anxiety, depression, paranoia and auditory hallucinations Ingestion of high doses results in a sympathomimetic toxicity, and patients experience palpitations, tachycardia and hypertension. Neurological effects include tremors, myoclonus and seizures (Elliot 2011; Arbo et al., 2012; Musselman and Hampton, 2014).

In humans, the piperazine designer drugs are readily absorbed from the gastrointestinal tract (Antia et al., 2009, 2010; Schep et al., 2011) and they are mainly metabolized in the liver (Maurer et al., 2004). The liver is an important organ that plays a central role in the metabolic homeostasis of the body, which consists of metabolism, synthesis, storage and redistribution of carbohydrates, fat, and vitamins. In addition, the liver produces a large number of proteins including serum albumin, enzymes, and cofactors (Taub, 2004). Xenobiotic metabolism is also one of the liver functions, making it a primary target for chemicals, drugs and microbial agents. Since the liver is the organ involved in and is a major target organ for chemicals, hepatoxicity is a major issue in pharmaceutical drug development and drug-induced liver injury is one of the most proeminent causes of market withdrawls (Sahu, 2007).

DNA microarray technology enables to monitor and quantify the expression of thousands of genes simultaneously. This technology has the potential to more comprehensively contribute to the understanding of toxicity than any available traditional approach, since toxic changes in cells generally result from alterations not just in a single or few molecules, but in many molecular cascades. It may also help to identify early, sensitive biomarkers of toxicity, since alterations in gene expression are thought to precede the toxic outcome. These markers could then be used to develop screening tests to predict the toxicity of particular compounds. The combination of microarrays with conventional toxicological tools is rapidly contributing to the knowledge of the mechanisms

underlying cellular toxicity, and has emerged as the field of toxicogenomics (Sawada et al., 2005).

In the corresponding drug scene, piperazine designer drugs have the reputation of being safe, however preliminary data show that these compounds exhibits cytotoxicity in different in vitro models. The aim of this work was to evaluate the hepatotoxicity of BZP, TFMPP, MeOPP, and MDBP, using the primary cultured rat hepatocytes and a toxicogenomic approach, that could help understanding the aforementioned detrimental effects of these drugs.

Material and Methods

Cell culture materials and chemicals

Williams medium E, penicillin/streptomycin solution, amino acids solution, SeraPlus (FBS) were purchased from PAN Biotech (Aidenbach, Germany). Gentamicin (10 mg/mL) was obtained from Invitrogen Corp. (Karlsruhe, Germany), and DMEM (10x) from Biozol (Eching, Germany). Dexamethasone, reduced glutathione (GSH), oxidized glutathione (GSSG), glutathione reductase (GR, EC 1.6.4.2), 2-vinylpyridine, reduced β-nicotinamide adenine dinucleotide (β-NADH), luciferin, and luciferase were obtained from Sigma-Aldrich (St. Louis, USA). Rat-tail tendon collagen I for sandwich culture was provided by Roche (Mannheim, Germany). N-Benzylpiperazine (BZP, 99.3% purity) was purchased from Chemos GmbH (Regenstauf, Germany), 1-(3-trifluoromethylphenyl)piperazine (TFMPP, 98% purity) from Alfa Aesar (Karlsruhe, Germany), 1-(4-methoxyphenyl)piperazine (MeOPP, 96% purity) from Acros Organics (New Jersey, USA), and 1-(3,4-methylenedioxybenzyl)piperazine (MDBP, 97% purity) from Aldrich Chemistry (Steinheim, Germany).

Animals

Male Wistar rats with a body weight of 300 – 400 g were purchased from Charles River (Sulzfeld, Germany). The animals had free access to food (sniff, Soest, Germany) and water and were kept under controlled temperature (18 – 26°C), humidity (30 – 70%) and lighting (12 h light/dark cycle conditions). Before the experiments, the animals were acclimated for a minimum of 6 days. This study was approved by the local committee for

the welfare of experimental animals and was performed in accordance with national legislation.

Isolation and culture of primary rat hepatocytes

Rat hepatocytes were isolated from male Wistar rats (300 – 400 g) using a modified two-step isolation described by Hengstler et al. (2000). The rats were anesthetized using an i.p. injection of a combination of 20 mg/kg xylazine (Rompun 2%, Bayer, Leverkusen, Germany) and 61.5 mg/kg ketamine (Ratiopharm, Ulm, Germany). The liver was perfused via the vena portae for 15 min with an EGTA-buffer at 37°C. Constant temperature was achieved using an inline heating system (SAHARAInline, Transmed Sarstedt Group, Bad Wünnenberg, Germany). The EGTA-buffer consists of 248 mL glucose-solution (9 g/L D-glucose), 40 mL KH-buffer (60 g/L NaCl, 1.75 g/L KCl, and 1.6 g/L KH_2PO_4; adjusted to pH 7.4), 40 mL HEPES-buffer (60 g/L HEPES; adjusted to pH 8.5), 60 mL amino acid solution (0.27 g/L L-alanine, 0.14 g/L L-aspartic acid, 0.4 g/L L-asparagine, 0.27 g/L L-citrulline, 0,14 g/L L-cysteine, 1.0 g/L L-histidine, 1.0 g/L L-glutamic acid, 1.0 g/L L-glycine, 0.4 g/L L-isoleucine, 0,8 g/L L-leucine, 1.3 g/L L-lysine, 0.55 g/L L-methionine, 0.65 g/L L-ornithine, 0.55 g/L L-phenylalanine, 0.55 g/L L-proline, 0.65 g/L L-serine, 1.35 g/L L-threonine, 0.65 g/L L-tryptophan, 0.55 g/L L-tyrosine, 0.8 g/L L-valine; (amino acids that could not be dissolved at neutral pH were dissolved by addition of 10 M NaOH at pH 11 and thereafter adjusted to pH 7.6), 2 mL glutamine solution (7 g/L L-glutamine; freshly prepared) and 0.8 mL EGTA-solution (47.5 g/L EGTA; dissolved by addition of NaOH, adjusted to pH 7.6). Subsequently, perfusion was continued for 15 min with collagenase buffer (37°C) consisting of 155 mL glucose solution, 25 mL KH-buffer, 25 mL HEPES-buffer, 38 mL amino acid solution, 10 mL $CaCl_2$ solution (19 g/L $CaCl_2$ x 2 H_2O), 2.5 mL glutamine solution and 90 mg collagenase type I (Sigma, Taufkirchen, Germany) that were dissolved in the prewarmed mixture of the aboved mentioned solutions immediately before use. After perfusion, the liver was dissected and dissociated in suspension buffer [124 mL glucose-solution, 20 mL KH-buffer, 20 mL HEPES-buffer, 30 mL amino acid solution, 2 mL glutamine solution, 1.6 mL $CaCl_2$ solution, 0.8 mL $MgSO_4$ solution (24.6 g/L $MgSO_4$ x 7 H_2O) and 0,4 g bovine serum albumine that was dissolved in the mixture of the solutions mentioned above]. The liver cell suspension was filtered through a 100 µm cell strainer, centrifuged for 5 min at 50 g, washed twice with suspension buffer, centrifuged again and resuspended in 30 mL suspension buffer. Trypan blue exclusion rate was determined and only hepatocyte suspensions with a viability greater than 80% were used. The collagen sandwich cultures were prepared as described by Schug et al. (2008). Collagen was dissolved by adding 12 mL of 0.2% (v/v)

acetic acid to the lyophilized powder. After dissolving overnight at 4 °C, 1.2 mL of 10x DMEM were added and the acid solution was neutralized by adding 1 M NaOH solution. After this, 250 µL of the collagen solution was added to each well of the 6-well plate (Sarstedt, Nümbrecht, Germany) and left to solidify for 1 h. For attachment, 2 mL of Williams Medium E (WME) (with 10% FBS, 100 U/mL penicillin, 0.1 mg/mL streptomycin, 10 µg/mL gentamicine, 100 nM dexamethasone) were added to each well. Hepatocytes were plated at a density of 1 x 10^6 cells per well. After a 3 h attachment at 37 °C and 5% CO_2 in a humidified atmosphere the cells were washed twice with warm (37 °C) WME. The medium was removed again and a second layer of collagen was added. After 30 min of gelation, WME was added, including the same additives mentioned before, but without FBS. The cells were incubated overnight before piperazine designer drugs treatment.

Cytotoxicity Assay

After incubation overnight, the sandwich cultures were exposed to the test drugs. Concentration-response curves were obtained by incubating the cells with 0 – 20 mM of BZP, TFMPP, MeOPP, or MDBP for 72 h at 37°C. Stock solutions of BZP were made up in PBS. Stock solutions of TFMPP, MeOPP and MDBP were made in DMSO. In these cases, 0.1% DMSO in culture medium was used as negative control. All stock solutions were stored at -20 °C and freshly diluted on the day of the experiment. Cytotoxicity was measured by the resazurin fluorometric method (CellTiter-Blue® Cell Viability Assay, Promega GMBH, Mannheim, Germany). This assay is based on the ability of living cells to convert a redox dye, resazurin, into a fluorescent product, resorufin. The assay was performed by adding 600 µL of the CellTiter-Blue® reagent directly to the medium 4 h before the end of the 72 h incubation-time. Resorufin was measured at a wavelength of 560 nm excitation and 590 nm emission with a fluorescence reader. Results were graphically presented as percentage of cell death versus concentration (µM). All drugs were tested in 3 independent experiments with each concentration tested in 3 replicates within each experiment.

Drugs challenge for the evaluation of toxicity biomarkers

Based on individual cytotoxicity data, three concentrations were chosen for each compound. The concentrations selected for energetic and redox status evaluation were

625, 210 and 0.5 µM for BZP; 35, 12 and 0.5 µM for TFMPP; 522, 175 and 0.5 for MeOPP and 467, 160 and 0.5 µM for MDBP. The highest concentrations correspond to EC_{20}, the intermediate to 1/3 of EC_{20} and the lowest are the common blood concentrations found in intoxication cases. For the microarray study, hepatocytes were incubated with 625, 35, 522 and 467 µM BZP, TFMPP, MeOPP and MDBP, respectively. Incubations were done at 37°C for 24 h.

Measurement of intracellular glutathione levels

After a 6 and 24 h incubation period, the medium was removed and the cells were kept on ice while being scraped in PBS, pH=7.4. After centrifugation (210 g, 5 min, 4 °C), the supernatant was removed. The pellet of cells was lysed with 5% $HClO_4$ and centrifuged (16,000 g, 10 min, 4 °C). The obtained supernatant was frozen at -20 °C until further determination of tGSH levels, evaluated by the DTNB-GSH reductase recycling assay, as previously described (Dias da Silva et al., 2014). Briefly, the acidic supernatant was neutralized with an equal volume of 0.76 M KHCO3 and centrifuged (16,000 g, 2 min, 4 °C). Total glutathione was determined by transfering, in triplicate, 100 µL of the neutralized supernatants, standards or blank (5% $HClO_4$, w/v) to a 96-well plate, followed by the addition of 65 µL of freshly prepared reagent containing 0.24 mM NADPH and 0.7 mM DTNB in phosphate buffer (71.5 mM Na_2HPO_4, 71.5 mM NaH_2PO_4 and 0.63 mM EDTA, pH 7.5). The plates were then incubated for 15 min, at 30 °C, in a microplate reader (BioTek Instruments, Vermont, USA), prior to the addition of 40 µL per well of a freshly prepared 10 U/mL glutathione reductase solution in phosphate buffer. The stoichiometric formation of 5-thio-2-nitrobenzoic acid (TNB) was followed every 10 s for 3 min at 415 nm at 30 °C, and compared with a standard curve performed for all readings. For the determination of GSSG, 10 µl of 2-vinylpyridine were added to 200 µl aliquots of the acidic supernatants and mixed continuously for 1 h at 0 °C for derivatization of the sulfhydryl groups (SH). GSSG was then measured as described for tGSH. The GSH content was calculated by subtracting the GSSG from the tGSH values [GSH = tGSH – (2 x GSSG)]. Data were normalized to the protein content, determined by the Lowry assay (Lowry et al., 1951), and the final results were expressed as nmol per mg of protein from 3 independent experiments with each concentration tested in 3 replicates within each experiment.

Measurement of intracellular ATP levels

After a 6 and 24 h incubation period, the medium was removed and the cells were kept on ice while being scraped in PBS, pH=7.4. After centrifugation (210 g, 5 min, 4 °C), the supernatant was removed. The pellet of cells was lysed with 5% $HClO_4$, centrifuged (16,000 g, 10 min, 4 °C), and the supernatant obtained was frozen at -20°C until further determination of the ATP intracellular content. The ATP levels were quantified by a bioluminescence assay, as described by Pontes et al. (2008). Briefly, the acidic supernatant was neutralized with an equal volume of 0.76 M KHCO3 and centrifuged (16,000 g, 1 min, 4 °C). The ATP contents were then measured in duplicate in 96-well white plates, by adding 100 µL of the neutralized supernatants, standards or blank (5% $HClO_4$, w/v) and 100 µL of the luciferin/luciferase solution [0.15 mM luciferin, 300,000 light units of luciferase from Photinus pyralis (American firefly), 50 mM glycine, 10mM $MgSO_4$, 1 mM Tris, 0.55 mM EDTA, 1% BSA (pH 7.6)]. The emitted light intensity was determined using a luminescence microplate reader (BioTek Instruments, Vermont, USA) and compared with a standard curve performed within each experiment. Data were normalized to the protein content, determined by the Lowry assay (Lowry et al., 1951) from 3 independent experiments with each concentration tested in 2 replicates within each experiment.

RNA isolation and processing

After the 24 h incubation time, the medium was removed and 1 mL of QIAzol (QIAGEN, Hilden, Germany) was added immediately. RNA isolation was performed according to the manufacturer's instructions. The RNA was quantified using a NanoDrop 2000 spectrophotometer (Thermo Scientific, Wilmington, DE, USA) and the integrity of RNA was confirmed with a standard sense automated gel electrophoresis system (Experion, Bio-Rad, Hercules, CA, USA).

Microarray analysis

For global gene expression profiling, the Affymetrix Rat GenChip® Genome 430 2.0 array was used. All labeling reagents and instrumentation regarding microarrays were acquired from Affymetrix (Santa Clara, USA).

Microarray analysis was done only for the highest concentration tested of each drug. A total of 100 ng RNA were transcribed into cDNA by oligo dT primers, and reverse transcribed to biotinylated cRNA with the GeneChip 3' IVT Express Kit. After 16 hours of in vitro transcription, the amplified RNA was purified using magnetic beads and 15 µg of amplified RNA was fragmented with the fragmentation buffer using the Affymetrix's protocol. In the next step, 12.5 µg of labeled and fragmented cRNA were hybridized to Rat Genome 430 2.0 AffymetrixGeneChips along with a hybridization cocktail and placed in a hybridization oven rotating at 60 RPM at 45 °C for 16 h. Microarrays were washed using an Affymetrix fluidics station 450 and stained initially with streptavidin-phycoerytherin. For each sample, the signal was further enhanced by incubation with biotinylated goat anti-streptavidin followed by a second incubation with streptavidin-phycoerytherin, and a second round of intensities were measured. Microarrays were scanned with an Affymetrix Gene-Chip Scanner-3000-7G controlled by GCOS software. Rat Genome 430 2.0 Affymetrix GeneChips contain over 45,000 probe sets from over 34,000 well-characterized mouse genes. GeneChips microarray study followed MIAME guidelines issued by the Microarray Gene Expression Data group.

Microarray data processing and statistical analysis

Concentration-response curves were fitted by the least squares method. The comparisons between curves (bottom, top and log EC_{50}) were made using the extra sum-of-squares *F* test. Results from biochemical measures were presented as mean ± standard error of the mean (SEM). Normality of the data distribution was assessed by the Kolmogorov-Smirnov normality test. Significance was accepted at $p<0.05$. Statistical comparisons between groups were performed with one-way ANOVA followed by Bonferroni post-hoc.

Affymetrix gene expression data were processed using the statistical programming language 'R-version 2.15.1'. For the normalisation of the entire set of Affymetrix gene expression arrays was used the Robust Multi-array Average (RMA) algorithm (Irizarry et al., 2003), that applies background correction, log2 transformation, quantile normalisation and a linear model fit to the normalised data to obtain a value for each probe set (PS) on each array. After normalisation, gene expression for each gene was adjusted by comparing the expression to the corresponding control array expression (paired design).

Differential expression was calculated using the R package limma (Smyth et al., 2005). Here, the combined information of the complete set of genes is used by an

empirical Bayes adjustment of the variance estimates of single genes. This form of a moderated *t* test is abbreviated here as 'Limma *t* test'. The resulting *p* values were multiplicity-adjusted to control the false discovery rate (FDR) by the Benjamini-Yekutieli procedure. As a result, for each compound a gene list was obtained, with corresponding estimates for fold change and *p* values of the Limma *t* test (unadjusted and FDR-adjusted).

Principal component analysis (PCA) plots were used to visualize expression data in two dimensions, representing the first two principal components, that is, the two orthogonal directions of the data with the highest variation. The software 'R – version 2.15.1' was used for all calculations and display of PCA. Genes which showed change ratios greater than 2 or less than 0.3-fold in the triplicate arrays have been considered as up or down-regulated and subjected to gene ontology (GO) and pathway analyses. Transcription factor binding sites enrichment (TFBSE) was performed using the PRIMA algorithm (Elkon et al., 2003) provided in the Expander software suite (version 6.04) (Ulitsky et al., 2010). The Venn diagrams for the comparison of gene expression, GO terms and transcription factor binding sites (TFBS) among the tested piperazine designer drugs were constructed according to Chow and Rodgers (2005). The size of the circles and areas was chosen proportional to the number of elements included.

Results

Piperazine designer drugs elicited concentration-dependent cytotoxicity to primary cultured rat hepatocytes

A comprehensive concentration-response analysis was carried out by incubating the primary rat heatocytes with 0-20 mM of each piperazine designer drug for 72 h. Figure 1 presents the obtained concentration-response curves showing that in the resazurin assay, all tested drugs produced concentration-dependent cytotoxic effects. A summary of the calculated EC_{50} values (representing the half-maximum-effect concentrations from the fitted curves) is presented in Table 1. Significant differences were observed for the EC_{50} values of the curves. Based on these data, it was evident that, under our experimental conditions, TFMPP (EC_{50} 0.104 mM) was the most cytotoxic of the tested piperazine designer drugs to primary rat hepatocytes, followed by MDBP (EC_{50} 1.01 mM), MeOPP (EC_{50} 1.23 mM) and BZP (EC_{50} 2.34 mM).

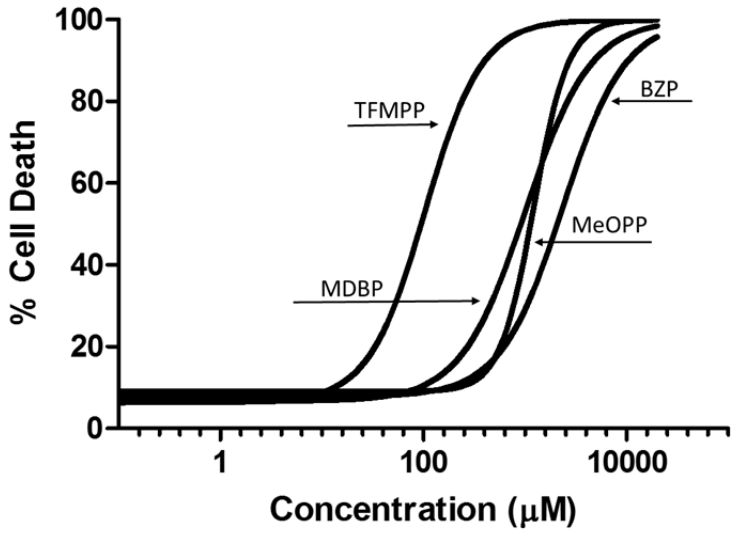

Figure 1. Concentration-response (cell death) curves of the tested piperazine designer drugs after 72 h incubations with primary rat hepatocytes at 37°C. Cell viability was evaluated by the rezasurin assay. Data are presented as percentage of cell death relative to the respective negative controls. Three independent experiments were performed (three replicates tested for each concentration within each experiment). Curves were fitted using least squares as the fitting method.

Table 1. EC_{50} values of the piperazine designer drugs

Designer Drug	EC_{50} (mM)
BZP	2.34
TFMPP	0.104*
MeOPP	1.23*#
MDBP	1.01*#$

* compares to BZP, # compares to TFMPP. The cytotoxicity curves were fitted using least squares as the fitting method. Comparisons were made using the extra sum-of-squares F test ($p<0.05$).

Piperazine designer drugs did not cause redox or energetic imbalance in primary rat hepatocytes

Changes in the intracellular amounts of GSH and GSSG are strong indicators of redox disturbances and were investigated with the DTNB-GSSG reductase recycling assay. No differences from control incubations were found after 6 h incubations for any of the tested drugs. However, a significant ($p<0.05$, ANOVA/Bonferroni) increase in total GSH of cells incubated with 625 µM BZP for 24 h was observed. This corresponded to a 24% and a 56% increase in reduced GSH and GSSG levels, respectively, in comparison to control (figure 2). All other compounds did not induce any change in total GSH, reduced GSH or GSSG levels. When intracellular ATP levels were evaluated, no alterations were

found at 6 or 24 h incubation-time (data not shown). Overall, the highest concentrations tested did not present cytotoxicity to the primary rat hepatocytes, being therefore suitable for microarray studies.

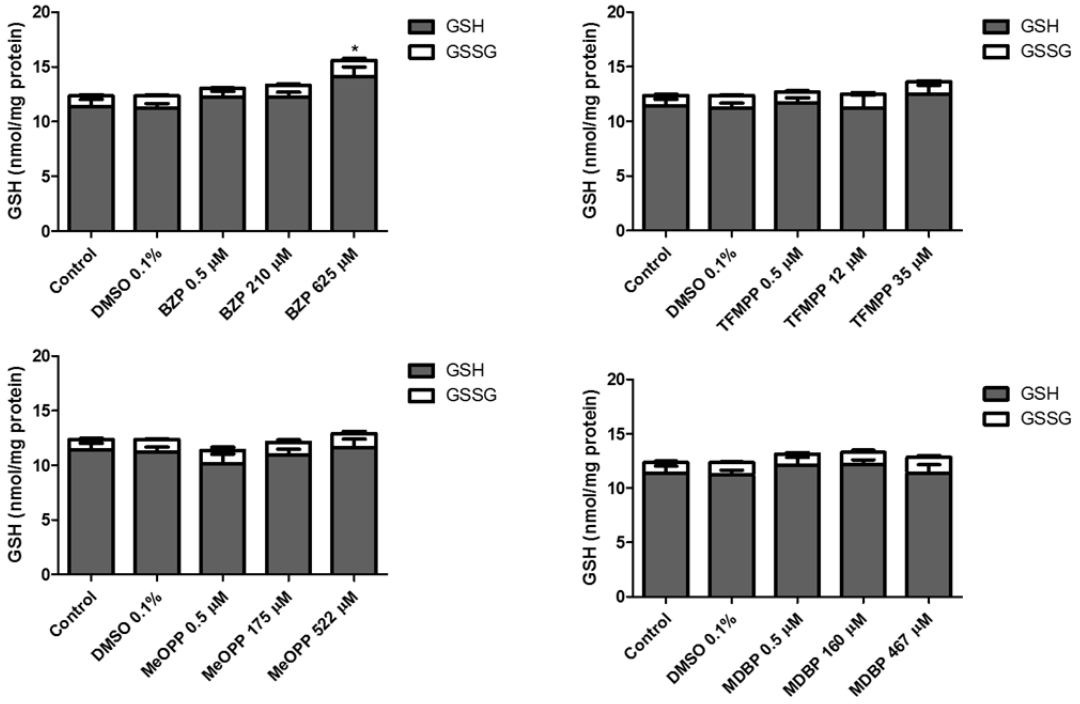

Figure 2. Intracellular contents of total glutathione (tGSH), reduced glutathione (GSH) and oxidized glutathione (GSSG) in primary rat hepatocytes after 24 h incubations with the tested piperazine designer drugs at 37 °C. Results are expressed as nmol/mg protein ± SEM (n=4 independent experiments run in triplicates). Statistical comparisons were made using one-way ANOVA/Bonferroni post-hoc test (* $p<0.05$ vs control).

Piperazine designer drugs induce transcriptional changes in rat primary hepatocytes

To identify global changes in gene expression associated with piperazine designer drugs induced hepatotoxicity, microarray analysis were performed. Figure 3 presents the number of probe sets significantly altered (up- or down-regulated) for each compound and the Venn diagram presenting the overlapping genes. MDBP presented the highest number of altered probe sets. Among the four piperazine designer drugs, 65 probes were found to be overlapped. From the total number of probe sets, genes with a fold change higher than 2.0 were selected as up-regulated, while genes with a fold change less than 0.3 were selected as down-regulated. The selected overlapped genes are summarized in table 2. As can be seen, the number of up-regulated genes is higher than the down-regulated ones. Among the overlapped genes are gpnmb, which codifies the transmembrane protein NMB, a molecule that participates in the cell adhesion processes,

and fads1 that codifies the enzyme fatty acid desaturase 1. Desaturase enzymes regulate unsaturation of fatty acids through the introduction of double bonds between defined carbons of the fatty acyl chain. Surprisingly, 5 of the up-regulated overlapped genes are related to the cholesterol pathway, according to the GO analysis. These genes are msmo1, idi1, cyp51, sqle, and fdps that codify the enzymes responsible for cholesterol biosynthesis. The first enzyme on cholesterol biosynthethic pathway up-regulated by the piperazine designer drugs is isopentenyl-diphosphate Δ isomerase (or isopentenyl pyrophosphate isomerase, IPP isomerase, idi1 gene), an isomerase that catalyzes the conversion of isopentenyl pyrophosphate (IPP) to the more-reactive electrophile dimethylallyl pyrophosphate (DMAPP). This isomerization is a key step in the biosynthesis of isoprenoids through the mevalonate pathway. Farnesyl pyrophosphate synthase (fdps gene), catalyzes the next reaction of this route, which are sequential condensation reactions of dimethylallyl pyrophosphate with 2 units of 3-isopentenyl pyrophosphate to form farnesyl pyrophosphate. Squalene epoxidase (sqle gene) is an enzyme that uses NADPH and molecular oxygen to oxidize squalene to 2,3-oxidosqualene (squalene epoxide). This is the first oxygenation step in sterol biosynthesis and it is thought to be one of the rate-limiting enzymes of this pathway. Lanosterol 14 α-demethylase (or CYP51A1, cyp51 gene) is a cytochrome P450 enzyme that is involved in the conversion of lanosterol to 4,4-dimethylcholesta-8(9),14,24-trien-3β-ol. This demethylation step is regarded as the initial checkpoint in the transformation of lanosterol to other sterols that are widely used within the cell. The last up-regulated enzyme is sterol-C4-methyloxidase that catalyzes one of the final reactions of cholesterol synthesis. Regarding the down-regulated probe sets, only one gene was common to all four piperazine derivatives, and this was related to the enzyme betaine-homocysteine-*S*-methyltransferase (bhmt gene). This is a zinc metallo-enzyme that catalyzes the transfer of a methyl group from betaine to homocysteine to produce dimethylglycine and methionine, participating in the metabolism of glycine, serine, threonine and also methionine. When the TFBS were analysed, four transcription factors overlapped among the four piperazine designer drugs evaluated (figure 4).

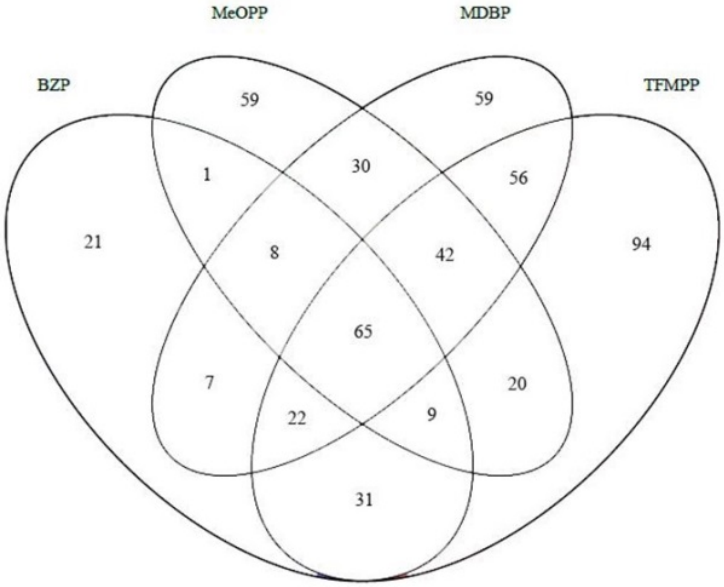

	Probe sets	
Designer drug	Up-regulated	Down-regulated
BZP	35	118
TFMPP	52	168
MeOPP	38	234
MDBP	74	242

Figure 3. Overlap of differentially expressed probe sets after 24h incubation of primary rat hepatocytes with piperazine designer drugs. Overlaps are displayed as Venn diagrams with absolute numbers of altered elements in the circles.

Table 2. Function and protein encoded by overlapped genes that were significantly altered

Gene	Protein	Function
	Up-regulated	
Gpnmb	transmembrane glycoprotein NMB	cell adhesion molecule
Fads1	fatty acid desaturase 1	fatty acid metabolism
Msmo1	sterol C4-methyloxidase	cholesterol biosynthesis
Idi1	isopentenyl-diphosphate-Δ-isomerase	cholesterol biosynthesis
Cyp51	lanosterol 14-α demethylase, CYP51A1	cholesterol biosynthesis
Sqle	squalene epoxidase	cholesterol biosynthesis
Fdps	farnesyl diphosphate synthase	cholesterol biosynthesis
	Down-regulated	
Bhmt	betaine-homocysteine S-methyltransferase	cysteine and methionine metabolism

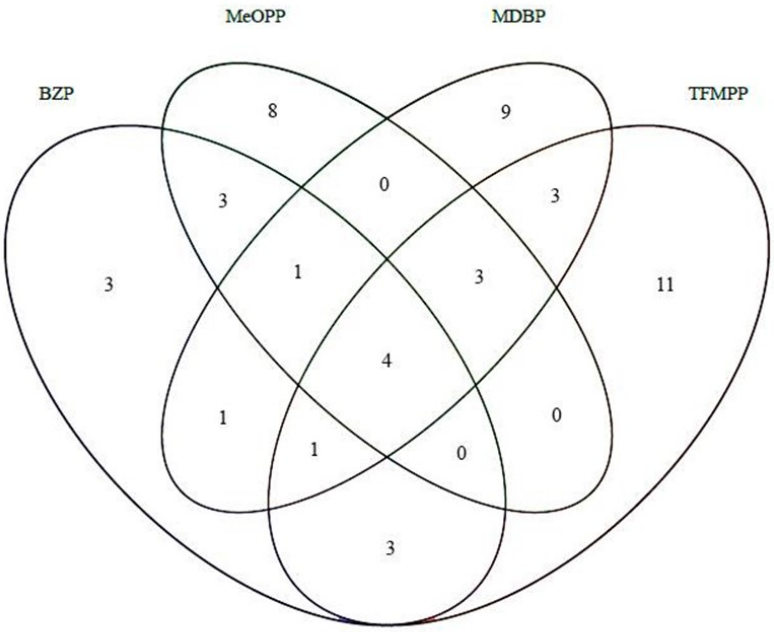

Overlapped Transcription Factors
MAZR
HNF4,_COUP
HNF-4
SREPB-1

Figure 4. Overlap of differentially expressed transcription factor binding sites (TFBS) after 24h incubation of primary rat hepatocytes with piperazine designer drugs. Overlaps are displayed as Venn diagrams with absolute numbers of altered elements in the circles.

Discussion

We have demonstrated here that piperazine designer drugs produce cytotoxicity to primary rat hepatocytes. Among the four tested piperazine designer drugs, TFMPP was the most potent in eliciting cytotoxic effects, which was in accordance with previous studies obtained in H9c2 cell line (Arbo et al., 2014). For toxicogenomic testing the highest nontoxic concentration was evaluated (Waldmann et al., 2014), which can explain the lack of effect in the redox and energetic status of the cells. The overall redox state of a cell is important for intracellular signalling and gene activation, and a vital aspect of cellular response to chemical stress and in terms of defence and cell repair (Mates and Sanchez-Jimenez, 1999). GSH also has a role in signal transduction, gene expression and apoptosis (Arrigo, 1999). A slight increase in GSH content was observed, and this can be understood as a compensatory mechanism, through which the increase of cellular antioxidant capacity tries to compensate the increase in oxidation (Finne et al., 2008).

The overall goal of the toxicogenomic study was to identify gene expression markers describing toxic effects elicited by the piperazine designer drugs. In recent years, cultivated hepatocytes have been applied in gene expression studies aimed at the identification of hepatotoxic or carcinogenic compounds (Klingmüller et al, 2006; Suzuki et al., 2008; Uehara et al., 2008; Legendre et al., 2014). Sandwich hepatocytes cultures supplemented with dexamethasone seem to be the most adequate model to detect gene expression alterations since they preserve a honeycomb shape and polarity of hepatocytes, transporters, and prevent up-regulation of epithelial to mesenchymal transition markers (Luttringer et al., 2002; Schug et al., 2008, Godoy et al., 2010; Kim et al., 2010). However, two major limitations when using cultivated primary hepatocytes in toxicogenomics must be considered. First, hepatocytes undergo massive gene expression alterations, particularly during the first 24 h in culture. Therefore, gene expression alterations induced by test compounds have to be analysed against a rather “noisy” background. Second, huge discrepancies between test compound-induced gene expression in the liver in vivo and in hepatocytes in vitro have been reported (Godoy et al., 2009; Schug et al., 2013). It is, therefore, necessary to phenotypically anchor the findings obtained after such toxicogenomic approaches.

In spite of the number of down-regulated probes being higher than the up-regulated ones, only the bhmt was commonly regulated by the four piperazine designer drugs. The bhmt gene codifies the enzyme betaine-homocysteine-S-methyltransferase (BHMT), a liver and kidney metaloenzyme that catalyzes the methyl transfer from betaine to homocysteine to form methionine and dimethylglycine (Kořínek et al., 2013). It has been shown that BHMT plays a protective role in homocysteine-induced injury in cultured hepatocytes (Ji et al., 2007). The major effect of BHMT inhibition is an increase in homocysteine and a decrease in S-adenosylmethionine levels. The decrease in S-adenosylmethionine activates a process leading to hepatocyte proliferation and transformation. Indeed, patients with hyperhomocysteinemia develop hepatic steatosis, which can progress into hepatocellular carcinoma (Selicharová et al., 2013). In agreement with a steatosis hepatotoxic mechanism, we also found an up-regulation of the Fads1 gene, which encodes fatty acid Δ^5-desaturase. Fads1 gene is known to be related with lipogenesis, suggesting that it participates in the process of steatogenesis (Glaser et al., 2010; Tateno et al., 2011). GPNMB is a type I transmembrane protein expressed in a wide variety of normal tissues, which was also found to be up-regulated by all the drugs. GPNMB is associated with poor prognosis in breast cancer and has been implicated in two different angiogenesis pathways (Agostini et al., 2012), so it is possible that GPNMB also plays a role in hepatocarcinoma.

Nevertheless, the majority of the up-regulated genes that were found are related to cholesterol biosynthesis. In the body, cholesterol is either derived from the diet or from *de novo* synthesis occurring mainly in the liver through the mevalonate pathway. This pathway comprises several enzymes, such as sterol C4-methyloxidase (msmo1), isopentenyl-diphosphate-Δ-isomerase (idi1), lanosterol 14-α demethylase (cyp51), squalene epoxidase (sqle), and farnesyl diphosphate synthase (fdps). Cholesterol metabolism may play a role in the development of non-alcoholic fatty liver disease. For example, in steatotic livers, cholesterol biosynthesis is still activated despite a cholesterol overload in hepatocytes, indicating that cholesterol metabolism is deregulated (Enjoji and Nakamuta, 2010). Additionally, in mice, dietary cholesterol exacerbates hepatic steatosis, and the expression of genes fdps, idi1, sqle and cyp51 were found to be altered after 3 weeks of treatment with an atherogenic, Western or high fat diets (Renaud et al, 2014).

Cholesterol, as well as phospholipids, are critical components of the plasma membrane of living cells. While cholesterol also functions as the precursor of steroid hormones, phospholipids function as emulsifying agents to maintain the proper colloidal state of the cytoplasm. Several toxicants are known to disrupt phospholipid metabolism. For example, lead exposure was associated with cholesterogenesis and phospholipidosis in exposed animals (Ademuyiwa et al., 2009). Phospholipidosis is often observed in various tissues, including liver, kidney, and lung, and it is characterized by intracellular accumulation of phospholipids and the appearance of membranous lamellar bodies (Hirode et al., 2008). Four possible mechanisms have been suggested for the induction of phospholipidosis based on toxicogenomic data: (1) inhibition of lysosomal phospholipase activity – this is generally regarded as the primary mechanism of induction; (2) inhibition of lysosomal enzyme transport; (3) enhanced phospholipid biosynthesis; and (4) enhanced cholesterol biosynthesis - this considered to be an indirect trigger (Sawada et al., 2005). In drug-induced phospholipidosis, accumulation of phospholipids in lamellar bodies is also accompanied by increased levels of neutral lipids and cholesterol. Changes of the cellular cholesterol turnover are sensored by the sterol regulatory element binding proteins (SREBP) type transcription factors. Specifically, the SREBPs regulate multiple genes of the cholesterol biosynthesis and uptake pathway (Anderson and Borlak, 2006). This transcription factor enters the nucleus, binds to sterol regulatory elements and induces several genes involved in sterol and lipid biosynthesis (Hubbert et al., 2007). Drugs known to induce phospholipidosis by up-regulation of cholesterol biosynthetic pathway include propiconazole (Murphy et al., 2012), fluoxetine, imipramine, and hydroxyzine (Sawada et al., 2005; Hirode et al., 2008).

Gene expression is primarily controlled through the action of transcription factors that respond to environmental, autocrine, or paracrine signals. The regulation of cholesterol levels is a complex process involving cross regulatory feedback mechanisms using a variety of sensors (Murphy et al., 2012). Hepatic lipid synthesis is regulated by the lipogenic transcription factor sterol regulatory element binding proteins (SREBPs), one of the overlapped transcription factors found on TFBSE analysis. SREBPs are ~130 kDa proteins attached to the endoplasmic reticulum and nuclear membranes through transmembrane-spanning domains. SREBP1 and SREBP2 are encoded by separate genes, and SREBP1 is expressed as two subtypes, 1a and 1c. In the liver, SREBP1c is the predominant subtype (Mater et al., 1999). A two-step proteolytic cleavage of SREBP occurs within the Golgi complex and releases a basic helix-loop-helix-leucine zipper transcription factor denoted nuclear SREBP (nSREBP). The cleavage is controlled by the endoplasmic reticulum cholesterol content, which is sensed by SREBP cleavage activating protein (SCAP). SCAP, together with Insig proteins, retains SREBP within the endoplasmic reticulum when cholesterol is abundant, but escorts it to the Golgi complex on cholesterol depletion (Yan et al., 2007). Processed SREBP1 and-2 bind to specific promoters and, in turn, enhance the transcription of genes involved in cholesterol biosynthesis and transport (Szántó et al., 2014). SREBP is also involved in a complex feedback regulation which includes insulin signalling (Ribaux and Iynedjian, 2003; Reed et al., 2008; Kohjima et al., 2008), FoxO transcription factors (Deng et al., 2012), and oxysterols (Ren et al., 2007).

Another overlapped transcription factor found among the four piperazine designer drugs evaluated is HNF4. This is a member of the nuclear hormone receptor family of transcription factors. It binds DNA as a homodimer and, although initially believed to be an orphan receptor, its activity may be modulated by the binding of fatty acyl-CoA thioesters. The ability of HNF4 to regulate liver genes, as well as its expression throughout hepatic development, suggested a significant role for this factor in differentiation of the hepatocyte lineage (Watt et al., 2003). Regarding to cholesterol pathways, HNF4 regulates the transcription of apolipoprotein A-I in hepatocytes (Mogilenko et al., 2009).

In conclusion, piperazine designer drugs elicited cytotoxicity in sandwich cultures of primary rat hepatocytes. In spite of the negligible toxicity observed through some classical biochemical markers, such as GSH/GSSG and ATP, microarray analysis showed to be more sensitive and revealed that piperazine designer drugs can enhance cholesterol biosynthesis, which may eventually lead to phospholipidosis. The hope is that, in the near future, gene biomarkers will allow the testing of multiple drug toxicities simply by

measuring gene expression. The toxicogenomic approach used in this study should be helpful in the examination of the mode of action and identification of gene markers for these drugs. However, these findings need validation through other tests.

References

Ademuyiwa O, Agarwal R, Chandra R, Behari JR (2009) Lead-induced phospholipidosis and cholesterogenesis in rat tissues. Chem Biol Int 179: 314-320.

Agostini J, Benoist S, Seman M, Julié C, Imbeaud S, Letourneur F, Cagnard N, Rougier P, Brouquet A, Zucman-Rossi J, Laurent-Puig P (2012) Identification of molecular pathways involved in oxaliplatin-associated sinusoidal dilatation, J Hepatol 56: 869-876.

Anderson N, Borlak J (2006) Drug-induced phospholipidosis. FEBS Letters 580: 5533-5540.

Antia U, Lee HS, Kydd RR, Tingle MD, Russell BR (2009) Pharmacokinetics of 'party pill' drug N-benzylpiperazine (BZP) in healthy human participants. Forensic Sci Int 186: 63-67.

Antia U, Tingle MD, Russel BR (2010) Validation of an LC-MS method for the detection and quantification of BZP and TFMPP and their hydroxylated metabolites in human plasma and its application to the pharmacokinetic study of TFMPP in humans. J Forensic Sci 55: 1311-1318.

Arbo MD, Bastos ML, Carmo H (2012) Piperazine compounds as drugs of abuse. Drug Alcohol Depend 122: 174-185.

Arbo MD, Silva R, Barbosa DJ, da Silva DD, Rossato LG, Bastos ML, Carmo H (2014). Piperazine designer drugs induce toxicity in cardiomyoblast H9c2 cells through mitochondrial impairment. Toxicol Lett 229: 178-189.

Arrigo, AP (1999). Gene expression and the thiol redox state. Free Radical Biol Med 27: 936-944.

Austin H, Monasterio E (2004) Acute psychosis following ingestion of 'Rapture'. Australasian Psychiatry 12: 406–408.

Baumann MH, Clark RD, Budzynski AG, Partilla JS, Blough BE, Rothman RB (2005) N-Substituted piperazines abused by humans mimic the molecular mechanism of 3,4-methylenedioxymethamphetamine (MDMA, or 'Ectasy'). Neuropsychopharmacol 30: 550-560.

Chow S, Rodgers P (2005) Extended abstract: constructing area-proportional Venn and Euler diagrams with three cycles. Paper presented at the Euler diagrams workshop 2005, Paris.

Deng X, Zhang W, O-Sullivan I, Williams JB, Dong Q, Park EA, Raghow R, Unterman TG, Elam MB (2012) FoxO1 inhibits sterol regulatory element-binding protein-1c (SREBP-1c) gene expression via transcription factors Sp1 and SREBP-1c. J Biol Chem 287: 20132-20143.

Dias da Silva D, Silva E, Carmo H (2014) Combination effects of amphetamines under hyperthermia – the role played by oxidative stress. J Appl Toxicol 34: 637-650.

Elliott S (2011) Current awareness of piperazines: pharmacology and toxicology. Drug Testing Anal 3: 430-438.

Elkon R, Linhart C, Sharan R, Shamir R, Shiloh Y (2003) Genome-wide in silico identification of transcriptional regulators controlling the cell cycle in human cells. Genome Res 13(5):773-780.

Enjoji M, Nakamuta M (2010) Is the control of dietary cholesterol intake sufficiently effective to ameliorate non-alcoholic fatty liver disease? World J Gastroenterol 16: 800-803.

Finne EF, Olsvik PA, Berntssen MHG, Hylland K, Tollefsen KE (2008) The partial pressure of oxygen affects biomarkers of oxidative stress in cultured rainbow trout (*Oncorhynchus mykiss*) hepatocytes. Toxicol in Vitro 22: 1657-1661.

Gee P, Richardson S, Woltersdorf W, Moore G (2005) Toxic effects of BZP-based herbal party pills in humans: a prospective study in Christchurch, New Zealand. NZ Med J 118: 1784–1794.

Glaser C, Heinrich J, Koletzko B (2010) Role of FADS1 and FADS2 polymorphisms in polyunsaturated fatty acid metabolism. Metabolism 59: 993-999.

Godoy P, Hengstler JG, Ilkavets I, Meyer C, Bachmann A, Müller A, Tuschl G, Mueller SO, Dooley S (2009). Extracellular matrix modulates sensitivity of hepatocytes to fibroblastoid dedifferentiation and transforming growth factor beta-induced apoptosis. Hepatology 49: 2031-2043.

Godoy P, Lakkapamu S, Schug M, Bauer A, Stewart JD, Bedawi E, Hammad S, Amin J, Marchan R, Schormann W, Maccoux L, von Recklinghausen I, Reif R, Hengstler JG (2010) Dexamethasone-dependent *versus* -independent markers of epithelial to mesenchymal transition in primary hepatocytes. Biol Chem 391: 73-83.

Hirode M, Ono A, Miyagishima T, Nagao T, Ohno Y, Urushidani T (2008) Gene expression profiling in rat liver treated with compounds inducing phospholipidosis. Toxicol Appl Pharmacol 229: 290-299.

Hubbert ML, Zhang Y, Lee FY, Edwards PA (2007) Regulation of hepatic Insig-2 by the farnesoid X receptor. Mol Endocrinol 21: 1359-1369.

Irizarry RA, Hobbs B, Collin F, Beazer-Barclay YD, Antonellis KJ, Scherf U, Speed TP (2003) Exploration, normalization, and summaries of high density oligonucleotide array probe level data. Biostatistics 4: 249-264.

Ji , Shinohara M, Kuhkenkamp J, Chan C, Kaplowitz N (2007) Mechanism of protection by the betaine-homocysteine methyltransferase/betaine system in HepG2 cells and primary mouse hepatocytes. Hepatology 46: 1586-1596.

Kim Y, Lasher CD, Milford LM, Murali TM, Rajagopalan P (2010) A comparative study of genome-wide transcriptional profiles of primary hepatocytes in collagen sandwich and monolayer cultures. Tissue Engeneering 16: 1449-1460.

Klingmüller U, Bauer A, Bohl S, Nickel PJ, Breitkopf K, Dooley S, Zellmer S, Kern C, Merfort I, Sparna T, Donauer J, Walz G, Geyer M, Kreutz C, Hermes M, Götschel F, Hecht A, Walter D, Egger L, Neubert K, Borner C, Brulport M, Schormann W, Sauer C, Baumann F, Preiss R, MacNelly S, Godoy P, Wiercinska E, Ciuclan L, Edelmann J, Zeilinger K, Heinrich M, Zanger UM, Gebhardt R, Maiwald T, Heinrich R, Timmer J, von Weizsäcker F, Hengstler JG (2006) Primary mouse hepatocytes for systems biology approaches: a standardized *in vitro* system for modelling of signal transduction pathways. IEE Proc Syst Biol 153: 433-447.

Kohjima M, Higuchi N, Kato M, Kotoh K, Yoshimoto T, Fujino T, Yada M, Yada R, Harada N, Enjoji M, Takayanagi R, Nakamuta M (2008) SREBP-1c, regulated by the insulin and AMPK signalling pathways, plays a role in non-alcoholic fatty liver disease. Int J Mol Med 21: 507-511.

Kořínek M, Šístek V, Mládková J, Mikeš P, Jiráček J, Selicharová I (2013) Quantification of homocysteine-related metabolites and the role of betaine-homocysteine S-methyltransferase in HepG2 cells. Biomed Chromatogr 27: 111-121.

Legendre A, Jacques S, Dumont F, Cotton J, Paullier P, Fleury MJ, Leclerc E (2014). Investigation of the hepatotoxicity of flutamide: pro-survival/apoptotic and necrotic switch in primary rat hepatocytes characterized by metabolic and transcriptomic profiles in microfluidic liver biochips. Toxicol in vitro 28: 1075-1087

Lowry OH, Rosebrough NJ, Farr AL, Randall RJ (1951) Protein measurement with the folin-phenol reagent. J Biol Chem 193: 265-275.

Luttringer O, Theil FP, Lavé T, Wernli-Kuratli K, Guentert TW, de Saizieu A (2002) Influence of isolation procedure, extracellular matrix and dexamethasone on the regulation of membrane transporters gene expression in rat hepatocytes. Biochem Pharmacol 64: 1637-1650.

Mater MK, Thelen AP, Pan DA, Jump DB (1999) Sterol response element-binding protein 1c (SREBP1c) is involved in the polyunsaturated fatty acid suppression of hepatic S14 gene transcription. J. Biochem Chem 274: 32725-32732.

Mates JM, Sanchez-Jimenez, F (1999) Antioxidant enzymes and their implications in pathopysiologic process. Front Biosci 4: D339-D345.

Meririne E, Kajos M, Kankaanpää A, Seppälä T (2006) Rewarding properties of 1-benzylpiperazine, a new drug of abuse, in rats. Basic Clin Pharmacol Toxicol 98: 346-250.

Mogilenko DA, Dizhe EB, Shavva VS, Lapikov IA, Orlov SV, Perevozchikov AP (2009) Role of the nuclear receptors HNF4α, PPARα, and LXRs in the TNFα-mediated inhibition of human apolipoprotein A-I gene expression in HepG2 cells. Biochem 48: 11950-11960.

Murphy LA, Moore T, Nesnow S (2012) Propiconazole-enhanced hepatic cell proliferation is associated with dysregulation of the cholesterol biosynthesis pathway leading to activation of Erk1/2 through Ras farnesylation. Toxicol Appl Pharmacol 260: 146-154.

Pontes H, Santos-Marques MJ, Fernandes E, Duarte JA, Remião F, Carvalho F, Bastos ML (2008) Effect of chronic ethanol exposure on the hepatotoxicity of ecstasy in mice: an ex vivo study. Toxicol in vitro 22: 910-920.

Reed BD, Charos AE, Szekely AM, Weissman SW, Snyder M (2008) Genome-wide occupancy of SREBP1 and its partners NFY and SP1 reveals novel functional roles and combinatorial regulation of distinct classes of genes. Plos Genetics 4: e1000133.

Ren S, Li X, Rodriguez-Agudo D, Gil G, Hylemon P, Pandak WM (2007) Sulfated oxysterol, 25HC3S, is a potent regulator of lipid metabolism in human hepatocytes. Biochem Biophys Res Comm 360: 802-808.

Renaud HJ, Cui JY, Lu H, Klaassen CD (2014) Effect of diet on expression of genes involved in lipid metabolism, oxidative stress, and inflammation in mouse liver-insights into mechanisms of hepatic steatosis. Plos One 9: e88584-e88584.

Ribaux PG, Iynedjian PB (2003) Analysis of the role of protein kinase B (cAKT) in insulin-dependent induction of glucokinase and sterol regulatory element-binding protein 1 (SREBP1) mRNAs in hepatocytes. Biochem J 376: 697-705.

Sahu SC (Ed) Hepatotoxicity: from genomics to *in vitro* and *in vivo* models. Wiley: West Sussex, England.

Sawada H, Takami K, Asahi S (2005) A toxicogenomic approach to drug-induced phospholipidosis: analysis of its induction mechanism and establishment of a novel *in vitro* screening system. Toxicol Sci 83: 282-292.

Schep LJ, Slaughter RJ, Vale A, Beasley M, Gee GP (2011) The clinical toxicology of the designer “party pills” benzylpiperazine and trifluoromethylphenylpiperazine. Clin Toxicol 49: 131–141.

Schug M, Heise T, Bauer A, Storm D, Blaszkewicz M, Bedawy E, Brulport M, Geppert B, Hermes M, Föllmann W, Rapp K, Maccoux L, Schormann W, Appel KE, Oberemm A, Gundert-Remy U, Hengstler JG (2008) Primary rat hepatocytes as in vitro system for gene expression studies: comparison of sandwich, Matrigel and 2D cultures. Arch Toxicol 82: 923-931.

Schug M, Stöber R, Heise T, Mielke H, Gundert-Remy U, Godoy P, Reif R, Blaszkewicz M, Ellinger-Ziegelbauer H, Ahr HJ, Selinski S, Günther G, Marchan R, Sachinidis A, Nüssler A, Oberemm A, Hengstler JG (2013) Pharmacokinectics explain in vivo/in vitro discrepancies of carcinogen-induced gene expression alterations in rat liver and cultivated hepatocytes. Arch Toxicol 87: 337-345.

Selicharová I, Kořínek M, Demianová Z, Chrudinová M, Mládková J, Jiráček J (2013) Effects of homocysteinemia and betaine-homocysteine S-methyltransferase inhibition on hepatocyte metabolites and the proteome. Biochim Biophys Acta 1834: 1596-1606.

Smyth GK, Gentleman R, Carey V, Dudoit S, Irizarry R, Huber W (2005) Limma: linear models for microarray data. Bioinformatics and Computational Biology Solutions using R and Bioconductor, Springer, New York, pp 397-420.

Suzuki H, Inoue T, Matsushita T, Kobayashi K, Horii I, Hirabayashi Y, Inoue T (2008) In vitro gene expression analysis of hepatotoxic drugs in rat primary hepatocytes. J Appl Toxicol 28: 227-236.

Szántó M, Brunyánszki A, Márton J, Vámosi G, Nagy L, Fodor T, Kiss B, Virág L, Gergely P, Bai P (2014) Deletion of PARP-2 induces hepatic cholesterol accumulation and decrease in HDL levels. Biochim Biophys Act 1842: 594-602.

Tateno C, Kataoka M, Utoh R, Tachibana A, Itamoto T, Asahara T, Miya F, Tsunoda T, Yoshizato K (2011) Growth hormone-dependent pathogenesis of human hepatic steatosis in a novel mouse model bearing a human hepatocyte-repopulated liver. Endocrinology 152: 1479-1491.

Taub R (2004) Liver regeneration: from myth to mechanism. Nat Rev Mol Cell Biol 5: 836-847.

Uehara T, Kiyosawa N, Hirode M, Omura K, Shimizu T, Ono A, Mizukawa Y, Miyagishima T, Nagao T, Urushidani T (2008) Gene expression profiling of methapyrilene-induced hepatotoxicity in rat. J Toxicol Sci 53: 37-50.

Ulitsky I, Maron-Katz A, Shavit S, Sagir D, Linhart C, Elkon R, Tanay A, Sharan R, Shiloh Y, Shamir R (2010) Expander: from expression microarrays to networks and functions. Nat Protoc 5(2): 303-322.

Waldmann T, Rempel E, Balmer NV, König A, Kolde R, Gaspar JA, Henry M, Hescheler J, Sachinidis A, Rahnenführer J, Hengstler JG, Leist M (2014) Design principles of concentration-dependent transcriptome deviations in drug-exposed differentiating stem cells. Chem Res Toxicol 27: 408-420.

Watt AJ, Garrison WD, Duncan SA (2003) HNF4: a central regulator of hepatocyte differentiation and function. Hepatol 37: 1249-1253.

Yan D, Lehto M, Rasilainen L, Metso J, Ehnholm C, Ylä-Herttuala S, Jauhiainen M, Olkkonen VM (2007) Oxysterol binding protein induces upregulation of SREBP-1c and enhances hepatic lipogenesis. Arterioscler Thromb Vasc Biol 27: 1108-1114.

Yarosh HL, Katz EB, Coop A, Fantegrossi WE (2007) MDMA-like behavioral effects of N-substituted piperazines in the mouse. Pharmacol Biochem Behav 88: 18-27.

CHAPTER IV

INTEGRATED DISCUSSION

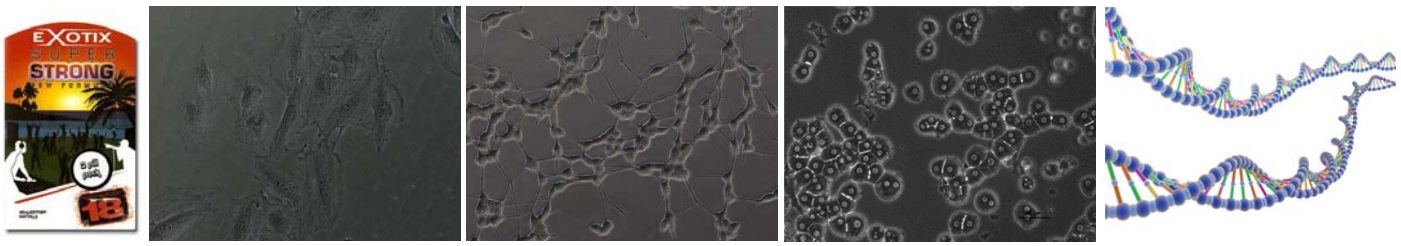

4.1 Integrated discussion

The consumption of drugs of abuse is a worldwide problem, and the internet has contributed to the easy access to such drugs. Piperazine designer drugs have been marketed in UK (Davies et al., 2010), Japan (Takahashi et al., 2009), Brazil (Lanaro et al., 2010), France (Gaillard et al., 2013), Bulgaria (Helander et al., 2014), Belgium (Kovaleva te al., 2008), Sweden (Wilkström et al., 2004), South Africa (Cohen and Butler, 2011), Poland (Biliński et al., 2012), New Zealand (Gee et al., 2005; Sheridan et al., 2007), Australia and in the USA (Gee and Fountain, 2007). In spite of they have been commercialized as a secure alternative to MDMA, studies and case-reports, reviewed by Schep and collegues (2011) and Arbo and co-workers (2012), indicate risks for humans. When this thesis was proposed, these drugs were freely commercialized in Portugal and other EU countries. However, at that time, there were no toxicological or mechanistic studies about them. Therefore, the present thesis aimed to study the mechanisms of toxicity of piperazine designer drugs exploring different *in vitro* models, corresponding to the main target organs usually affected by drugs of abuse. To achieve this objective we used i) H9c2 rat cardiomyoblasts, to study the cardiotoxicity; ii) differentiated human neuroblastoma derived SH-SY5Y cells, to evaluate the neurotoxicity; and iii) four *in vitro* approaches to evaluate the hepatotoxicity, the human derived HepG2 and HepaRG cells, and the monolayers and sandwich cultures of primary rat hepatocytes.

The H9c2 is a clonal cardiomyoblast cell line derived from embryonic rat ventricles. These cells maintain many molecular markers of cardiomyocytes and show morphological characteristics of immature embryonic cardiomyocytes (Hescheler et al., 1991). On the other hand, H9c2 cells adopt features of skeletal muscle because the cells express nicotinic receptors and synthesize a muscle-specific creatine phosphokinase isoenzyme (Kimes and Brandt, 1976). Also, the cells do not express gap junctions, T tubules, or myofibrils with organized sarcomeres. However, they are considered a valuable model to assess *in vitro* cardiotoxicity, especially because these cells have preserved several elements of the electrical and hormonal signal pathway found in adult cardiac cells (Hescheler et al., 1991) and adequately mimic the metabolic capacity of the rat heart (Zordoky and El-Kadi, 2007; Aboutabl and El-Kadi, 2007). Recently, our group showed through this model that mitoxantrone cause energetic imbalance in the cardiac cells and that the metabolism contributes to the toxicity (Rossato et al., 2013ab).

Human SH-SY5Y cells are a comparatively homogeneous neuroblast-like cell line, frequently used as an *in vitro* neuronal model. Although they do not present all the characteristics of adult neurons in the brain, these cells may acquire a neuronal

dopaminergic phenotype after stimulation with several agents, making them a useful research tool to elucidate the toxicity mechanism of drugs (Presgraves et al., 2003). They exhibit neuronal marker enzyme activity (tyrosine and dopamine-β-hydroxylases), specific uptake of NE, and express one or more neurofilament proteins. They also express opioid, muscarinic, and nerve growth factor receptors. Although SH-SY5Y cells have been widely used either in their undifferentiated or differentiated state, use of undifferentiated cells involves some limitations, such as the proliferation during the experiment, which makes it difficult to distinguish whether neurotoxic agents influence the proliferation rate or the rate of cell death (Datki et al., 2003). Furthermore, SH-SY5Y cells in culture are unsynchronized and do not always exhibit the typical markers of mature neurons, which leads to uncertainty in experiments. Differentiation leads to a functionally mature neuronal phenotype. Upon differentiation, cells stop proliferating, become a more stable population and show extensive neurite outgrowth, with morphological similarity to living neurons in the brain. In addiction, SH-SY5Y differentiated cells possess more biochemical, ultrastructural, morphological and electrophysiological similarity to neurons and express a variety of neuronal-specific markers (Presgraves et al., 2003). However, according to the differentiation agent used, cells may acquire different phenotypes. SH-SY5Y cells differentiated with retinoic acid present a mature cholinergic phenotype, with no significant differences in DAT and tyrosine hydroxylase expression (Cheung et al., 2009). However, they present higher expression of choline acetyl transferase and vesicular monoamine transporter (VMAT), confirming the enhancement of cholinergic phenotype. On the other hand, SH-SY5Y cells differentiated with 12-*O*-tetradecanoylphorbol-13-acetate (TPA) acquire a more characteristic adrenergic neuronal phenotype, as observed by the increase of tyrosine hydroxylase expression and NE and neuropeptide Y biosynthesis (Presgraves et al., 2003). When used retinoic acid/TPA in combination, differentiated SH-SY5Y cells develop a dopaminergic phenotype and have higher levels of tyrosine hydroxylase, DAT, and dopaminergic D_2 and D_3 receptors but lower levels of VMAT than undifferentiated cells (Xie et al., 2010). Differentiated SH-SY5Y cells have been used by our group to study the neurotoxic effects of MDMA and metabolites (Ferreira et al., 2013; Barbosa et al., 2014ab) and other neurotoxicants (Martins et al., 2013).

The human-derived hepatoblastoma cell line HepG2 has been extensively used as a test system for the prediction of hepatic toxicity, carcinogenicity and cell mutagenicity in humans. These cells show many liver specific functions, express conjugating enzymes, but lack a functional expression of almost all the relevant human liver CYP450 enzymes (Donato et al., 2008). Most of the CYP450 isoforms examined in HepG2 cells presented values that were 2-3 orders of magnitude lower than in human hepatocytes (Guo et al.

2011; Lin et al. 2012). In our lab, this *in vitro* system was previously used for the characterization of the cytotoxic effects of amphetamine derivatives (Dias da Silva et al. 2013ab, 2014ab).

The HepaRG cells are derived from a human hepatocellular carcinoma and also show features of a well differentiated hepatocyte. When seeded at a low density, they acquire an elongated undifferentiated morphology, actively divide, and after having reached confluency, form typical hepatocyte-like colonies surrounded by biliary ephitelial-like cells. Moreover, contrary to other human hepatoma cell lines, including the HepG2 cells, HepaRG cells not only express several CYP450s, but also the nuclear constitutive androstane receptor (CAR) and pregnane X receptor (PXR) at levels comparable to those found in cultured primary human hepatocytes (Donato et al., 2008). Comparing to HepG2 cells, HepaRG present a higher level of CYP1A1, CYP2B6, CYP2C9, CYP2E1 and CYP3A4 mRNA and lower CYP2D6 mRNA (Aninat et al. 2006, Rodrigues et al. 2013). Interestingly, the main metabolic pathways described for the piperazine designer drugs in animals and in humans comprise reactions catalyzed by CYP2D6, which include the hydroxylation of BZP (Staack and Maurer 2005), TFMPP (Staack et al. 2003), and MeOPP (Staack et al. 2004) and the demethylenation of MDBP (Staack and Maurer 2004).

Hepatoma cells have been recognized as a good model to evaluate enzyme induction and non-metabolic dependent toxicity. However, they do not constitute a real alternative to primary hepatocytes to screen chemicals bioactivated by drug-metabolizing enzymes (Donato et al., 2008). Cultured hepatocytes are the most suitable model for investigating induction of CYPs by chemical inducers and metabolic profiles of new drugs (Aninat et al. 2006), so this *in vitro* model was also included in this work. Nevertheless, dedifferentiation is well know to occur in primary monolayer cultures, where hepatocytes lost many of their specific properties such as reduced synthesis of serum proteins; a progressive fall in levels of glucose-6-phosphatase; and a decrease in CYP450s and NADPH CYP450-reductase (Luttringer et al., 2002). Moreover, hepatocytes features such as polarity and bile canalicular transport are progressively lost in monolayer cultures. After a few days, hepatocytes start to spread and acquire a fibroblast-like shape (Godoy et al., 2009). In spite of these disandvantages, monolayer hepatocyte cultures have been used successfully by our group to describe the toxic effects of MDMA and ethanol consumption (Pontes et al., 2008), paraquat (Sousa et al., 2009) and synthetic cathinones (Araújo et al., 2014).

After the isolation procedure, the hepatocytes can be maintained in different extracellular matrice configurations (single or double collagen matrices, Matrigel, Vitrogen) in customized culture media (Luttringer et al., 2002). In collagen-sandwich cultures, hepatocytes are mantained between two collagen gels and remain stable over extended periods. Moreover, in this extracellular matrice, the cells preserve a honeycomb shape and polarity, and prevents upregulation of epithelial to mesenchymal transition markers (Godoy et al., 2009). Besides, collagen-sandwich cultures exhibit the preservation of other differentiated functions, including secretion of urea, expression of plasma proteins such as albumin and fibrinogen, the presence of bile canaliculi, as well as the synthesis of gap junction and tight junction proteins (Kim et al., 2010). However, even the collagen sandwich culture technique is not able to completely abolish dedifferentiation. Therefore, further factors, such as hormonal additives might be required. For instance, dexamethasone has been reported to contribute to the maintenance of differentiated hepatocytes functions, increase fibronectin secretion, induce tyrosine aminotransferases, promote an ordered arrangement of the cytoskeleton , enhance gap junctions expression and function, regulate the P-glycoprotein expression, support CYP450 activity and curtail the decrease in protein synthesis observed in hepatocytes during the initial 24 h after isolation (Luttringer et al., 2002; Godoy et al., 2010). On the other hand, it is known that culture conditions may influence signal transduction pathways (Klingmüller et al., 2006). RNA expression levels *in vitro* strongly depend on culture conditions and may deviate from *in vivo* situation. Studing the gene expression patterns induced by the hepatotoxicant methapyrilene in three different systems (sandwich, Matrigel and 2D cultures), Schug et al (2008) proved that collagen-sandwich cultures were the most adequate system for detection of gene expression alterations. Based on this, we selected this *in vitro* model in our toxicogenomic studies.

Previous works have demonstrated that different cell lines shown equal predictivity to most toxicants. That happens because all cell lines have the same machinery for cell survival and replication. Besides, in immortalized cells, the endpoints utilized for toxicity evaluation, such as oxidative stress, inflammation, apoptosis, energetic dysfunction, can potentially contribute to a variety, or the majority, of organ toxicities (Lin and Will, 2012). Our studies showed that piperazine designer drugs presented different responses in our *in vitro* models. TFMPP, MeOPP and MDBP were highly cytotoxic to differentiated human neuroblastoma SH-SY5Y cells, presenting the lowest EC_{50} values among all models, while BZP was more cytotoxic to H9c2 rat cardiomyoblasts. The effects in cardiac cells were somehow expected, since these drugs have a predominance of adrenergic effects in the periphery (Schep et al., 2011). Therefore, these data might indicate that BZP has a

greater affinity for adrenoceptors than the other drugs. Comparing the hepatic *in vitro* models, the primary rat hepatocytes were clearly more susceptible to cytotoxicity than the immortalized cells, which presented the highest EC_{50} values. This indicates the importance of the metabolism to the piperazine designer drugs cytotoxicity since the main difference among these 3 models is their metabolic capacity. Regarding the relative potency of the drugs, it was clear that TFMPP was the most cytotoxic derivative in all *in vitro* models.

Besides the cytotoxicity studies, some common toxicological mechanisms of drugs of abuse were also evaluated, namely the oxidative stress, the Ca^{2+} homeostasis, the energetic status, the mitochondrial function and the cell death mode.

The formation of reactive species and the resulting oxidative and/or nitrosative stress is a common toxicological pathway of several drugs of abuse, including amphetamines, cocaine and alcohol (Carvalho et al., 2012; Uys et al., 2014). Cellular homeostasis is regulated through reduction and oxidation (redox) reactions resulting from the transfer of electrons from one species to another. The formation of oxidative and nitrosative species (ROS/RNS) is a consequence of redox reactions that are important to physiology, whose dysregulation is attributed to pathology. Oxidative stress corresponds to a disturbance in the pro-oxidant/antioxidant balance in favor of the former, resulting in potential damage. Reactive species are capable of irreversibly modifying and damaging lipids and proteins or compromising the function of enzymes or transporters (Sies, 1997). Oxidative stress can occur in all tissues and organs. Our data showed that piperazine designer drugs significantly ($p<0.05$, ANOVA/Dunn's) induced reactive species formation only in rat primary hepatocytes, at all concentrations tested. Using equipotent concentrations of the drugs at their EC_{20}, EC_{40} and EC_{60}, the highest increase in ROS/RNS was observed after MeOPP incubations. In the other *in vitro* models evaluated, namely H9c2 and SH-SY5Y cells, no overproduction of reactive species was observed. Primary hepatocytes are an efficient metabolic *in vitro* system, whose reactions could lead to an increased production of reactive species. Indeed, this is observed in the metabolism of MDMA, where the *N*-demethylation reactions lead to the formation of a free catecholic group, which, in turn, can auto-oxidate into reactive *o*-quinones (Carvalho et al., 2004). The metabolism of piperazine designer drugs, catalyzed by CYP450 isoenzymes, can lead to several products, namely catechol intermediates (Staack and Maurer, 2004) and paracetamol (Staack et al., 2004), which can be further metabolized into *N*-acetyl-*p*-benzoquinone imine, a highly oxidative molecule.

In mammalian cells, GSH is considered the major cytosolic redox buffer. Under normal physiological conditions, GSH is mainly in the reduced form. GSH can directly scavenge ROS or indirectly through a reaction catalyzed by glutathione peroxidase (GPx). The elimination of H_2O_2 by GPx is accomplished with the concomitant oxidation of reduced GSH, leading to formation of oxidized glutathione (GSSG). Therefore, the reduction of GSH accompanied by an increase in GSSG levels is considered a good indicator of oxidative stress (Griffith, 1999). Our results showed that in H9c2 cells, only MDBP, at 1000 and 2000 μM, significantly ($p<0.05$, ANOVA/Bonferroni) reduced the total GSH intracellular levels. However, in differentiated SH-SY5Y cells, 500 and 1000 μM BZP, 100 μM TFMPP, and 250 and 500 μM MeOPP and MDBP elicited a significant ($p<0.01$, ANOVA/Bonferroni) total GSH depletion. A similar result was observed using equipotent concentrations of the drugs in rat primary hepatocytes. The piperazine designer drugs, with the exception of TFMPP and of the lowest concentration of MeOPP, significantly ($p<0.001$, ANOVA/Dunn's) depleted GSH intracellular levels. For MeOPP, this depletion was concentration-dependent ($p<0.001$, ANOVA/Dunn's) and it was the highest among all the piperazines. In hepatocytes, the reduction in GSH levels is accompainned by an overproduction of reactive species, therefore, this GSH depletion would be a physiological response to the oxidative stress. Moreover, in hepatocytes incubated with BZP, an increase in GSSG was also observed, corroborating to this hypothesis. However, the increase in GSSG levels can promote the GSSG efflux from the cell through multidrug resistance proteins or the formation of mixed disulfides in cellular proteins (Cole and Deeley, 2006). This GSSG efflux is a cellular response that protects the cells from oxidative stress that is why an increase in intracellular GSSG is, sometimes, not seen. In SH-SY5Y and H9c2 cells, whose metabolic capacity is much lower than hepatocytes, other GSH depletion mechanisms should be considered, which include formation of GSH-conjugates and enzymatic inhibition of GSH biosynthesis (Gao et al., 2010).

One of the GSH biosynthetic pathways was investigated through the *in vitro* incubation of piperazine designer drugs with the enzyme glutathione reductase (GR). The formed GSSG is reduced to two molecules of GSH by the action of GR. This enzyme presents thiol groups that are sensitive to chemical modifications induced by redox conditions. Under extreme oxidising environments, aggregates of GR may be formed, which decrease its activity (Remião et al., 2000). Under our experimental conditions, the piperazine designer drugs do not seem to have any influence on the GR activity, indicating that other enzymes from the GSH homeostasis could be involved.

Interestingly, GSH depletion has been observed after cocaine, methamphetamine and cronic alcohol abuse (Uys et al., 2014). In hepatocytes, formation of GSH-conjugates with amphetamine derivatives is a classical feature (Hiramatsu et al. 1990; Carvalho et al. 1996; Carvalho et al. 2004; Dias da Silva et al. 2014a). The aromatic hydroxylation of amphetamine into *p*-hydroxyamphetamine leads to the formation of the glutathione-S-yl-*p*-hydroxiamphetamine conjugate through a reaction catalyzed by CYP2D6 (Carvalho et al. 1996). The formation of catechol metabolites, which are oxidized into quinone intermediates following demethylenation of MDMA (Hiramatsu et al. 1990) and MDA (Carvalho et al. 2004) has also been shown to produce the corresponding glutathione-S-yl-*N*-methyl-α-methyldopamine and glutathione-S-yl-α-methyldopamine conjugates. Due to the similarity between the main metabolic pathways that were already described for the piperazine designer drugs (Staack and Maurer 2005) and those of the amphetamines, the formation of such GSH-conjugates with the piperazines is possible. The biosynthesis of GSH occurs in the cytosol, and it is dependent on two enzymes: γ-glutamylcysteine ligase and GSH synthase (Marí et al., 2013). Besides, the break down of extracellular GSH to provide cysteine is the rate-limiting substrate for the intracellular *de novo* GSH synthesis, a reaction catalyzed by the enzyme γ-glutamyl transpeptidase (GGT) (Zhang et al., 2005). It is possible that these three enzymes might be targets for inhibition by piperazine designer drugs or their metabolites.

Mitochondria are considered the ‘powerhouse’ of the cell, since one of them major functions is energy production through ATP generation. Mitochondria provide ATP via oxidative phosphorylation, which occurs in the electron transport chain, localized in the inner mitochondrial membrane (Van Laar and Berman, 2013). Mitochondria also participate in other pathways of normal cell functioning, namely Ca^{2+} handling and apoptotic cell death. Ca^{2+} uptake is driven by the electrochemical potential gradient generated by the combination of the mitochondrial membrane potential (Δψm) and the low concentration of Ca^{2+} in the matrix (Duchen, 1999). It is well established that mitochondria accumulate Ca^{2+} ions during cytosolic Ca^{2+} elevations in a variety of cell types (Kumar et al., 2012). The downward electrochemical gradient across the inner membrane directs Ca^{2+} into the mitochondria through an uniporter. Once inside the mitochondria it can either be buffered or it can be transported back out of the mitochondria via a Na+/Ca^{2+} antiporter (Szabadkai and Duchen, 2008). If mitochondrial buffering capacity is overwhelmed by elevated Ca^{2+}, mitochondrial matrix Ca^{2+} increases to levels high enough to trigger the opening of the mitochondrial permeability transition pore (MPTP). This involves the formation of pores in the inner membranes with ≤1.5 kDa, allowing the influx of water and solutes into the matrix. Although MPTP can ‘flicker’ and be reversible, sustained

transitions lead to the collapse of Δψm, cessation of ATP production, and cell death (Dong et al., 2006). In cell death, one well understood role of mitochondria is to regulate the release of proteins from the space between the inner and outer mitochondrial membranes to the cytosol, such as cytochrome c, apoptosis inducing factor (AIF) or SMAC/Diablo, thus leading to downstream caspase activation and apoptotic cell death (Danial and Korsmeyer, 2004).

Due to the importance of mitochondria to normal cell processes, several aspects of mitochondrial function were evaluated. A significant increase ($p<0.05$, Kruskal-Walis/Dunn's) of intracellular free Ca^{2+} levels were observed after incubation with 1000 μM BZP, 50 and 100 μM TFMPP, 500 μM MeOPP, and 1000 μM MDBP in H9c2 cardiomyoblasts and 350 μM BZP, 1 and 5 μM TFMPP, 25 and 50 μM MeOPP and 1000 μM MDBP in neuroblastoma SH-SY5Y cells, indicating that these drugs cause perturbations in cellular Ca^{2+} homeostasis. However, when we evaluated the Δψm, distinct responses were noted, which includes a significant ($p<0.01$, ANOVA/Bonferroni) Δψm loss at 100, 500 and 1000 μM TFMPP and 500, 1000 and 2000 μM MeOPP or MDBP in H9c2 cells and a significant ($p<0.05$, ANOVA/Bonferroni) hyperpolarization of differentiated SH-SY5Y neurons at 1000 μM BZP, 50 and 100 μM TFMPP and 1000 and 2000 μM MeOPP or MDBP. With the increase in Ca^{2+} levels, the mitochondria buffering capacity was overwhelmed and led to the loss of Δψm, mitochondrial depolarization and the significant ($p<0.05$, ANOVA/Bonferroni) depletion of ATP, which was verified at 1000 and 2000 μM BZP, 500 μM TFMPP, 2000 μM MeOPP and 1000 and 2000 μM MDBP. This happens in response to mitochondrial depolarization, when the ATP synthase reverts to an ATPase activity, consuming ATP and pumping protons outwards, in a futile, energy consuming cycle (Duchen, 1999), in an attempt of Δψm maintenance (Mathur et al., 2000). All these events led to the MPTP opening, which was confirmed by the significant ($p<0.05$, two-way ANOVA/Bonferroni) increase in cell viability after co-incubation of 1500 and 2000 μM BZP, 50 and 100 μM TFMPP and 2000 μM MeOPP or MDBP with 1 μM cyclosporine A, a MPTP inhibitor. MPTP opening is catastrophic for the cell and will lead inexorably to cell death, either through ATP consumption, acute energy failure and necrosis or through the leakage of cytochrome c from mitochondria and the initiation of apoptosis (Duchen, 1999).

On the other hand, in differentiaded SH-SY5Y cells in spite of the increase in the intracellular free Ca^{2+} levels, cells exhibited a mitochondrial hyperpolarization. This is a physiological response, there is evidence that neurons displaying a more pronounced Δψm hyperpolarization survives longer (Ward et al., 2007). This happens because

hyperpolarization reduces neuronal activity and lowers ATP consumption, maintaining ion gradients and protecting neurons from death. However, it may also reduce the expression of activity-dependent genes, such as neurotrophins (Guatteo et al., 2005). This is supported by our data once ATP remained unaltered, even with the increased intracellular Ca^{2+} levels.

On the contrary, in primary rat hepatocytes, it was observed a significant ($p<0.01$, ANOVA/Dunn's) loss of Δψm for the piperazine designer drugs at all concentrations tested, with the exception of EC_{20} TFMPP, with subsequent overproduction of reactive species and ATP depletion. The reduction of intracellular ATP levels was significant ($p<0.05$, ANOVA/Dunn's) for all concentrations, with the exception of EC_{20} BZP and TFMPP and EC_{40} TFMPP. In the liver, depletion of ATP is a typical feature of hypoxic and toxic injury, and leads to inhibition of two hepatic anabolic processes, namely gluconeogenesis and plasma protein synthesis, which have in common a substantial requirement for ATP (Ponsoda et al. 1995). As it occurred in H9c2 cardiomyoblasts, the MPTP opening in hepatocytes can be expected since reactive species production, loss of Δψm and ATP depletion are key events that end up in mitochondrial collapse.

Similarly, studies conducted with MDMA also showed involvement of increased intracellular Ca^{2+} concentrations and loss of Δψm in the cytotoxic effects using H9c2 cells (Tiangco et al., 2005). Increases in the intracellular free Ca^{2+} levels for the mixture of MDMA and its metabolites were also noted in differentiated SH-SH5Y cells. However, by using an intracellular Ca^{2+} quelator, the authors concluded that Ca^{2+} did not participate in the cell death pathway caused by this mixture. On the other hand, the antioxidant *N*-acetylcysteine prevented the mitochondrial disruption (Barbosa et al., 2014b), proving that for MDMA neurotoxicity the oxidative stress plays an important role. In HepG2 cells, a mixture of amphetamines led to increase of reactive species and loss of Δψm (Dias da Silva et al., 2014a). Mytochondrial dysfunction was also observed in MDMA-treated rats (Song et al., 2010). The involvement of reactive species and MPTP opening is also described in mitochondria isolated from rat liver and incubated with different concentrations of methamphetamine (Mashayekhi et al., 2014).

As stated before, mitochondrial disfunction can lead to MPTP opening and thus, to cell death, that occur either by necrosis or apoptosis. Necrosis is an unregulated phenomenon involving damage of membrane integrity, cellular disruption and swelling of cytoplasmic organelles; whereas apoptosis is characterized by organized plasma membrane blebbing, cell shrinkage and typical modifications of nuclear morphology, such as chromatin condensation and fragmentation (Eguchi et al., 1997). Our experiments

showed that piperazine designer drugs induced apoptotic pathways in all *in vitro* models, namely H9c2 cardiomyoblasts, human neuroblastoma SH-SY5Y cells and primary rat hepatocytes. The early marker of apoptosis is the exposition of phosphatidilserine on the cell surface, which is normally concentrated in the luminal layer of the cytoplasmic membrane. At the later stage, the entire phosphatidylserine is flipped on the outer membrane (Kumar et al., 2012). When the rate of apoptosis is substantially increased, the cells undergo secondary necrosis (or late apoptosis) with breakdown of membrane potential, cell swelling and cell contents release. After staining H9C2 cells approximately at EC_{30} with annexin V-FITC and PI, there was a significantly ($p<0.01$, ANOVA/Bonferroni) higher number of cells at an early apoptotic stage and low necrotic cells. However, there was also a significantly ($p<0.05$, ANOVA/Bonferroni) elevated number of cells double-stained and most likely undergoing secondary necrosis. On the other hand, in SH-SY5Y cells a clear apoptotic pattern was observed, with a significant increase ($p<0.01$, ANOVA/Bonferroni) in the number of early apoptotic cells for all drugs at non cytotoxic concentrations. Interestingly, only in primary rat hepatocytes the activation of the downstream effector caspase-3 was noticed. A significant ($p<0.01$, ANOVA/Dunn's) increase in caspase-3 activity was observed for all concentrations, except for EC_{20} BZP and TFMPP and EC_{40} TFMPP, showing that while the hepatocytes signalize for classical apoptotic pathways, in other tissues alternative mechanisms for apoptosis induction that are independent of caspases activation may be occurring.

In fact, apoptosis has been described for amphetamines. In primary cultures of hippocampal neurons, 400 μM MDMA and 50 μM 2,5-dimethoxy-4-iodoamphetamine (DOI) induced caspase dependent and independent mechanisms of death, involving both the mitochondria machinery and the activation of cell death receptors (Capela et al., 2013). In differentiated SH-SY5Y cells, a mixture of MDMA and metabolites elicited apoptosis through caspase-3 activation (Barbosa et al., 2014b). In HepG2 cells, the death mechanisms induced by different amphetamines, alone or in combination, seemed to depend on both temperature and time of exposure. In spite of the overexpression of several apoptosis markers, including proteins of BCL-2 family and activation of caspase3/7, at 37 ºC, in unfavorable environments, such as hyperthermia (40.5 ºC) and long incubation periods (48 h), necrotic features were also observed (Dias da Silva et al., 2013b). Corroborating these findings, while MDMA induced apoptosis in hepatic stellate cells (Montiel-Duarte et al., 2004), the combination of MDMA and ethanol evoked necrotic features (Pontes et al, 2008).

An alternative apoptotic pathway involved in cardiomyocite (Parra et al., 2013) and neuronal cell death (Reimertz et al., 2001; O'Donovan et al., 2001) includes activation of calpains. Calpains are Ca^{2+}-dependent proteases involved in apoptotic and necrotic processes which could, in turn, be activated by piperazine designer drugs due to the increased intracellular Ca^{2+} levels (Jiang et al., 2010).

The potential genotoxicity of the piperazine designer drugs was evaluated through the comet assay in differentiated SH-SY5Y cells. Under our experimental conditions, no signs of genotoxicity were observed, however, it was observed a significant ($p<0.01$, ANOVA/Bonferroni) increase in DNA degradation caused by endonuclease activity during apoptosis or necrosis at 100 μM TFMPP and 250 and 500 μM MeOPP or MDBP.

Our data pointed to mitochondria and GSH homeostasis as targets of piperazine designer drugs toxicity. However, toxic changes in cells generally result from alterations not just in a single or few molecules, but in many molecular cascades. Moreover, mitochondrial dysfunction and oxidative stress are common mechanisms of toxicity and they are generally secondary events in the toxic insult. The DNA microarray technology has the potential to more comprehensively contribute to the understanding of toxicity than any available traditional approach. This technology also helps to identify early, sensitive biomarkers of toxicity, since alterations in gene expression are thought to precede the toxic outcome. The combination of microarrays with conventional toxicological tools has contributed to the knowledge of the mechanisms underlying cellular toxicity of several xenobiotics (Sawada et al., 2005).

The sandwich cultures of primary rat hepatocytes were selected as the best *in vitro* model for toxicogenomic studies (Schug et al., 2008). The sandwich cultures were incubated with a non cytotoxic concentration of each piperazine designer drug. The transcriptomic data were generated through the Affymetrix microarray technology and analyzed based on previous works (Grinberg et al., 2014).

In spite of the number of down-regulated probes being higher than the up-regulated ones, the number of common up-regulated probes by the four piperazine designer drugs was higher. The four piperazine designer drugs presented a very homogenous response, therefore we looked for a common pathway played by the drugs in liver toxicity. The majority of the up-regulated genes were related to cholesterol biosynthesis. In the body, cholesterol is either derived from the diet or from *de novo* synthesis occurring mainly in the liver through the mevalonate pathway. This pathway comprises several enzymes, such as sterol C4-methyloxidase (msmo1), isopentenyl-

diphosphate-Δ-isomerase (idi1), lanosterol 14-α demethylase (cyp51), squalene epoxidase (sqle), and farnesyl diphosphate synthase (fdps), whose genes were up-regulated.

Phospholipids, including cholesterol, are critical components of the plasma membrane of living cells. Phospholipids function as emulsifying agents to maintain the proper colloidal state of the cytoplasm, while cholesterol also functions as the precursor of steroid hormones. Phospholipidosis is observed in various tissues, including liver, kidney, and lung, and it is characterized by intracellular accumulation of phospholipids and the appearance of membranous lamellar bodies (Hirode et al., 2008). Based on previous toxicogenomic data, four possible mechanisms have been suggested for the induction of phospholipidosis: (1) inhibition of lysosomal phospholipase activity – this is generally regarded as the primary mechanism of induction; (2) inhibition of lysosomal enzyme transport; (3) enhanced phospholipid biosynthesis; and (4) enhanced cholesterol biosynthesis - this considered to be an indirect trigger (Sawada et al., 2005). The last one seems to fit in the overexpression genes found after piperazine designer drugs incubation, however, this data needs *in vivo* confirmation. Drugs known to induce phospholipidosis by up-regulation of cholesterol biosynthetic pathway include propiconazole (Murphy et al., 2012), fluoxetine, imipramine, and hydroxyzine (Sawada et al., 2005; Hirode et al., 2008).

Gene expression is primarily controlled by transcription factors, which respond to environmental, autocrine, or paracrine signals. The regulation of cholesterol levels is a complex process involving cross regulatory feedback mechanisms using a variety of sensors (Murphy et al., 2012). In the liver, lipid synthesis is regulated by the lipogenic transcription factor sterol regulatory element binding proteins (SREBPs). In accordance to our data, SREBP was one of the overlapped transcription factors found in common for all piperazine designer drugs.

Overall, the results of the thesis show that piperazine designer drugs are potentially cardio, neuro and hepatotoxic compounds *in vitro*, raising concerns about its use, in spite of being marketed as safe by smartshops and websites. It also raises questions about the use of piperazine designer drugs in combinations among them, namely the association of BZP and TFMPP in the same tablet, or with other drugs, such as ethanol, tobacco, amphetamines and cannabinoids. As previously observed with amphetamine designer drugs (Dias da Silva et al., 2013abc, 2014ab), marked toxicity can occur when the drugs are combined at individually non-cytotoxic concentrations.

4.2 References

Aboutabl ME, El-Kadi AOS. Constitutive expression and inducibility of CYP1A1 in the H9c2 rat cardiomyoblast cells. Toxicol In vitro 2007, 21: 1686-1691.

Araújo AM, Valente MJ, Carvalho M, Dias da Silva D, Gaspar H, Carvalho F, et al. Raising awareness of new psychoactive substances: chemical analysis and in vitro toxicity screening of 'legal high' packages containing synthetic cathinones. Arch Toxicol 2014 doi: 10.1007/s00204-014-1278-7

Arbo MD, Bastos ML, Carmo H. Piperazine compounds as drugs of abuse. Drug Alcohol Depend 2012, 122: 174-185.

Aninat C, Piton A, Glaise D, Le Charpentier T, Langouët S, Morel F, et al. Expression of cytochromes P450, conjugating enzymes and buclear receptors in human hepatoma HepaRG cells. Drug Met Disp 2006, 34: 75-83.

Barbosa DJ, Capela JP, Silva R, Ferreira LM, Branco PS, Fernandes E, et al. "Ecstasy"-induced toxicity in SH-SY5Y differentiated cells: role of hyperthermia and metabolites. Arch Toxicol 2014a, 88: 515-531.

Barbosa DJ, Capela JP, Silva R, Villas-Boas V, Ferreira LM, Branco PS, et al. The mixture of "ecstasy" and its metabolites is toxic to human SH-SY5Y differentiated cells at in vivo relevant concentrations. Arch Toxicol 2014b, 88: 455-473.

Biliński P, Hołownia P, Kapka-Skrzypczak L, Wojtyła A. Designer drugs (DD) abuse in Poland; a review of the psychoactive and toxic properties of substances found from seizures of illegal drug products and the legal consequences thereof. Part II - Piperazines/piperidines, phenylethylamines, tryptamines and miscellaneous 'others'. Ann Agric Environ Med 2012, 19: 871-882.

Capela JP, Araújo SC, Costa VM, Ruscher K, Fernandes E, Batsos ML, et al. The neurotoxicity of hallucinogenic amphetamines in primary cultures of hippocampal neurons. Neurotoxicology 2013, 34, 254-263.

Carvalho F, Remião F, Amado F, Domingues P, Ferrer Correia AJ, Bastos ML. d-Amphetamine interactions with glutathione in freshly isolated rat hepatocytes. Chem Res Toxicol 1996, 9: 1031-1036.

Carvalho M, Carmo H, Costa VM, Capela JP, Pontes H, Remião F, et al. Toxicity of amphetamines: an update. Arch Toxicol 2012, 86: 1167-1231.

Carvalho M, Milhazes N, Remião F, Borges F, Fernandes E, Amado F, et al. Hepatotoxicity of 3,4-methylenedioxyamphetamine and α-methyldopamine in isolated rat hepatocytes: formation of glutathione conjugates. Arch Toxicol 2004, 78: 16-24.

Cheung Y, Lau WK, Yu M, Lai CS, Yeung S, So KF, et al. Effects of all-trans-retinoic acid on human SH-SY5Y neuroblastoma as in vitro model in neurotoxicity research. Neurotoxicology 2009, 30: 127-135.

Cohen BMZ, Butler R. BZP-party pills: a review of research on benzylpiperazine as recreational drug. Int J Drug Policy 2011, 22: 95-101.

Cole SPC, Deeley RG. Transport of glutathione and glutathione conjugates by MRP1. Trends Pharmacol 2006, 27: 438-446.

Danial NN, Korsmeyer SJ. Cell death: critical control points. Cell 2004, 116: 205-219.

Datki Z, Juhász A, Gálfi M, Soós K, Papp R, Zádori D, et al. Method for measuring neurotoxicity of aggregating polypeptides with the MTT assay on differentiated neuroblastoma cells. Brain Res Bull 2003, 62: 223-229.

Davies S, Wood DM, Smith G, Button J, Ramsey J, Archer R, et al. Purchasing 'legal highs' on the internet – is there consistency in what you get? Q J Med 2010, 103: 489-493.

Dias da Silva D, Carmo H, Silva E. The risky cocktail: what combination effects can we expect between ecstasy and other amphetamines? Arch Toxicol 2013a, 87: 111-122.

Dias da Silva D, Carmo H, Lynch A, Silva E (2013b) An insight into the hepatocellular death induced by amphetamines, individually and in combination: the involvement of necrosis and apoptosis. Arch Toxicol 2013b, 87: 2165-2185.

Dias da SIlva D, Silva E, Carmo H. Cytotoxic effects of amphetamine mixtures in primary hepatocytes are severely aggravated under hyperthermic conditions. Toxicol In Vitro 2013, 27, 1670-1678.

Dias da Silva D, Silva E, Carmo H. Combination effects of amphetamines under hyperthermia – the role played by oxidative stress. J Appl Toxicol 2014a, 34: 637-650.

Dias da Silva D, Silva E, Carvalho F, Carmo H. Mixtures of 3,4-methylenedioxymethamphetamine (ecstasy) and its major human metabolites act additively to induce significant toxicity to liver cells when combined at low, non-cytotoxic concentrations. J Appl Toxicol 2014b, 34: 618-627.

Donato MT, Lahoz A, Castell JV, Gómez-Lechón MJ. Cell lines: a tool for in vitro drug metabolism studies. Curr Drug Metab 2008, 9: 1-11.

Dong Z, Saikumar P, Weinberg JM, Venkatachalam MA. Calcium in cell injury and death. Annu Rev Pathol Mech Dis 2006, 1: 405-434.

Duchen MR. Contributions of mitochondria to animal physiology: from homeostatic sensor to calcium signalling and cell death. J Physiol 1999, 516: 1-17.

Eguchi Y, Shimizu S, Tsujimoto Y. Intracellular ATP levels determine cell death fate by aopotosis or necrosis. Cancer Res 1997, 36: 1835-1840.

Ferreira PS, Nogueira TB, Costa VM, Branco PS, Ferreira LM, Fernandes E, et al. Neurotoxicity of "ecstasy" and its metabolites in human dopaminergic differentiated SH-SY5Y cells. Toxicol Lett 2013, 216, 159-170.

Gaillard YP, Cuquel AC, Boucher A, Romeuf L, Bevalot F, Prevosto JM, et al. A fatality following ingestion of the designer drug meta-chlorophenylpiperazine (mCPP) in an asthmatic - HPLC MS/MS detection in biofluids and hair. J Forensic Sci 2013, 58: 263-269.

Gao W, Mizukawa Y, Nakatsu N, Minowa Y, Yamada H, Ohno Y, et al. Mechanism-based biomarker gene sets for glutathione depletion-related hepatotoxicity in rats. Toxicol Appl Pharmacol 2010, 247: 211-221.

Gee P, Fountain J. Party on? BZP party pills in New Zealand. N Z Med J 2007, 120: U2422.

Gee P, Richardson S, Woltersdorf W, Moore G. Toxic effects of BZP-based herbal party pills in humans: a prospective study in Christchurch, New Zealand. N Z Med J 2005, 118: 1784-1794.

Godoy P, Hengstler JG, Ilkavets I, Meyer C, Bachmann A, Müller A, et al. Extracellular matrix modulates sensitivity of hepatocytes to fibroblastoid dedifferentiation and transforming growth factor beta-induced apoptosis. Hepatology 2009, 49: 2031-2043.

Godoy P, Lakkapamu S, Schug M, Bauer A, Stewart JD, Bedawi E, et al. Dexamethasone-dependent versus -independent markers of epithelial to mesenchymal transition in primary hepatocytes. Biol Chem 2010, 391: 73-83.

Griffith OW. Biologic and pharmacologic regulation of mammalian glutathione synthesis. Free Radical Biol Med 1999, 27: 922-935.

Grinberg M, Stöber RM, Edlund K, Rempel E, Gofoy P, Reif R, et al. Toxicogenomics directory of chemically exposed human hepatocytes. Arch Toxicol 2014. *In press*.

Guatteo E, Marinelli S, Geracitano R, Tozzi A, Federici M, Bernardi G, et al. Dopamine-containing neurons are silenced by energy deprivation: a defensive response or beginning of cell death? Neurotoxicology 2005, 26: 857-868.

Guo L, Dial S, Shi L, Branham W, Liu J, Fang JL, et al. Similarities and differences in the expression of drug-metabolizing enzymes between human hepatic cell lines and primary human hepatocytes. Drug Metab Dispos 2011, 39: 528-538.

Helander A, Bäckber M, Hultén P, Al-Saffar Y, Beck O. Detection of new psychoactive substance use among emergency room patients: results from the Swedish STRIDA project. Forensic Sci Int 2014, 243: 23-29.

Heschler J, Meyer R, Plant S, Krautwurst D, Rosenthal W, Schultz G. Morphological, biochemical, and electrophysiological characterization of a clonal cell (H9c2) line from rat heart. Circ Res 1991, 69: 1476-1486.

Hiramatsu M, Kumagai Y, Unger SE, Cho AK. Metabolism of methylenedioxymethamphetamine: formation of dihydroxymethamphetamine and a quinone identified as its glutathione adduct. J Pharmacol Exp Ther 1990, 254: 521-527.

Hirode M, Ono A, Miyagishima T, Nagao T, Ohno Y, Urushidani T. Gene expression profiling in rat liver treated with compounds inducing phospholipidosis. Toxicol Appl Pharmacol 2008, 229: 290-299.

Jiang SX, Zheng R-Y, Zeng J-Q, Li X-L, Han, Z, Hou ST. Reversible inhibition of intracellular calcium influx through NMDA receptors by imidazoline I2 receptor antagonists. Eur J Pharmacol 2010, 629: 12-19.

Kim Y, Lasher CD, Milford LM, Murali TM, Rajagopalan P. A comparative study of genome-wide transcriptional profiles of primary hepatocytes in collagen sandwich and monolayer cultures. Tissue Engeneering 2010, 16: 1449-1460.

Kimes BW, Brandt BL. Properties of a clonal muscle cell line from rat heart. Exp Cell Res 1976, 98: 367-381.

Klingmüller U, Bauer A, Bohl S, Nickel PJ, Breitkopf K, Dooley S, et al. Primary mouse hepatocytes for systems biology approaches: a standardized in vitro system for modelling of signal transduction pathways. IEE Proc Syst Biol 2006, 153: 433-447.

Kovaleva J, Devuyst E, De Paepe P, Verstraete A. Acute chlorophenylpiperazine overdose: a case report and review of the literature. Ther Drug Monit 2008, 30: 394-398.

Kumar S, Kain V, Sitasawad SL. High glucose-induced Ca2+ overload and oxidative stress contribute to apoptosis of cardiac cells through mitochondrial dependent and independent pathways. Biochim Biophys Acta 2012, 1820: 907-920.

Lanaro R, Costa JL, Zanolli-Filho LA, Cazenave SOS. Identificação química da clorofenilpiperazina (CPP)em comprimidos apreendidos. Quim Nova 2010, 33: 725-729.

Lin J, Schyschka L, Mühl-Benninghaus R, Neumann J, Hao L, Nussler N, et al. Comparative analysis of phase I and II enzyme activities in 5 hepatic cell lines identifies Huh-7 and HCC-T cells with the highest potencial to study drug metabolism. Arch Toxicol 2012, 86: 87-95.

Lin Z, Will Y. Evaluation of drugs with specific organ toxicities in organ-specific cell lines. Toxicol Sci 2012, 126: 114-127.

Luttringer O, Theil FP, Lavé T, Wernli-Kuratli K, Guentert TW, de Saizieu A. Influence of isolation procedure, extracellular matrix and dexamethasone on the regulation of membrane transporters gene expression in rat hepatocytes. Biochem Pharmacol 2002, 64: 1637-1650.

Marí M, Morales A, Colell A, García-Ruiz C, Kaplowitz N, Fernández-Checa JC. Mitochondrial glutathione: features, regulation and role in disease. Biochim Biophys Acta 2013, 1830: 3317-3328.

Martins JB, Bastos ML, Carvalho F, Capela JP. Differential effects of methyl-4-phenylpyridinium ion, rotenone, and paraquat on differentiated SH-SY5Y cells. J Toxicol 2013; 2013: 347312.

Mashayekhi V, Eskandari MR, Kobarfard F, Khajeamiri A, Hosseini MJ. Induction of mitochondrial permeability transition (MPT) pore opening and ROS formation as a mechanism for methamphetamine-induced mitochondrial toxicity. Naunyn Schmiedebergs Arch Pharmacol 2014, 387: 47-58.

Mathur A, Hong Y, Kemp BK, Barrientos AA, Erusalimsky JD. Evaluation of fluorescent dyes for the detection of mitochondrial membrane potential changes in cultured cardiomyocytes. Cardiovasc Res 2000, 46: 126-138.

Murphy LA, Moore T, Nesnow S. Propiconazole-enhanced hepatic cell proliferation is associated with dysregulation of the cholesterol biosynthesis pathway leading to

activation of Erk1/2 through Ras farnesylation. Toxicol Appl Pharmacol 2012, 260: 146-154.

O'Donovan CN, Tobin D, Cotter TG. Prion protein fragment PrP-(106-126) induce apoptosis via mitochondrial disruption in human neuronal SH-SY5Y cells. J Biol Chem 2001, 23: 43516-43523.

Parra V, Moraga F, Kuzmicic J, López-Crisosto C, Troncoso R, Torrealba N, et al. Calcium and mitochondrial metabolism in ceramide-induced cardiomyocyte death. Biochim Biophys Acta 2013, 1832: 1334-1344.

Ponsoda X, Bort R, Jover R, Gómez-Lechón MJ, Castell JV. Molecular mechanism of diclofenac hepatotoxicity: association of cell injury with oxidative metabolism and decrease in ATP levels. Toxicol in Vitro 1995, 9: 439-444.

Pontes H, Sousa C, Silva R, Fernandes E, Carmo H, Remião F, et al. Synergistic toxicity of ethanol and MDMA towards primary cultured rat hepatocytes. Toxicology 2008, 254: 42-50.

Presgraves S, Ahmed T, Borwege S, Joyce J. Terminally differentiated SH-SY5Y cells provide a model system for studying neuroprotective effects of dopamine agonists. Neurotox Res 2003, 5: 579-598.

Reimertz C, Kögel D, Lankiewicz S, Poppe M, Prehn JHM. Ca^{2+}-induced inhibition of apoptosis in human SH-SY5Y neuroblastoma cells: degradation of apoptotic protease activating factor-1 (APAF-1). J Neurochem 2001, 78: 1256-1266.

Remião F, Carmo H, Carvalho FD, Bastos ML. Inhibition of glutathione reductase by isoproterenol oxidation products. J Enzym Inhib 2000, 15: 47-61.

Rodrigues RM, Bouhifd M, Bories G, Sacco MG, Gribaldo L, Fabbri M, et al. Assessment of an automated in vitro basal cytotoxicity test system based on metabolically-competent cells. Toxicol in Vitro 2013, 27: 760-767.

Rossato LG, Costa VM, Pinho PG, Arbo MD, Freitas V, Vilain L, et al. The metabolic profile of mitoxantrone and its relation with mitoxantrone-induced cardiotoxicity. Arch Toxicol 2013a, 87: 1809-1820.

Rossato LG, Costa VM, Vilas-Boas V, Bastos ML, Rolo A, Palmeira C, et al. Therapeutic concentrations of mitoxantrone elicit energetic imbalance in H9c2 cells as an earlier event. Cardiovasc Toxicol 2013b, 13: 413-425.

Sawada H, Takami K, Asahi S. A toxicogenomic approach to drug-induced phospholipidosis: analysis of its induction mechanism and establishment of a novel in vitro screening system. Toxicol Sci 2005, 83: 282-292.

Schep LJ, Slaughter RJ, Vale A, Beasley MG, Gee P. The clinical toxicology of the designer "party pills" benzylpiperazine and trifluoromethylphenylpiperazine. Clin Toxicol 2011, 49: 131-141.

Schug M, Heise T, Bauer A, Storm D, Blaszkewicz M, Bedawy E, et al. Primary rat hepatocytes as in vitro system for gene expression studies: comparison of sandwich, Matrigel and 2D cultures. Arch Toxicol 2008, 82: 923-931.

Sheridan J, Butler R, Wilkins C, Russel B. Legal piperazine- containing party pills – a new trend in substance misuse. Drug Alcohol Rev 2007, 26: 335-343.

Sies H. Oxidative stress: oxidants and antioxidants. Exp Physiol 1997, 82: 291-295.

Song BJ, Moon KH, Upreti VV, Eddington MD, Lee IJ. Mechanisms of MDMA (Ecstasy)-induced oxidative stress, mitochondrial dysfunction, and organ damage. Curr Pharm Biotechnol 2010, 11: 434-443.

Sousa C, Pontes H, Carmo H, Dinis-Oliveirs RJ, Valentão P, Andrade PB, et al. Water extracts of *Brassica oleracea* var. *costata* potentiate paraquat toxicity to rat hepatocytes *in vitro*. Toxicol in Vitro 2009, 23: 1131-1138.

Staack RF, Fritschi G, Maurer HH. New designer drug 1-(3-trifluoromethylphenyl)piperazine (TFMPP): gas chromatography/mass spectrometry and liquid chromatography/mass spectrometry studies on its phase I and II metabolism and on its toxicological detection in rat urine. J Mass Spectrom 2003, 38: 971-981.

Staack RF, Maurer HH. New designer drug 1-(3,4-methylenedioxybenzyl)piperazine (MDBP): studies on its metabolism and toxicological detection in rat urine using gas chromatography/mass spectrometry. J Mass Spectrom 2004, 39: 255-261.

Staack RF, Maurer HH. Metabolism of designer drugs of abuse. Cur Drug Metab 2005, 6: 259-274.

Staack RF, Theobald DS, Paul LD, Springer D, Kraemer T, Maurer HH. In vivo metabolism of the new designer drug 1-(4-methoxyphenyl)piperazine (MeOPP) in rat and identification of the human cytochrome P450 enzymes responsible for the major metabolic step. Xenobiotica 2004, 34: 179-192.

Szabadkai G, Duchen MR. Mitochondria: the hub of cellular Ca^{2+} signaling. Physiology 2008, 23: 84-94.

Takahashi M, Nagashima M, Suzuki J, Seto T, Yasuda I, Yoshida T. Creation and application of psychoactive designer drugs data library using liquid chromatography with photodiode array spectrophotometry detector and gas chromatography-mass spectrometry. Talanta 2009, 77: 1245-1272.

Uys JD, Mulholland PJ, Townsend PM. Glutathione and redox signaling in substance abuse. Biomed Pharmacother 2014, 68: 799-807.

Van Laar VS, Berman SB. The interplay of neuronal mitochondrial dynamics and bioenergetics: implications for Parkinson's disease. Neurobiol Dis 2013, 51: 43-55.

Ward MW, Huber HJ, Weisová P, Düssmann H, Nicholls DG, Prehn JHM. Mitochondrial and plasma membrane potential of cultured cerebellar neurons during glutamate-induced necrosis, apoptosis, and tolerance. J Neurosci 2007, 27: 8238-8249.

Wikström M, Holmgren P, Ahlner J. A2 (*N*-benzylpiperazine) a new drug of abuse in Sweden. J Anal Toxicol 2004, 28: 67-70.

Xie H, Hu L, Li G. SH-SY5Y human neuroblastoma cell line: in vitro cell model of dopaminergic neurons in Parkinson´s disease. Chin Med J 2010, 123: 1086-1092.

Zhang H, Forman HJ, Choi J. Gamma-glutamyl transpeptidase in glutathione biosynthesis. Methods Enzymol 2005, 401: 468-483.

Zordoky BNM, El-Kadi AOS. H9c2 cell line is a valuable in vitro model to study the drug metabolizing enzymes in the heart. J Pharmacol Toxicol Methods 2007, 56: 317-322

CHAPTER V

CONCLUSIONS

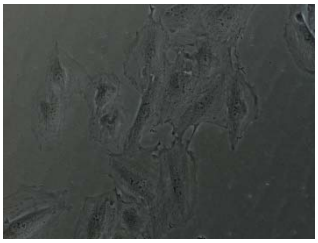
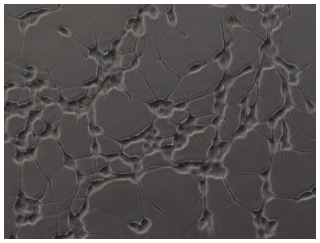
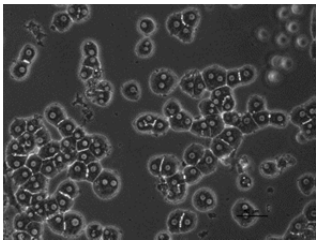


From the experimental studies herein described, it was possible to conclude that:

a) Piperazine designer drugs presented cytotoxicity to different *in vitro* models, including H9c2 rat cardiomyoblasts, human neuroblastoma SH-SY5Y cells, human hepatoma derived HepG2 and HepaRG cells and rat primary hepatocytes;

b) *In vitro* cardiotoxicity of piperazine designer drugs seems to be related with increased intracellular Ca^{2+} levels, mitochondrial depolarization, ATP depletion and MPTP opening, leading to cell death either by apoptsis or necrosis;

c) *In vitro* neurotoxicity seems to be related with increased intracellular Ca^{2+} levels, mitochondrial hyperpolarization and induction of apoptotic pathways;

d) Piperazine designer drugs did not present genotoxicity to differentiated SH-SY5Y cells when evaluated by the comet assay;

e) Primary rat hepatocytes were more sensitive to piperazine designer drugs than HepG2 and HepaRG cells, indicating a potential role of the metabolism in the cytotoxicity;

f) *In vitro* hepatotoxicity seems to be related with overproduction of reactive species and GSH depletion, causing oxidative stress, and mitochondrial dysfunction, ultimately leading to apoptosis;

g) Mitochondria seem to be an important target of piperazine designer drugs;

i) Gene expression analysis pointed to a possible phospholipidosis mechanism of toxicity however, this should be further confirmed *in vivo*.

CHAPTER VI

FUTURE PERSPECTIVES

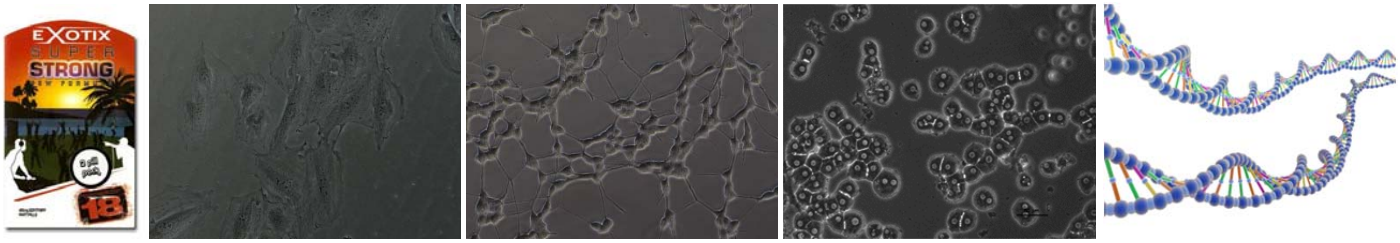

Future studies are required in order to confirm and better understand some findings. Regarding the role of GSH in the piperazine designer drugs cytotoxicity, the formation of GSH adducts should be further investigated. Moreover, the role of oxidative stress in the *in vitro* cardio and neurotoxicity should be confirmed by other biomarkers, such as carbonilated proteins and lipoperoxidation. The apoptotic pathways involved in piperazine designer drugs-induced cell death need a better comprehension by studing alternative cascades such as the calpains activation, cytochrome c release or the induction of pro-apoptotic factors such as the proteins from the BCL-2 family. The role of dopaminergic and serotonergic receptors in the piperazine designer drugs-induced neurotoxicity should be considered. Also, the influence of MPTP opening in the piperazine designer drugs-induced *in vitro* hepatotoxicity deserves experimental evaluation. Regarding the gene array studies, the potential phospholipidosis mechanisms should be confirmed, since discrepancies between gene expression *in vitro* and the real *in vivo* situation are not uncommon. *In vivo* metabolomics could be an interesting tool to better elucidate the phospholipidosis hypothesis and the role of the metabolism in piperazine designer drugs toxicity. The evaluation of potential nephrotoxicity is needed, since there are case-reports on acute renal effects of these drugs.

The recreational abuse of substances is a very complex issue since new drugs of abuse are continually appearing in the market. Continuous research can lead to a better understanding of the mechanisms of toxicity of these drugs and to improve treatments and diagnosis. Finally, future research should aim to evaluate the interaction among different compounds, since in a real life scenario these drugs are often consumed in association with ethanol, tobacco and other drugs of abuse.